EXPLORING the POTENTIAL of IMINES as ANTI-PROTOZOAN AGENTS with FOCUS on *T. BRUCEI* and *P. FALCIPARUM*

A thesis submitted in fulfilment of the requirement for the degree of

DOCTOR OF PHILOSOPHY

Of

RHODES UNIVERSITY

By

KOLA AUGUSTUS OLUWAFEMI

B.Sc. (Hons.) [Akungba], M.Sc. (Ibadan)

December, 2017

ABSTRACT

This work focuses on the design, synthesis and evaluation of imine-containing heterocyclic and acyclic compounds with special focus on their bioactivity against parasitic protozoans (*P. falciparum* and *T. brucei*) - given the context of drug resistance in the treatment of malaria and Human African sleeping sickness and the fact that several bioactive organic compounds have been reported to possess the imino group.

Starting from 2-aminopyridine, novel *N*-alkylated-5-bromo-7-azabenzimidazoles and substituted 5-bromo-1-(carbamoylmethy)-7-azabenzimidazole derivatives were prepared, and their bioactivity against parasitic protozoans was assessed. NMR spectra of the substituted 5-bromo-1-(carbamoylmethy)-7-azabenzimidazole derivatives exhibited rotational isomerism, and a dynamic NMR study was used in the estimation of the rate constants and the free-energies of activation for rotation. The free-energy differences between the two rotamers were determined and the more stable conformations were predicted.

Novel 2-phenyl-7-azabenzimidazoles were also synthesised from 2-aminopyridine. A convenient method for the regioselective formylation of 2,3-diaminopyridines into 2-amino-7-(benzylimino)pyridine analogues of 2-phenyl-7-azabenzimidazole was developed, and some of the resulting imino derivatives were hydrogenated to verify the importance of the imino moiety for bioactivity. The 2-phenyl-7-azabenzimidazoles and the 2-amino-7-(benzylimino)pyridine analogues were screened for their anti-protozoal activity and their cytotoxicity level was determined against the HeLa cell line.

In order to validate the importance of the pyridine moiety, novel *N*-(phenyl)-2-hydroxybenzylimines, *N*-(benzyl)-2-hydroxybenzylimines and (±)-*trans*-1,2-bis[2-hydroxybenzylimino]cyclohexanes were also synthesized and screened for activity against the parasitic protozoans and for cytotoxicity against the HeLa cell line.

The biological assay results indicated that these compounds are not significantly cytotoxic and a good number of them show potential as lead compounds for the development of new malaria and trypanosomiasis drugs.

ACKNOWLEDGMENTS

My sincere appreciations go to my supervisor, Dr Rosalyn Klein for her support, general guidance, mentorship and her encouragement throughout the period of carrying out this research work; I gained a lot from her wealth of experience. I am also indebted to my co-supervisor, Prof Perry T. Kaye, the quantum of his contribution is not measurable.

My appreciations also go to the Department of Chemistry, Rhodes University – under the leadership of Prof Rui Krause and the secretary – Mrs Benita Tarr, for allowing an excellent environment for creative research work. I also thank Mrs Michelle Isaacs and Prof Heinrich Hoppe of the Centre for Chemico-and Biomedical Research, Rhodes University – they conducted the anti-parasitic protozoan assays.

Many thanks to my colleagues, Dr O. J. Jesumoroti, Dr Emmanuel Olawode, Dr Bankole Owolabi, Mr Ogunyemi Oderinlo, Melody, Tarryn Potts, Sinalo, Siyolise, Lukhanyiso, Teresa, Urbain and John Achadu. I acknowledge Adekunle Ajasin University, Akungba-Akoko, Ondo State, Nigeria, for granting me a study leave. I thank my bosses at Adekunle Ajasin University for their support, specifically, Dr Adebisi Olonisakin, Dr Isaac Ololade, Prof C. O. Aboluwoye, Prof Oluwafemi Mimiko, Prof Nurudeen Oladoja are all appreciated.

I thank my family members, especially, Prof C. O. Oluwafemi, Mrs Olusola Oluwafemi, Mr. Olabode Williams Oluwafemi, Adeola Oluwafemi, Mr. Adetunji Oluwafemi, Oreoluwa Oluwafemi, Akuneme Grace, Mr. Ajepe Alaba, Mr. Ojo Oginni, Mr. Adebowale Aderemi, Mrs Ayo Oluwafemi, Mrs Taiwo Obele, Mrs Kehinde Omojasola, Barr. Banji Abuloye and Mr. Taiwo Awe.

Financial support was received from the Tertiary Education Trust Fund (TETFund), Nigeria with fund from Education Tax under its Academic Staff Training and Development Initiative. This research work was also supported by the South African Medical Research Council (SAMRC) with funds from National Treasury under its Economic Competitiveness and Support Package, and Rhodes University Sandisa Imbewu.

LIST OF ABBREVIATIONS

$CDCl_3$	–	deuterated chloroform
DMSO-d_6	–	deuterated dimethyl sulfoxide
DCM	–	dichloromethane
DDT	–	dichlorodiphenyltrichloroethane
DEPT-135	–	distortionless enhancement polarization transfer
Global Fund	–	Global fund to fight AIDS, tuberculosis and malaria
GMEP	–	Global Malaria Eradication Program
HMBC	–	heteronuclear multiple bond correlation
HPLC-MS	–	high performance liquid chromatography–mass spectrometry
HSQC	–	heteronuclear single quantum coherence
HAT	–	human African trypanosomiasis
COSY	–	homonuclear correlation spectroscopy
MeOD	–	deuterated methanol.
MDG	–	Millennium Development Goals
NMP	–	*N*-methyl pyrrolidone
NMR	–	nuclear magnetic resonance
pLDH	–	parasite lactate dehydrogenase
P. falciparum	–	*Plasmodium falciparum.*
RBM	–	Roll Back Malaria program
s-cis and *s-trans*	–	single-bond *cis* and single-bond *trans*
T. brucei	–	*Trypanosoma brucei.*
WHO	–	World Health Organization

Table of Contents **pages**

1. INTRODUCTION

1.1. PROTOZOANS

Protozoans are a class of single-celled eukaryotic microorganisms which belong to the Kingdom Protista.[1-3] They exhibit heterotrophism and the absence of filaments are notable characteristics of protozoans. Some protozoans are parasitic while some are free-living; others are saprophytic in nature and the rest are mutualistic.[1-3] The protozoans of interest in this project are parasites; specifically, *Plasmodium* species which cause malaria and *Trypanosomes* which are responsible for Human African Trypanosomiasis and African cattle Trypanosomiasis.

1.2. HUMAN AFRICAN TRYPANOSOMIASIS (HAT)

Trypanosoma belongs to the protozoan sub-group called zooflagellates and it is the causative agent of African sleeping sickness in humans (HAT). Trypanosomiasis is an infection by a parasitic protozoan called *Trypanosoma* whose vector is the tsetse fly (*Glossina genus*). The *Glossina genus* acquires the infection when they bite an infected person or animal.[1, 4, 5] In 1901, Forde, in the Gambia, West Africa, analysed a blood sample of a fever patient and found some parasites. Dutton identified and named these parasites *Trypanosoma gambiense*.[6] Trypanosomiasis can be divided into two types, namely, African Trypanosomiasis (*Trypanosoma brucei gambiense* and *Trypanosoma brucei rhodesiense)* and American Trypanosomiasis (*Trypanosoma cruzi* and *Trypanosoma rangeli*).[5]

1.2.1. Life-Cycle of *Trypanosomes*

It takes a period of three weeks to complete the life cycle of trypanosomes in tsetse flies. Humans are the major reservoir for *Trypanosomas*, but the parasites are also found in animals.[7] Figure 1 describes the life-cycle of *Trypanosoma brucei*,[7] the parasite responsible for African cattle sleeping sickness. When an infected tsetse fly bites a human in order to take a blood meal (1), it infects the human host with *Trypanosoma* (metacyclic *trypomastigotes*). The parasites migrate to the lymphatic system and then into the blood stream (2). The parasites are then transformed into blood stream *trypomastigotes* which maintain bloodstream infection The parasites penetrate the blood vessel endothelium and invade the extravascular tissues (lymph) and spinal fluid (central nervous system) where they replicate by binary fission (3,4). When an uninfected tsetse fly takes a blood meal from an infected person, the

tsetse fly becomes` infected with bloodstream *trypomastigotes* (5) and the cycle begins again[1, 7, 8]

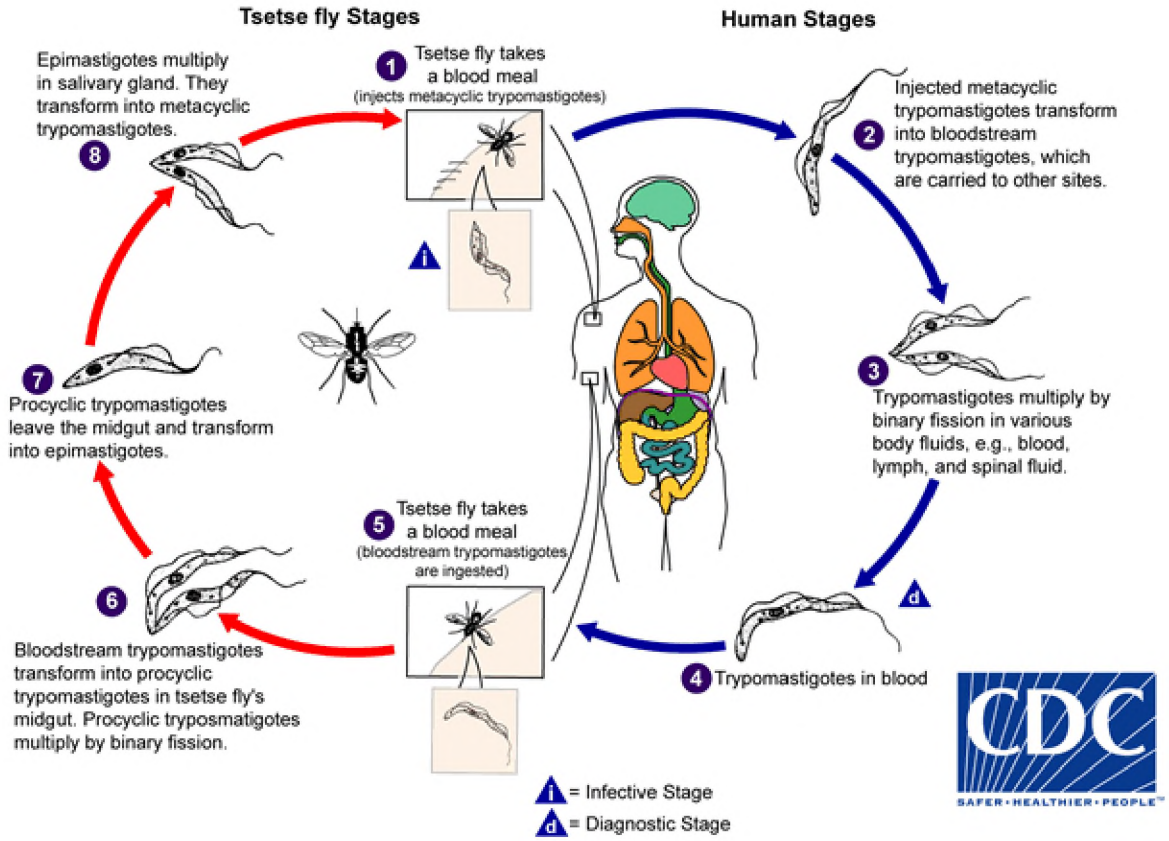

Figure 1. Life cycle of *Trypanosoma brucei*.[7] (Reproduced with permission of Centres for Disease Control and Prevention)

The parasite resides in the tsetse fly's midgut and matures into procyclic *trypomastigotes* (6). The procyclic *trypomastigotes* differentiate by binary fission after which they leave the midgut and transform into *epimastigotes* (7). The *epimastigotes* have the ability to migrate to the tsetse fly's salivary glands and continue their multiplication by binary fission (8).[1, 7, 8]

1.2.2. Clinical Symptoms and Diagnosis

Generally, victims experience anxiety, drowsiness, fever, headache, insomnia, uncontrollable sleep, weakness, sweating, mood change, a swollen red and painful nodule at the site of the bite and swollen lymph nodes all over the body. The World Health Organization (WHO) recommends three stages in testing for trypanosomiasis. The first step involves checking for clinical symptoms like swollen cervical lymph nodes. The second step is to establish if the parasite is actually present in body fluid of the patient and the last step is to determine the state of the parasites' progression and this requires examining the cerebral fluid of the patient. In general, the tests undertaken to examine suspected cases are a blood smear to check for

parasites, cerebrospinal fluid examination, a complete blood count and lymph node aspiration.[5,9-11]

1.2.3. Epidemiology and Eradication Efforts

Between the years 1896 and 1906, there was an epidemic in Uganda and the Congo and between 200 000 and 500 000 people died of the infection.[11-14] By 1920, more African countries were affected, and a severe trypanosomiasis epidemic was recorded between 1970 and 1990. The outbreak in 1920 was minimal as only five thousand cases were recorded in Africa, but a major set-back occurred in 1970 when the epidemic recurred. Efforts by the WHO, national control programmes, bilateral cooperations and non-governmental organizations have helped to reduce the occurrence of trypanosomiasis.[11] The Democratic Republic of Congo (DRC) recorded over 70% of the recently reported cases. Only about 200 cases were reported in Central Africa in 2015, and less than one hundred cases were reported in Nigeria and other neighbouring countries (Chad, Cameroon, Ghana and Côte d'Ivoire).[11, 12]

Between 2000 and 2012, recorded cases were reduced by about 73%,[3] and the World Health Organization has set the year 2020 as the elimination date for trypanosomiasis.[11]

Previous efforts to eradicate trypanosomiasis have included the use of sodium arsenite, nifurtimox **1**, quinapyramine **2**, trypan red **3**, isometamidium chloride **4**, melarsoprol **5,** pentamidine **6** suramin **7** and a more recent drug called eflornithine.[5, 15-21]

Recent reports have shown that *Trypanosoma* parasites have developed resistance to existing drugs being used for treatment of the infection in humans and animals.[19-21]

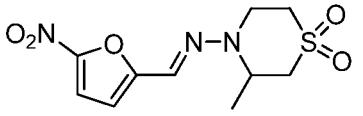

1

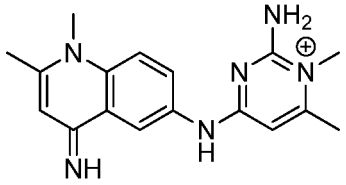

2

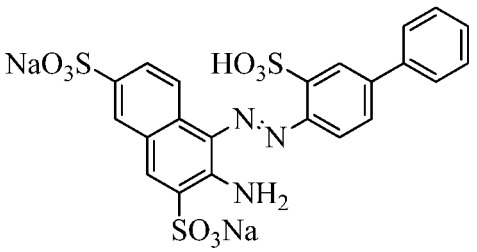

3

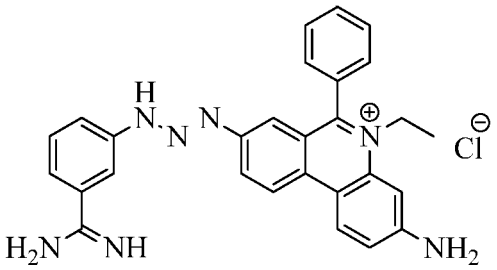

4

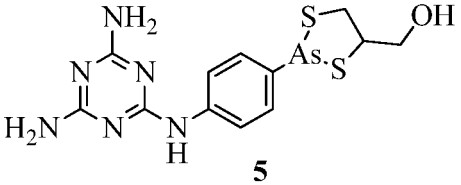

5

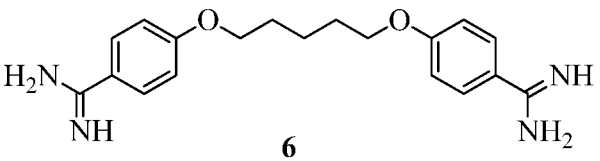

6

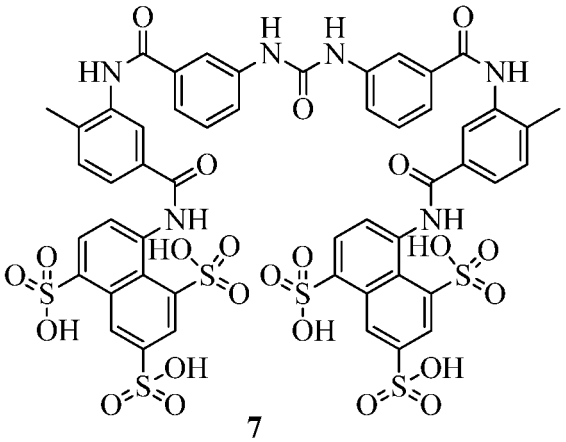

7

1.3. MALARIA

1.3.1. Etiology of Malaria

Malaria is a vector-borne parasitic (protozoan) disease. It occurs in humans as a result of infection by *Plasmodium falciparum, Plasmodium malariae, Plasmodium vivax, Plasmodium ovale* and *Plasmodium knowlesi*. *Plasmodium* is an apicomplexan eukaryotic protozoan parasite (Sporozoan).[22, 23] This disease is usually transmitted when a female *Anopheles* mosquito takes a blood meal from an infected person, thereby becoming infected and capable of infecting an uninfected person.[23] An unnatural mode of transmission of malaria is through shared needles and by blood transfusion from malaria-infected blood donors.[23]

Nei Ching was the first to describe the symptoms of malaria in Chinese records dating back to 2700 BCE. In 1550 BCE, the Egyptian Eber Papyrus discussed oil isolated from the Balantines tree as mosquito repellent. In the 6th century BCE, Cuneiform writings referred to a malaria-like fever affecting people living in Tigris–Euphrates region.[24, 25] On the 6th of November, 1880, Charles Louis Alphonse Laveran (a French army surgeon in Algeria, North Africa) was the first person to detect malaria parasites in the blood sample of a malaria-infected patient.[25] On the 29th of August, 1897, Ronald Ross of the Indian Medical Service proved that it is possible for the malaria parasite to be transmitted from infected persons to mosquitoes. Giovanni Batista, Amico Bignami and Giuseppe Bastianelli, in 1899, demonstrated that malaria infected mosquitos can transmit the infection to uninfected persons.[25]

1.3.2. Life-Cycle of *Plasmodium falciparum*

The parasite passes successively through two hosts, female Anopheles mosquitos and humans in a complex life-cycle [23, 26, 27] involving different stages as it passes from one host to another.[28] The female Anopheles mosquito is known to be responsible for transmission of malaria parasites. Female Anopheles mosquitoes need blood meals for reproduction and they survive in stagnant water or water bodies with very slow mobility. Within a period of 7-14 days, mosquitos can complete their reproductive life-cycle, eggs are hatched after 3 days and the emerging larvae grow into pupae. The pupae mature into mosquitos within a few days.[28]

Figure 2 summarises the life cycle of a malaria parasite;[30] when an infected female Anopheles mosquito takes a blood meal from an uninfected person (1), sporozoites are introduced into the human host (2) and they quickly migrate to the human liver cells (3) where they undergo asexual multiplication. When eruption of the liver cells occurs, merozoites (4) are released into the bloodstream which results in the inevitable invasion of the red blood cells.[23, 28-31] Merozoites can be regarded as blood-stage parasites and they are responsible for the clinical manifestation of malaria. Merozoites are characterized by their ability to multiply asexually and their ability to infect and destroy all erythrocytes they come into contact with. Each merozoite matures into a trophozoite which in turn grows to become a schizont. The Schizonts rupture and release more merozoites. In the course of the female Anopheles mosquitoes taking a blood meal from an infected person (5), they ingest both male (microgametocyte) and female (macrogametocyte) merozoites. The parasites multiply in mosquitoes by a process known as the sporogenic cycle.[23, 28, 30, 31]

During the sporogenic cycle, microgametes and macrogametes fuse to produce diploid zygotes. The zygotes grow to become ookinetes and invade the mid-gut wall and mature into oocysts. Mitotic division of matured oocysts results in the release of sporozoites. The released sporozoites migrate to the mosquitos' salivary gland where they are ready to be transmitted into humans to continue the malaria life-cycle.[28, 29]

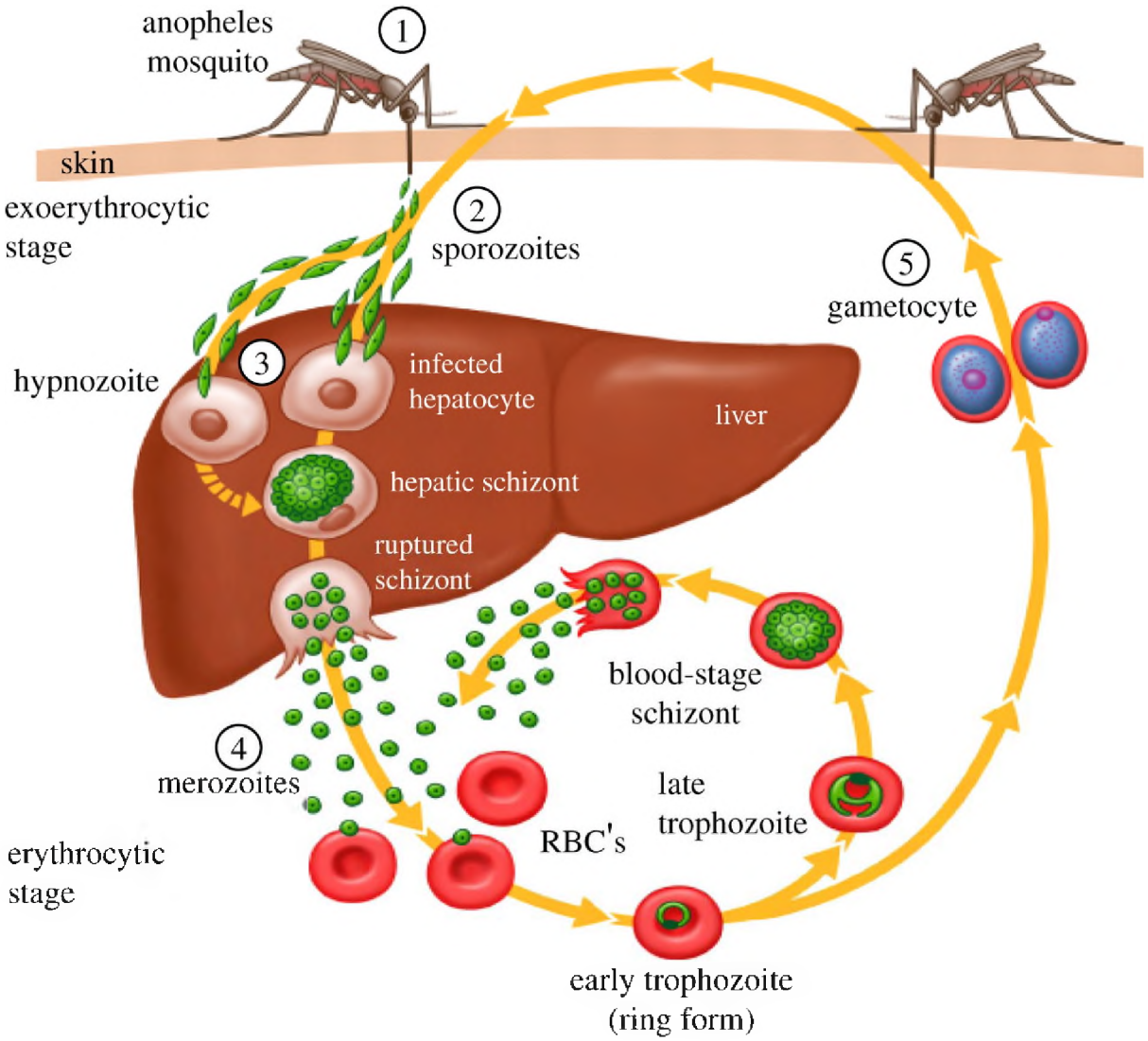

Figure 2. Life-cycle of malaria parasite

(Reproduced with permission).[30]

1.3.3. Epidemiology of Malaria

A study on malaria transmission by Shiff at Johns Hopkins Bloomberg School of Public Health showed that temperature, water availability, seasonal fluctuation of mosquito

populations, vectoral capacity of common vector species and duration of conditions suitable for mosquito's survival are the factors responsible for malaria transmission.[32]

Malaria infections are prevalent in Sub-Saharan Africa, Latin America and Southern Asia (Figure 3).[34, 35] Estimates have shown that more than 200 million people suffer from malaria infection every year and this huge number of cases is estimated to have been responsible for about a million deaths annually. Therefore, malaria infection has been listed as one of the three deadliest diseases across the world.[31, 33-35a] A recent WHO report showed that the global death toll due to malaria has been successfully reduced from 839,000 per year in 2000 to 438,000 in 2015).[34]

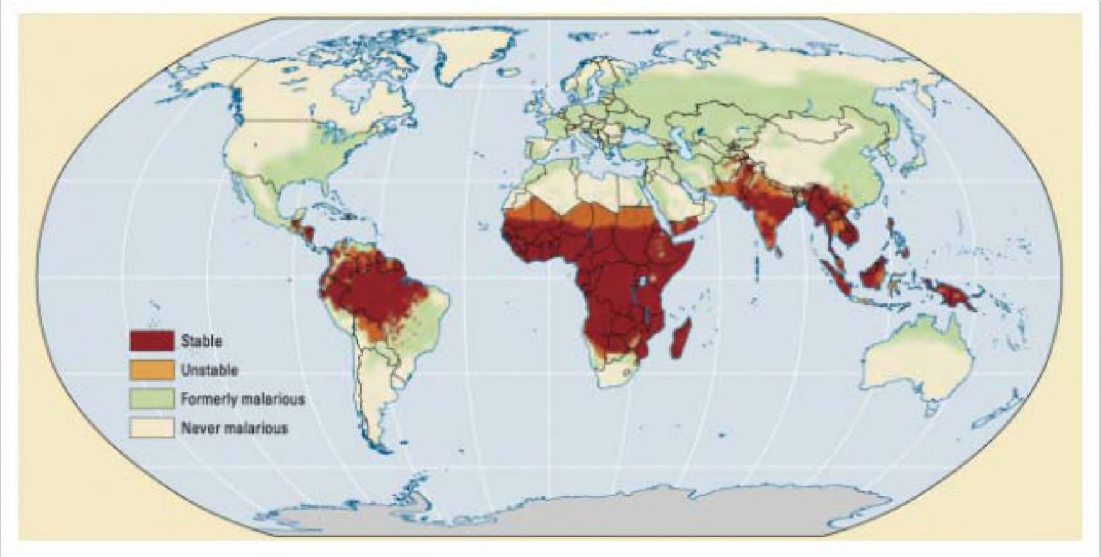

Figure 3: World map showing malaria prevalence. (Reproduced from World development report, 2009).[35]

1.3.4. Malaria Symptoms and Eradication Efforts

Destruction of red blood cells and asexual replication of malaria parasites within a human host are responsible for some symptoms of malaria infection. For an uncomplicated infection, symptoms like fever, chills, headache, body pains, diarrhoea and vomiting occur after about 10-15 days of infection. Other physical conditions like elevated body temperature, body weakness, perspiration and an enlarged spleen are symptoms as well.[36, 37]

In a severe malaria infection, symptoms include severe anaemia and haemoglobinuria that result from the destruction of erythrocytes. Low blood pressure and kidney failure may also occur. In cerebral malaria infection, conscience impairment, abnormal behaviour, seizure, coma and other abnormalities are signs and symptoms.[37]

Malaria eradication is a difficult task because a person that survives an initial infection can get infected again and again. Malaria infected people are difficult to identify without diagnosis because many symptoms are common to other infections and malaria-infected mosquitoes are not identifiable.[38] Major eradication efforts in the past have included the following.

1. *Elimination of mosquitoes by the use of dichlorodiphenyltrichloroethane (DDT) at homes and administration of chloroquine to clear infection in infected persons.*[35-38] This proved to be effective for a while, but the malaria parasites developed resistance to chloroquine, and so a need for new antimalarial drugs developed. Mosquitos have also developed resistance to DDT, and DDT is harmful to the ecological system in toxic amounts, having the potential to seep into groundwater and accumulate in humans and animals. DDT in human bodies is stored in the adrenal glands, testes, thyroid, liver and kidneys. It also has negative effects on the human nervous system.[39-42]
2. *Alma ata declaration in 1978*: This event was an international conference on primary healthcare and health systems in African nations. It was declared at the conference that nations should adopt the recommended primary healthcare principles outlined in the conference.[43]
3. *Bill & Melinda Gates Foundation.* This foundation made known its goal for malaria eradication in 2007. In 2014, Bill Gates announced his intention to commit more than $500 million for an intervention fund for malaria eradication and for diseases such as pneumonia, diarrhoea and other parasitic infections. Bill Gates also made known his efforts to eradicate malaria by the middle of the 21st century; his foundation would make a commitment to increase the yearly funding for malaria by 30 percent. In his words, ''The only way ahead of the natural evolution of infectious diseases is to stay fully invested in the R&D pipeline for new drugs, new vaccines, new diagnostics and innovative approaches to vector control''.[44]

Other programmes designed for the eradication of malaria include the WHO's Global Malaria Eradication Program (GMEP), Millennium Development Goals (MDG), Roll Back Malaria Programme (RBM) and Global Fund to Fight AIDS, Tuberculosis and Malaria (Global Fund).[33, 38, 45, 46]

1.3.5. Antimalarial Compounds

Antimalarial compounds can be categorized according to their actions on certain stages in the life-cycle of the malaria parasite. Bruce-Chwatt of the Division of Malaria Eradication, World Health Organization in Geneva, Switzerland, classified antimalarial compounds into the following five groups. [47]

1. Primary tissue schizontocidal compounds which are mainly effective at the pre-erythrocyte stage. Examples in this class are primaquine, pamaquine, proguanil and pyrimethamine. These compounds are also referred to as casual prophylactics.
2. Blood schizontocides whichare active against the asexual red-blood cell form of malaria. 4-Aminoquinolines, quinine and mepacrine are examples in this class.
3. Gametocytocidal Compounds which are effective against the sexual stage of parasites that cause malaria. The 8-aminoquinolines, pamaquine, primaquine and plasmocide are examples of gametocytocidal drugs.
4. Sporontocidal compounds which are active against the sporogonic stage of the malaria parasite in the vector. Compounds that have anti-sporogonic activity are pyrimethamine, proguanil and chlorproguanil.
5. Secondary tissue schizontocidal agents which are toxic to the secondary exo-erythrocytic stage of *Plasmodium vivax* and *Plasmodium malariae*. Pamaquine and primaquine are good agents against this stage of parasite infection.

1.3.5.1. Quinolines and Amino Alcohols

Quinoline **8** can be referred to as a heterocyclic analogue of naphthalene **9** just as pyridine **10** is to benzene **11**. Quinoline is closely related to isoquinoline **12**, indole **13** and purine **14**.[48] Quinoline is a heterocycle made up of benzene (A) and pyridine (B) rings fused together. Quinolines are useful in the treatment and prevention of malaria at the blood stage. It is believed that quinolines act by interfering with the polymerization of heme to hemozoin.[49]

The quinoline derivative, Quinine (**15**), is historically important in that it is said to be the first molecule used successfully in the treatment of disease.[50, 52] Quinine is an alkaloid isolated from the bark of cinchona trees. [50, 51]

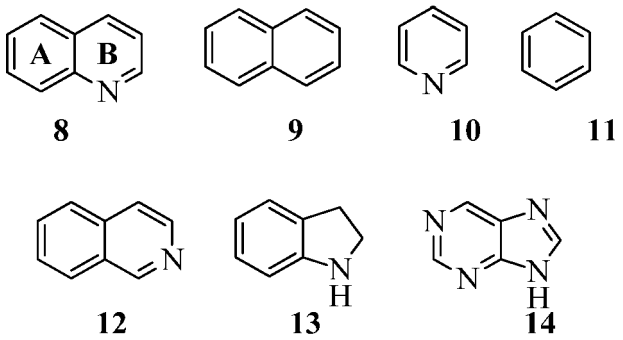

Synthetic quinolines such as the 4-aminoquinolines and 8-aminoquinolines have been particularly useful in malaria treatment. 4-Aminoquinolines were shown to have low effective concentrations against blood stage malaria and it was assumed that they killed parasites by preventing the formation of hemazoin; therefore, they are referred to as blood schizontocides[50, 54] Examples of 4-aminoquinolines are chloroquine **16**, which acts against the trophozoite stage of the malaria parasite, amodiaquine **17**, (the use of which has been limited due to its adverse effects of hepatitis and agranulocytosis), hydroxychloroquine **18**, napthoquine **19** and fluoroamodiaquine **20**.[53, 55] On the other hand, 8-aminoquinlines such as pamaquine **21**, pentaquine **22**, primaquine **23** and quinocide **24**, are active against all gametocyte stages of malaria. Amino alcohols are also active against all gametocyte stages of malaria. Examples of such amino alcohols are lumefantrine **25**, mefloquine **26** and halofantrine **27**.[50, 51, 55] Chloroquine is the most important 4-aminoquinoline. It is accepted that chloroquine works by binding to haematin (ferriprotoporphyrin IX).[37] Chloroquine is a weak base and its neutral form is able to diffuse into the acidic food vacuole where it binds to protons and gets trapped.[55, 56] Malaria-infected red blood cells can accumulate chloroquine in high concentration probably due to pH trapping.[55-59] Accumulation of the toxic chloroquine-haematin complex results in destruction of the parasite's membrane by lipid peroxidation.[60] Other suggested mechanisms of action include:

1. Inhibition of haemozoin generation leading to toxic ferriprotoporphyrin IX build-up within the malaria parasite.[55, 61, 62]
2. Inhibition of the malaria parasite's digestive vacuole protease which is an important enzyme that is responsible for the parasite's feeding mechanism.[55]

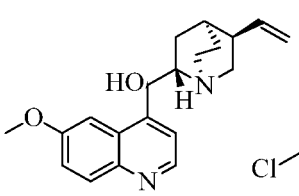

15

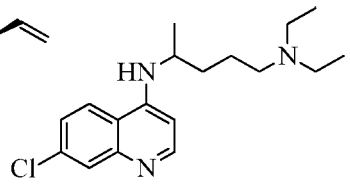

16

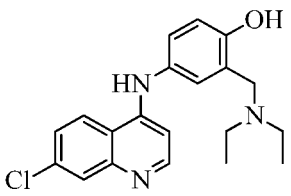

17

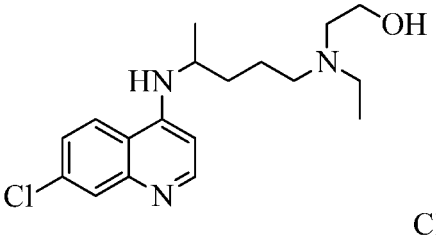

18

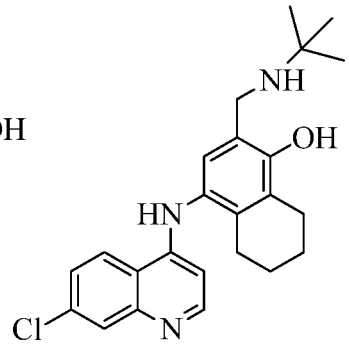

19

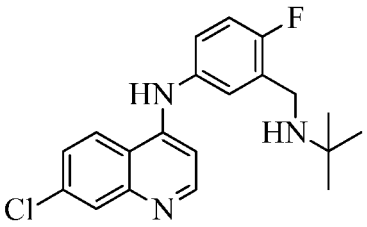

20

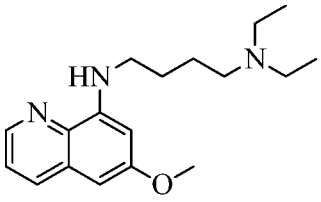

21

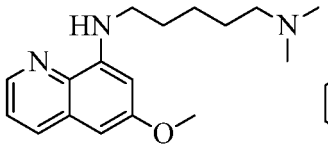

22

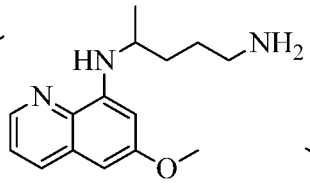

23

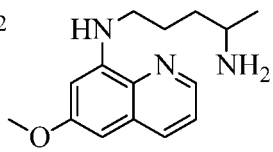

24

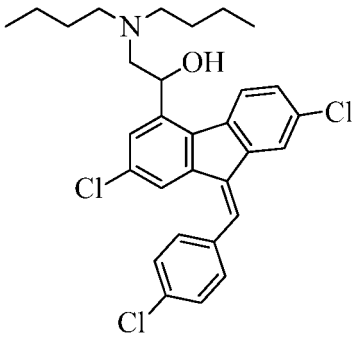

25

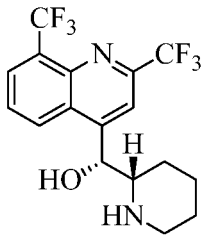

26

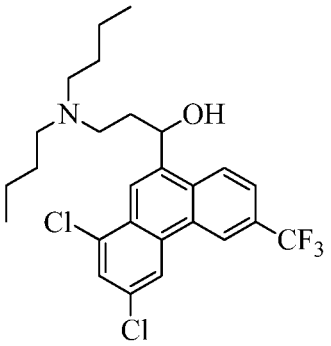

27

It is generally agreed that 4-aminoquinolines work to generate toxic ferriprotoporphyrin IX or quinolone-ferriprotoporphyrin complexes.[55] However, malaria parasites have developed resistance to 4-aminoquinolines. Reported experimental evidence has shown that chloroquine resistant isolates are characterized by diminished accumulation of chloroquine when compared with chloroquine sensitive isolates.[55, 59, 63]

1.3.5.1.1. Synthesis of Quinolines

Several methods have been reported for the preparation of quinolines. A well-established procedure for quinoline synthesis is the Skraup method which involves the reflux of anilines **28**, acrolein **29**, concentrated sulphuric acid, anhydrous glycerol and nitrobenzene (Scheme 1).[64, 65] Another important method is the Combes Synthesis. In Combes method, arylamines **31** are condensed with 1,3-dicarbonyls **32** leading to phenylimines **33**, key intermediates that can be cyclized to yield substituted quinolones **34**. A direct method for preparation of 3-substituted quinolones **37** is called the Friedlander synthesis. This method has to do with the condensation of 2-aminobenzaldehyde **35** with ketones or aldehydes (**36**) using a suitable base.[65]

A more recent procedure for the preparation of 2-aminoquinolines **40** was reported by Zhang and co-workers in 2014.[65] In the procedure, a mixture of 1-phenyl-1*H*-tetrazole **38** and 1,2-diphenylacetylene **39** in the presence of 2.5 mol % of $[CpRhCl_2]_2$, $Cu(OAc)_2 \cdot H_2O$) were refluxed at 130 °C for 6 h. The desired product was isolated in good yield (Scheme 1).[66]

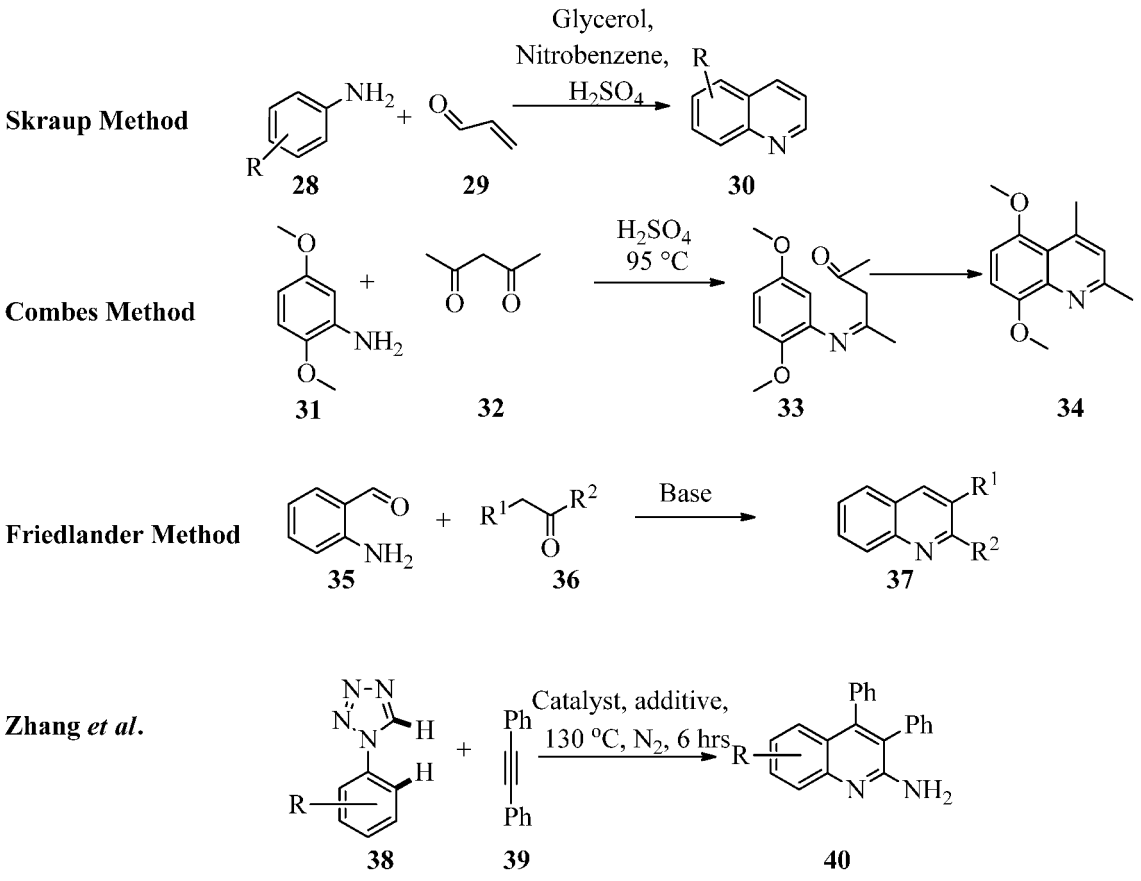

Scheme 1. Synthesis of quinolines.

I.3.5.2. Artemisinins and endoperoxides

As a response to the order given by Chinese government to scientists in China to find a solution to the problem of malaria, the antimalarial activity of organic extracts from the leaves of the plant *Artemisia annua* was determined, and Artemisinin **41** was isolated from the aerial part of the plant in 1972.[55, 67-69] In recognition of her contribution, the 2015 Nobel Prize for Medicine was awarded to Tu Youyou for her work in the discovery of artemisinin, and William C. Campbell and Satoshi Omura for their work on therapy against roundworm.[67] Artemisinin itself is a sesquiterpene lactone with a 1,2,4-trioxane ring. Its therapeutic advantage against *P. falciparum* is diminished because of its low solubility in oil and water.[55] Derivatives of artemisinin (semi-synthetic), such as dihydroartemisinin **42** which was generated by reduction of artemisinin, were then explored. Compound **42** gave way for the preparation of artemether **43**, arteether **44**, artesunate **45** and dihydroartemisinin **46**.[53, 70, 71] These derivatives are more active than artemisinin but the major short-coming of these derivatives is their short plasma half-life.[65] Artemisinin derivatives form the major components in the artemisinin-based combination therapy (ACT) recommended by the World Health Organization.

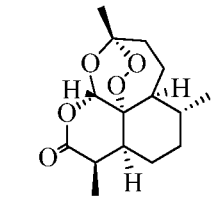

41

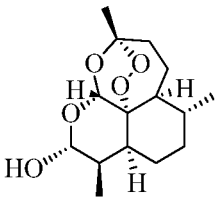

42

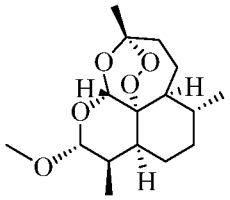

43

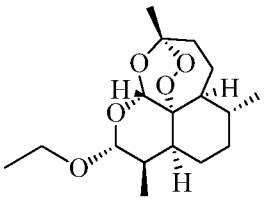

44

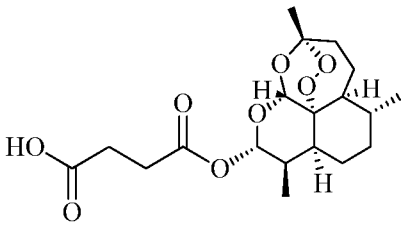

45

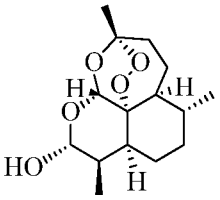

46

The antiparasitic strength of artemisinins is due to the 1,2,4-trioxane pharmacophore.[68, 72] Deoxyartemisinin is not active against the *Plasmodium* parasite; this demonstrated that the

peroxy group is very important for the antiplasmodial activity of trioxanes.[73] On this basis, compounds with endoperoxide cores or simplified artemisinin analogues were designed, prepared and assayed. Examples of such synthetic analogues are compounds **47**[74] 3,3,4,4-tetramethyl-1,2-dioxethane **48,**[75] the adamantyltrioxanes **49, 50 and 51**[75] and the dispiro-1,2,4,5-tetraoxanes **52, 53 and 54**.[75]

Argument was made for artemisinin-mediated oxidative stress as a possible mode of action for endoperoxides. This mechanism involves the interaction of lipid-solubilized heme with artemisinin to generate lipid hydroperoxides by triplet ground-state oxygen capture. This can damage the food vacuole of the malaria parasite.[73] It was also argued that the oxygen atoms of artemisinins interact with reducing ferrous ions to generate primary and / or secondary carbon-centred radicals because of the asymmetric nature of artemisinins. These radicals can alkylate heme and specific proteins or targets and in turn lead to the death of the *Plasmodium* parasite.[76] It should be noted that consensus has not been reached on the endoperoxide target and the mechanism of action.

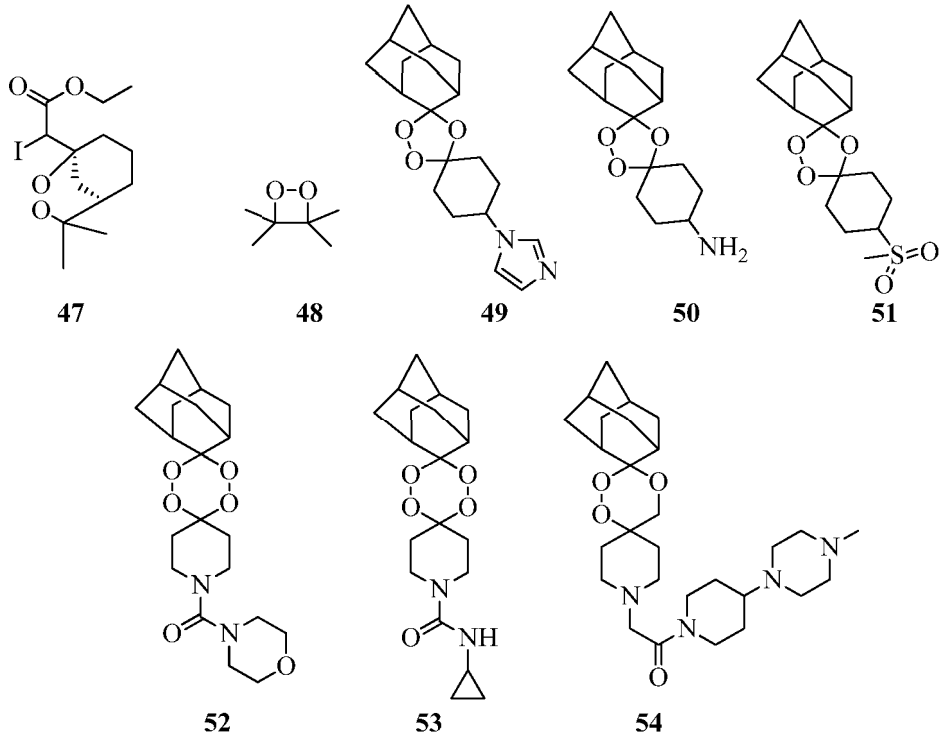

1.3.5.2.1. Synthesis of (+)-Artemisinin

Starting from (+)-isopulegol **55**, Constantino and co-workers[76] reported the synthesis of (+)-artemisinin. Through hydroboration-oxidation of **55**, cyclohexanol **56** was prepared. The *O*-benzylation of the isolated cyclohexanol **56** was accomplished by treatment with sodium hydride and benzyl chloride to give compound **57**. The hydroxyl group of **57** was oxidized to a ketone group to give **58** which was then transformed *via* **59**to give the Robinson annelation product **60**. Hydrogenation of the alkene group in **60** and hydrogenolysis of the benzyloxy unit using palladium-oncarbon catalyst gives **61**. Oxidation of **61** by pyridinium dichromate gave **62**, a keto-acid derivative of **61**. Methylation of the carbonyl group of **62** using methyllithium gave **63a** and **63b** as epimers. In the presence of *p*-toluenesulfonic acid, **63a** and **63b** were converted to dihydroartemisinic acid **65** and a regio-isomer **64**. The isolated artemisinic acid **65** was oxidized in the presence of ultraviolet light to artemisinin **41**.

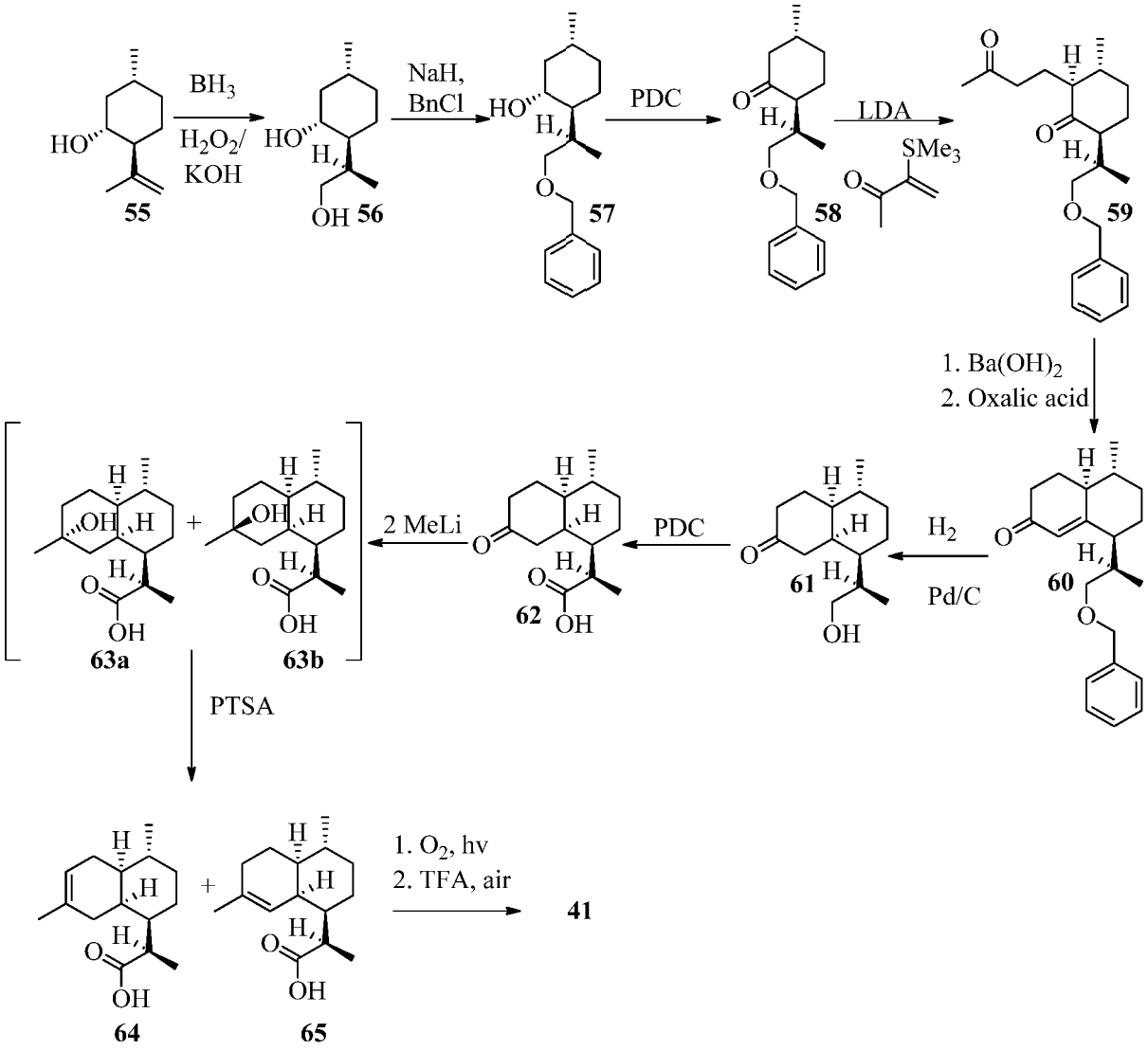

Scheme 2. Synthesis of (+)-artemisinin.

1.3.5.2.2. Synthesis of 1,2,4, 5-Tetraoxane

Achiral tetraoxanes are readily obtained endoperoxide analogues. An example is illustrated in the synthesis of 3-benzyl-7,8,12,13-tetraoxaspiro[5.7]tridecanes **69** (Scheme 3), reported by Ellis and co-workers in 2008.[77] In this example, the 4-benzylcyclohexanones **67** were obtained by deprotection of the ketals **66** using 10% hydrochloric acid in acetone. The crucial, intermediate *gem*-dihydroperoxides **68** were generated using hydrogen peroxide and iodine as catalyst. The *gem*-dihydroperoxides were alkylated using diiodopropane in the presence of silver(I) oxide and the 1,2,4,5-tetraoxanes were isolated in good yields (Scheme 3).[77]

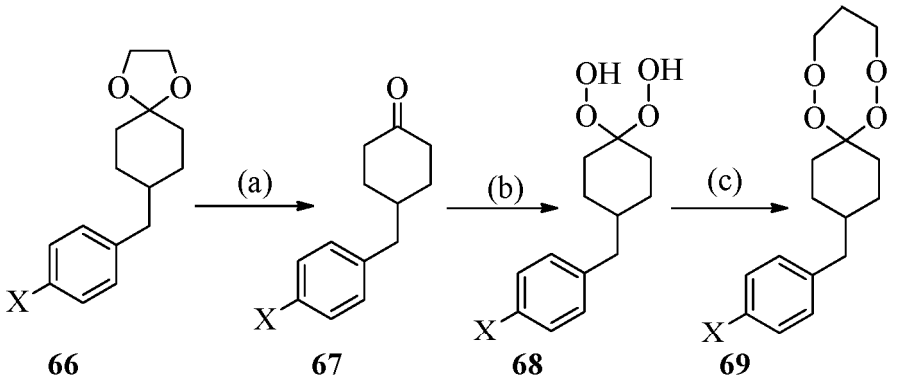

(a) 10% $HCl_{(aq)}$, Acetone; (b) H_2O_2, I_2, Acetonitrile; (c) 1,3-diiodopropane.

Scheme 3. Synthesis of 7, 8, 12, 13-tetraoxane.

1.3.5.3. Antifolates

Antifolates act to deprive *Plasmodium* parasites of the essential folate cofactors. They do this by inhibiting dihydropteroate synthase (DHPS), which is essential in the biosynthesis of folates, and dihydrofolate reductase (DHFR) which is a key enzyme in biosynthesis of tetrahydrofolate. These enzymes exist in protozoans and are important antimalarial drug targets in that DHPS is absent in humans while DHFR is also absent in humans and is quite different from human enzymes. [78-81]

Notable examples of antifolates are dihydrofolic acid **70**, pyrimethamine **71**, and an inhibitor of dihydrofolate reductase enzyme, proguanil **72** (the *in vivo* active metabolite of which is cycloguanil **73**), lometrexol **74** and sulphadoxine **75** which specifically inhibit dihydropteroate synthase.[79, 80]

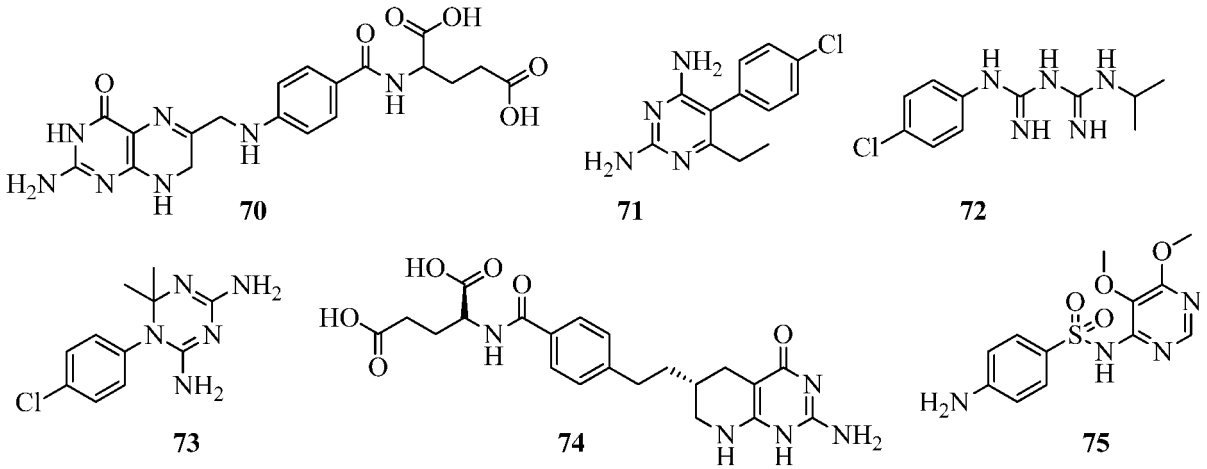

1.3.5.4. Antibiotics

Antibiotics are molecules that have been established to be active against bacterial infections.[82] Antibiotics work as antimalarial drugs in that they can inhibit ribosome and DNA gyrase.[83] Good examples of antibiotics that are used in treating malaria infections are azithromycin **76** which is a synthetic molecule made from the natural product erythromycin **77**. Clindamycin **78** is another antibiotic that is effective against *P. falciparum*; it is a synthetic derivative of lincomycin **79** which is a natural product. Other active antibiotics used against malaria infections are doxycycline **80** and the tetracycline **81**.[84-87]

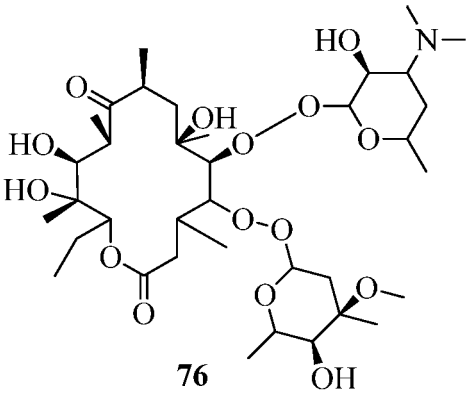

76

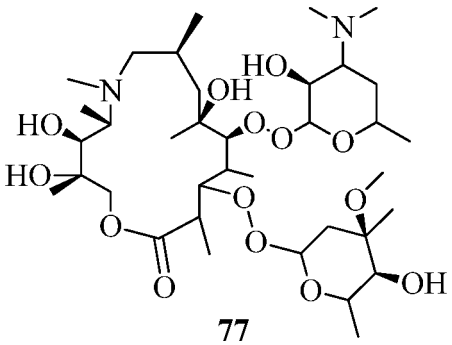

77

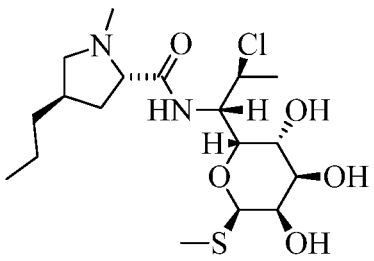

78

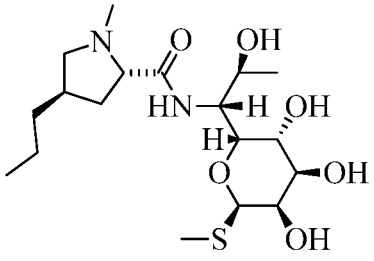

79

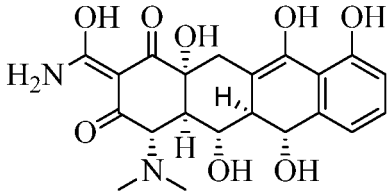

80

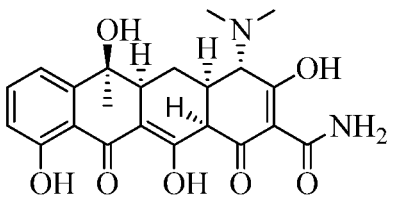

81

1.3.5.5. 1-Deoxy-D-xylulose-5-phosphate reductoisomerase (DXR) Inhibitors

1-Deoxy-D-xylulose-5-phosphate reductoisomerase (DXR) is an essential enzyme in the Rohman pathway for the biosynthesis of isoprene. 1-Deoxy-D-xylulose-5-phosphate (DXP) and 2-methyl-D-erythritol-4-phosphate (MEP) are the vital precursors for the biosynthesis of isoprenoids and terpenoids. Using Mg^{2+} or Mn^{2+} and nicotinamide adenine dinucleotide phosphate (NADP) as cofactors, DXP undergoes reductive isomerization to MEP and DXR is the catalyst for this process [88-91] Isoprenoids are essential to several core bacterial cellular functions.[89] The non-mevalonate pathway (or DOXP, Rohman or 2-C-methyl-D-erythriol-4-phosphate pathway) is essential in protozoan malaria parasites (*P. falciparum).*[92, 93] The basic isoprenoid building blocks, isopentenyl diphosphate and dimethylallyl diphosphate (IPP and DMAPP) are generated in cells by one of two distinct biosynthetic routes.[90, 93] The DXR enzyme is a validated drug target in the treatment of malaria and has the significant advantage of being absent in humans and animals in which the mevalonate pathway is used for the biosynthesis of isoprenoid building blocks.[93-96]

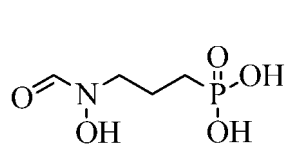

82

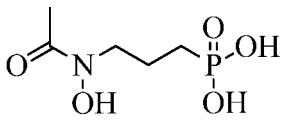

83

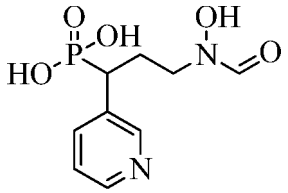

84

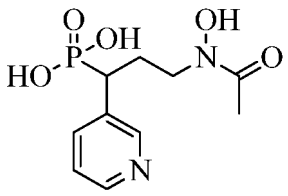

85

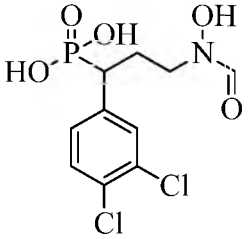

86

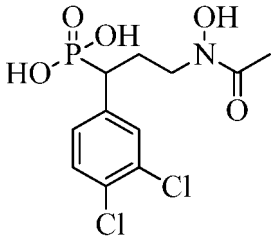

87

Examples of DXR inhibitors are the natural product, fosmidomycin **82**, and FR900098 **83**. [86, 88, 97] Other notable inhibitors are the meta-substituted pyridyl fosmidomycin derivatives **84** and **85** [89] and the dichloro-substituted fosmidomycin derivatives **86** and **87**.[97]

1.3.5.5.1. Synthesis of DXR Inhibitors

The Michael-Arbuzov reaction is a very popular way of preparing DXR inhibitors. It is a bimolecular nucleophilic substitution reaction of trialkyphosphites **88** with an alkyl halide **89** at high temperature to generate an intermediate phosphonium cation **90** which reacts in a second bimolecular nucleophilic substitution with the halide anion displaced in the first step (Scheme 4). The products of this reaction are dialkyl phosphonic esters **91** and an alkyl halide **92**.[98, 99]

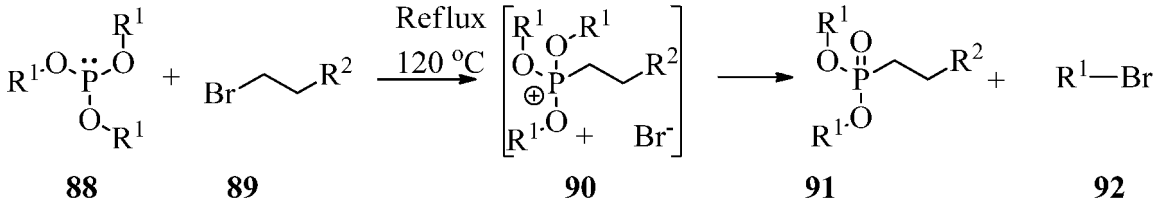

88 **89** **90** **91** **92**

Scheme 4. The Michael-Arbuzov reaction.

1.3.5.6. *Plasmodium falciparum* Calcium Dependent Protein Kinase 1 (*Pf*CDPK1) Inhibitors

Plasmodium falciparum Calcium Dependent Protein Kinase 1 (*Pf*CDPK 1) was reported to have been isolated from *P. falciparum* in 1993 by Zhao *et al.*[100, 101] *Pf*CDPK1 is located in the periphery of *P. falciparum* and it is a key enzyme for signalling roles in motility, secretion and maturation at the blood stage.[101-106] It is one of the seven calcium dependent protein kinases (CDPKs) present in *P. falciparum*.[102]

*Pf*CDPK1 has been proven to play a vital role in the life cycle of apicomplexan parasites as well as in the life cycle of *P. falciparum*. It is the only well-characterized protein kinase out of the seven CDPKs.[102] Structurally, it possesses an *N*-terminal kinase domain and a *C*-terminal calmodulin-like domain with calcium-binding EF hands.[100, 106] CDPKs are present in higher plants, algae and alveolates. Apicomplexa is a family member of alveolates and this family includes the parasitic protozoa under which *P. falciparum* can be found. CDPKs are absent in the human host, and the enzyme was therefore proposed as a drug target.[100-103]

*Pf*CDPK1 inhibitors have been reported to include imidazolopyridazines **93**, pyrazolopyrimidines **94**, azabenzimidazoles **95**, isoxazole amides **96** and pyrazinones **97**.[103]

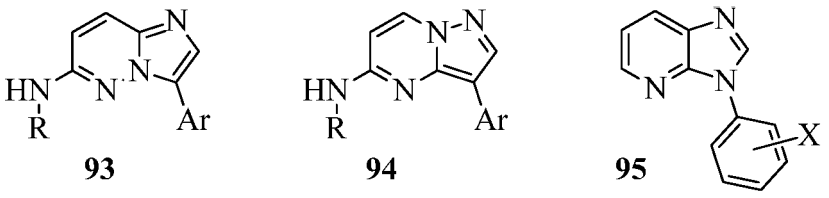

93 **94** **95**

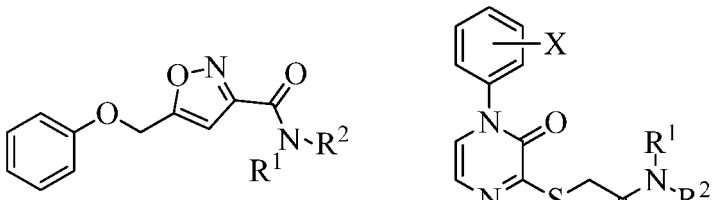

96 **97**

1.3.5.6.1. Synthesis of Azabenzimidazoles as *Pf*CDPK1 Inhibitors

Any method that is suitable for the synthesis of benzimidazole **98** from phenylendiamine **100** appears to be suitable for the preparation of azabenzimidazole **99** from diaminopyridine **101**.

98 **99**

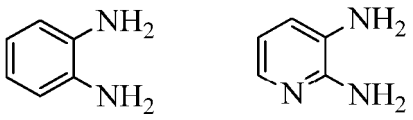

100 **101**

A few representatives of synthetic routes to azabenzimidazoles are presented in Scheme 5. The condensation of triethyl orthoformate **102** with diaminopyridines using acetic anhydride as solvent at about 90°C generates azabenzimidazoles.[107] Reaction of diaminopyridines with aldehydes at high temperature using nitrobenzene as solvent also gives azabenzimidazoles in high yields.[108] In the presence of ceric ammonium nitrate (CAN) catalyst or boric acid, benzimidazoles or azabenzimidazoles can be prepared at moderate reaction temperature.[109, 110] Carboxylic acids can also be used as the source of the imidazole carbon in the synthesis of benzimidazoles **98** and azabenzimidazoles **99**.[111]

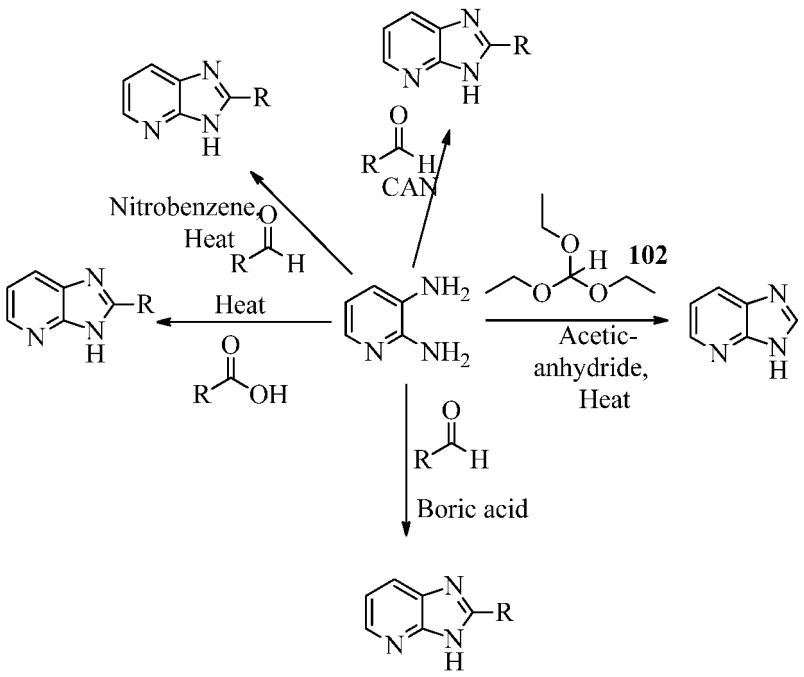

Scheme 5. Synthesis of azabenzimidazoles.

1.4. RATIONALE BEHIND THE PRESENT STUDY

An extensive literature review on bioactive organic molecules revealed that many organic compounds with biological activities are characterized by the possession of an imine (C=N) functional group – either within a ring (heterocycles) or in a straight chain structure. The following systems are notable representatives of such organic compounds.

1. Pyrazolo[1,5-*a*] pyrimidine derivatives, an example of which is compound **103** which was developed and reported to be an inhibitor of pim-1 (Provirus insertion site of Moloney murine leukaemia virus).[112]
2. Benzimidazoles: Pyrido[1,2-*a*]benzimidazoles **104** exemplifies this class of compounds. It was reported that such compounds are active against drug resistant K1 strain of *P. falciparum*.[113]
3. Azabenzimidazoles: Shahul *et al.* identified amino imidazoles as active antimalarial compounds and this led to their synthesis and antimalarial studies of the amino azabenzimidazole **105**.[114] Other azabenzimidazoles which are active against specific enzymes are the 6-arylazabenimidazoles which were demonstrated to inhibit TANK-binding kinase 1(TBK1) and the nuclear facto κb kinase subunit epsilon (Ikk-ε).[115]

4. Isoquinolines: Rathelot *et al.* reported the preparation and evaluation of the antimalarial properties of 5-nitroisoquinolines; compound **106** {(*E*)-*N*-[(5-nitroisoquinolin-1-yl) methylene]-1-[(2-(trifluoromethyl)phenyl]methanamine} is a derivative of such nitroisoquinolines.[116]
5. Imidazolopyridines: Compounds **107** and **108** are examples of well-established imidazolopyridazines which are active against malaria, specifically, as *Pf*CDPK1 inhibitors.[103]
6. Ancistrocladidine **109** (an alkaloid) is a natural product that contains an imino group. It was isolated from *Ancistrocladus tanzaniensis*. This alkaloid shows activity against the K1 strain and the 3D7 strain of *P. falciparum*.[117]
7. Quinolin-4-(1*H*)-imines **110** were reported to be active against liver stage *P. falciparum* infection at nanomolar concentrations.[118]

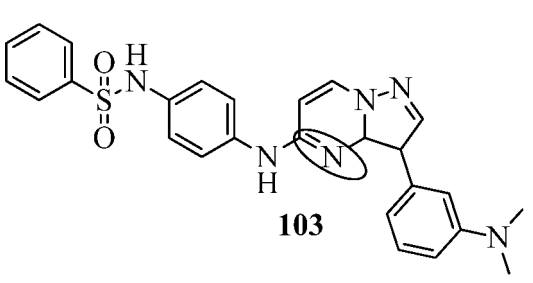

103

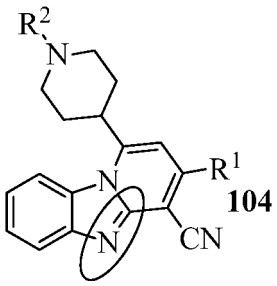

104

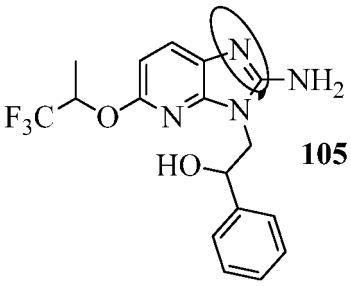

105

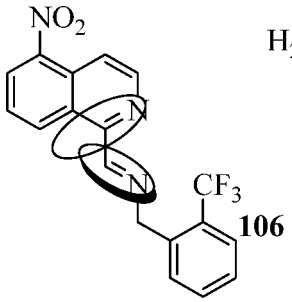

106

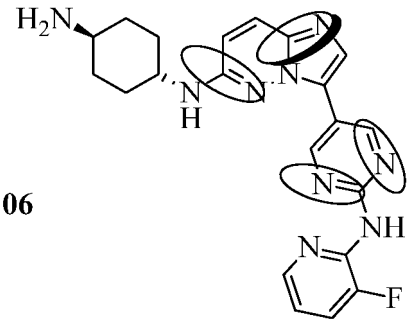

107

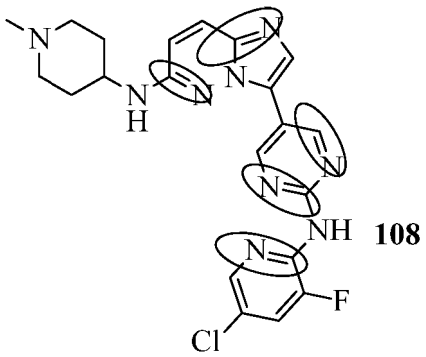

108

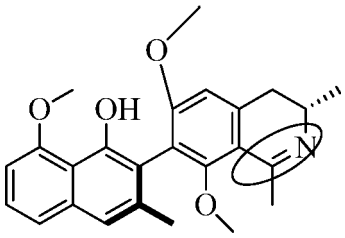

109

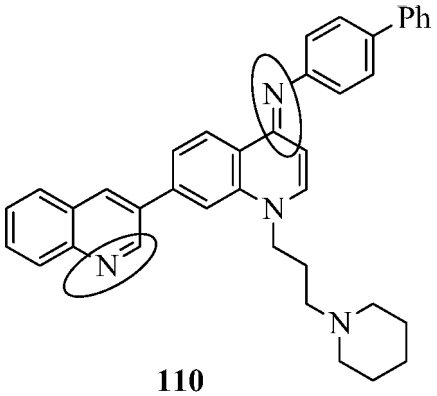

110

Therefore, this research is aimed at designing, synthesising and evaluating novel, stable heterocyclic and acyclic molecules, which possess the imine functional group (C=N), as potential lead scaffolds in the development of anti-*P. falciparum* and anti-*T. brucei* compounds and the identification of possible lead compounds for the treatment of co-infection of both parasites. More specifically, the project has involved the following objectives:

1. Exploring the development of potential dual target scaffolds.
2. Screening the synthesized compounds for their parasite-inhibition potential against *T. brucei* and *P. falciparum* as well as exploring their cytotoxicity on human cell lines.
3. Spectroscopic (NMR, IR, and ESI HPLC-MS) analysis of synthesized molecules and detailed DNMR studies to elucidate rotational isomerism effects.

2. RESULTS AND DISCUSSION

This discussion will focus on the synthesis of imine-containing heterocyclic and acyclic organic molecules, investigation of their biological activities against *P. falciparum* and *T. brucei*.

The following areas will be covered.

2.1. Synthesis and antiprotozoal activities of 2,3-diaminopyridine derivatives: The synthesises under this heading are divided into:

2.1.1. Preparation of 2,3-diamino-5-bromopyridine

2.1.2. Synthesis of 5-bromo-7-azabenzimidazoles and its 1-alkylated derivatives.

2.1.3. Synthesis of substituted 5-bromo-1-[(*N*-carbamoyl)methyl]-7-azabenzimidazoles.

2.1.4. Determination of rotational energy of activation by dynamic NMR study for 1-{[*N*-(3-chlorobenzyl)carbamoyl]methyl}-5-bromo-7-azabenzimidazole and 1-{[*N*-(2-furfuryl)carbamoyl]methyl}-5-bromo-7-azabenzimidazole.

2.1.5. Synthesis of *N,N'*-bis-[2-(5-bromo-7-azabenzimidazol-1-yl)-2-oxoethyl]ethylene and -1,2-cyclohexyldiamines.

2.1.6. Biological activity of substituted 5-bromo-1-[(*N*-carbamoyl)methyl]-7-azabenzimidazoles, *N,N'*-bis[2-(5-bromo-7-azabenzimidazol-1-yl)-2-oxoethyl]ethylene and -1,2-cyclohexyldiamines.

2.2. Preparation of 2-phenyl-7-azabenzimidazoles and their anti-protozoan activity.

2.3. Regioselective formylation of 2,3-diamino-5-bromopyridine to generate 2-amino-5-bromo-7-(benzylimino)pyridines and their anti-protozoan activity.

2.4. Synthesis and anti-protozoan properties of *N*-(phenyl)-2-hydroxybenzylimines

2.5. Synthesis and anti-protozoan evaluation of *N*-(3,4-difluorobenzyl)-2-hydroxybenzylimines.

2.6. Synthesis and anti-protozoan activities of (±)-*trans*-1,2-bis[5-chloro-2-hydroxybenzylimino]cyclohexanes.

2.1. SYNTHESIS OF 2,3-DIAMINOPYRIDINE DERIVATIVES

Scheme 6 provides a summary of the routes to the preparation of 2,3-diamino-5-bromopyridine derivatives. 2,3-Diamino-5-bromopyridine **115** is shown as a key starting material for the different reaction routs as shown in this scheme.

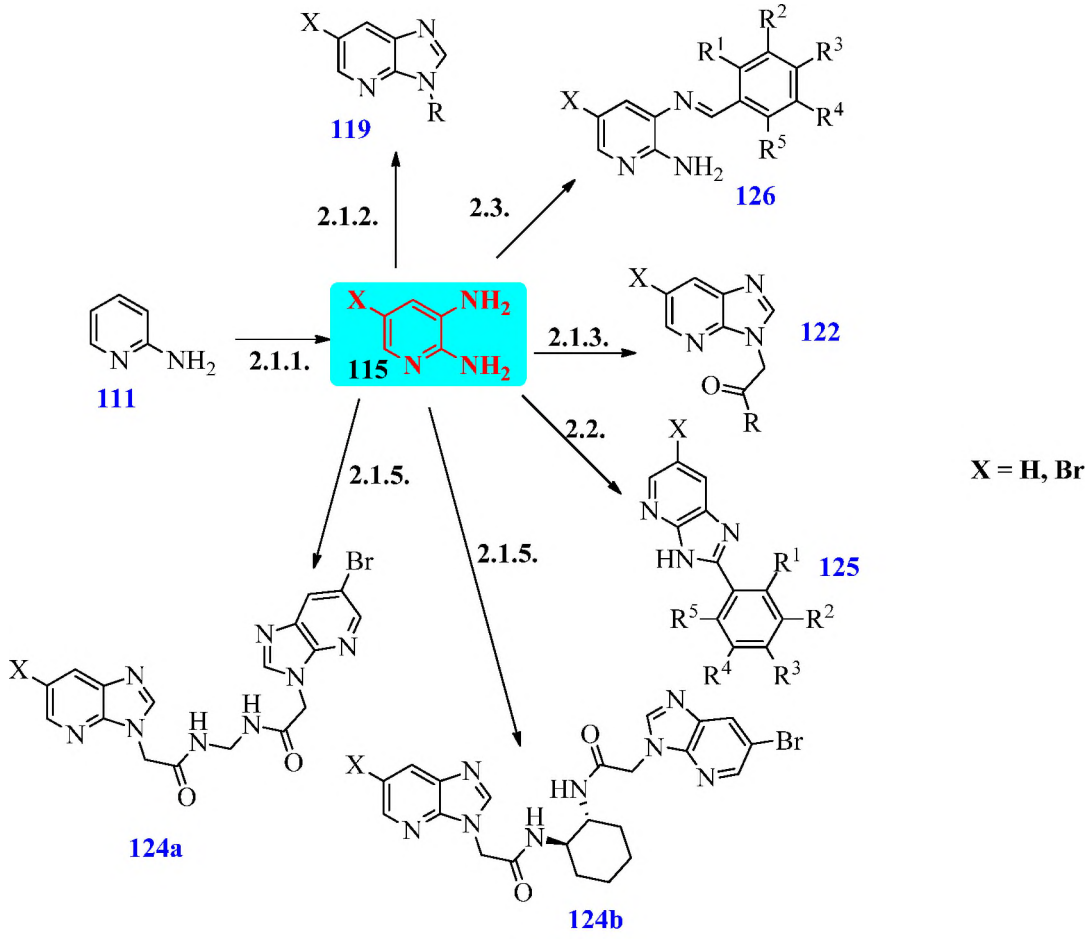

Scheme 6. Strategic reaction plan for 2,3-diaminopyridine derivatives.

2.1.1. Preparation of 2,3-Diamino-5-bromopyridine

The method for the synthesis of 2,3-diaminopyridine **101** reported by Fox and Threlfall [119] was adopted for the preparation of 2,3-diamino-5-bromopyridine **115**. It was a 3-step process that involved bromination, nitration and reduction (Scheme 7). The first step involved electrophilic aromatic substitution of pyridine (bromination). This was a challenging step

because pyridines are not reactive towards electrophiles. In attempts to perform an electrophilic substitution reaction on pyridines, the interaction of an electrophile and the basic pyridine nitrogen atom can easily lead to the deactivation of the ring. Other factors that contribute to the inactive nature of pyridines towards electrophilic substitution are delocalisation of π–electron density towards the electronegative nitrogen leaving the ring atoms electron-deficient, and the electron-withdrawing inductive effect of the nitrogen- particularly on the adjacent α-carbons. The net effect is that the carbon atoms accommodate partial positive charges and the nitrogen atom a partial negative charge.[120, 121]

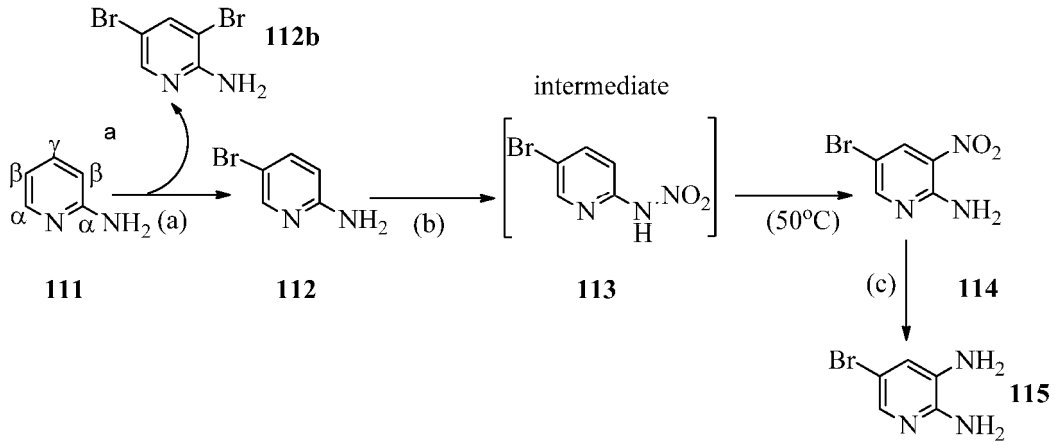

Reagents and conditions: (a) Br_2, Acetic acid (b) HNO_3, H_2SO_4 (c) Fe, HCl, H_2O, EtOH

Scheme 7. Synthesis of 2,3-diamino-5-bromopyridine.

Bromination of 2-aminopyridine **111** favours the positions 3 and 5 (β-positions of pyridines are favoured towards electrophilic attacks) and 2-amino-5-bromopyridine **112** may be obtained in 76% yield.[120, 121] A very small amount of 2-amino-3,5-dibromopyridine **112b** was isolated as by-product (Scheme 7).

The second step involved nitration of **112** to form 2-nitroamino-5-bromopyridine **113** using nitric acid in sulphuric acid at a temperature between 0 – 5 °C, which then rearranged to 2-amino-3-nitro-5-bromopyridine **114**, a yellow solid at about 50 °C. This pathway was published in the PhD theses of Viron and Kasman in 1952 and 1955, respectively.[122, 123] The last step was a reduction of **114** to generate the required 2,3-diamino-5-bromopyridine **115**. Reduced iron in the presence of a catalytic amount of hydrochloric acid was very effective for this step and a yield of 78% was obtained in this work.

2.1.2. Synthesis of 1-Substituted-5-bromo-7-azabenzimidazoles.

In the synthesis of 5-bromo-7-azabenzimidaozole **116** (Scheme 8), triethyl orthoformate **102** was used as a source of the imidazole carbon. The reaction was carried out in acetic anhydride as solvent at a temperature of 90 °C for four hours.[107] The desired product was isolated as a brown solid.

Mechanistically, the nucleophilic 3-amino centre of β-amino of the 2,3-diamino-5-bromopyridine **115** (being more basic than the 2-amino group),[123, 124, 125] attacks the carbon centre of the triethyl orthoformate first and one molecule of ethanol is eliminated to give 5-bromo-(diethoxymethyl)pyridine-2,3-diamine **117**.The same process occurs at the 2-amino group of **117** and a further molecule of ethanol is eliminated to form 6-bromo-2-ethoxy-2,3-dihydro-7-azabenzimidazole **118**. This can eliminate the last molecule of ethanol to generate 5-bromo-7-azabenzimidazole **116**.

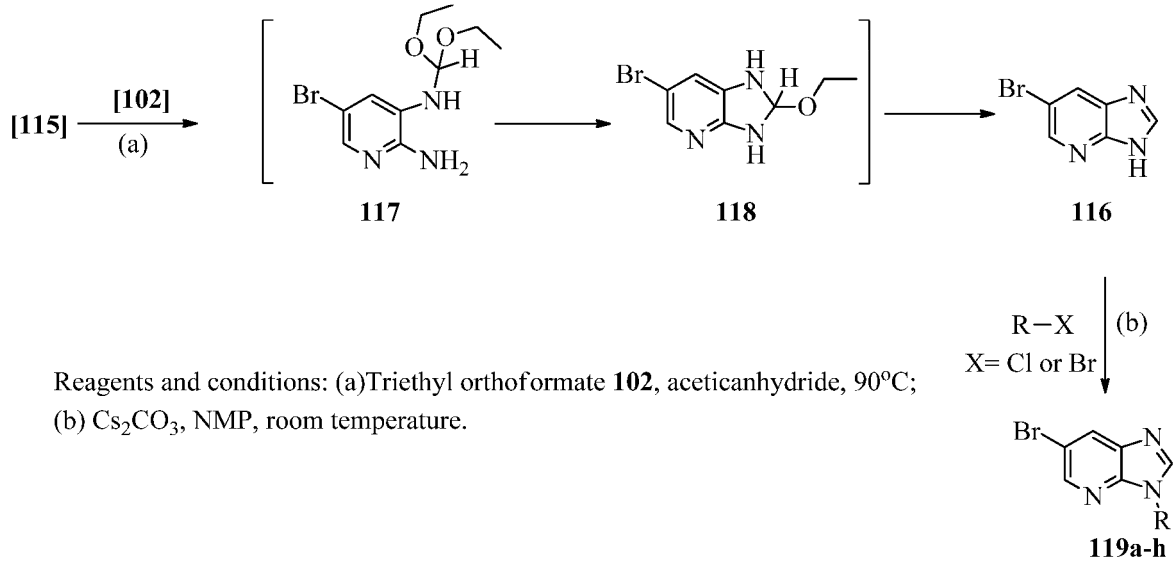

Reagents and conditions: (a)Triethyl orthoformate **102**, aceticanhydride, 90°C; (b) Cs_2CO_3, NMP, room temperature.

Scheme 8. Synthesis of 5-bromo-7-azabenzimidazole and its *N*-alkylated derivatives.

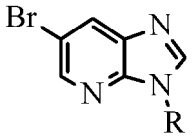

119a-h

Table 1. Synthesis of Substituted-5-bromo-7-azabenzimidazoles.

C 119	R	Yield (%)	Time (min.)
a	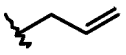	96	60
b	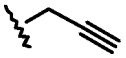	54	60
c	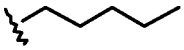	70	60
d	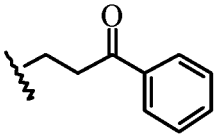	47	60
e	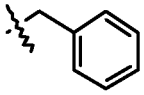	78	30
f	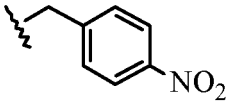	71	30
g	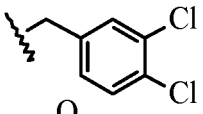	77	30
h	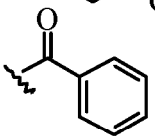	81	20

Proton nuclear magnetic resonance (^{1}H NMR) spectroscopy confirmed the successful preparation of the desired product (Figure 4). The amino proton of the imidazole ring resonates as a broad signal at 13.12 ppm. As a result of the *meta*-arrangement of protons 4-H and 6-H, there is a small coupling observed between these protons resulting in a coupling constant of 1.8 Hz. 4-H is represented by the doublet resonating at 8.29 ppm, while the doublet at 8.43 ppm corresponds to 6-H. Proton 2-H corresponds to the singlet resonating at 8.49 ppm. The high performance liquid chromatography-mass spectrometric (HPLC-MS) analysis for 5-bromo-7-azabenzimidazole **116** ($C_6H_4BrN_3$ 196.9589) indicated the presence of $[M]^+$ 196.9583 peak.

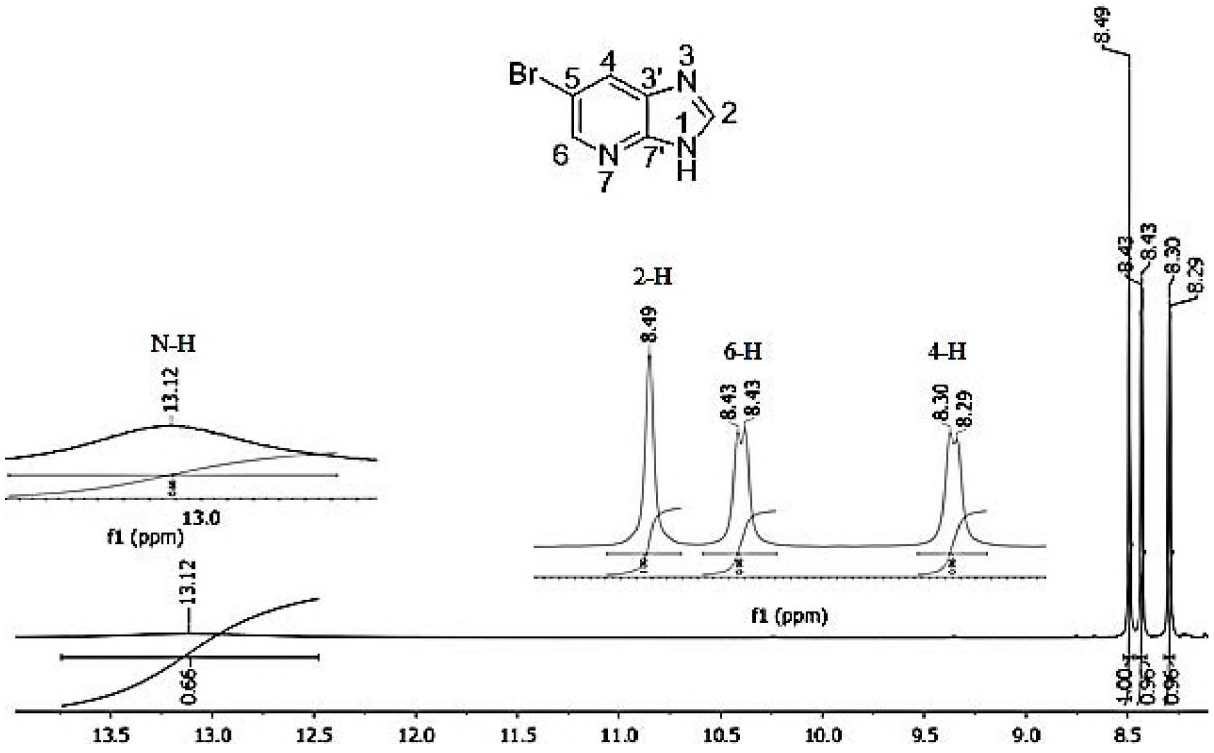

Figure 2. 400 MHz ^{1}H NMR spectrum of **116** in DMSO-d_6.

Step two of Scheme 8 is a nucleophilic substitution reaction which required the use of caesium carbonate to abstract the NH proton from azabenzimidazole **116** to generate a nucleophilic centre. Simultaneous charging of the reaction flask with the substrates (5-bromo-7-azabenzimidazole **116**), the electrophile (alkyl halide) and the base led to a long reaction time and poor yield. These problems were overcome by using a step-wise process of abstracting the proton from the substrate first with one equivalent of caesium carbonate followed by the introduction of the electrophile. The reaction proceeded to completion at room temperature within 20-60 minutes and the desired derivatives **119a-h** were isolated in good yields. *N*-methyl pyrrolidone (NMP) was the solvent of choice for this reaction because it dissolved the 5-bromo-7-azabenzimidazole **116** effectively and could be extracted completely into water during the work-up process.

1-Allyl-5-bromo-7-azabenzimidazole **119a** as a representative derivative of this series was fully characterized using MS, ^{1}H, ^{13}C, homonuclear correlation spectroscopy (COSY), distortionless enhancement polarization transfer spectroscopy using a 135 degree decoupler pulse (DEPT-135) and heteronuclear single quantum coherence (HSQC) NMR experiments

(Figures 4 to 9). The HPLC-MS analysis for 1-ally-5-bromo-7-azabenzimidazole **119a** ($C_9H_8BrN_3$ 236.9902) indicated the presence of $[M]^+$ 237.2171 peak.

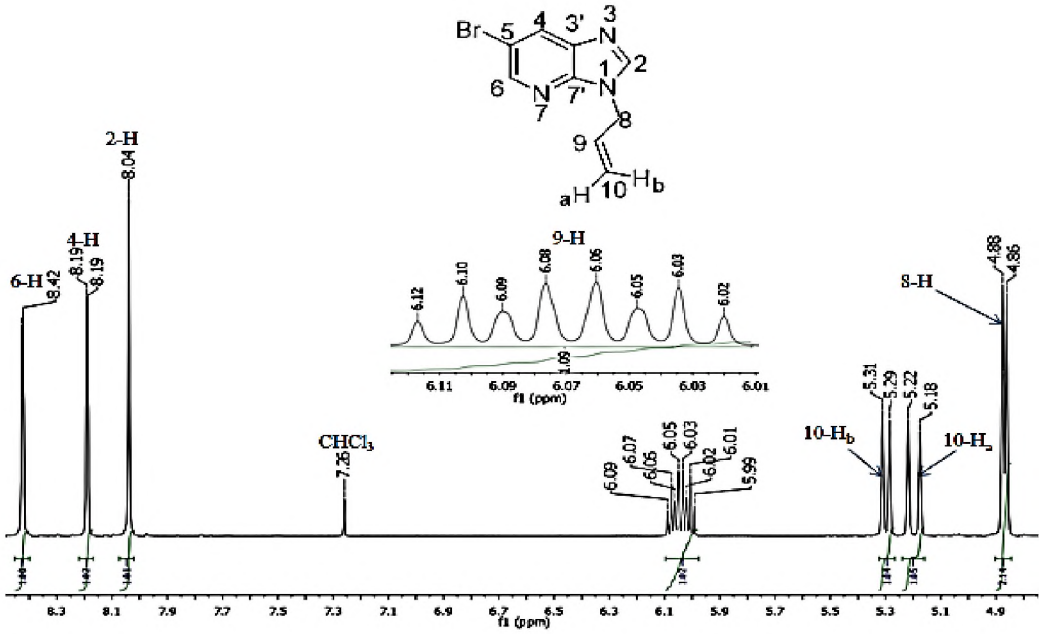

Figure 4. 400 MHz ^{1}H NMR spectrum of **119a** in $CDCl_3$.

From Figure 4, it was seen that the *meta*-arrangement of protons 4-H and 6-H again resulted in a small coupling between the two protons with a coupling constant of 2 Hz. The ^{1}H NMR signal at 8.19 ppm corresponds to 4-H while the signal which corresponds to 6-H appears further downfield (8.42 ppm) because it is alpha to the pyridine nitrogen atom of the azabenzimidazole core. The singlet at 8.04 ppm represents 2-H. The 8-methylene proton signal at 4.87 ppm is a doublet as expected because it couples to the vinylic methine proton 9-H and their coupling constant is 5.7 Hz. The vinylic proton 10-H_a (*cis* to the vinylic methine proton 9-H) and the 10-H_b proton (*trans* to the vinylic methine proton 9-H) couple to 9-H as revealed by the COSY experiment (Figure 5). 10-H_a signal at 5.20 ppm reveals a coupling constant of 17.1 Hz with the 9-H proton, while the 10-H_b resonates at 5.30 ppm with coupling constant of 10.2 Hz (because J_{trans} is greater than J_{cis}). 9-H which couples to protons 8-H, germinal protons 10-H_a and 10-H_b, corresponds to the signal at 6.04 ppm (doublet of doublet of doublets) with coupling constants of 5.7 Hz due to coupling to 8-H, 17.1 Hz (J_{trans}) due to its coupling to 10-H_a and 10.2 Hz (J_{cis}) resulting from its coupling to10-H_b (Figures 4 and 5).

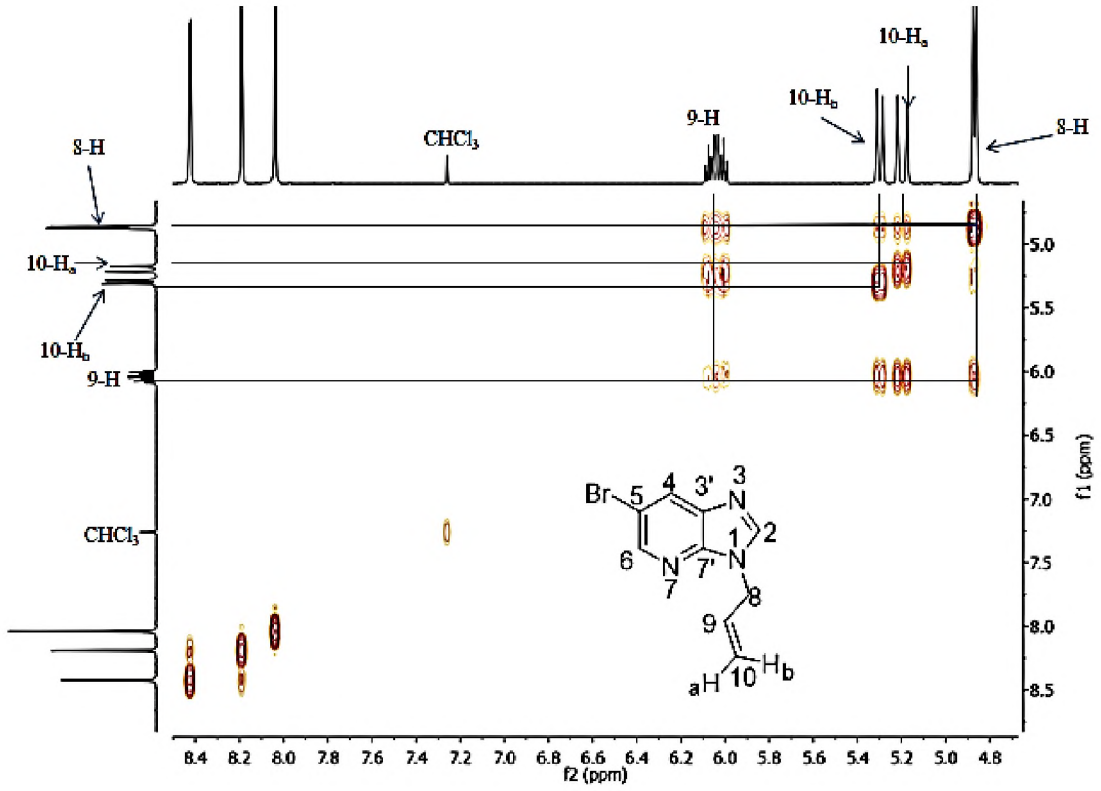

Figure 5. 400 MHz COSY NMR spectrum of **119a** in $CDCl_3$.

The DEPT-135 spectrum (Figure 6) clearly shows two negative signals with chemical shifts of 45.8 and 119.1 ppm. Using the HSQC spectrum with the DEPT-135 spectrum, it was confirmed that the carbon signals at 45.9 and 119.2 ppm, on the ^{13}C spectrum (Figures 6 and 8) correspond to C-8 and C-10, respectively.

The HSQC spectrum (Figure 9) was used in assigning the carbon-13 signals that correspond to the assigned proton signals. The four positive signals (C-2, C-4, C-6 and C-9) in the DEPT-135 spectrum were assigned with the aid of an HSQC experiment (Figure 9). It was observed from Figure 9 that, C-6 resonated at 145.3 ppm while C-4 at 130. 5 ppm (C-6 is shifted downfield because it is alpha to the 7-aza unit); C-2 was at 145.1 ppm. The ^{13}C signal for the vinylic methine carbon C-9 was observed at 131.8 ppm. Other, unassigned carbon signals in the ^{13}C spectrum represent the quaternary carbon atoms (C-3', C-5 and C-7').

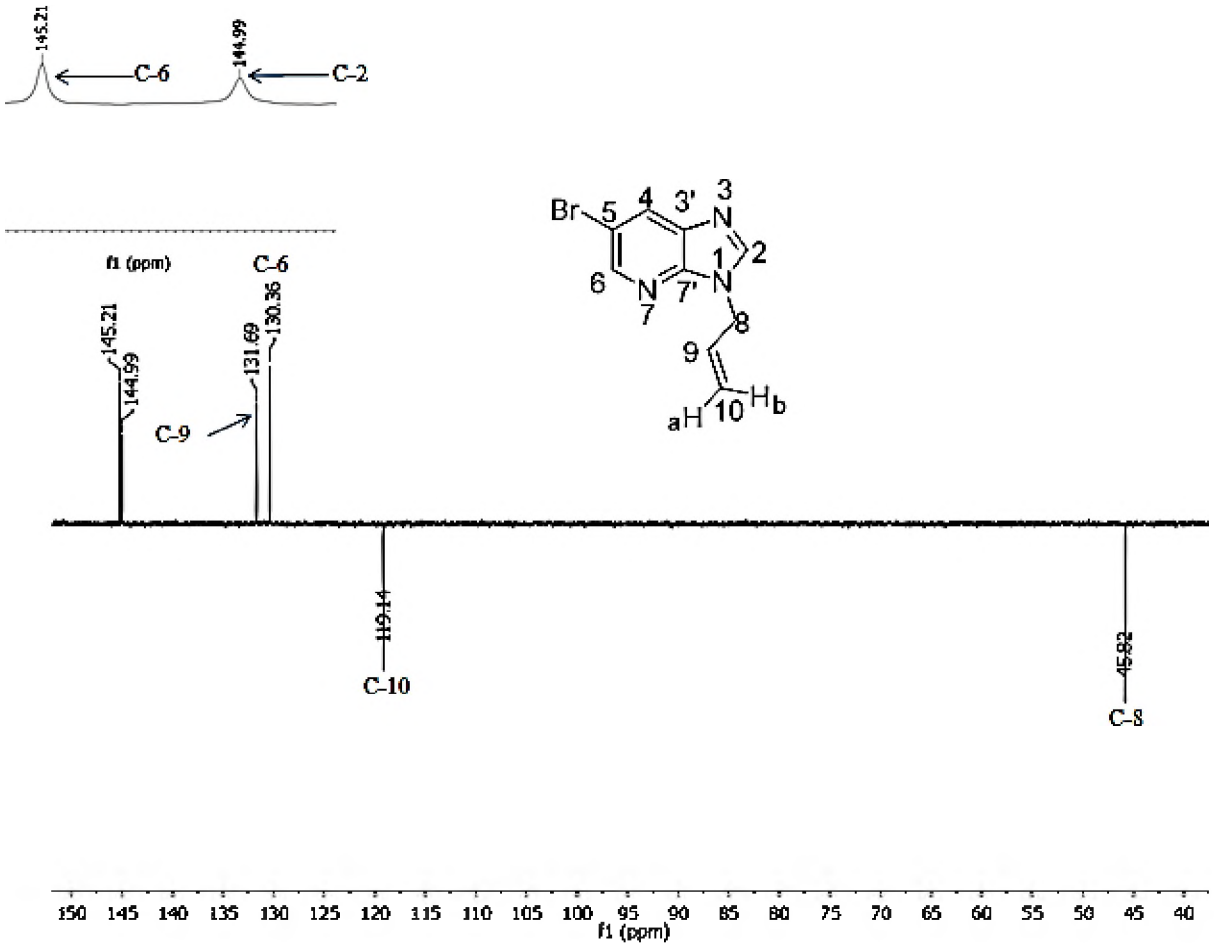

Figure 6. 100 MHz DEPT-135 NMR spectrum of **119a** in $CDCl_3$.

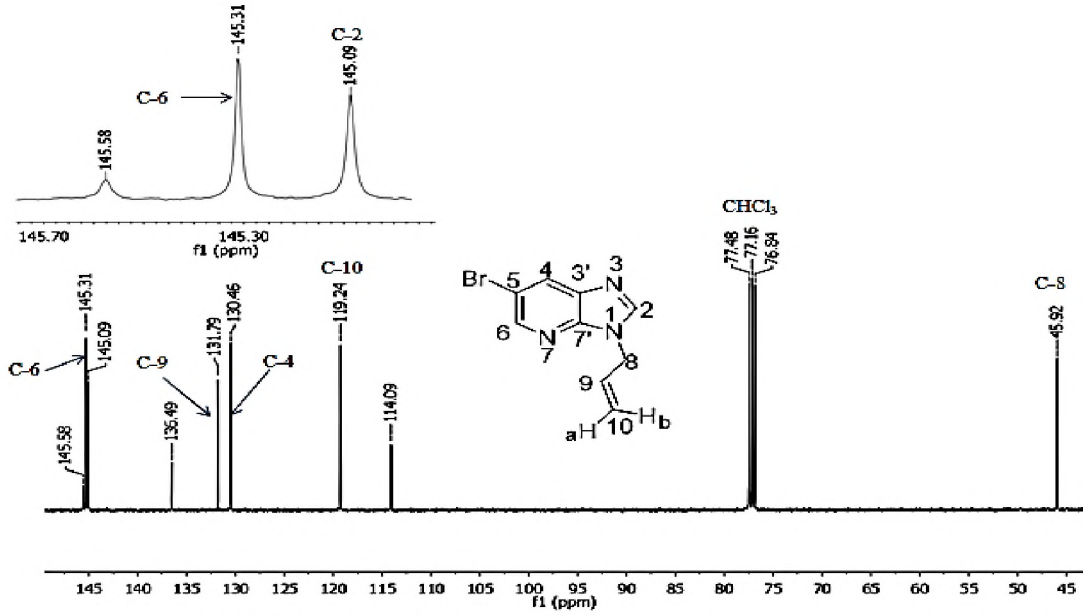

Figure 7. 100 MHz ^{13}C NMR spectrum of **119a** in $CDCl_3$.

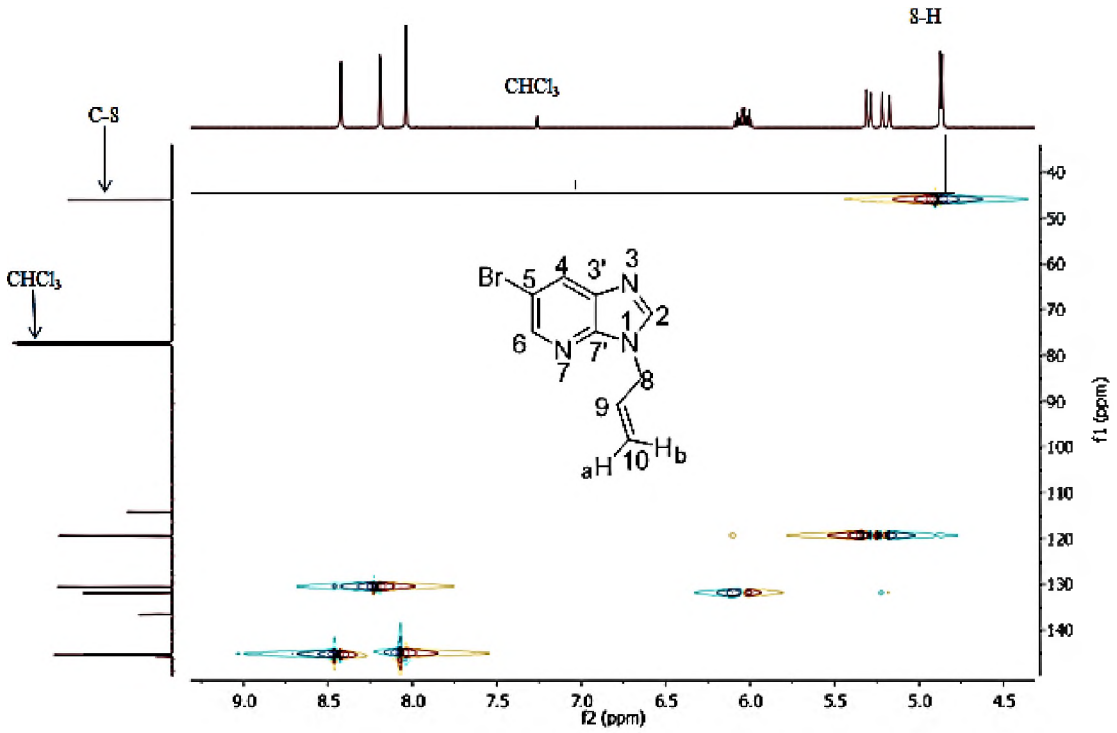

Figure 8. HSQC spectrum of **119a** in $CDCl_3$.

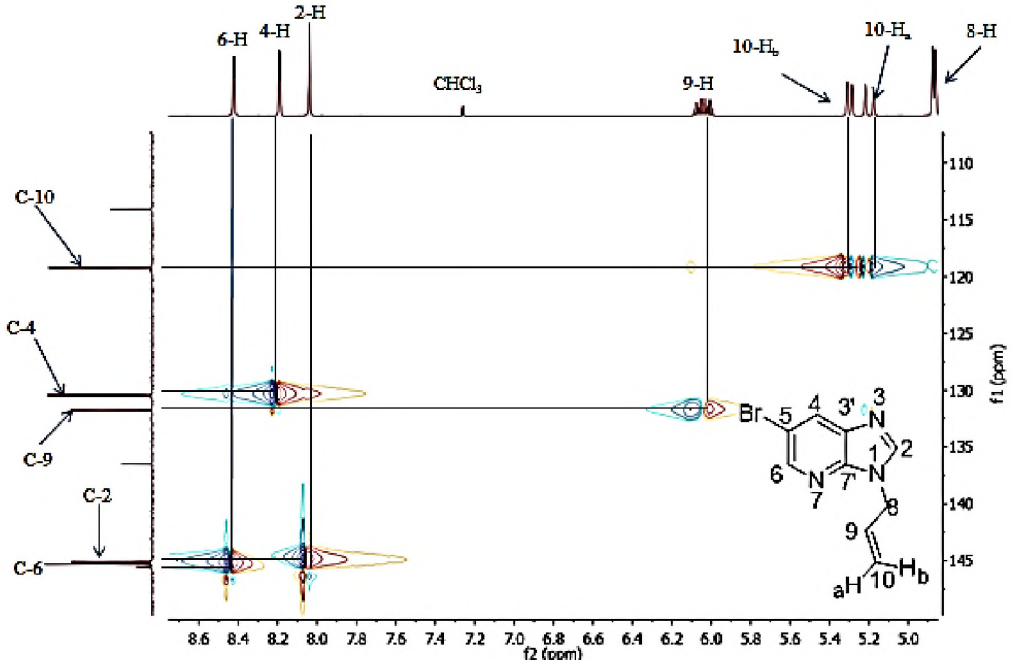

Figure 9. HSQC of **119a** in $CDCl_3$ (expanded).

2.1.3. Synthesis of substituted 5-bromo-1-[(*N*-carbamoyl)methyl]-7-azabenzimidazole derivatives 122a-l.

Access to compounds **122a-l** required the preparation of the series of *N*-substituted α-bromo acetamides **121a-l** which are lachrymatory in nature were prepared under nitrogen using bromoacetyl bromide **120** and selected benzylamines, phenethylamine, anilines, morpholine, 2-furfurylamine and 3-aminoisoxazole (Scheme 9). The reactions were performed by first abstracting an amino proton from the amines using potassium carbonate in dichloromethane (DCM) as solvent. After cooling to 0 °C, one equivalent of bromoacetyl bromide **120** was added slowly under nitrogen and the desired product was formed within 20 minutes as determined thin layer chromatography.

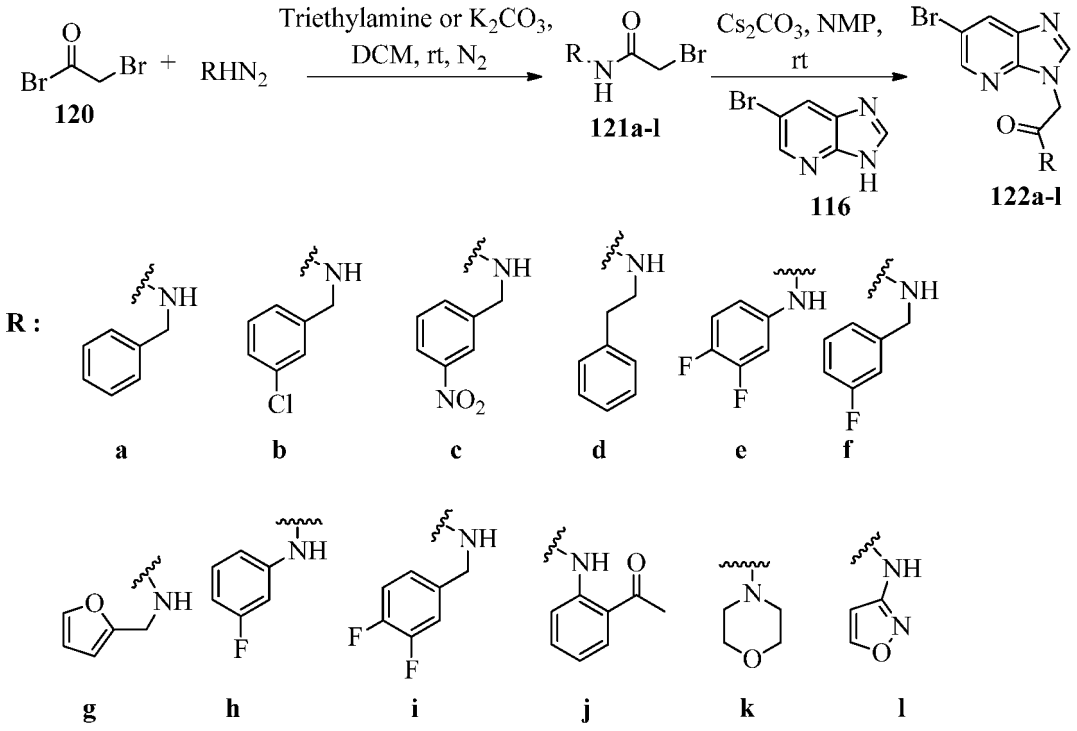

Scheme 9. Preparation of substituted the 5-bromo-1-[(*N*-carbamoyl)methyl]-7-azabenzimidazole derivatives **122a-l**.

^{1}H and ^{13}C NMR analysis indicated that the isolated products were obtained in essentially pure form. Figures 10 and 11 are the ^{1}H and ^{13}C NMR spectra of compound **121k**. The ^{1}H signal at 3.82 ppm (Figure 10) corresponds to the 8-methylene protons (8-CH_2) while the corresponding ^{13}C signal is at 25.5 ppm (Figure 11) The proton signals at 3.72 – 3.47 ppm represent the morpholino methylene protons (Figure 10), the presence of four signals instead of two can be attributed to rotational isomerism. The corresponding ^{13}C signals (Figure 11)

for the morpholino carbons (2,6, 5 and 3) are at 47.4, 47.2, 66.4 and 66.6, ppm, further confirming that there is a barrier to rotation in this molecule due to delocalization of the amide group. The carbonyl carbon (C-7) is represented by the signal at 165.4 ppm.

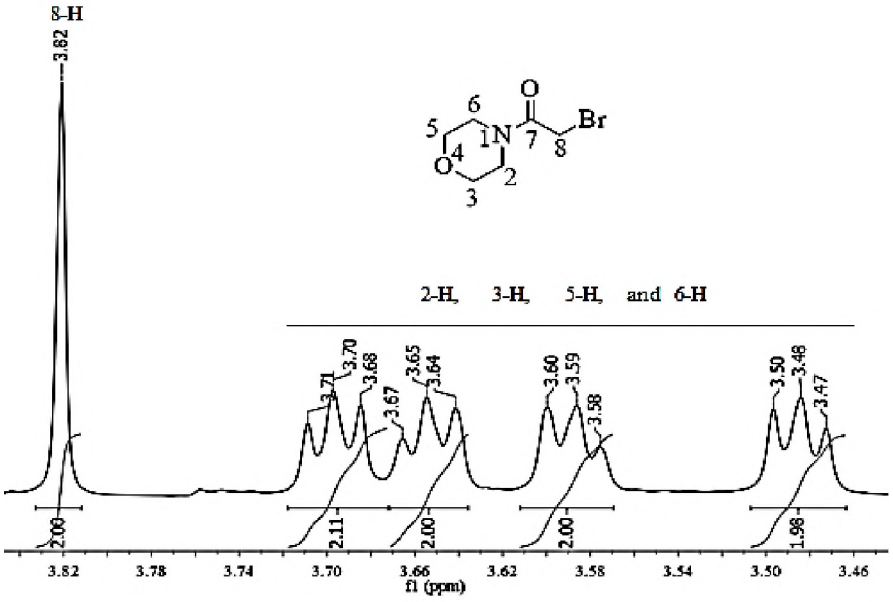

Figure 10. 400 MHz ^{1}H NMR spectrum of **121k** in $CDCl_3$.

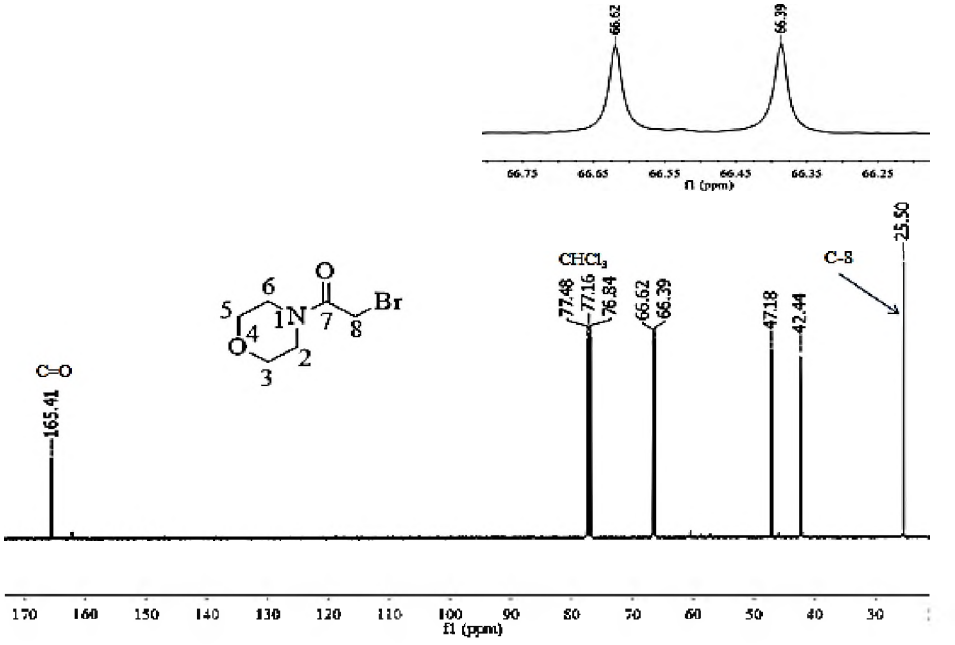

Figure 11. 100 MHz ^{13}C NMR spectrum of **121k** in $CDCl_3$.

The bromoacetamides **121a-l** were successfully reacted with 5-bromo-7-azabenzimidazole **116** at room temperature using NMP as solvent and caesium carbonate as a base. The resulting azabenzimidazole derivatives **122a-l** were purified and characterized by NMR analysis and the obtained yields ranged between 70 to 88%. Using 5-bromo-1-[2-(morpholino)-2-oxoethyl]-7-azabenzimidazole **122k** as a representative example for this series, its HPLC-MS ($C_{12}H_{14}BrN_4O_2$ 325.0300) indicated the presence of $[M+H]^+$ 325.0351 peak. ^1H, ^{13}C, COSY, DEPT, and HSQC NMR experiments (Figures 12 to19), were performed and assignments for the various proton and carbon atoms present are elucidated below.

The ^1H NMR spectrum of compound **122k** (Figure 12) indicated doubling of some of the signals. The 8-methylene protons resonate as singlets at 5.34 and 5.30 ppm (Figure 12), their integral ratio (*ca.* 1:20) indicating the rotamer ratio. The HSQC experiment indicated the carbon atom attached to these protons resonates at 44.2 ppm (Figures 13 and 14).

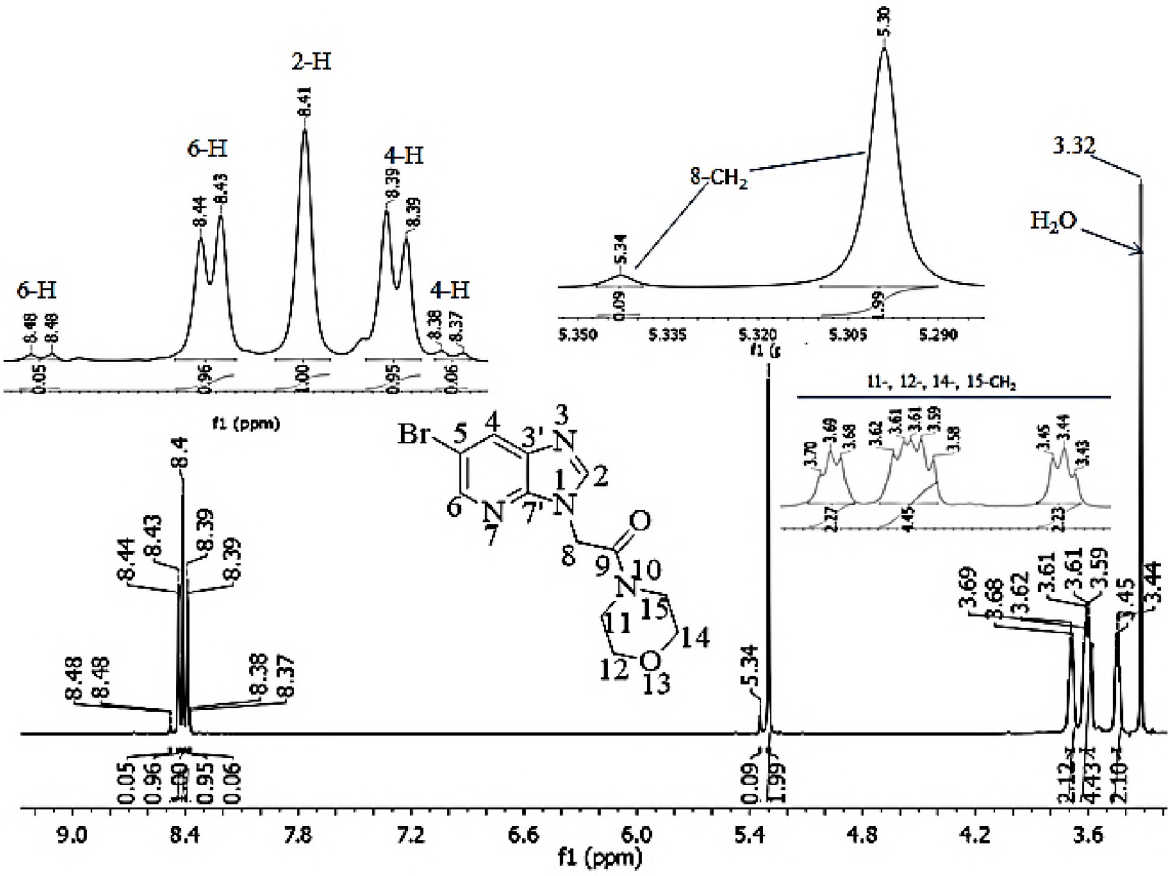

Figure 12. 400MHz ^1H NMR spectrum of **122k** in DMSO-d_6.

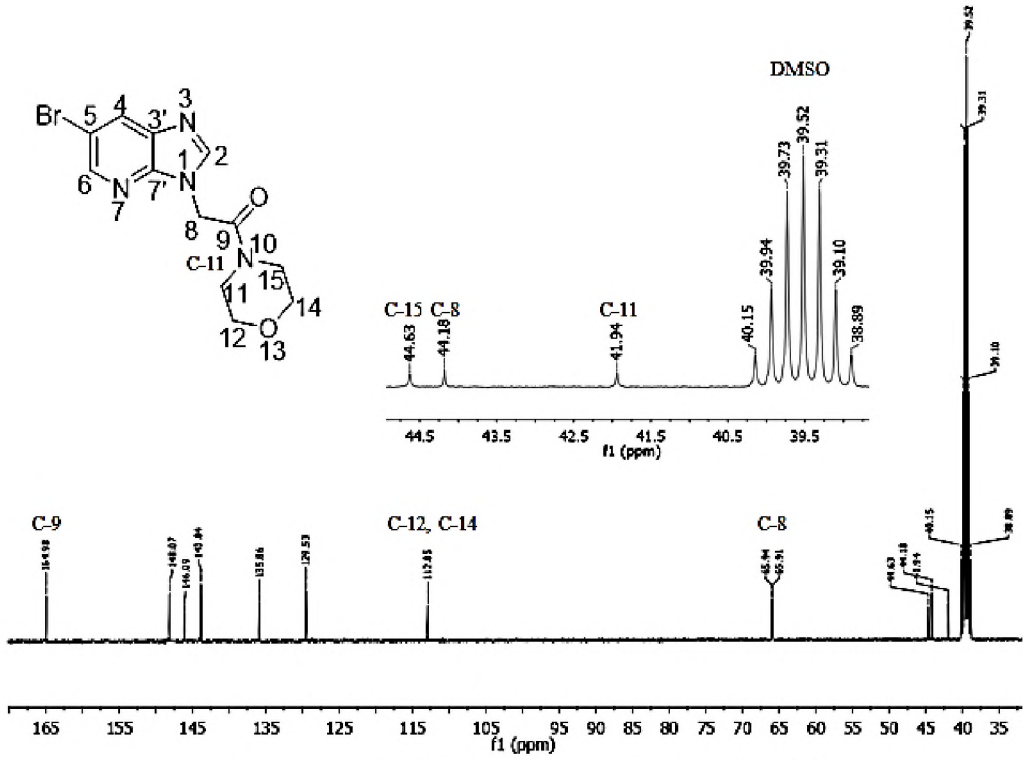

Figure 13. 100MHz ^{13}C spectrum of **122k** in DMSO-d*6*.

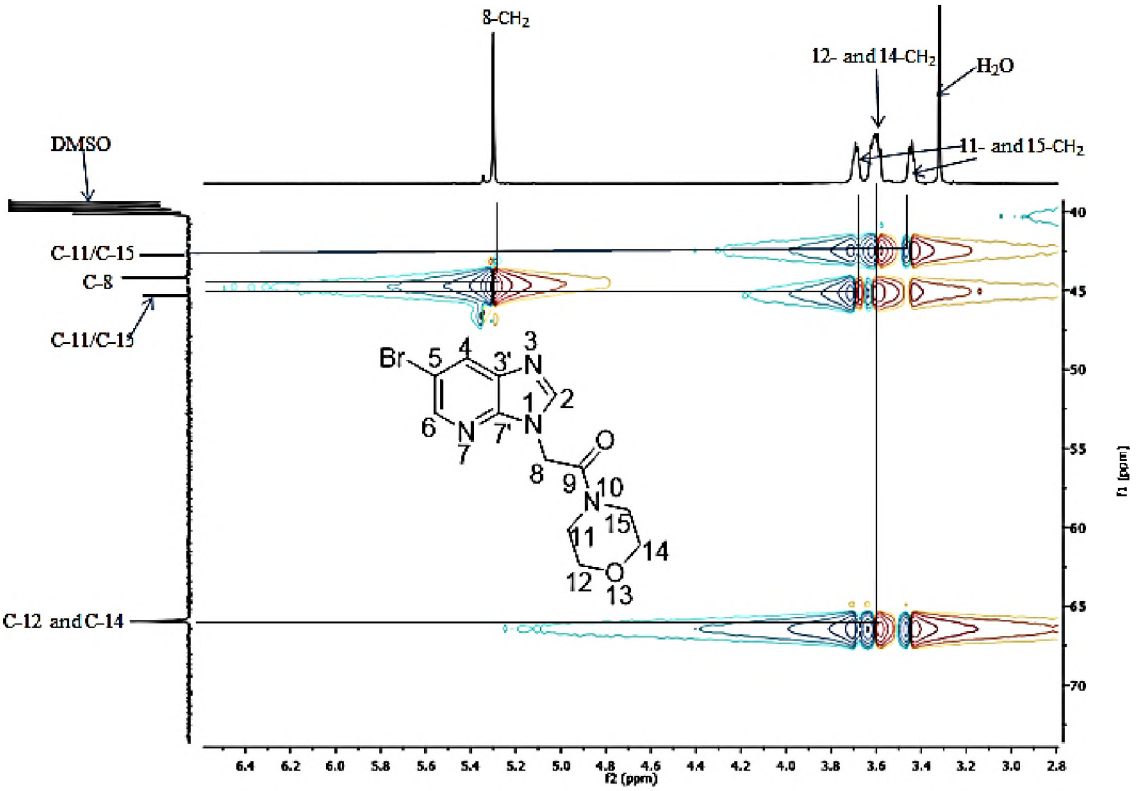

Figure 14. Partial HSQC spectrum of **122k** in DMSO-d*6*.

The 7-azabenzimidazole protons 2-H, 4-H and 6-H are represented by the signals at 8.41 (2-H), 8.39, 8.37 (4-H) and 8.4, 8.48 (6-H) ppm, respectively. The doubling of signals is again attributed to hindered rotation about the amide [C(O)-N)] bond, indicating that this molecule exists as a mixture of rotational isomers at the normal probe temperature (298 K). Data from the HSQC spectrum (Figure 15) showed that the ^{13}C signals at 148.1, 143.8 and 129.5 ppm, correspond to the carbon atoms C-2, C-6 and C-4, respectively.

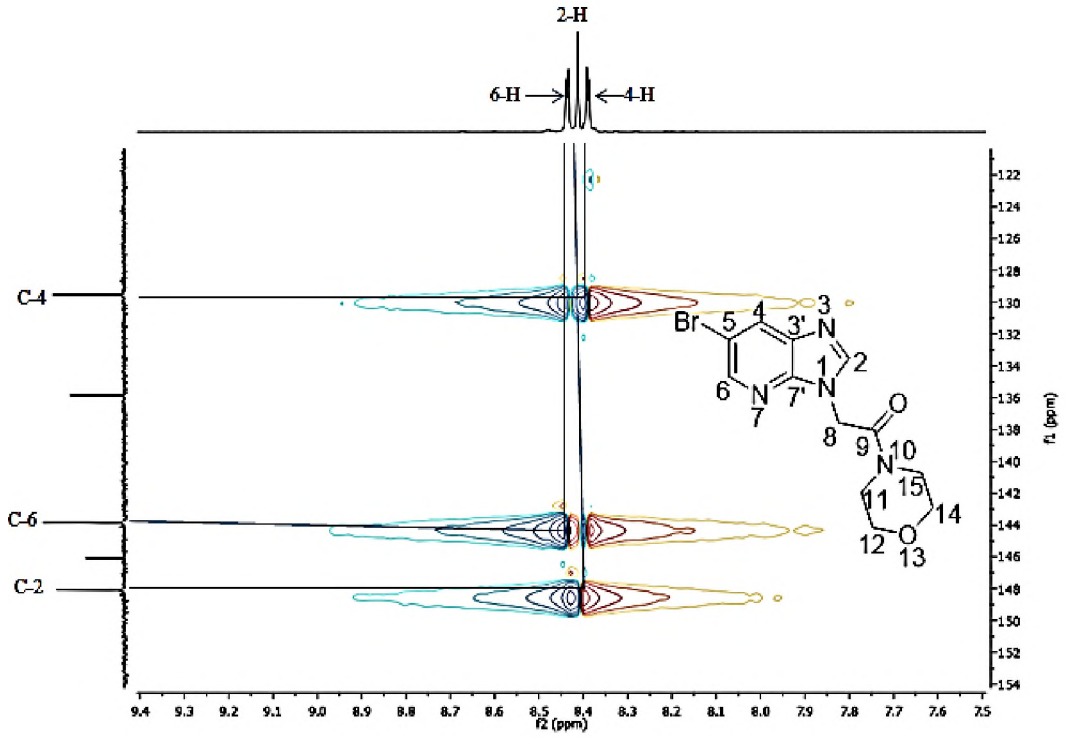

Figure 15. Partial HSQC spectrum of **122k** in DMSO-d_6.

The partial ^{13}C NMR spectrum (Figure 16) reveals splitting of the 12- and 14-CH_2 signal at 65.9 ppm and of the signal corresponding to the 11- and 15-methylene carbons (41.9and 44.6 ppm) due to rotational isomerism effects. The signal at 44.7 ppm is attributed to the methylene 8-methylene carbon. Assignment of these signals to the methylene carbons is supported by the corresponding negative signals in the DEPT-135 spectrum (Figure 17).The carbonyl carbon atom (C-9) corresponds to the signal at 164.5 ppm and appears unchanged relative to the precursor.

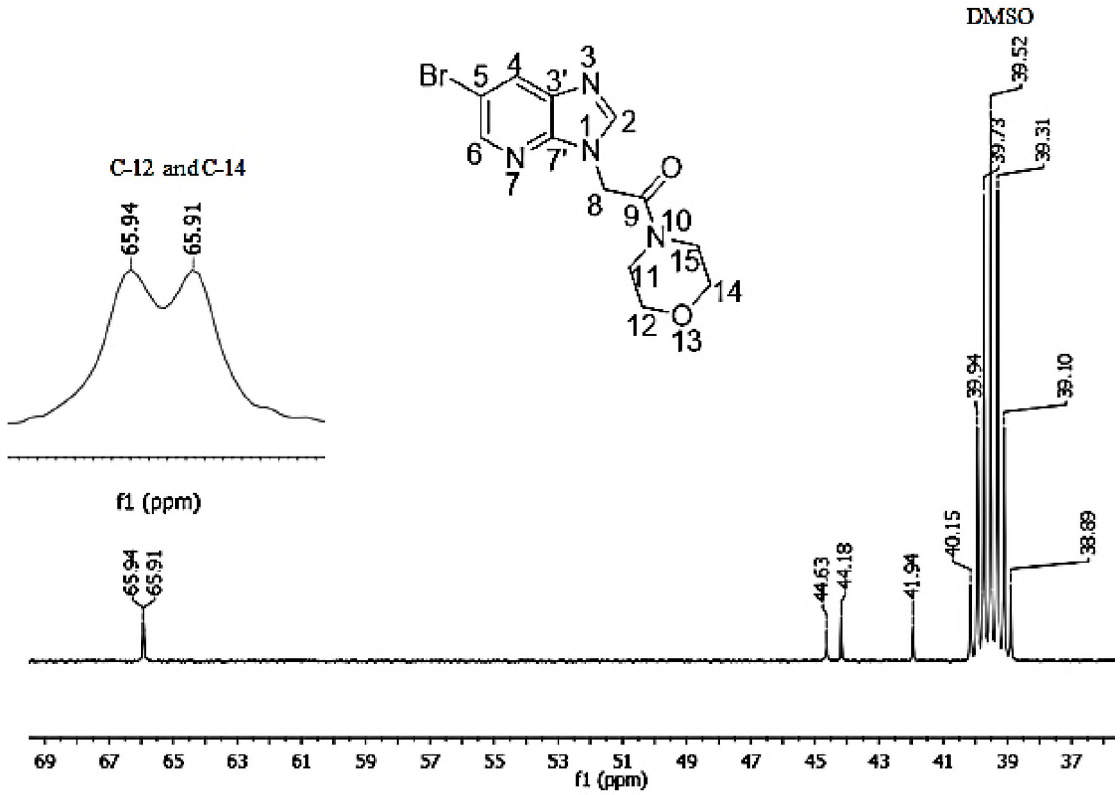

Figure 16. Patial 100MHz ^{13}C NMR spectrum of **122k** in DMSO-d_6 (expanded).

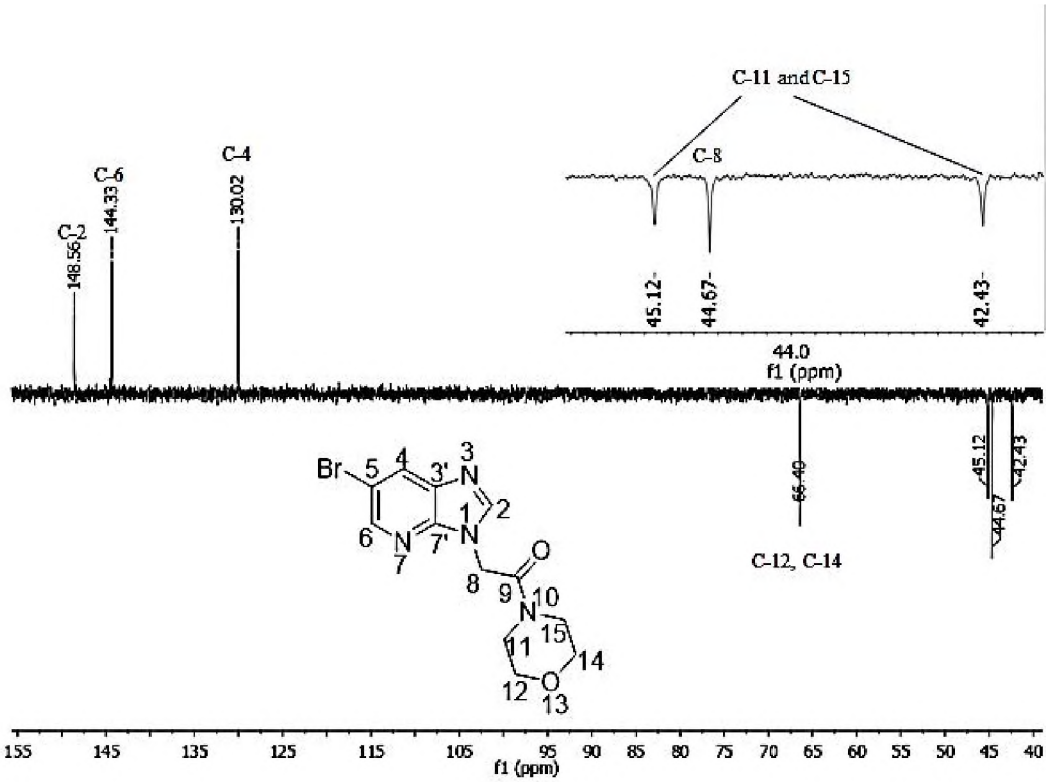

Figure 17. 100MHz DEPT-135 spectrum of **122l** in DMSO-d_6.

As evidenced by the doubling of certain signals, all of the *N*-benzylcarbamoyl, isoxazolylcarbamoyl, phenethylcarbamoyl and 2-furfurylcarbamoyl derivatives of this series (**121**) appear to display rotational isomerism. The ^{1}H NMR spectra of 1-{[*N*-(3-chlorobenzyl)carbamoyl]methyl}-5-bromo-7-azabenzimidazole **122b** and 1-{[*N*-(2-furfuryl)carbamoyl]methyl}-5-bromo-7-azabenzimidazole **122g** also clearly indicate the doubling of signals (Figures 18 and 19) when the NMR experiments were conducted at 298 K. Stabilization of the rotamers involved is due to delocalization of the lone-pair electrons on the nitrogen atom of the carbamoyl system. This leads to a partial double bond and consequent restricted rotation about the C(O)-N bond.

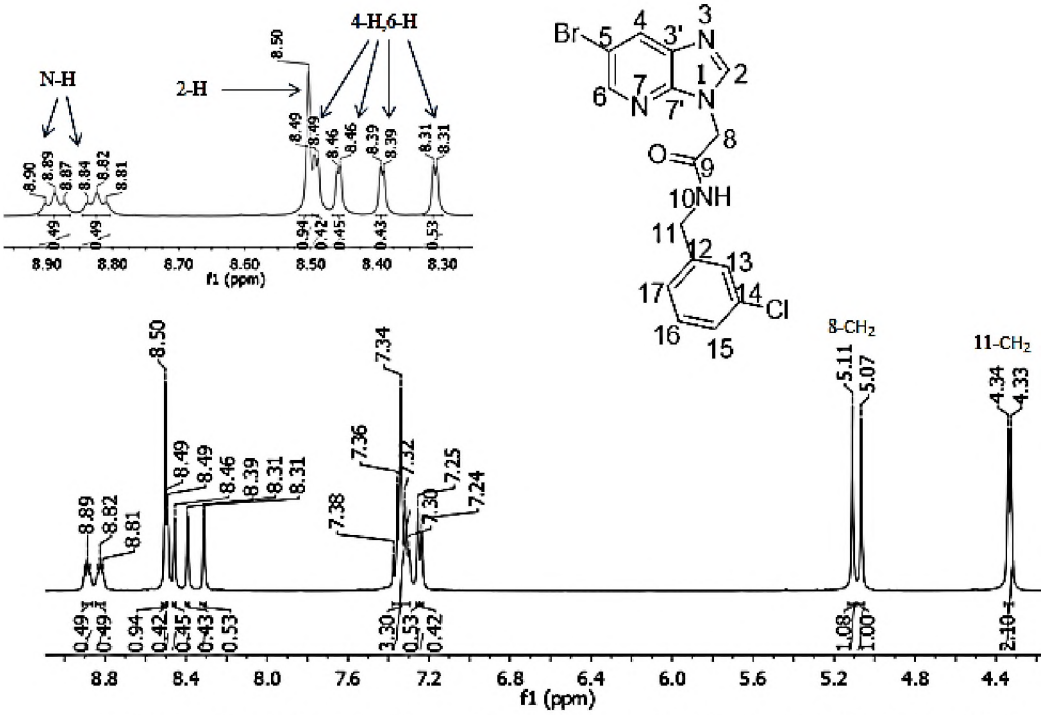

Figure 18. 400 MHz ^{1}H NMR spectrum of **122b** in DMSO-d_6 at 298 K.

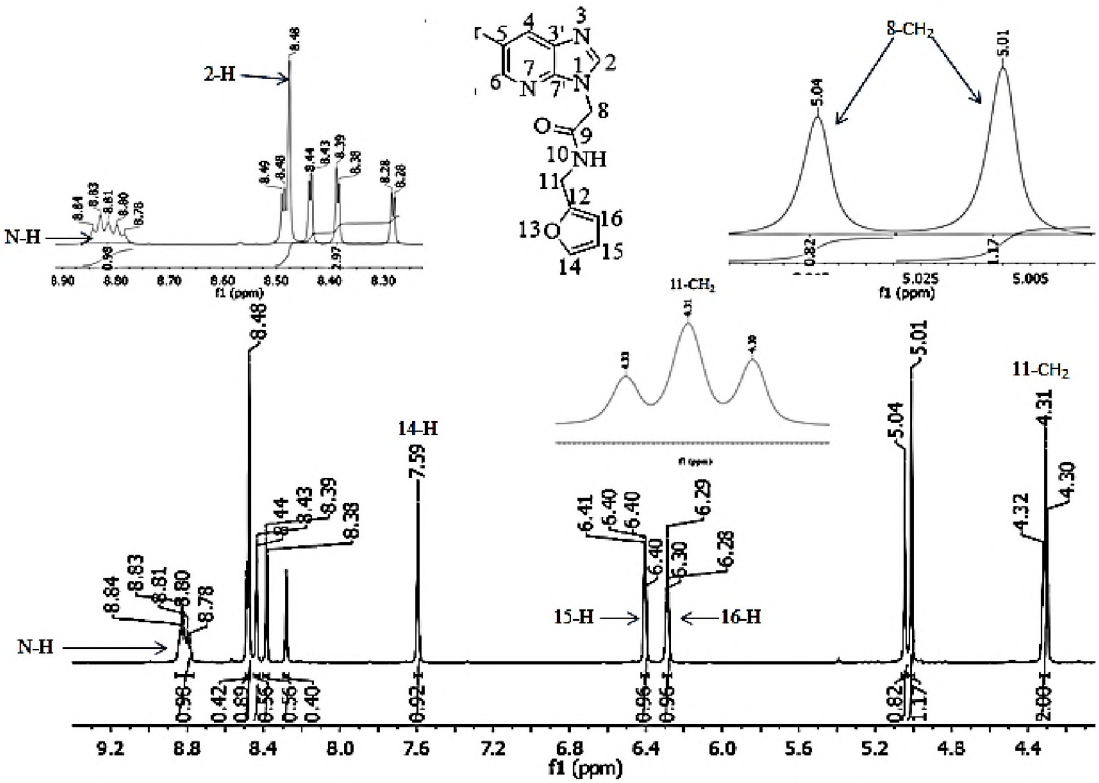

Figure 19. 400 MHz 1H NMR spectrum of **122g** in DMSO-d_6 at 298 K.

The canonical forms (A), which contribute to the resonance hybrids (B) and which correspond to the *s-cis* and *s-trans* rotamers of compound **122b,** are illustrated in Figure 20. The presence of an equilibrium mixture of the *s-cis* and *s-trans* rotamers at ambient temperature is responsible for the doubling of signals in the NMR spectra (Figures 18 and 19). In the ^{1}H NMR spectrum of compound **122g** (Figure 19), it seems that coupling of the 11-methylene protons with the amino proton leads to a pair of doublets which overlap to afford an apparent triplet.

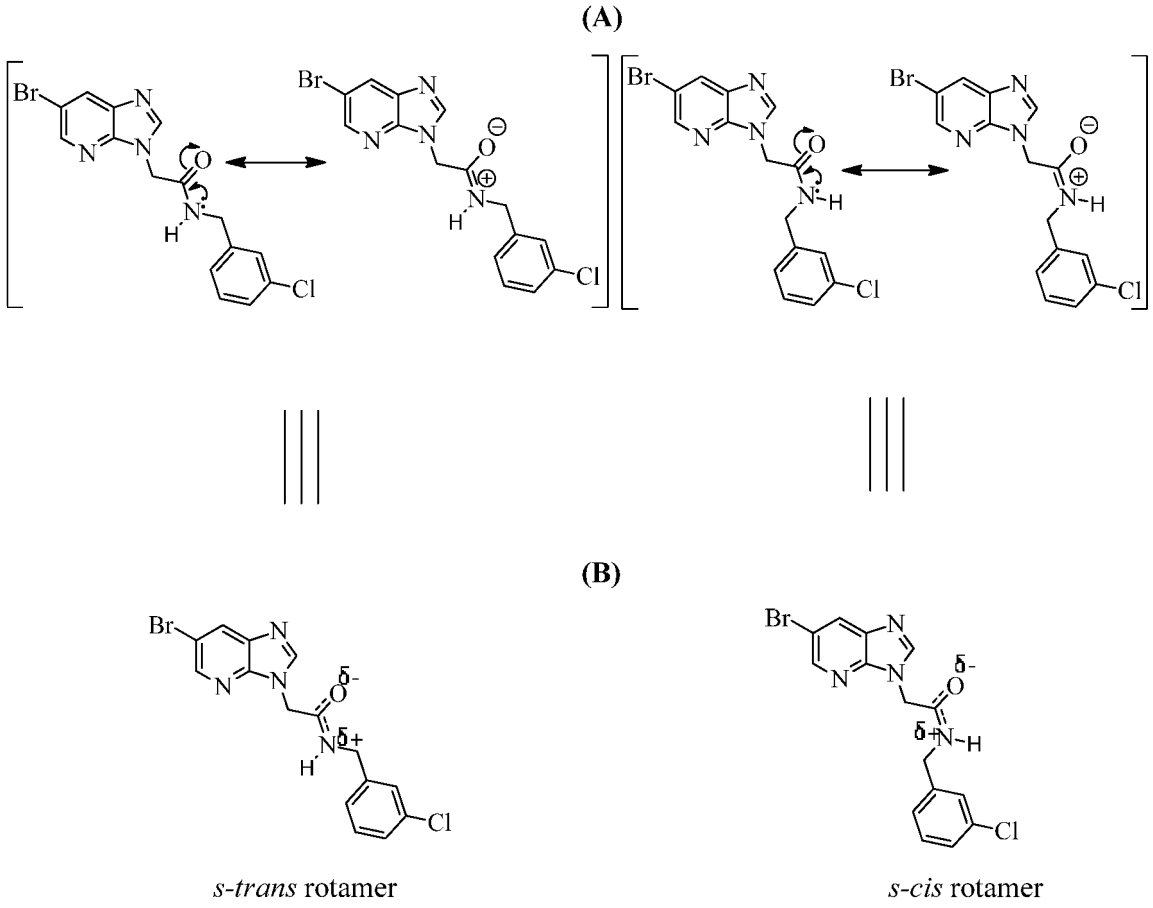

Figure 20. The canonical forms (A), contributing to the resonance hybrids (B) which correspond to the *s-trans* and *s-cis* rotamers of compound **122b.**

2.1.4. Dynamic NMR studies of rotamerism in 1-{[*N*-(3-chlorobenzyl)carbamoyl]methyl}-5-bromo-7-azabenzimidazole 122b and 1-{[*N*-(2-furfuryl)carbamoyl]methyl}-5-bromo-7-azabenzimidazole 122g.

For a mixture of chemically equivalent molecules whose nuclei undergo site exchange through an intramolecular process (internal rotation in the case of rotamers), the associated doubling of NMR signals is a function of the resonance frequency difference ($\Delta\omega$) between the signals for a particular nucleus and the rate constant (k) for the exchange.[126] In the dynamic NMR study, variable temperature ^{1}H NMR experiments were conducted and the coalescence temperature Tc was determined using the signals for the amide proton in **122b** and the 8-methylene proton signals in **122g**. The coalescence rate constants kc were determined using equation 1 and the rotational barriers (Figures 21 and 22) were also determined.

$$k_C = \pi \frac{\Delta\omega}{\sqrt{2}} \quad (1)$$

The free energy of activation ΔG^* corresponding to each of the rotational barriers (Figures 21 and 22) was also determined.

The free energy difference ΔG_o between any two rotamers can be estimated using equation 2.

$$\Delta G_o = -RTInK \quad (2)$$

Where K = is the equilibrium constant between the rotamers as determined from the NMR signal integrals for the two rotamers at a given temperature.

T = absolute temperature in Kelvin (298 K)

R = the universal gas constant (8.3144 J K^{-1} mol^{-1})

Therefore, the value of K for **122b** is 1.045 while that of **122g** is 1.247.

The free energy difference ΔG_o at 298 K between the *s-trans* and *s-cis*- rotamers of 1-{[*N*-(3-chlorobenzyl)carbamoyl]methyl}-5-bromo-7-azabenzimidazole **122b** is -0.11 kJ mol^{-1} while the free energy difference ΔG_o at 298 K between the *s-trans* and *s-cis* rotamers of 1-{[*N*-(2-furfuryl)carbamoyl]methyl}-5-bromo-7-azabenzimidazole **122g** is -0.55 kJ mol^{-1}.

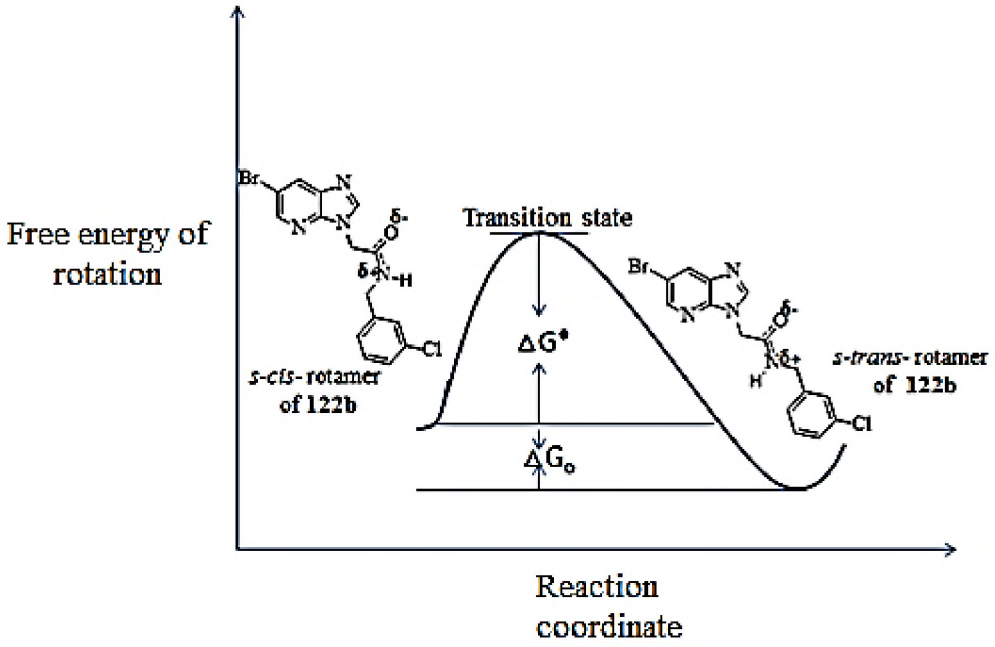

Figure 21. Energy barrier for rotational interconversion of *s-trans* and *s-cis* rotamers of 1-{[*N*-(3-chlorobenzyl)carbamoyl]methyl}-5-bromo-7-azabenzimidazole **122b**.

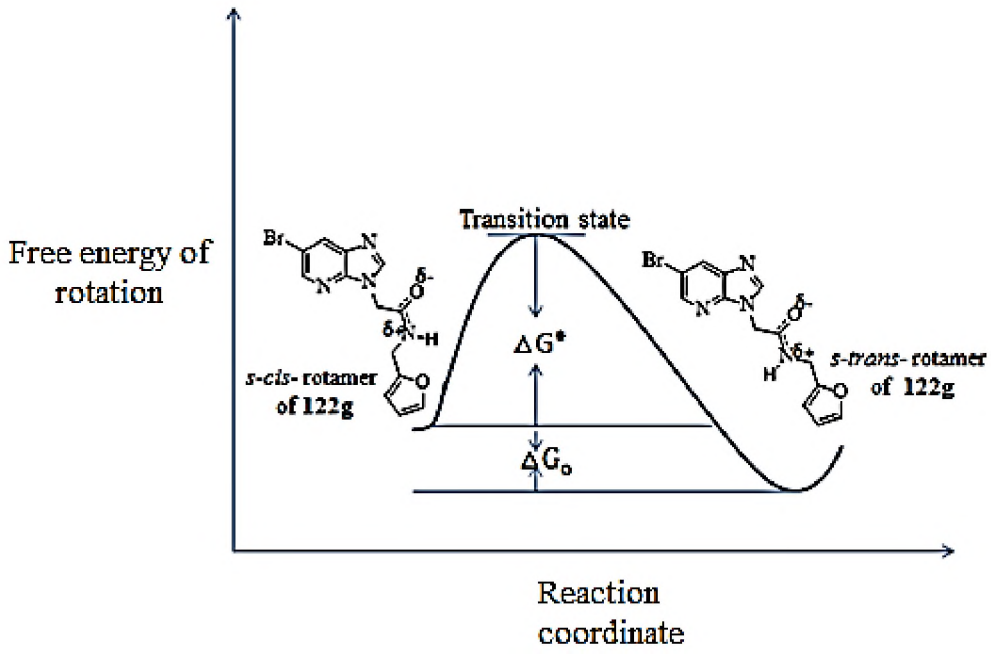

Figure 22. Energy barrier for rotational interconversion of *s-trans* and *s-cis* rotamers of 1-{[*N*-(2-furfuryl)carbamoyl]methyl}-5-bromo-7-azabenzimidazole **122g**.

The *s-trans* rotamer is presumed to be more stable than the *s-cis* rotamer because of the steric interaction between the (5-bromo-7-azabenzimidazolyl)methyl group and the 3-chlorobenzyl group in **122b** and the furfuryl group in **122g**(Figures 20-22).

In order to determine the activation parameters, ^{1}H NMR spectra were recorded for **122b** and **122g** at 298 K, 303 K, 313 K, 323 K, 333 K, 343 K, 353 K, 363 K and 373 K. The experimental results indicated that the site exchange was slow at 298 K, 303 K and 313 K for **122b** while intermediate site exchange was evident at 323 K, 333 K, 343 K and 353 K, with the signals broadening and coming close together. Coalescence was visible at 353 K while increasing the probe temperature to 373 K led to fast site exchange to give a single unresolved signal (Figure 23). A dynamic NMR study,conducted similarly for compound **122g,** indicated that the exchange was slow between 298 K and 323 K. Intermediate exchange was evident between 333 K and 353 K, and coalescence was visible at 363 K. Increasing the NMRprobe temperature to 373 K led to fast site exchange and a single peak was observed (Figure 24).

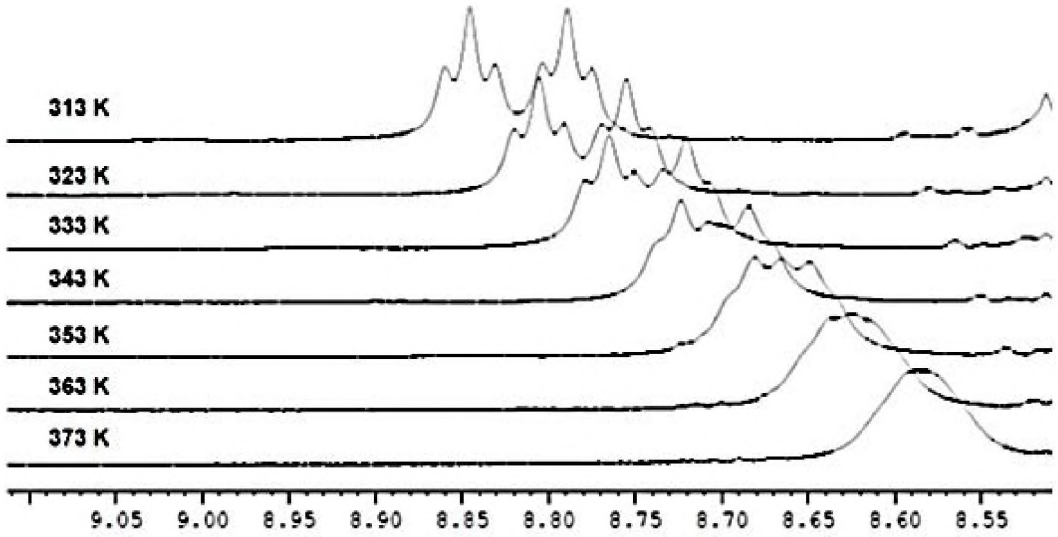

Figure 23. The effect of temperature change on line-widths and exchange rates for the *s-trans* and *s- cis* rotamers of 1-{[*N*-(3-chlorobenzyl)carbamoyl]methyl}-5-bromo-7-azabenzimidazole **122b**.

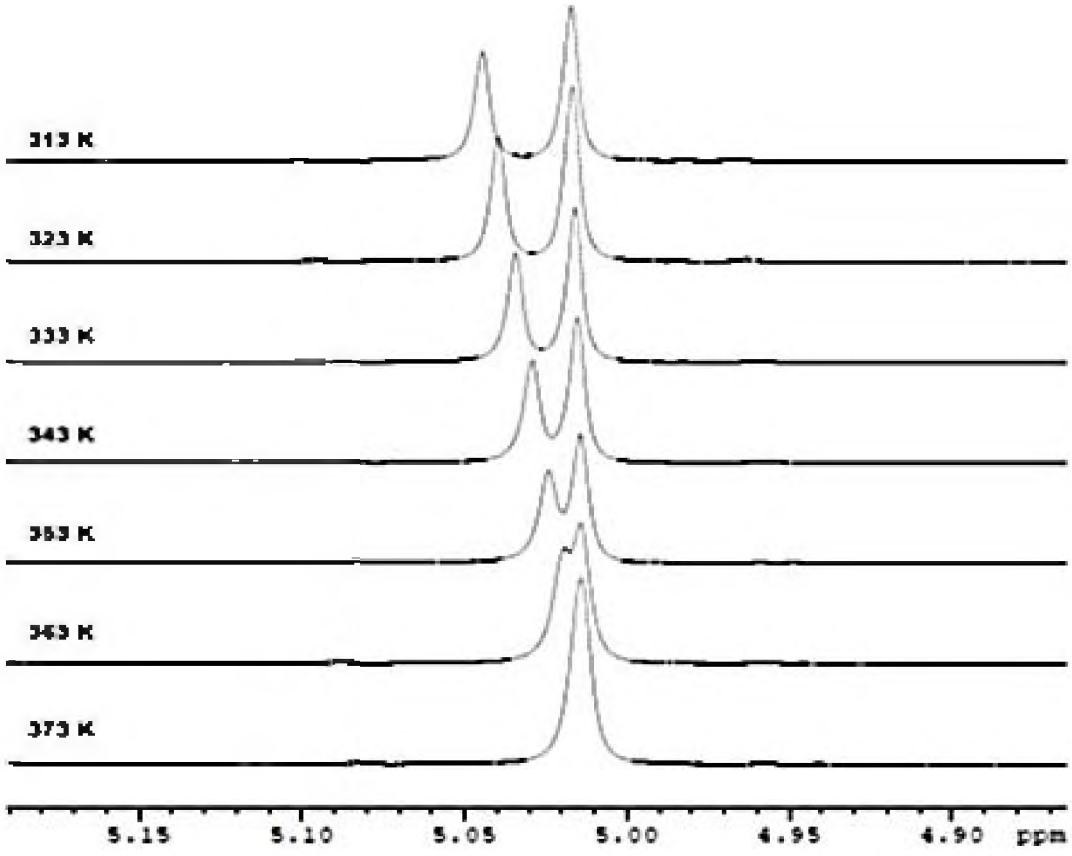

Figure 24. The effect of temperature change on line-widths and exchange rates for *s-trans* and *s-cis* rotamers of 1-{[*N*-(2-furfuryl)carbamoyl]methyl}-5-bromo-7-azabenzimidazole **122g**.

In each case, the chemical shift difference ωc at coalescence was obtained by extrapolation of a plot of $\Delta\omega$ against temperature. The frequency separation at coalescence was found to be 12.6 Hz for **122b** and 2.4 Hz for **122g** (Figures 25 and 26).

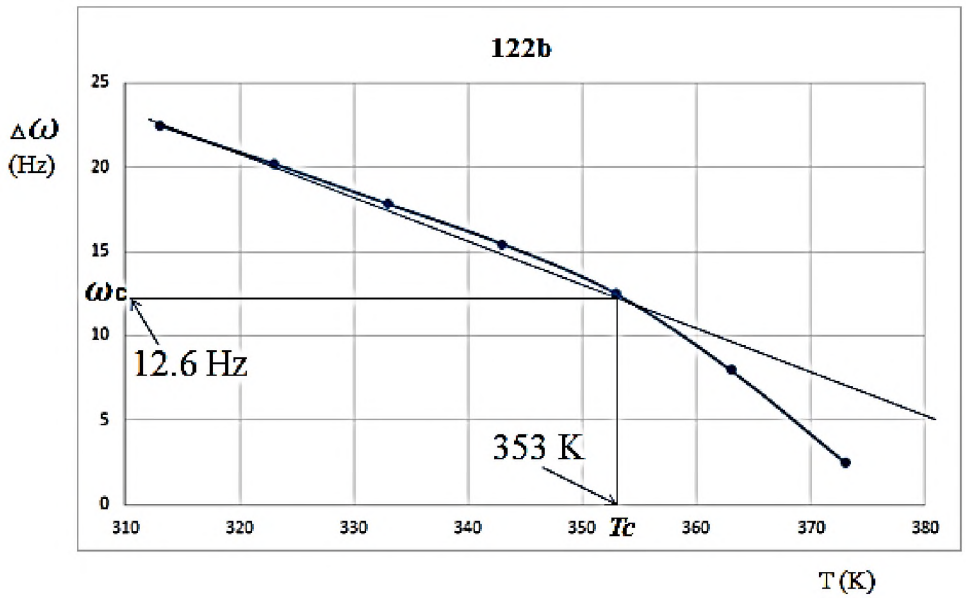

Figure 25. A plot of frequency separation between rotamer peaks of **122b** versus temperature.

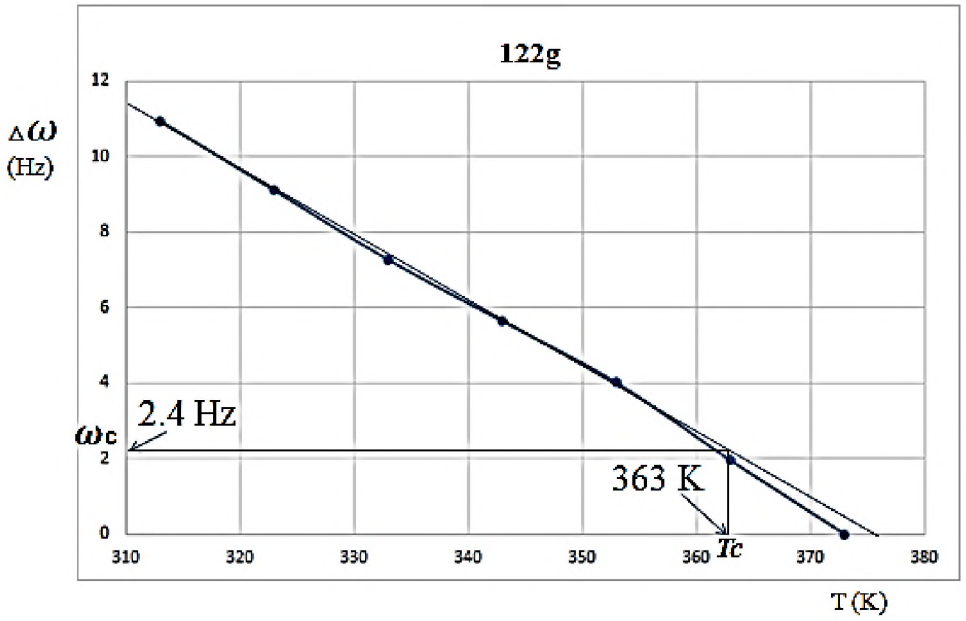

Figure 26. A plot of frequency separation between rotamer peaks of **122g** versus temperature.

The free-energy of activation ΔG^* can be calculated from the coalescence data using equation 3.[127]

$$\Delta G^* = RT_C [23 + \ln(T_C/\Delta\omega C)] \quad (3)$$

Therefore, using equation 3, ΔG^* is 77.3 kJ mol^{-1} for **122b** (Figure 26) and 84.6 kJ mol^{-1} for **122g (**Figure 27).

The free-energy of activation can also be estimated using the Eyring equation (equation 4)

$$k = \kappa . K_B.T/h . e^{-\Delta G^*/RT} \quad (4)$$

Where K_B = the Boltzmann constant (3.2998 x 10^{-23} J/K),

h = Planck's constant (6.626 x 10^{-34} J.s),

T = absolute temperature in kelvin,

R = the universal gas constant (8.3144 J K^{-1} mol^{-1}) and

κ = the transmission coefficient (1)

The free energy of rotation ΔG^* can thus be calculated in kilojoules per mole using equation 5.[128, 129]

$$\Delta G^* = 1.914 \text{ X } 10^{-2} T_c [10.319 + \log(T_c/k_c) \quad (5)$$

Therefore, using equation 5, the free-energy of activation for **122b** was calculated to be 73.3 kJ mol^{-1} while that of **122g** was 79.6 $kJmol^{-1}$.

The results obtained using both methods afford mean values of 75.3 ± 2.0 kJ mol^{-1} for **122b** and 82.1 ± 2.5 kJ mol^{-1} for **122g**. However, the free energy of activation calculated using the frequency separation (ωc) from extrapolation of the plot of temperature versus change in frequency of separation ($\Delta\omega$) is believed to be more acccurate because this method involves use of experimental data at all the temperatures while the latter method (Erying equation) uses only the coalescence temperature (Tc).

2.1.5. Synthesis of *N,N'*-bis[2-(5-bromo-7-azabenzimidazol-1-yl)-2-oxoethyl]ethylene-1,3-diamine 124a and the –cyclohexyl-1,2-diamine 124b.

In an attempt to investigate the anti-protozoan activity and rotational isomerism of bis-azabenzimidazole analogues, compounds **124a** and **124b** were synthesized. The key

intermediates **123a** and **123b** for these reactions were prepared under nitrogen. Ethylenediamine and (±)-*trans*-1,2-diaminocyclohexane were each treated with two equivalents of anhydrous potassium carbonate, using dichloromethane as solvent, to abstract the amino protons and generate the nucleophilic centres (scheme 10). Two equivalents of bromoacetyl bromide **120** were then added and the required products **123a,b** were isolated after 20 minutes, completion of the reaction having been determined by thin layer chromatography. ^{1}H and ^{13}C NMR analysis indicated the success of this step, and the isolated diamides **123a** and **123b** were shown to be pure enough for use in the second step.

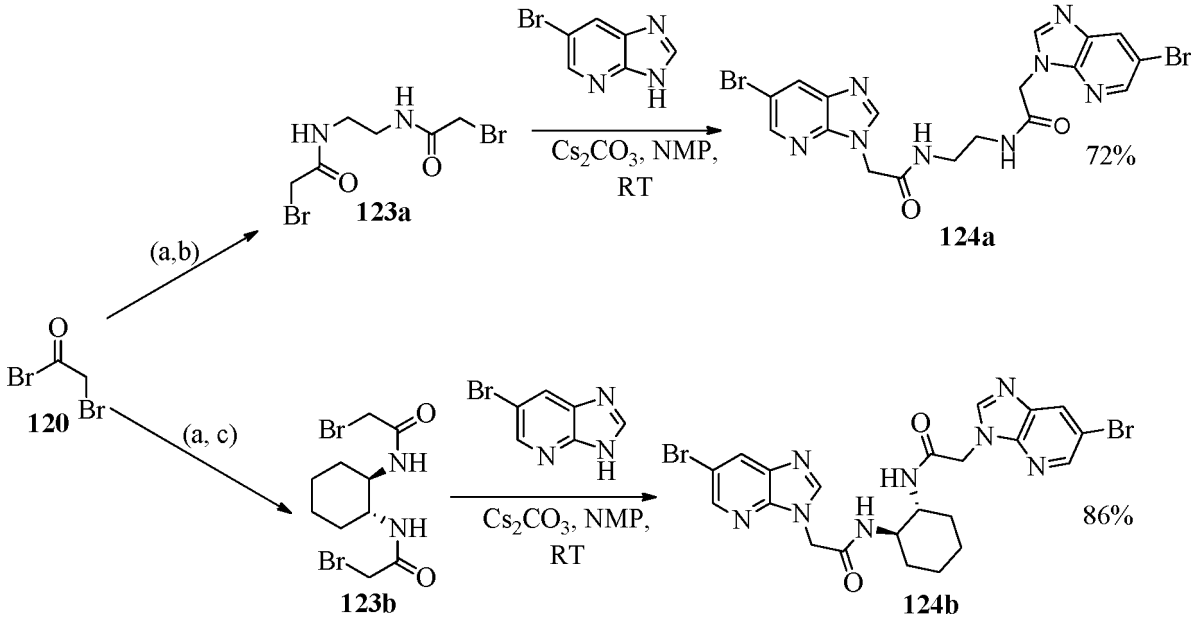

Reagents and conditions. (a) K_2CO_3, DCM, r.t., N_2; (b) Ethylenediamine; (c) (±)-Trans-1,2-diaaminocyclohexane.

Scheme 10. Synthesis of bis-[2-(5-bromo-7-azabenzimidazol-1-yl)acetamides].

The ^{1}H NMR spectrum of symmetrical diamides **123a** (Figure 27) shows the amido N-H signal at 8.32 ppm, the ethylene proton signal as a multiplet (due to rotational isomerism) at 3.17-3.13 ppm and the bromomethylene as singlet at 3.84 ppm (Figure 27). The ^{13}C NMR spectrum of **123a** shows the carbonyl carbon signal at 166.7 ppm, the ethylene carbon signals at 30.0 ppm and the bromomethylene signal almost overlapping the DMSO multiplets at 39.0 ppm (Figure 28).

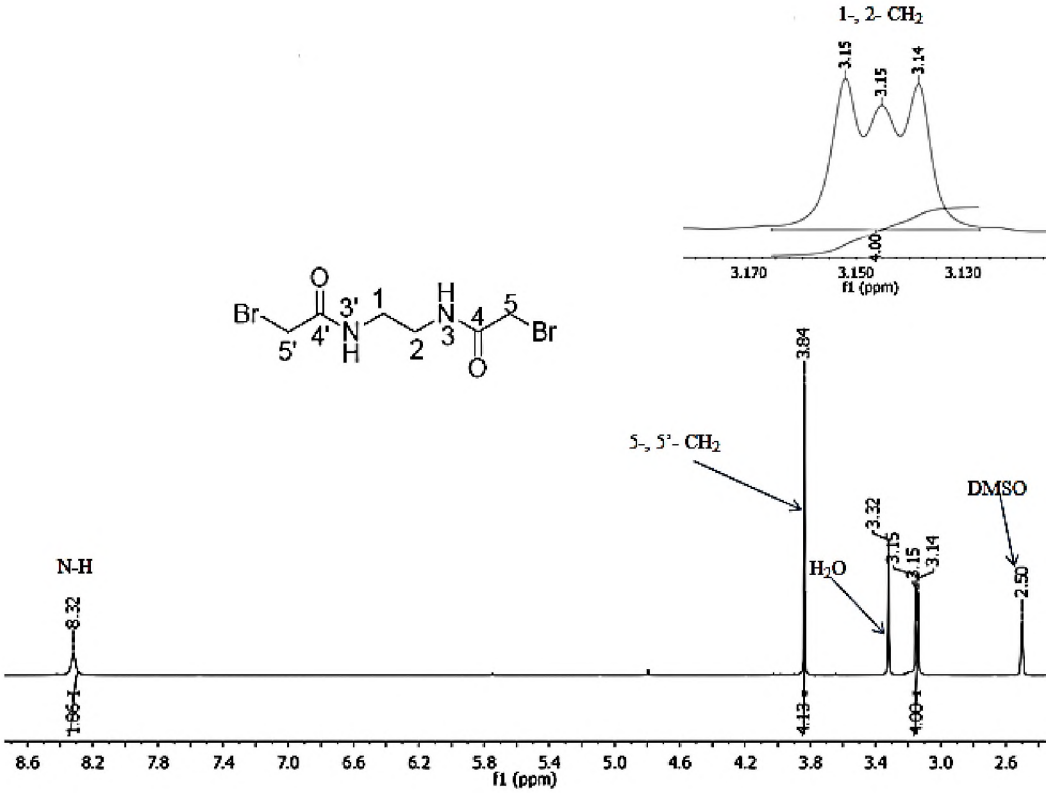

Figure 27. 400 MHz ^{1}H NMR spectrum of **123a** in DMSO-*d*$_6$.

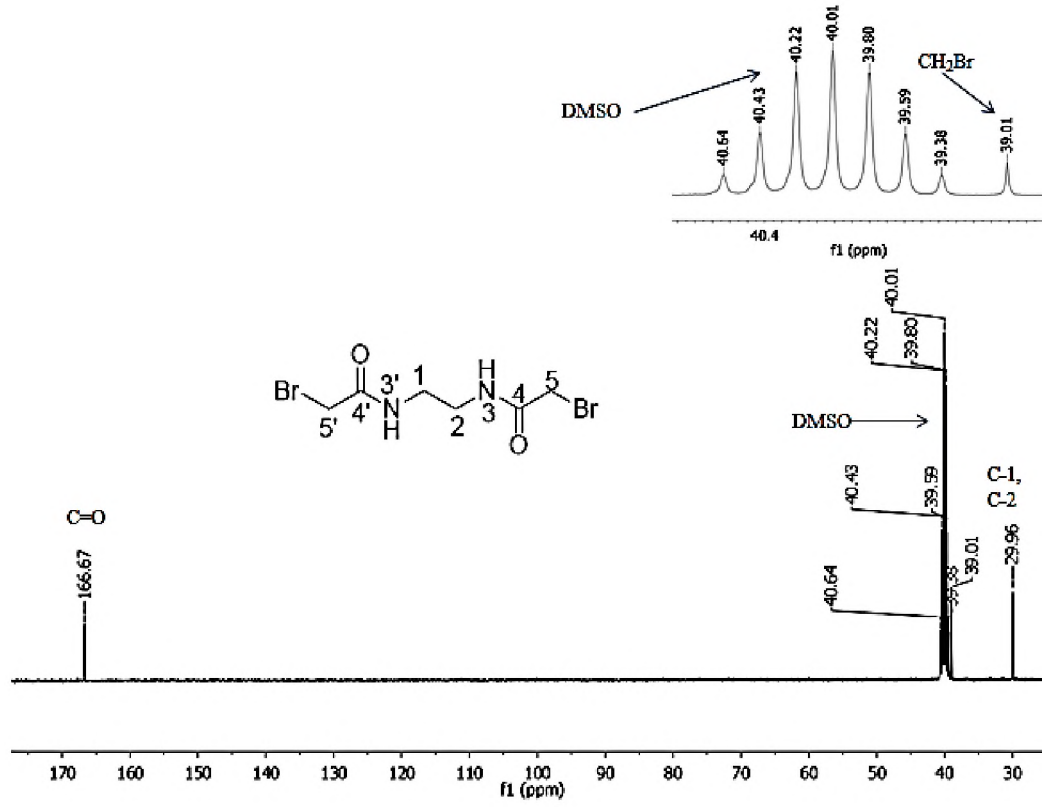

Figure 28. 100 MHz ^{13}C NMR spectrum of **123a** in DMSO- *d*$_6$.

The second step in this synthetic sequence involved the use of caesium carbonate as a base and *N*-methylpyrrolidone (NMP) as the solvent. The two reactants involved in this step were soluble in NMP – a solvent that can easily be extracted into water at the end of the reaction process (during work-up). However, the products **124a and 124b** were difficult to purify because of their polarity. Consequently, care was taken to make sure that exactly two equivalent of 5-bromo-7-azabenzimidazole and two equivalent of caesium carbonate were used to eliminate the possibility of having excess starting materials in the crude product mixture. The formation and purity of the desired products were confirmed by NMR analysis and 72 and 86% yields were obtained for the two compounds, respectively. The HPLC-MS analysis for **124a** ($C_{18}H_{17}Br_2N_8O_2$ 534.9841) indicated the presence of $[M+H]^+$ 534.9838 peak.

The COSY experiment showed that the aliphatic proton signals appeared as singlets - no crosspeaks between the protons, as expected (Figure 29). The ^1H NMR spectrum of *N,N'*-bis[2-(5-bromo-7-azabenzimidazol-1-yl)acetyl]-1,2-ethylenediamine **124**a indicated that the ethylene protons (1- and 2-CH_2) resonated at 3.19 ppm (Figure 30) while the HSQC spectrum assisted in deducing that these protons correlate with the ^{13}C signal resonating at 38.4 ppm, thus confirming that the signal corresponds to C-1 and C-2 (Figures 31 and 32). The methylene protons 5- and 5'-CH_2 correspond to the NMR signal at 4.96 ppm while HSQC spectrum correlates this signal to the ^{13}C signal at 45.6 ppm – evidently corresponding to C-5 and C-5'.

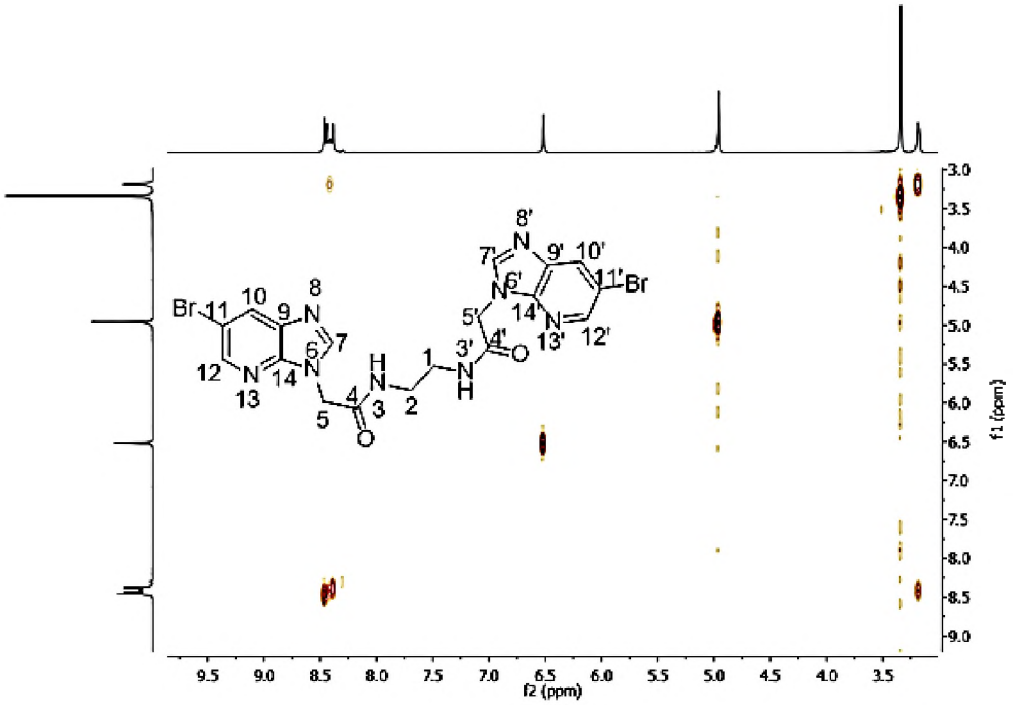

Figure 29. 400 MHz COSY NMR spectrum of **124a** in DMSO-d_6.

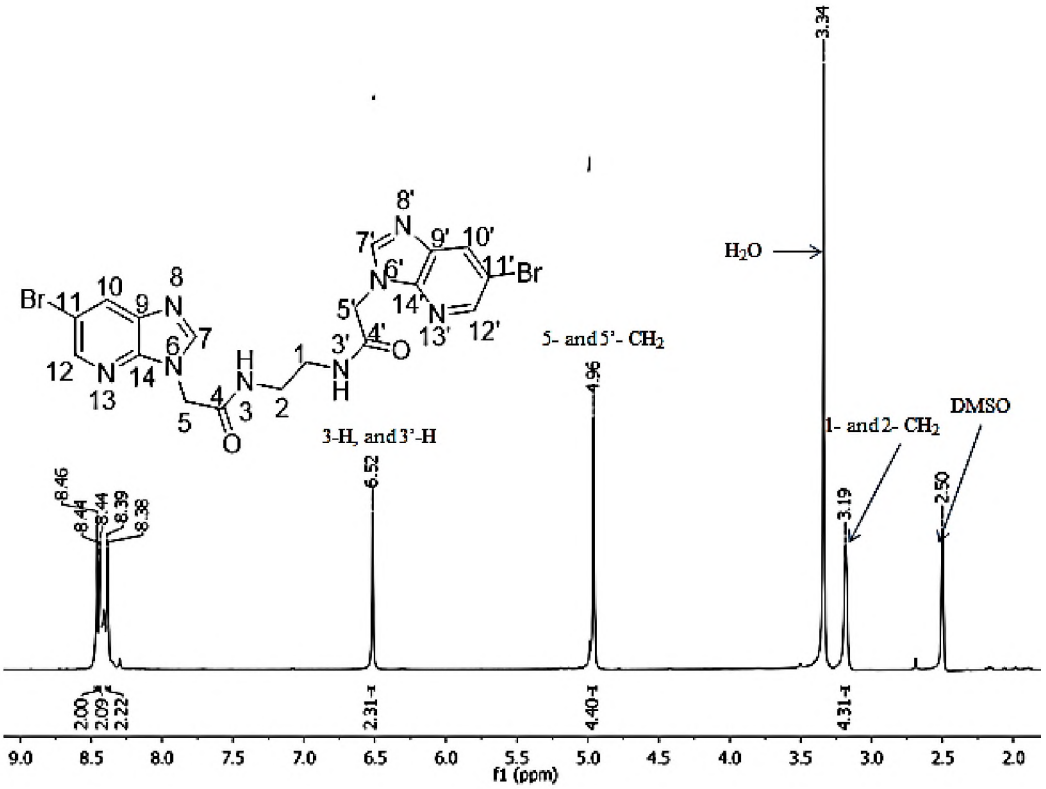

Figure 30. 400 MHz ^{1}H NMR spectrum of **124a** in DMSO- d_6.

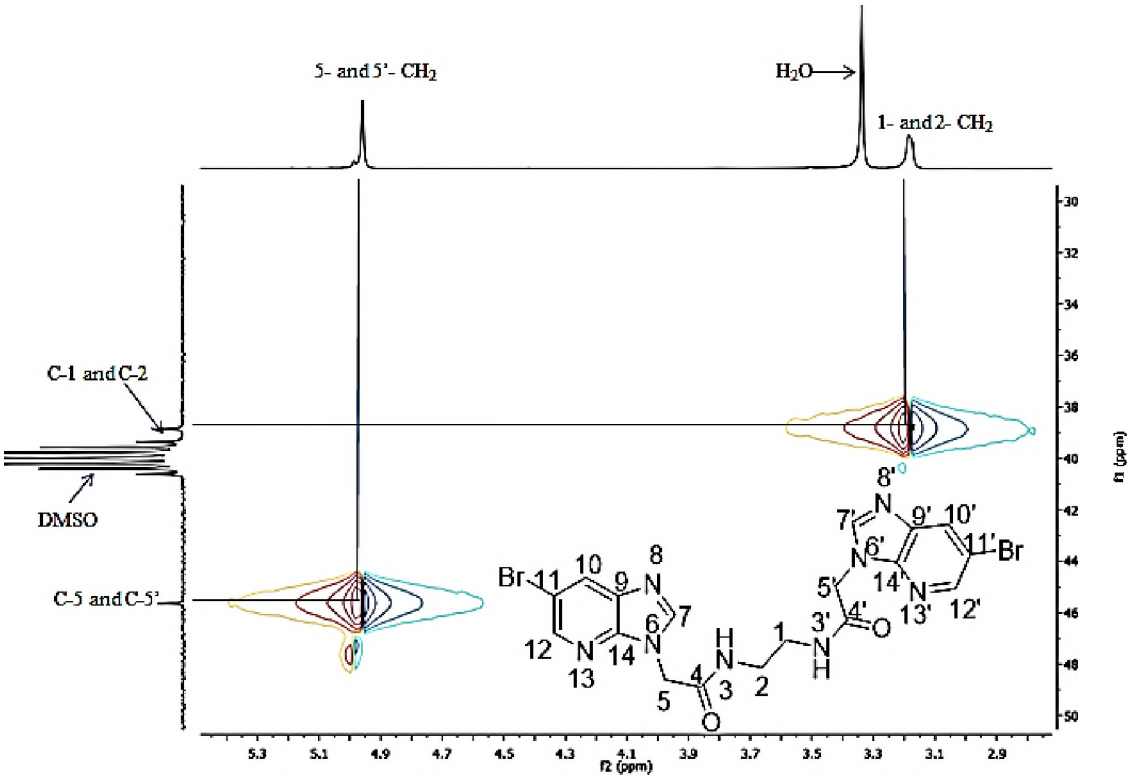

Figure 31. Partial 400 MHz HSQC NMR spectrum of **124a** in DMSO-d_6.

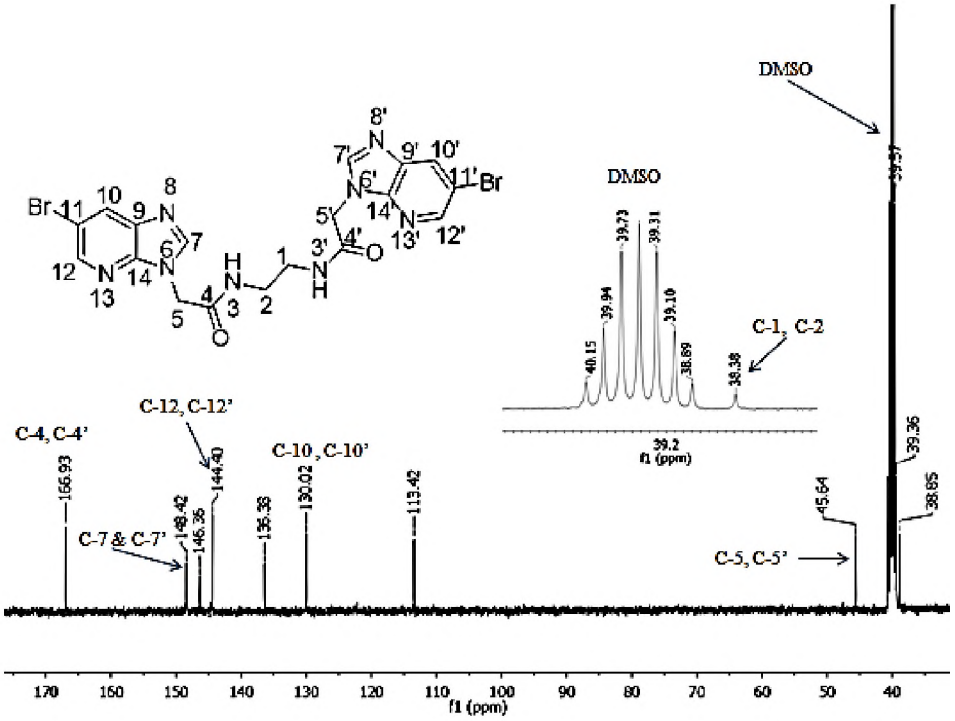

Figure 32. 100 MHz ^{13}C NMR spectrum of **124a** in DMSO- d_6.

The 7-azabenzimidazole protons 7-H and 7'-H (which are far removed from other aromatic protons) gave rise to the singlet at 8.46 ppm (Figure 33). With the aid of an HSQC experiment, it was shown that this proton signal correlates with the ^{13}C signal at 148.4 ppm on the ^{13}C spectrum; corresponding to C-7 and C-7' (Figures 32 and 34). Protons 10-H/ 10'-H and protons 12-H/ 12'-H however have a *meta*-arrangement and this results in a small coupling between the pairs. The 10-H/ 10'H signal appears at 8.38 ppm with a coupling constant of 1.5 Hz. The C-10/ C-10' correspond to the signal at 130.0 ppm on the ^{13}C NMR spectrum. The 12-H, 12'-H are represented by the proton signal at 8.44 ppm in the ^{1}H NMR spectrum and C-12 and C-12' correspond to the signal at 140.4 ppm on the ^{13}C NMR spectrum. The carbonyl carbons C-4/ C-4' correspond to the signal at 166.9 ppm on the ^{13}C NMR spectrum (Figure 32).

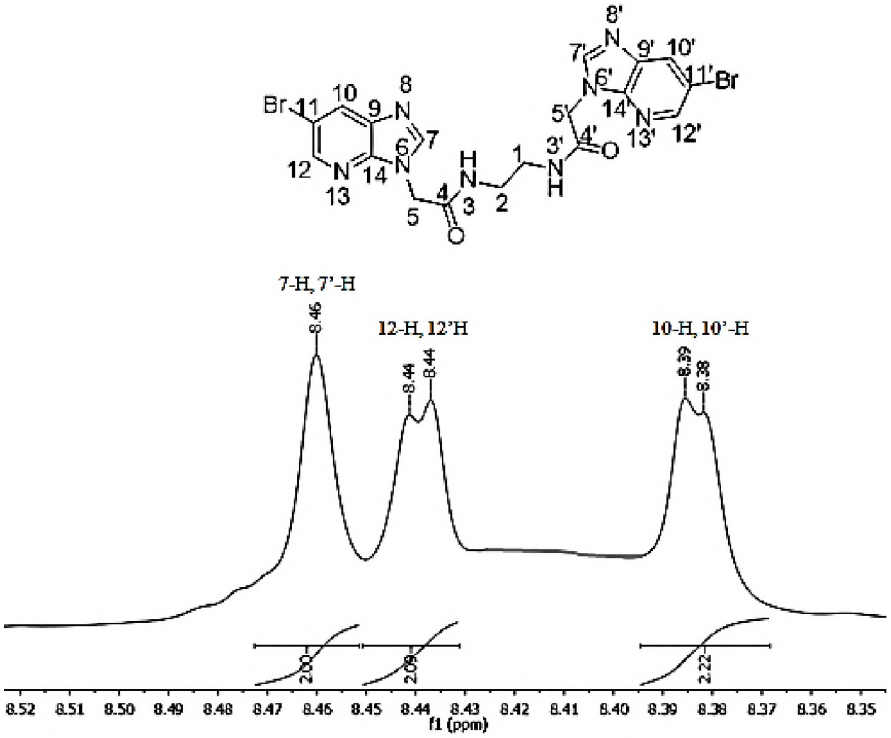

Figure 33. 400 MHz ^{1}H NMR spectrum of **124a** in DMSO-*d6* (expanded).

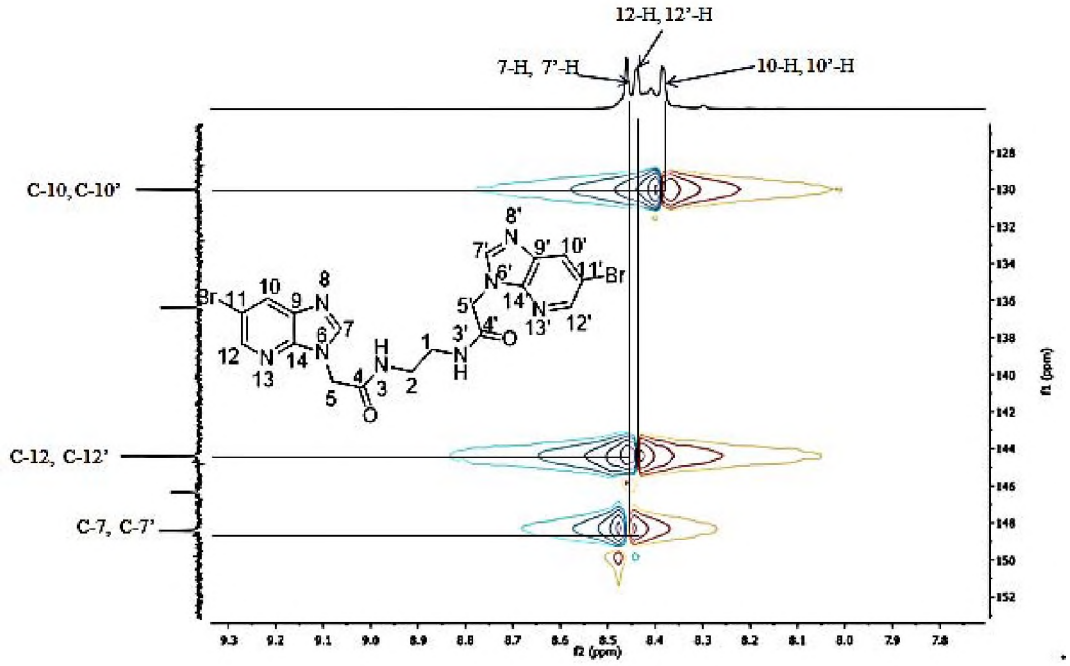

Figure 34. 400 MHz HSQC NMR spectrum of **124a** in DMSO- d_6 (expanded).

2.1.6. Biological Activity of substituted 5-Bromo-1-[(*N*-carbamoyl)methyl]-7-azabenzimidazoles 122a-l, *N,N'*-bis[2-(5-bromo-7-azabenzimidazol-1-yl)-2-oxoethyl]ethylene-1,3-diamine 124a and –cyclohexyl-1,2-diamine 124b.

The compounds **122a-l** and **124a,b** were assessed against HeLa (human cervix adenocarcinoma) cells to determine their cytotoxicity. A resazurin-based assay was used to determine the percentage of surviving cells by reading the resorufin fluorescence data using a multiplate reader. The cytotoxicity results (as presented in Table 2) show that none of the tested compounds is significantly cytotoxic (Figure 35). It is also to be noted that none of the twelve compounds was significantly viable against *P. faciparum* and *T. brucei*.

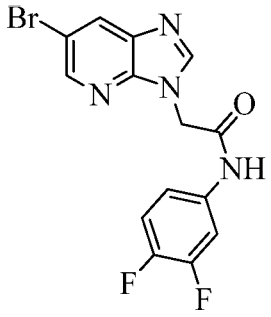

122e

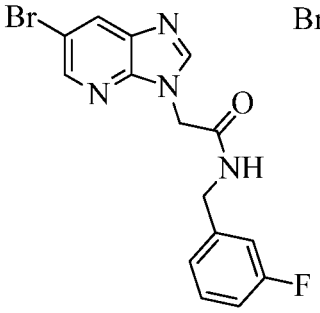

122f

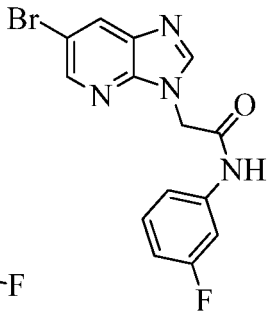

122h

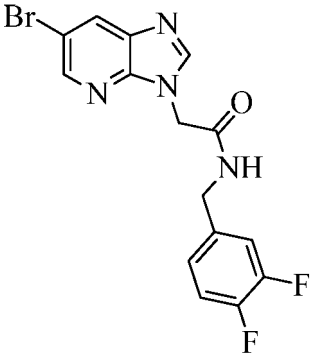

122i

Table 2. Viability of HeLa cell and parasite viability in the presence of **122a-l** and **124a-b** at 20 μM.

Compound	**HeLa Cell viability (%)**	***P. f.* strain 3D7 Parasite viability (%)**	***T.brucei* Parasite viability (%)**
122a	104	71	95
122b	110	88	105
122c	91	104	101
122d	98	106	102
122e	92	66	92
122f	101	123	88
122g	94	101	99
122h	100	77	96
122i	99	79	99
122j	88	106	100
122k	90	120	102
122l	89	116	96
124a	96	120	95
124b	92	105	100

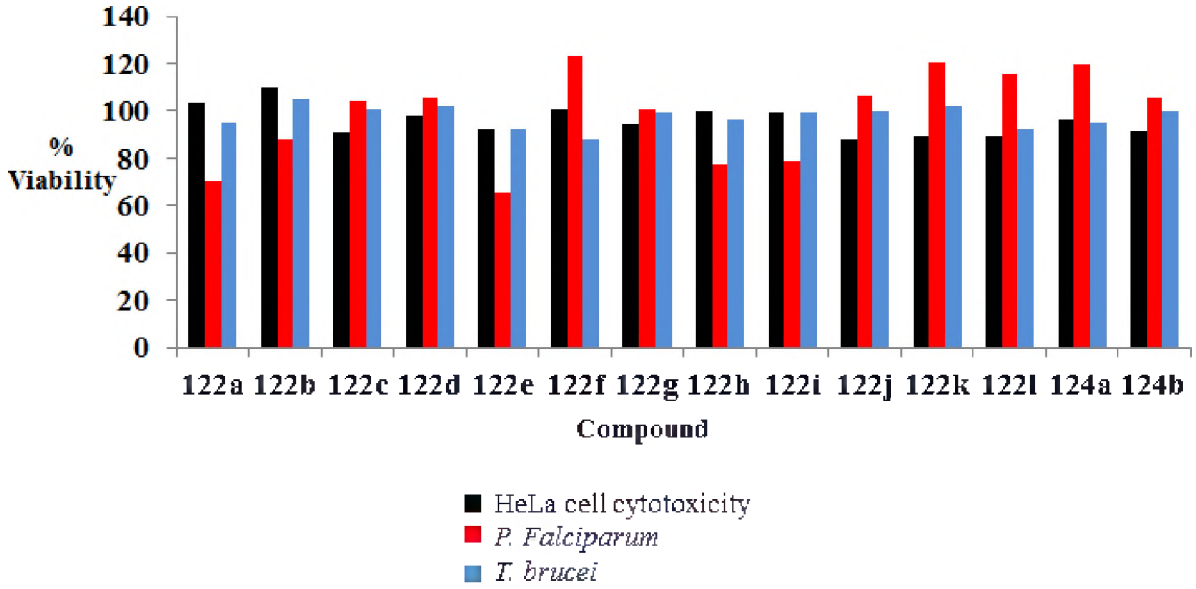

Figure 35. HeLa Cells survival and parasite viability in the presence of **122a-l** and **124a-b** at 20 μM**.**

2.2. PREPARATION OF 2-PHENYL-7-AZABENZIMIDAZOLES 125a-m.

In an attempt to retain the amino proton of 7-azabenimidazole while extending the aromatic system, 2-phenyl-7-azabenzimidazoles **125a-m** were prepared from 2,3-diaminopyridine **101** and 5-bromo-2,3-diaminopyridine **114**. The target compounds could be achieved by acetic acid mediated condensation between the diaminopyridines and triethyl orthoformate **102** followed by C-2-arylation, but this would pose a serious challenge in that the C-2-arylation process requires an expensive catalyst and ligands, and the number of possible derivatives is limited. We opted for a modified method reported by Singh *et al*., which is a thermal condensation of in selected benzaldehydes with **101** and **114** in refluxing nitrobenzene. [108]

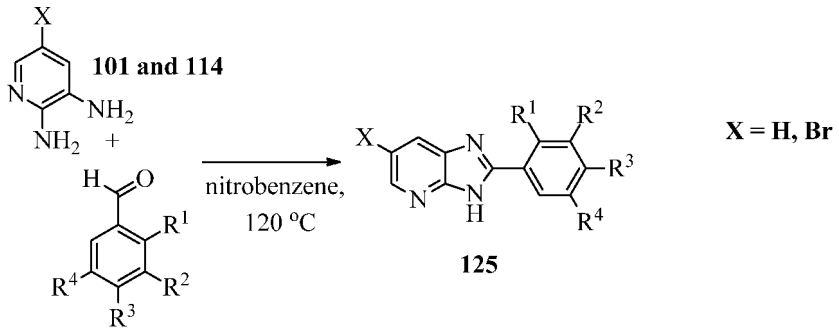

Scheme 11. Synthesis of 2-phenyl-7-azabenzimidazoles.

In the report published by Singh *et al.*, after 24 hours the nitrobenzene was evaporated and the crude product was purified by flash chromatography using an equal volume of hexane and ethyl acetate as eluent.[108] Given that nitrobenzene boils at 210.9 °C (there was difficulty in evaporating off the solvent even under vacuum) and the high polarity of the azabenzimidazoles (they interact with silica gel and were therefore difficult to purify by chromatography using silica gel), it was envisaged that generating precipitates of the 2-phenyl-7-azabenzimidazoles will be less tedious as a work-up procedure and isolated yields could be maximized. The major modifications were lower reaction temperature (lowered by 30 °C) and, in the work-up procedure, the crude mixture was allowed to cool to room temperature and diluted with ethyl acetate to generate the precipitates which were filtered and washed thoroughly with ethyl acetate. Yields of 61-89% were recorded for the isolated products (Table 3). It is to be noted that the ethyl acetate was able to dissolve and wash away the unreacted starting materials.

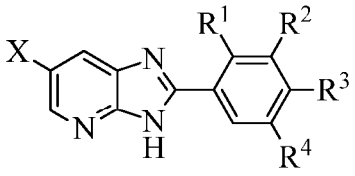

X = H, Br

125

Table 3. 2-Phenyl-7-azabenzimidazole derivatives and yields.

Compounds	R^1	R^2	R^3	R^4	X	Yield %
125a	OH	H	H	NO_2	H	78
125b	OH	OH	OH	H	H	73
125c	OH	Cl	H	Cl	H	80
125d	OH	OH	H	H	H	68
125e	H	OH	H	H	H	61
125f	H	H	Cl	H	H	88
125g	OH	H	H	Cl	H	77
125h	NO_2	OCH_3	H	H	H	81
125i	OH	H	H	NO_2	Br	75
125j	OH	H	H	Cl	Br	89
125k	OH	OCH_3	H	H	Br	63
125l	H	OH	OH	H	Br	63
125m	OH	OH	H	H	Br	67

NMR experiments were employed to verify the formation and purity of the target compounds. Figure 36 shows the proton NMR spectrum for 2-(2-hydroxyl-3,5-dichlorophenyl)-7-azabenzimidazole **125c**. The broad signal at 14.04 ppm in the ^{1}H NMR spectrum confirmed the presence of the phenolic OH, and the broadness of the signal suggests hydrogen bonding with the imidazole nitrogen. The doublet of doublets at 7.37 ppm can only be attributed to 5-H on the pyridyl ring, as the only proton flanked by two different protons. Thus, according to the correlation observed in the HSQC spectrum (Figure 37), the ^{13}C at 119.3 ppm corresponds to the attached C-5.

The COSY spectrum (Figure 38) showed crosspeaks with 5-H at 8.45 ppm and 8.14 ppm, corresponding to the pyridyl protons 4-H and 6-H. These were differentiated by comparison of the chemical shifts of the attached carbons – C-6 being significantly deshielded by the attached nitrogen, resonating at 145.3 ppm (thus, 6-H appears at 8.45 ppm). The remaining aromatic signals at 8.20 and 7.72 ppm have a small coupling constant (J = 2.2 Hz) consistent with a *meta* arrangement and were reasonably assigned to 11-H and 13-H, respectively.

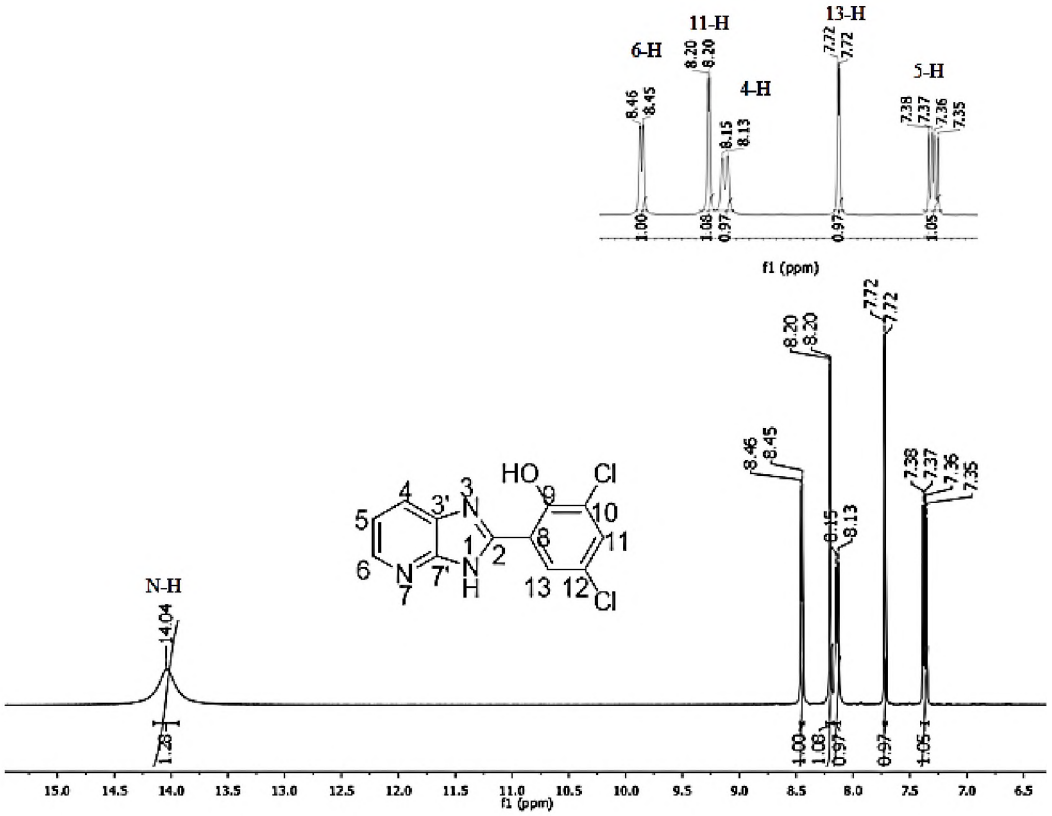

Figure 36. 400 MHz ^{1}H NMR spectrum of **125c** in DMSO-d_6.

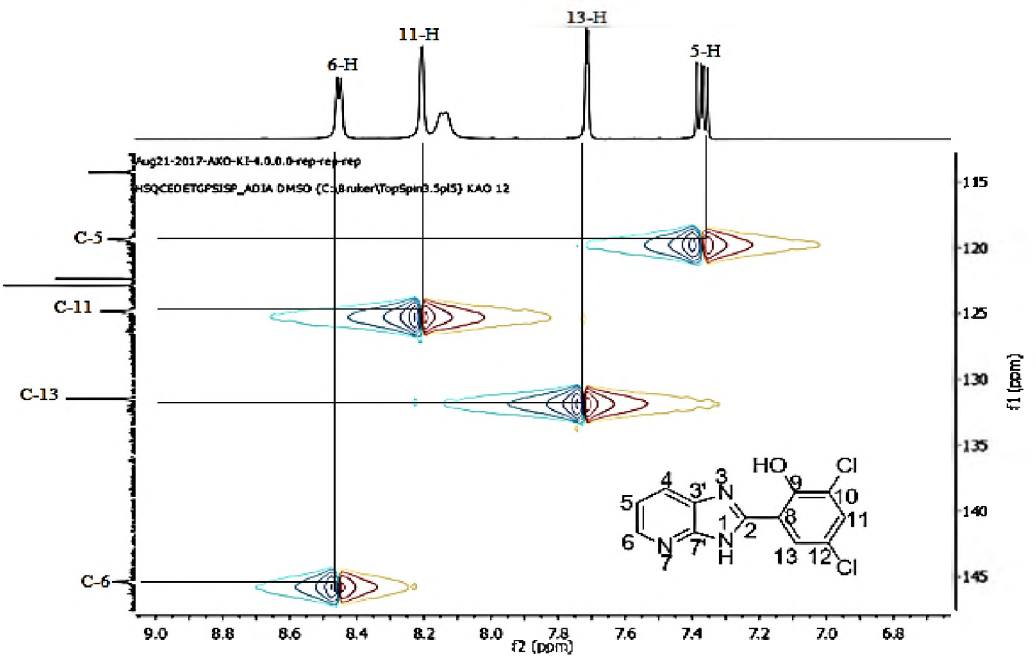

Figure 37. HSQC NMR spectrum of 125c in DMSO-d_6

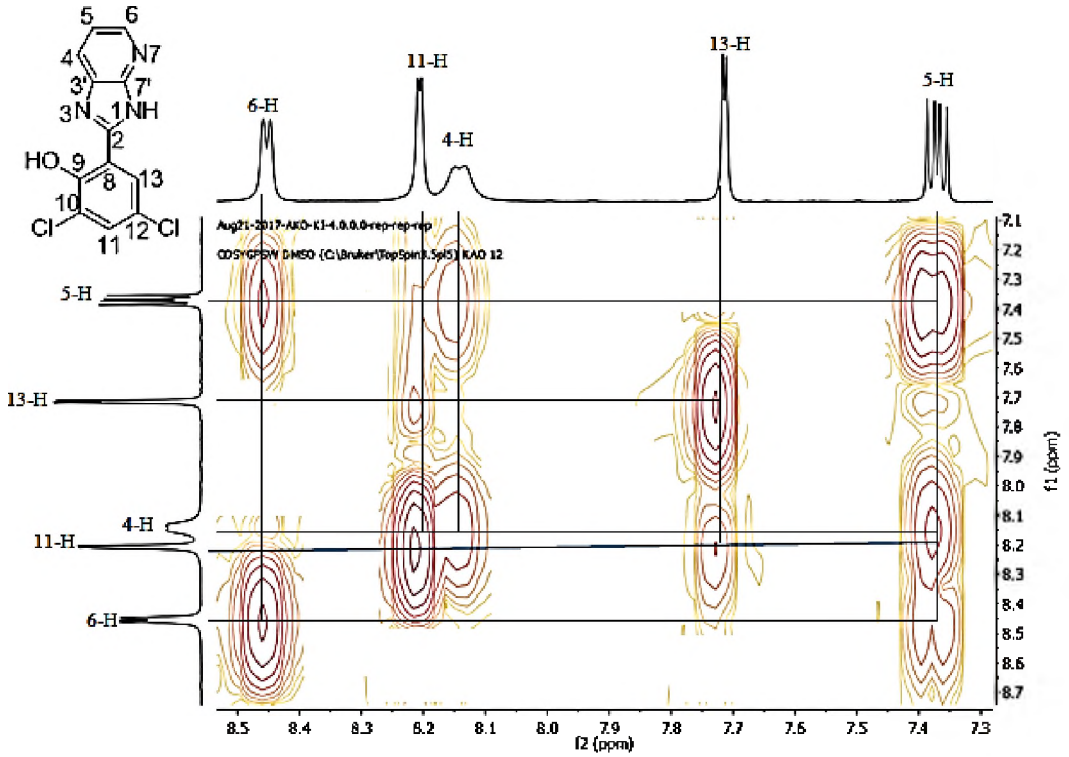

Figure 38. 400 MHz COSY NMR spectrum of **125c** in DMSO-d_6.

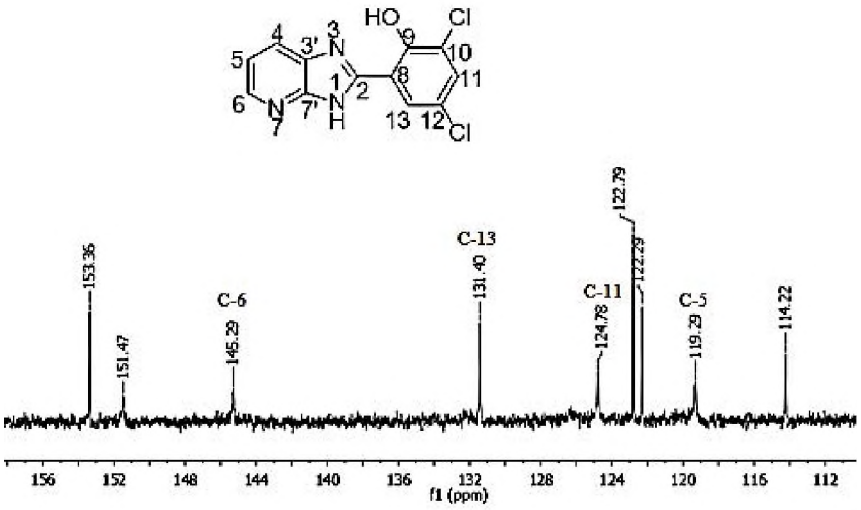

Figure 39. 100 MHz ^{13}C NMR spectrum of **125c** in DMSO-d_6.

The apparent absence of the signals corresponding to the quaternary carbons (Figure 39) in the 7-azabenzimidazole system is presumed to be due to line broadening effects associated with proton transfer between the tautomers **125c$_i$** and **125c$_{ii}$**.

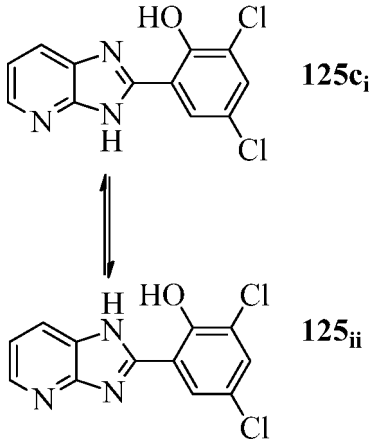

125c$_i$

125$_{ii}$

.

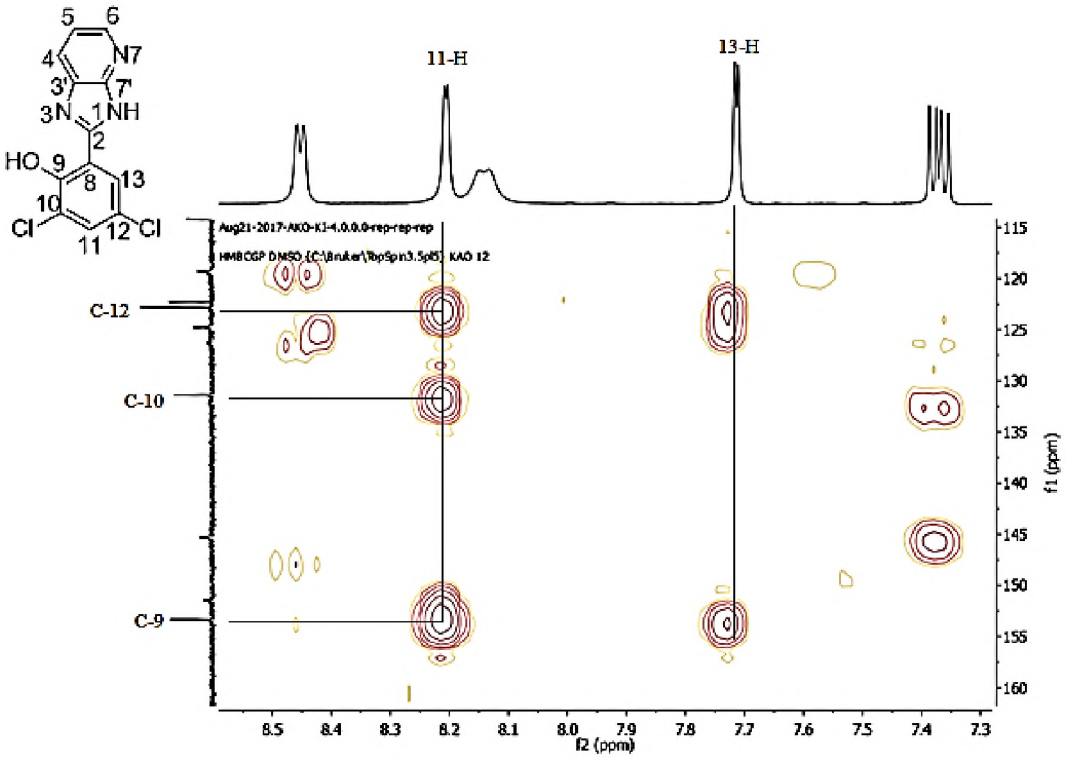

Figure 40. HMBC NMR spectrum of **125c** in DMSO-d_6.

Heteronuclear multiple bond correlation (HMBC) was used to assign chemical shifts for quaternary carbons for C-9, C-12 and C-10, the HMBC spectrum indicated that there is a two-bond coupling of proton 11-H to C-12 and a two-bond coupling of 13-H to C-12. The HMBC experiment also shows a three-bond coupling of 13-H to C-9 and a three-bond coupling of 11-H to C-9 (Figure 40).

The HPLC-MS analysis for compound **125c** ($C_{12}H_8Cl_2N_3O$ 280.0044) showed the presence of $[M+H]^+$ 279.9831 peak.

2.2.1. Anti-Parasitic Protozoan Activities of 2-Phenyl-7-azabenzimidazoles

A series of the above 2-phenyl-7-azabenzimidazoles **127a-m** were assessed against HeLa (human cervix adenocarcinoma) cells at a concentration of 20 μM in order to determine the overt cytotoxicity of these compounds as described earlier.

On these compounds, only **125a** and **125h** showed some toxicity (41% and 55%, respectively) against HeLa cells (Table 4 and Figure 41). It is to be noted that those that have an electron withdrawing bromine atom as substituent 'X' have the lowest toxicity of these compounds and this is particularly noticeable when comparing compound **125a** which had a

percentage cell viability of 41% and compound **125i** with a percentage cell viability of 87%. This was further confirmed by comparing **125d** (75%) and **125m** (107%) Figure 42).

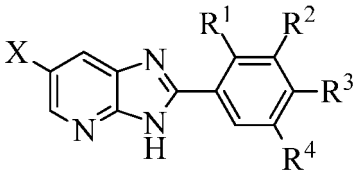

125a-m

Table 4. Percentage cell viability of **125a-m** against HeLa cells and standard deviation at 20 μM.

Compound	Cytotoxicity HeLa Cell viability (%)	Standard deviation
125a	41	2
125b	70	0.3
125c	86	11
125d	75	2
125e	79	4
125f	80	5
125g	94	7
125h	55	8
125i	87	15
125j	94	1
125k	81	14
125l	82	1
125m	107	9

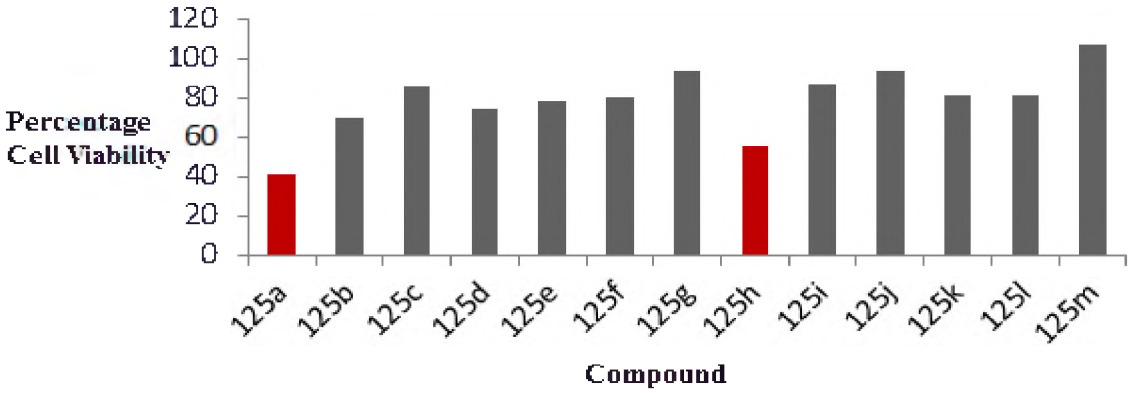

Figure 41. % HeLa cell viability obtained for 125a-m 20 μM.

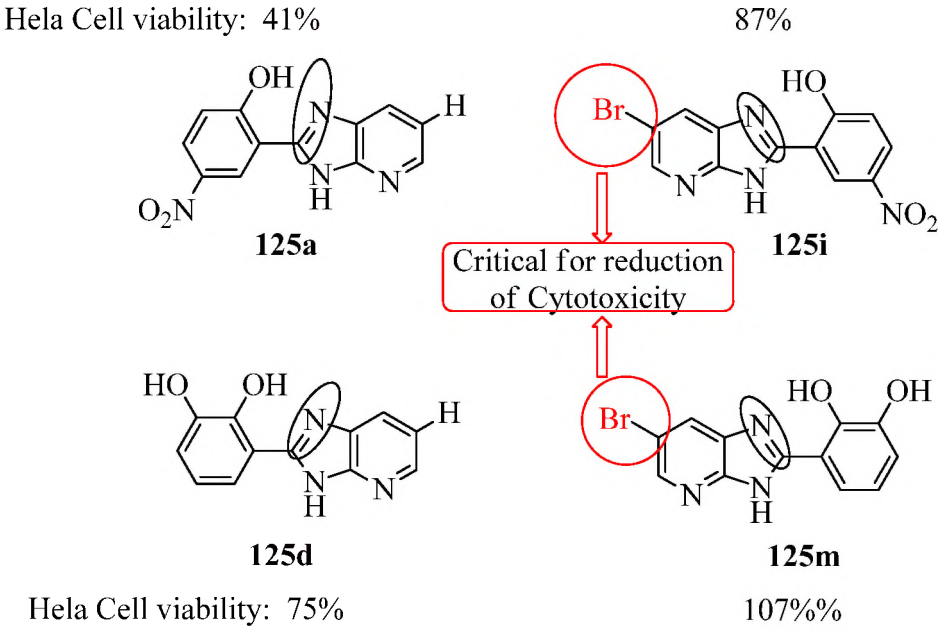

Figure 42. The presence of bromine at position-5 correlates with reduction of cytotoxicity.

These compounds were also tested against *T. brucei* at 20 μM. Compounds **125b**, **125d**, **125i**, **125k**, **125l** and **125m** show significant activity against *T. brucei* (Table 5). Compound **125a** has a parasite viability of 88% (against *T.brucei*) but on substituting the hydrogen at position with a bromine atom in compound **125a**, the activity of this compound was significantly increased and a parasite viability of 33% was recorded. By contrast compounds **125d** in which 'X' is a hydrogen atom and **125m** where 'X' is a bromine atom had the same percentage parasite viability against *T. brucei*. The best performance against *T. brucei* was by **125b** with a parasite viability of 17% (Table 5, Figures 43 and 44) compared with Hela cell viability of 70%.

Table 5. Percentage viability of *T. brucei* in the presence of **125a-m** at 20 μM.

Compound	*T.brucei* Parasite viability (%)	Standard deviation
125a	88	3
125b	17	1
125c	104	7
125d	20	3
125e	83	3
125f	99	1
125g	97	0.1
125h	61	2

125i	33	3
125j	111	2
125k	36	1
125l	43	3
125m	20	1

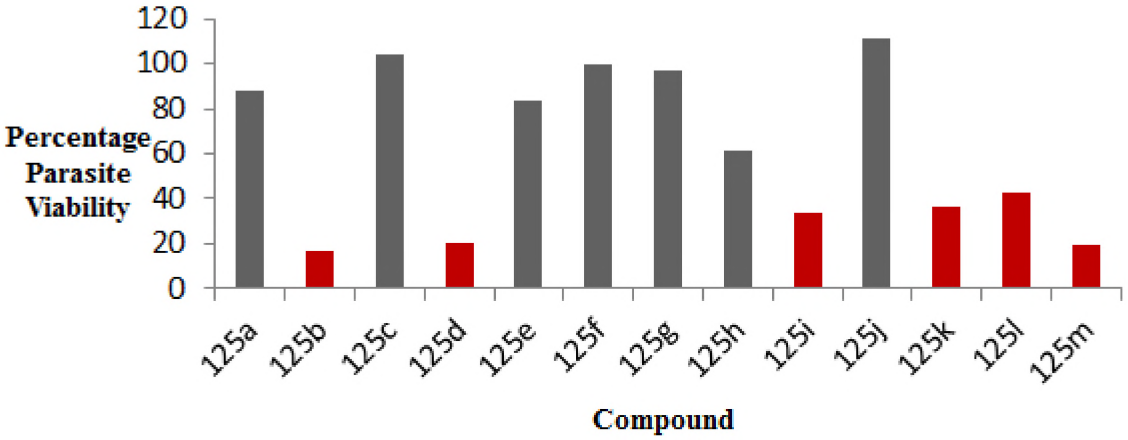

Figure 43. % *T. brucei* parasite viability obtained for **125a-m** 20 μM.

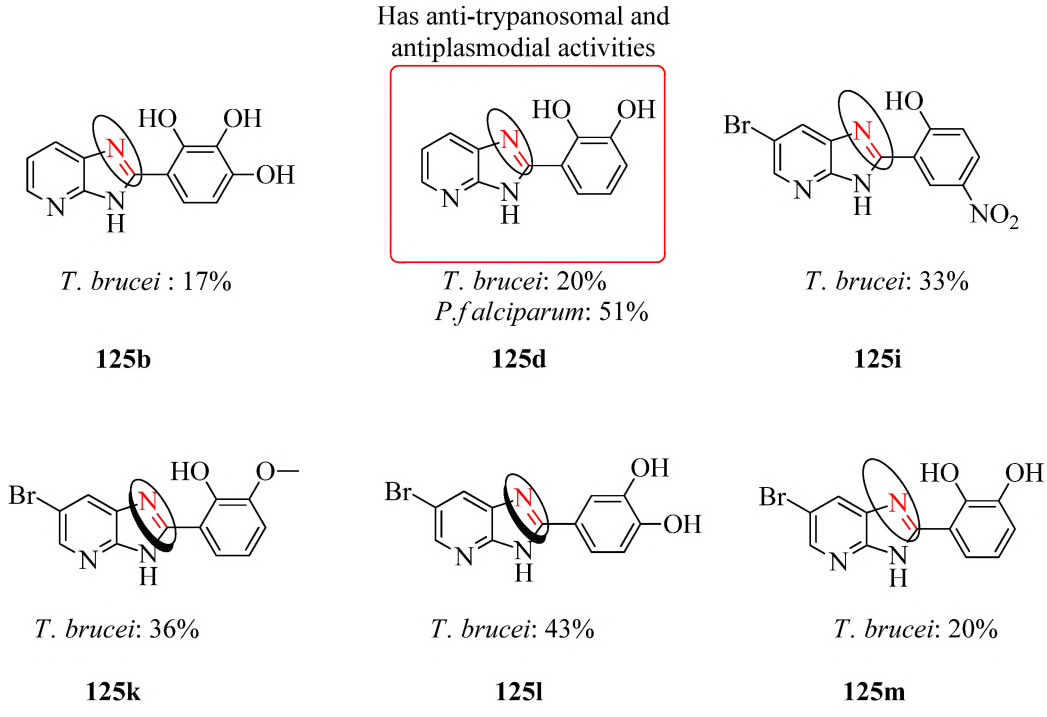

Figure 44. Active 2-phenyl-7-azabenzimidazoles from this study.

On screening these compounds for antimalarial activity, compound **125d** proved to be the best scaffold for further optimization. Other compounds do not show significant activities against the parasite lactate dehydrogenase (pLDH) [Table 6 and Figures 44 and 45].

Table 6. **125a-m** against *P. f.* strain 3D7 at 20 μM.

Compound	*P. falciparum* strain 3D7 Parasite viability (%)	Standard deviation
125a	148	4
125b	123	3
125c	128	0.3
125d	51	9
125e	125	15
125f	113	27
125g	71	4
125h	83	11
125i	112	11
125j	124	6
125k	106	3
125l	100	13
125m	93	0.3

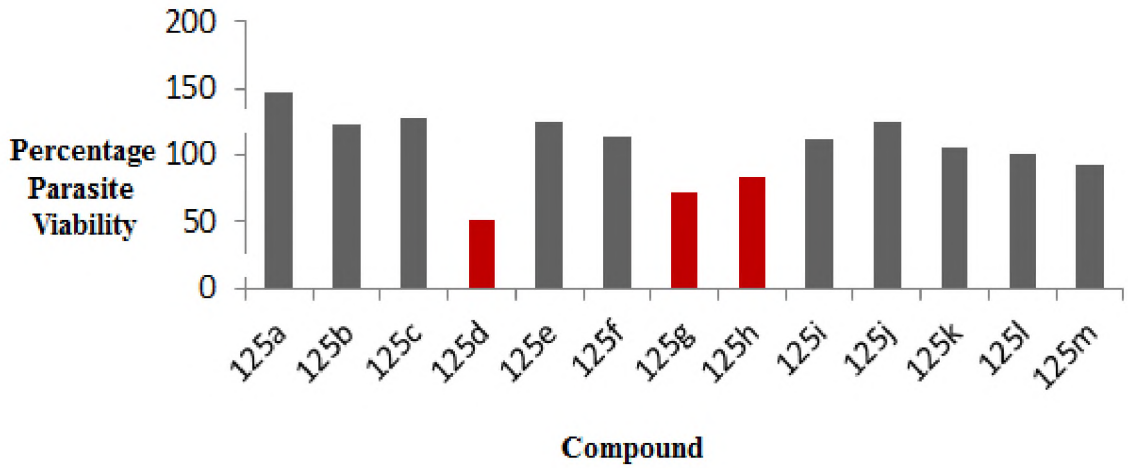

Figure 45. % parasite viability obtained in the presence of **125a-m** at 20 μM.

2.3. REGIOSELECTIVE FORMYLATION OF 2,3-DIAMINO-5-BROMO-PYRIDINE TO GENERATE 2-AMINO-5-BROMO-7-(BENZYLIMINO)PYRIDINES AND THEIR BENZYLAMINO ANALOGUES

This reaction was the result of an idea to open ring **B** of compound **125** to generate 2-amino-5-bromo-7-(benzylimino)pyridines **126a-h** (scheme 12). This was rationale in order to increase the flexibility between the pyridyl and phenyl rings, with the hope to prepare 2-amino-7-(benzylimino)pyridines, believed to be intermediates in the above synthesis 2-phenyl-7-azabenzimidazoles. However, they were not isolable by the synthetic method we used.

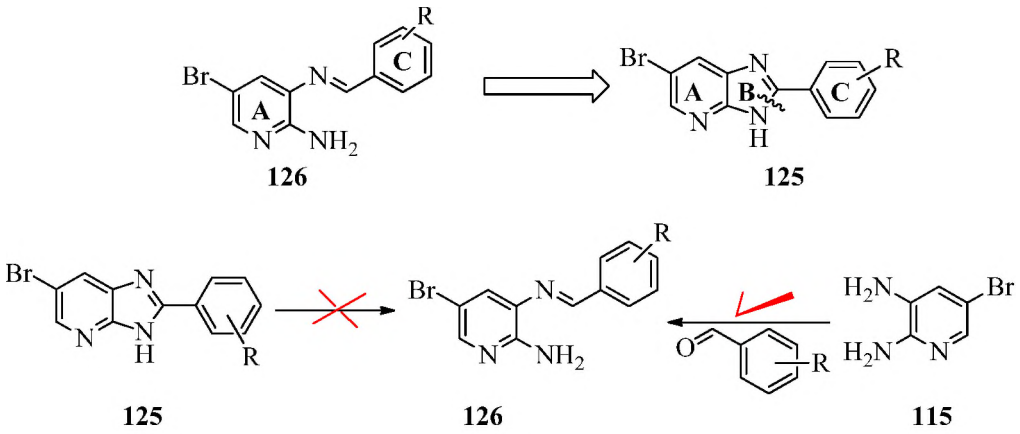

Scheme 12. Rationale for design of 2-amino-5-bromo-7-(benzylimino)pyridines **126a-h**.

A thorough literature search showed no synthetic route to compound **126** from **125** but it was proposed that 2,3-diamino-5-bromopyridine **115** could be formylated regio-selectively at the β-amino substituent. This regio-selectivity towards the β-amino substituent is possible because the α-amino substituent is less basic than the β-amino substituent (*o*-amino and *o*-nitro groups on pyridine rings enhance the acidity of their conjugate acids). The amino substituent at position 3 of 2,3-diamino-5-bromopyridine **115** is more basic and consequently, more nucleophilic than the amino substituent at position 2.[124, 125, 130, 131]

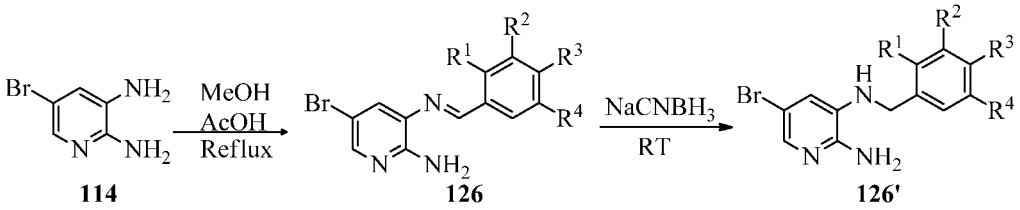

Scheme 13. Synthesis of 2-amino-5-bromo-7-(benzylimino)pyridines.

In this preparation of 2-amino-5-bromo-7-(benzylimino)pyridines **126a-h**, 2,3-diamino-5-bromopyridine **115** was condensed with one equivalent of the appropriate benzaldehyde in the presence of a catalytic amount of glacial acetic acid using methanol as solvent (Scheme 13). ^{1}H, ^{13}C and 2-D NMR analysis showed that the desired product were the only isolated entities after reacting for 20 minutes under reflux with yields between 65% and 88% (Table 7).

Table 7. 2-Amino-5-bromo-7-(benzylimino)pyridines.

Compound	R^1	R^2	R^3	R^4	Yield %
126a	OH	OH	OH	H	65
126b	OH	OCH_3	H	H	81
126c	OH	H	H	Cl	76
126d	OH	Cl	H	Cl	76
126e	OH	Br	H	Br	88
126f	OH	H	OCH_3	H	78
126g	H	OH	OH	H	71
126h	OH	OC_2H_5	H	H	86
126b'	OH	OCH_3	OH	H	89
126e'	OH	Br	H	Br	90
126f'	OH	H	OCH_3	H	94

The structures of the products were confirmed by infrared, ^{1}H and ^{13}C NMR spectroscopy as well as mass spectroscopy (MS). The HPLC-MS analysis for **126f** ($C_{13}H_{13}BrN_3O_2$ 322.0191) indicated the presence of $[M+H]^+$ 322.0006 peak. The ^{1}H NMR spectrum of 2-amino-5-bromo-7-(2-hydroxy-4-methoxybenzylimino)pyridine **126f** (Figure 46) contained only eight signals. The three methoxyl protons ($O-CH_3$) correspond to the singlet at 3.81 ppm, and HSQC analysis confirmed that the ^{13}C signal at 55.5 ppm corresponds to the methyl group C-15 (Figures 47 and 49). The singlet at 6.07 ppm most likely corresponds to the two α-amino protons (NH_2) and the singlet at 8.78 ppm (8-H) is consistent with a proton on the imine (N=C-H). HSQC analysis correlated this proton signal to the ^{13}C signal at 163.8 ppm (Figures 48 and 50). The broad signal at 12.30 ppm corresponds to the hydroxyl proton (OH).

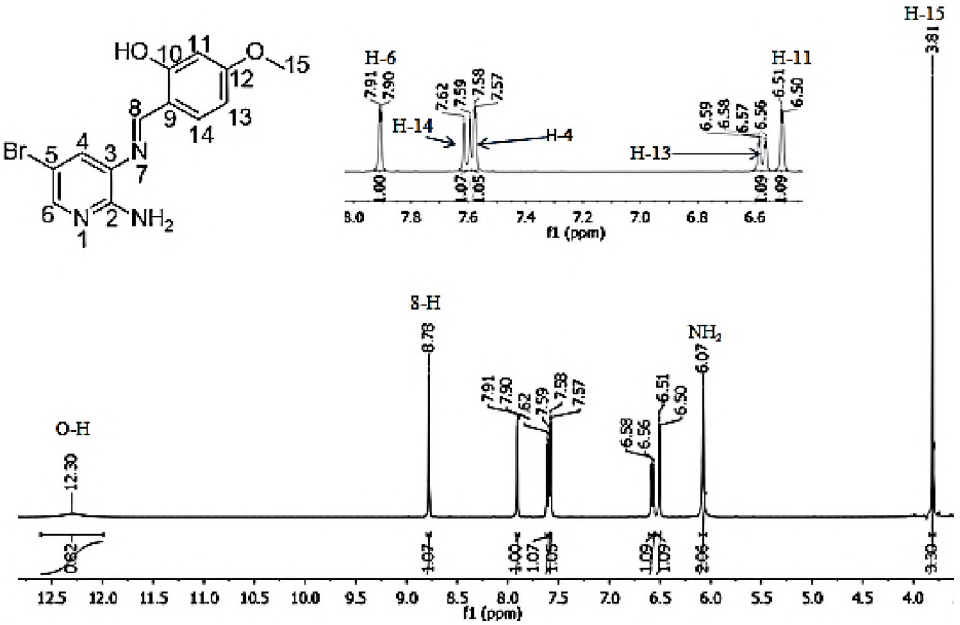

Figure 46. 400 MHz ^{1}H NMR spectrum of **126f** in DMSO-d_6.

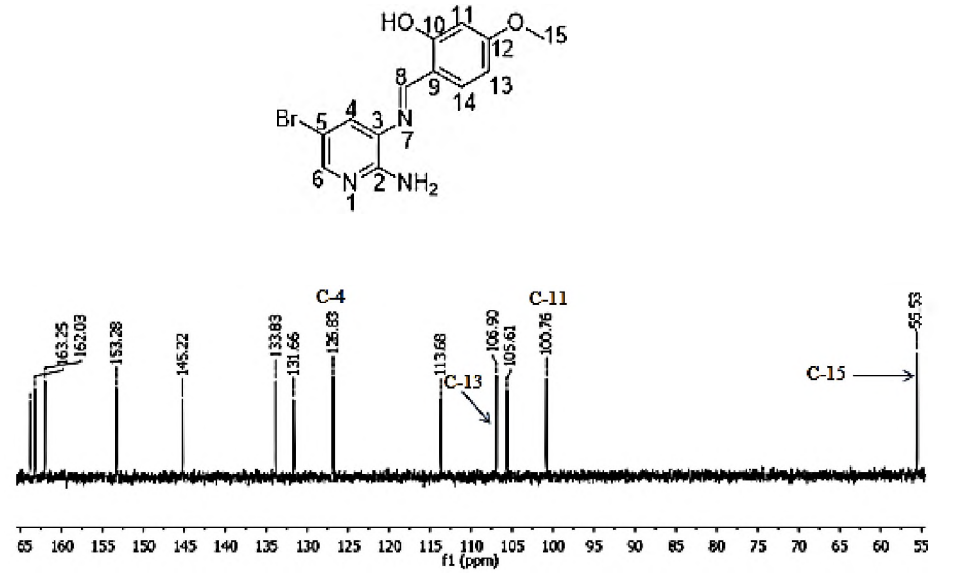

Figure 47. 100 MHz ^{13}C NMR spectrum of **126f** in DMSO-d_6.

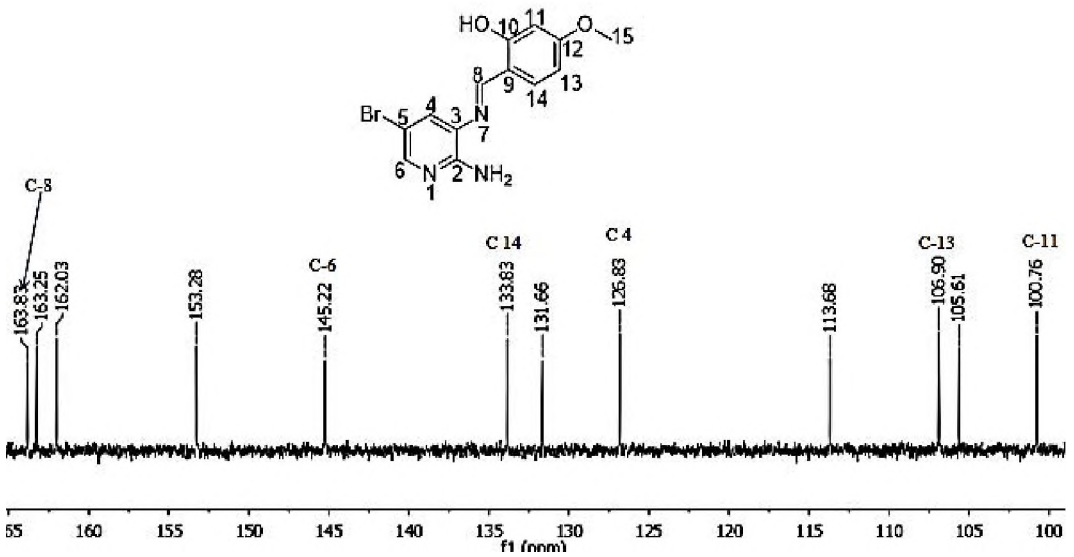

Figure 48. 400 MHz ^{13}C NMR spectrum of **126f** in DMSO- *d*$_6$ (expanded).

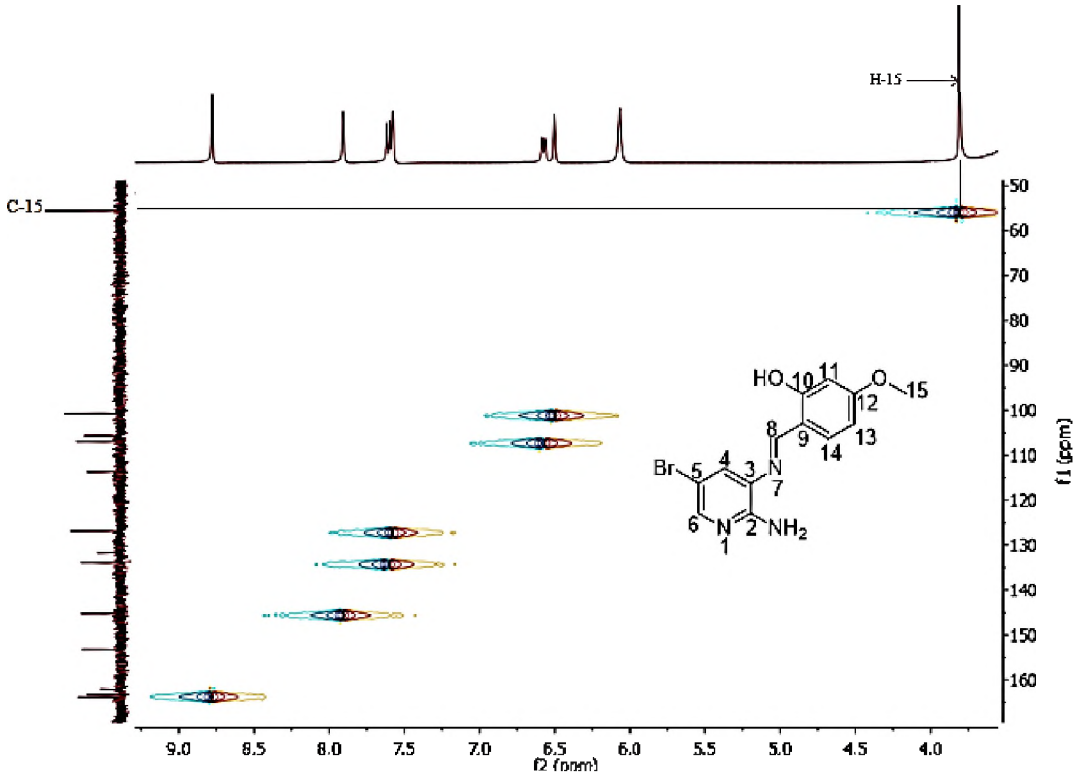

Figure 49. HSQC spectrum of **126f** in DMSO-*d*$_6$.

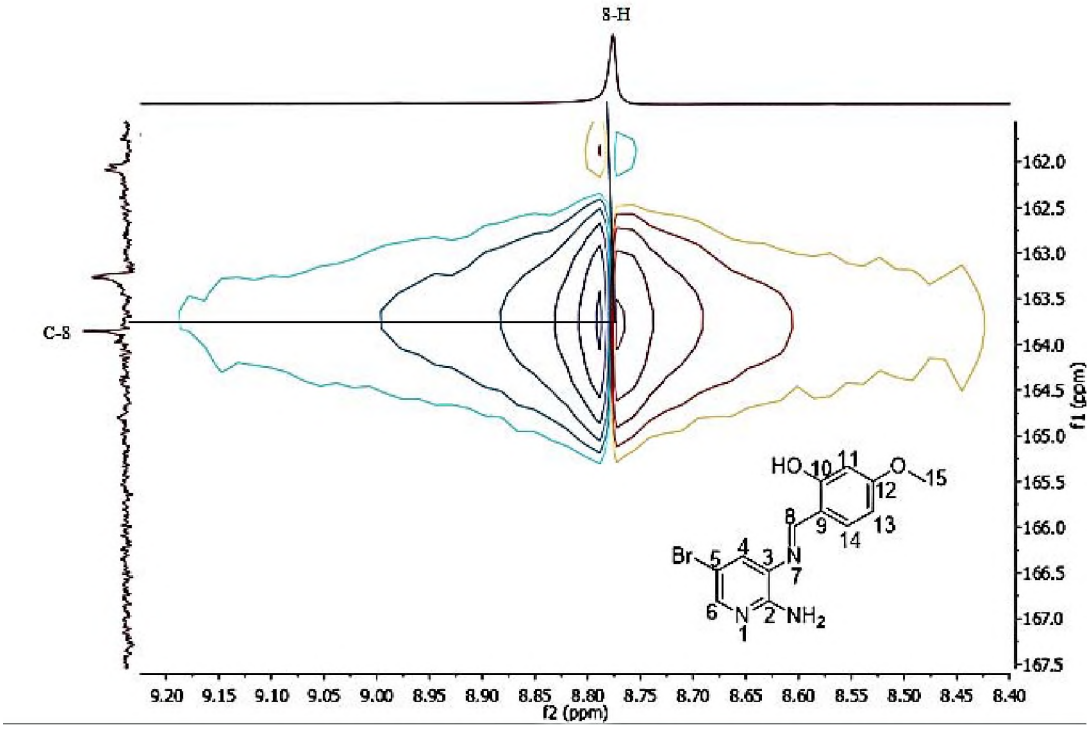

Figure 50. Partial HSQC spectrum of **126f** in DMSO-d_6 (expanded).

Other proton signals include the aromatic 13-H whose corresponding signal is a doublet of doublets resonating at 6.57 ppm. As expected, the proton signal appeared as doublet because it couples to14-H (J = 8.6 Hz) and doublet of doublets because of the small coupling with 11-H (J=2.3 Hz). 11-H resonates as a doublet at 6.50 ppm (2.3 Hz). 14-H couples to 13-H as seen in the COSY spectrum (Figure 51) and at 7.60 ppm with coupling constant of 8.6 Hz. The pyridyl protons 6-H and 4-H exhibit *meta*-coupling; a doublet at 7.91 ppm with coupling constant of 2.0 Hz corresponds to 6-H because it is alpha to the pyridyl nitrogen atom while 4-H resonates as a doublet at 7.58 ppm (J = 2.0 Hz).

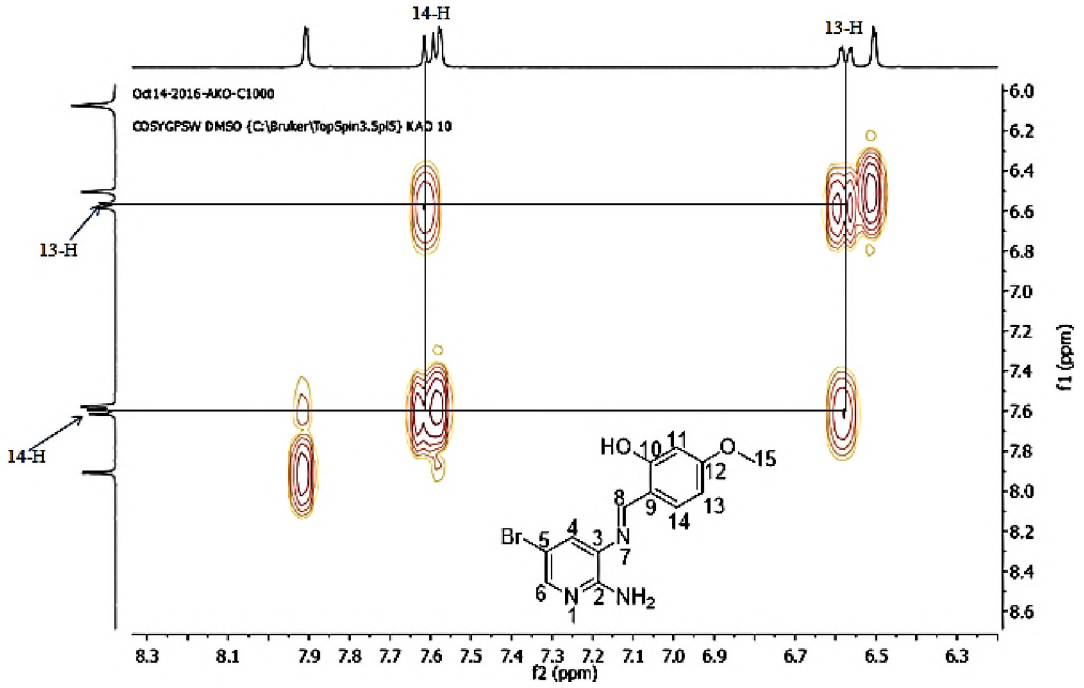

Figure 51. COSY spectrum of **126f** in DMSO- d_6.

The ^{13}C spectrum (Figures 51) clearly shows the signals necessary for all the appropriate ^{13}C atoms. The signals resonating at 145.2 and 126.8 ppm correspond to C-6 and C-4 as confirmed from the HSQC spectrum (Figure 50). Notable carbon signals of the phenyl ring resonate at 100.2 ppm (C-11), 106.9 ppm (C-13), 133.8 ppm (C-14) – all confirmed by correlations in the HSQC spectrum (Figures 47, 48 and 52).

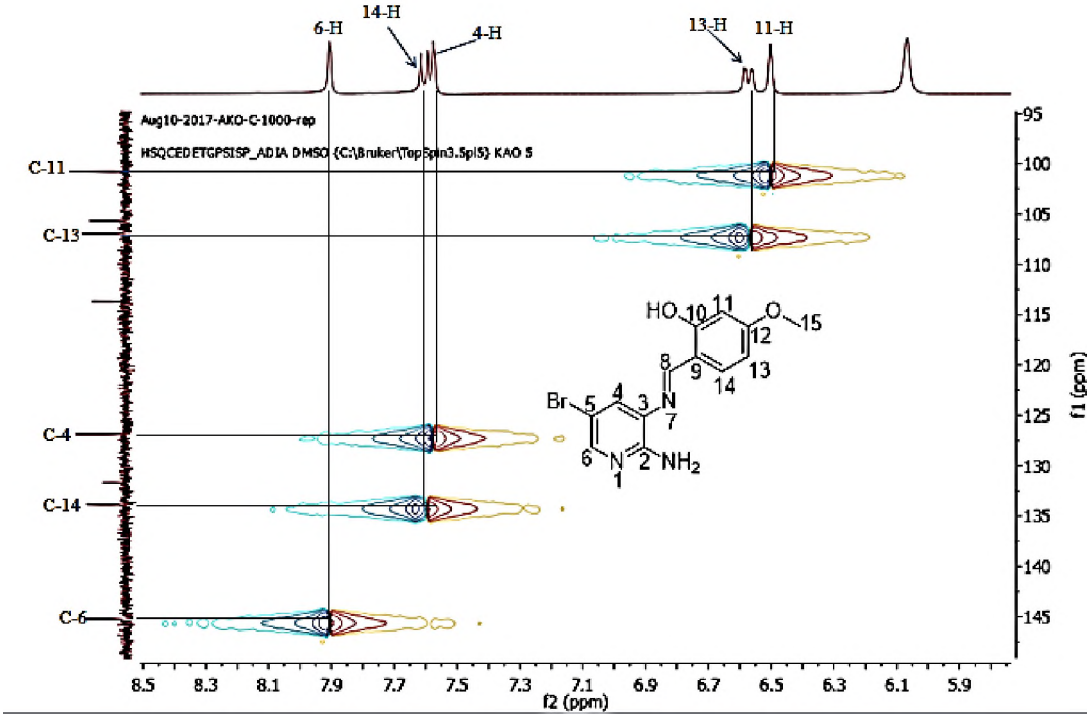

Figure 52. HSQC spectrum of **126f** in DMSO-d_6 (expanded).

The last step is the approach to the benzylamino pyridines and it involves hydrogenation of the imine group of compounds **126**. The reduction was performed using sodium cyanoborohydride, a well-known and effective reagent for the hydrogenation of the imines to amines. [132] The process was carried out in methanol as solvent at room temperature over a period of two hours. ^{1}H and ^{13}C NMR spectra of compound **126f** confirmed the success of this reaction process. The disappearance of the imino proton and the appearance of a methylene signal at 4.10 ppm and an amino signal (N-H) resonating at 5.45 (J = 5.5 Hz) were clear and unmistakeable (Figure 53). The COSY spectrum (Figure 54) shows the coupling between of amino and the methylene protons – the signal at 4.10 ppm has a coupling constant of 5.5 Hz confirming its identification as the corresponding methylene protons (CH_2) signal. The ^{13}C spectrum (Figure 55) exhibited a new signal corresponding to the methylene carbon atom at 40.8 ppm (C-8), and the DEPT-135 spectrum further confirms conversion of the imino group to a secondary amino group by showing the presence of the methylene carbon atom C-8 resonating at 41.3 ppm (Figure 56).

It is noteworthy to consider the fact that hydrogenation of the imines to amines lowers the chemical shift of surrounding proton signals (Table 8) due to the removal of both the

magnetic anisotropic deshielding effects and the delocalization potential of the imine group located between two aromatic rings. These proton assignments were made with the aid of the ^{1}H, COSY and HSQC spectra (Figures 52, 55-58).

Table 8. Effect of the reduction of the imino group in **125f** to the amino group in **126f** on chemical shifts (in ppm) of surrounding protons.

	Imines/ppm	**Secondary amine/ppm**
O-H	12.30	9.63
4-H	7.58	6.56
6-H	7.91	7.26
11-H	6.50	6.41
13-H	6.57	6.36
14-H	7.58	7.05
15-H	3.81	3.67

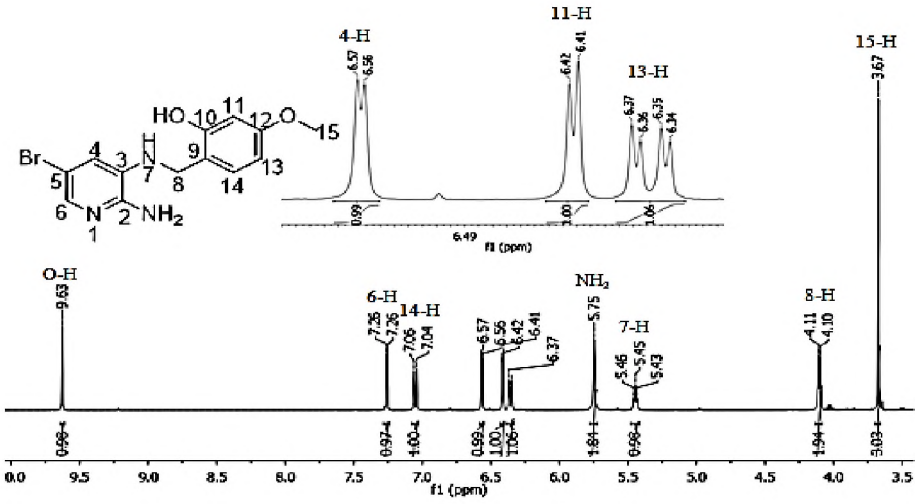

Figure 53. 400MHz ^{1}H NMR spectrum of **126f'** in DMSO-d_6.

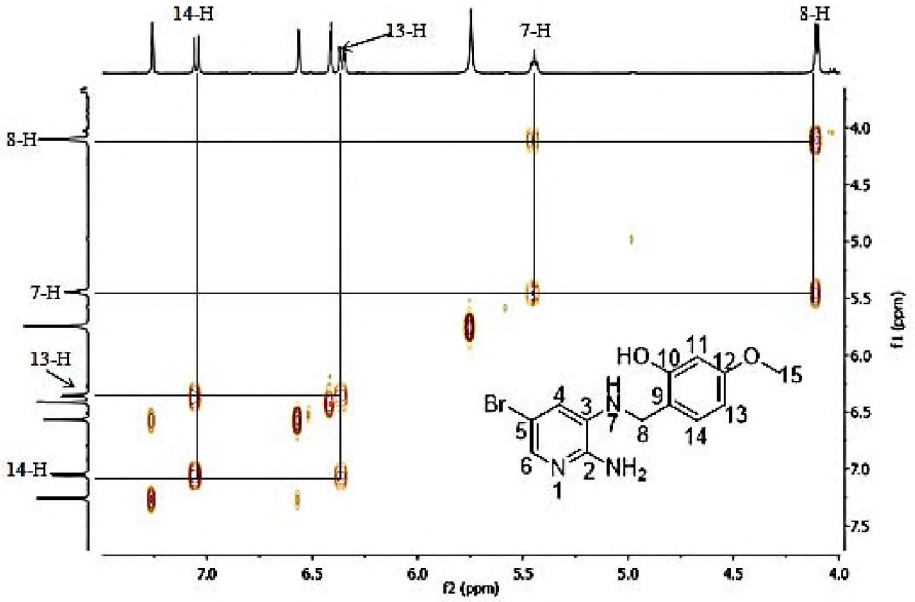

Figure 54. 400 MHz COSY spectrum of **126f'** in DMSO-d_6.

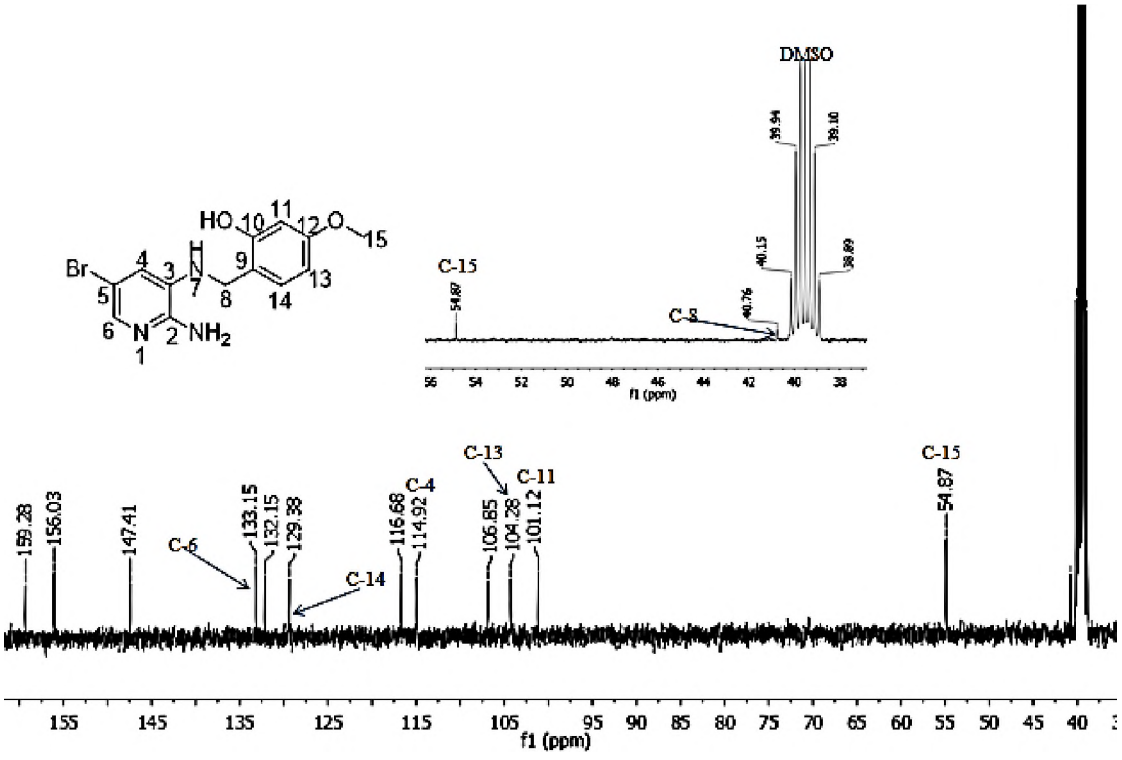

Figure 55. 100 MHz ^{13}C NMR spectrum of **126f'**in DMSO-d_6.

With the aid of ^{13}C (Figure 57) and HSQC spectra, it was established that the methoxyl carbon atom (C-15) resonates at 54.9 ppm while the pyridyl carbon atoms (C-6 and C-4) resonate at 133.2 and 115.4 ppm, respectively. The phenyl carbon atoms C-11, C-13 and C-14 correspond to the signals resonating at 101.1, 104.3 and 129.4 ppm, respectively.

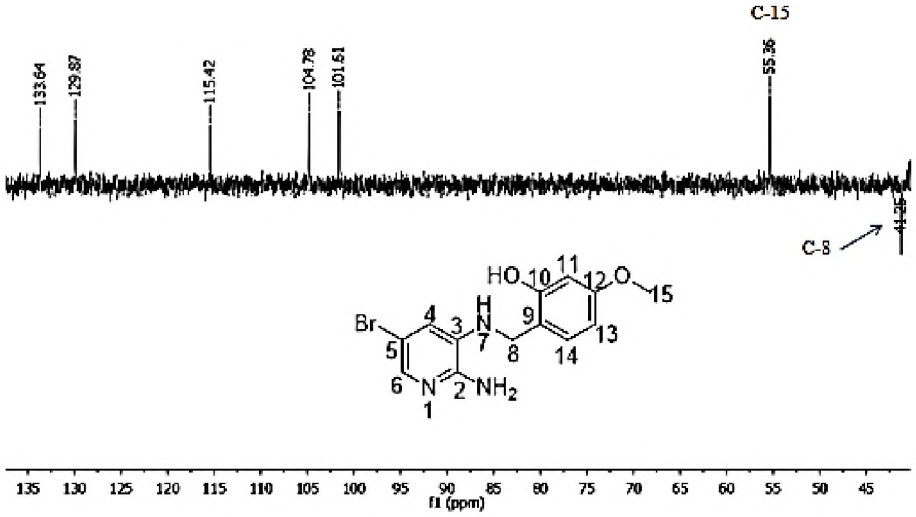

Figure 56. 100 MHz DEPT-135 spectrum of **126f'** in DMSO- d_6.

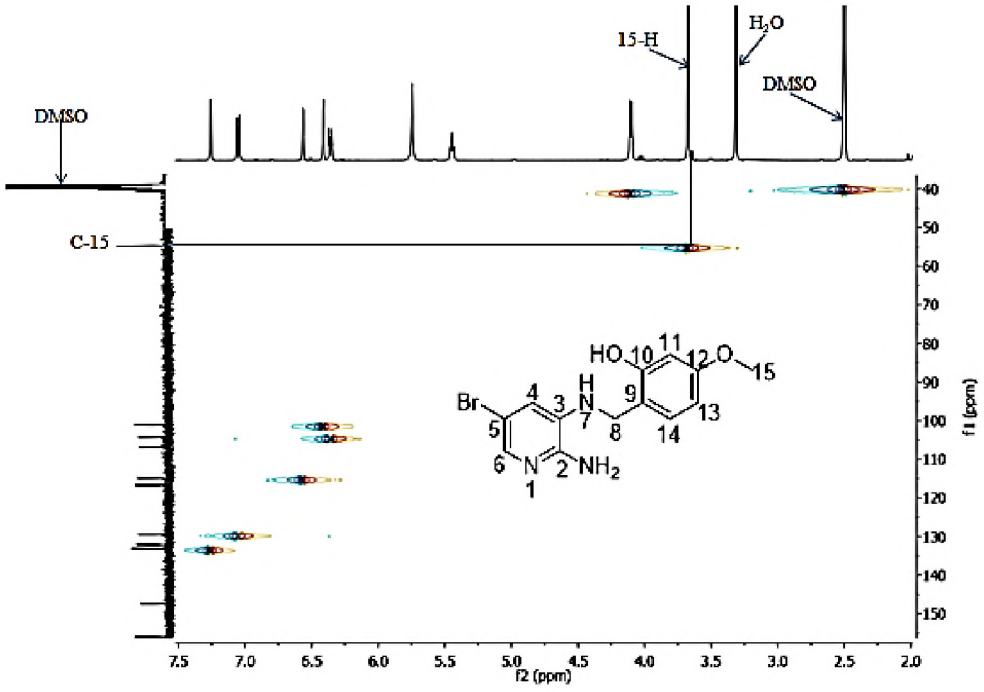

Figure 57. HSQC spectrum of **126f'** in DMSO-d_6.

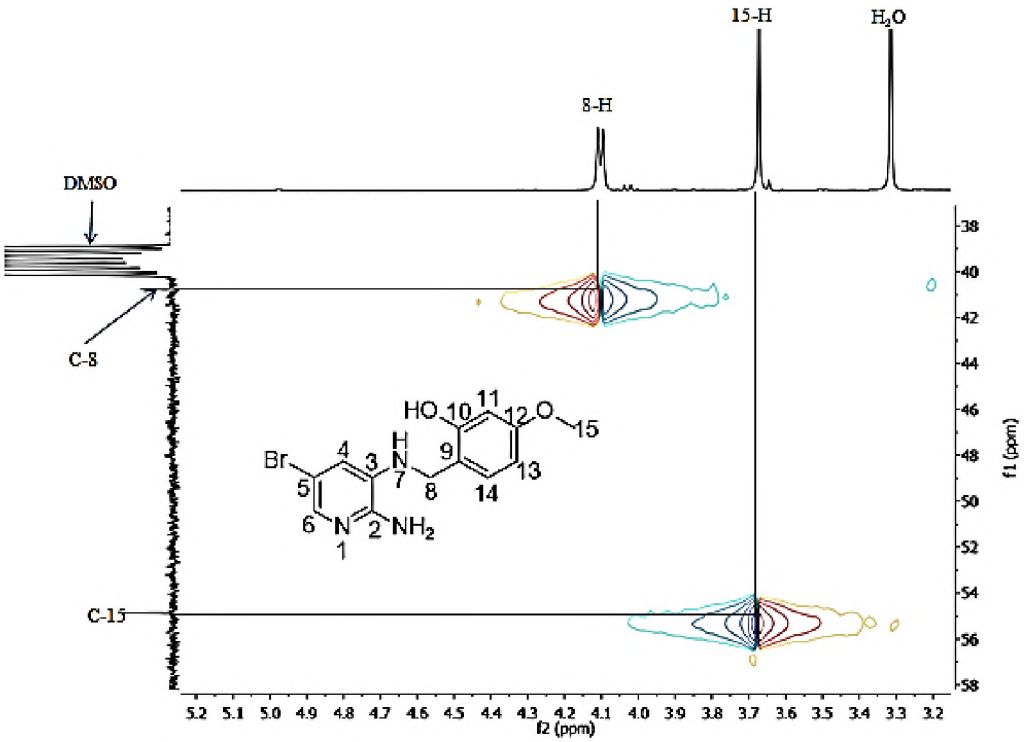

Figure 58. HSQC spectrum of **126f'** in DMSO-d_6 (expanded).

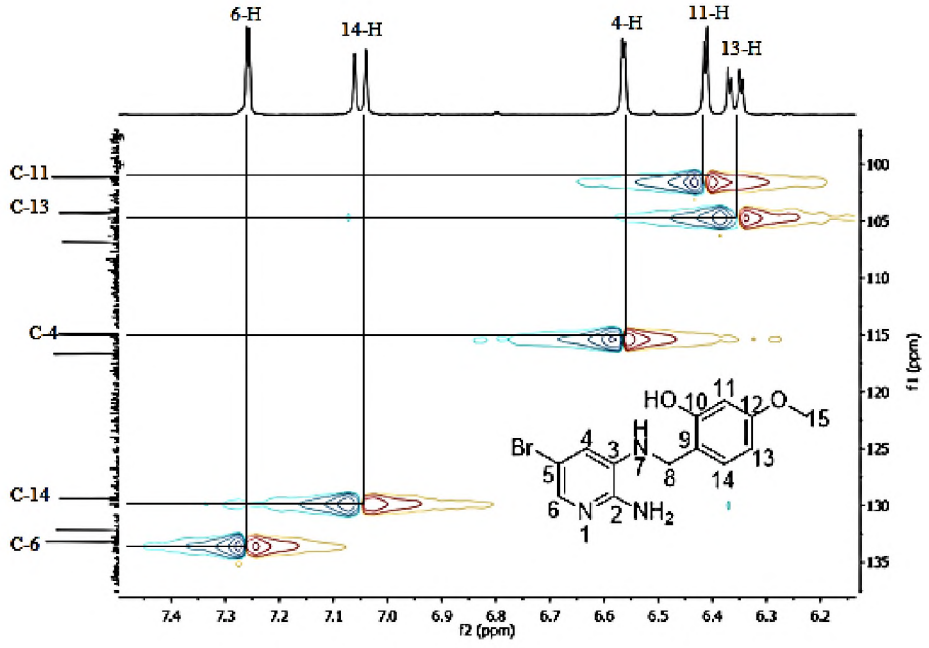

Figure 59. HSQC spectrum of **126f'** in DMSO-d_6 (expanded).

It should be noted that an attempt to regio-selectively formylate the β-amino group of 2,3-diamino-5-bromopyridine with one equivalent of salicylaldehyde failed. 5-Bromo-2,3-bis-(2-hydroxybenzylimino)pyridine **127** was the only product isolated even at room temperature (Scheme 14). Two equivalents of sodium cyanoborohydride was sufficient to hydrogenate the imino groups to secondary amino groups.

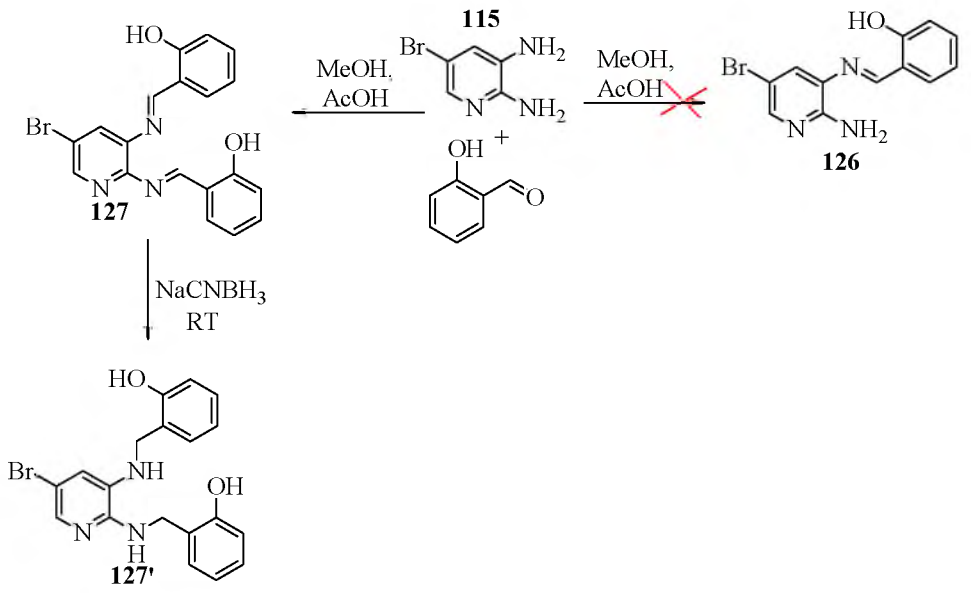

Scheme 14. Synthesis of 5-bromo-2,3-bis(2-hydroxybenzylimino)pyridine.

The ^{1}HNMR spectrum (Figure 60) for this product reveals the presence of a pair of signals resonating at 12.45 and 12.91 ppm corresponding to the two hydroxyl protons (O-H). Similarly, the signals corresponding to the two imino protons (9-H and 9'-H) appear at 9.50 and 9.00 ppm, but they could not be distinguished. The ^{13}C NMR spectrum shows the signals for nineteen carbon atoms as expected (Figure 61). Together, these NMR analyses confirmed that the di-imino derivative was the only product isolated for this reaction..

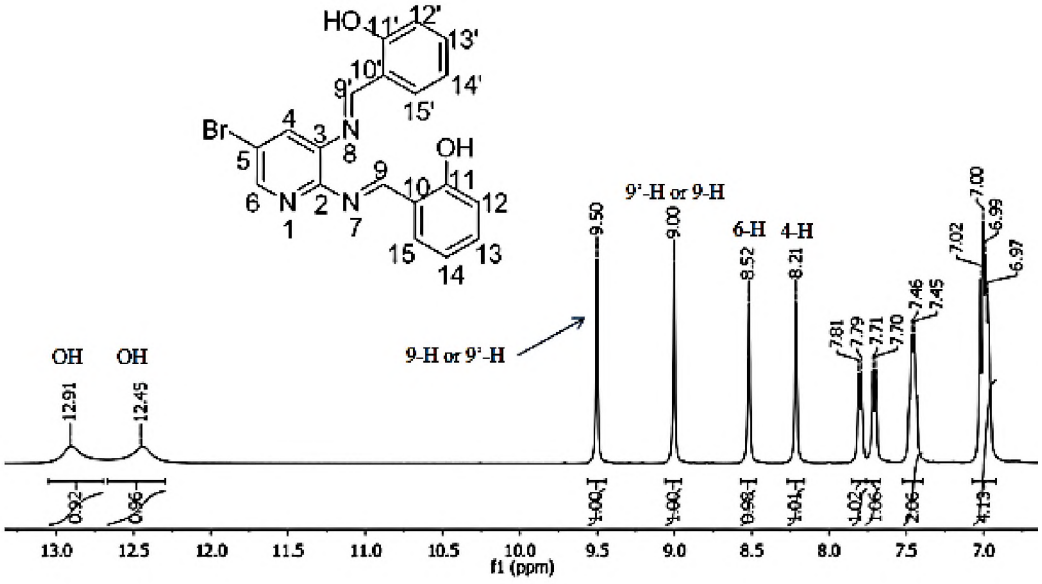

Figure 60. 400 MHz ^{1}H NMR spectrum of **127** in DMSO-d_6.

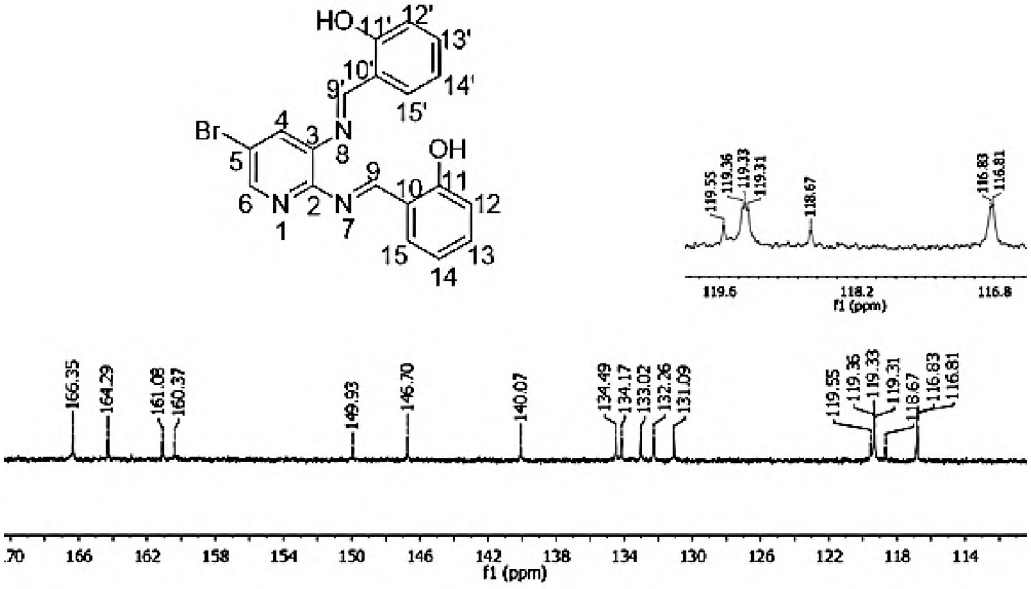

Figure 61. 100 MHz ^{13}C NMR spectrum of **127** in DMSO-d_6.

2.3.1. Anti-Parasitic Protozoan Activity of 126a-h, 127 and 127'.

The compounds **126a-h**, **127** and **127'** in this series were assessed for their ability to act against the parasitic protozoans, *T. brucei* and *P. falciparum*.

The compounds' cytotoxicity at concentration of 20 μM determined against HeLa cells using resazurin-based reagent. None of these compounds are significantly cytotoxic; the results of the cytotoxicity assessment indicated that the viability of the HeLa cell culture ranges from 53% and 109% (Table 9 and Figure 62).

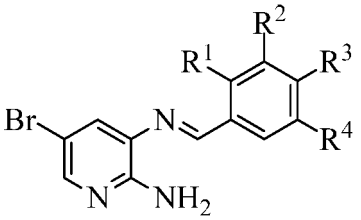

126a-h

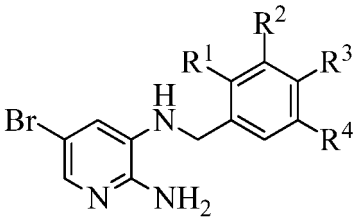

126'

Table 9. Percentage cell viability of HeLa cells in the presence of **126a-h**, **127** and **127'** at 20 μM.

Compound	Cytotoxicity HeLa Cell viability (%)	Standard deviation
126a	75	1
126b	78	3
126c	94	12
126d	53	1
126e	78	6
126f	78	2
126g	77	12
126h	85	1
126b'	93	16
126e'	109	5
126g'	97	5
127	91	2
127'	107	14

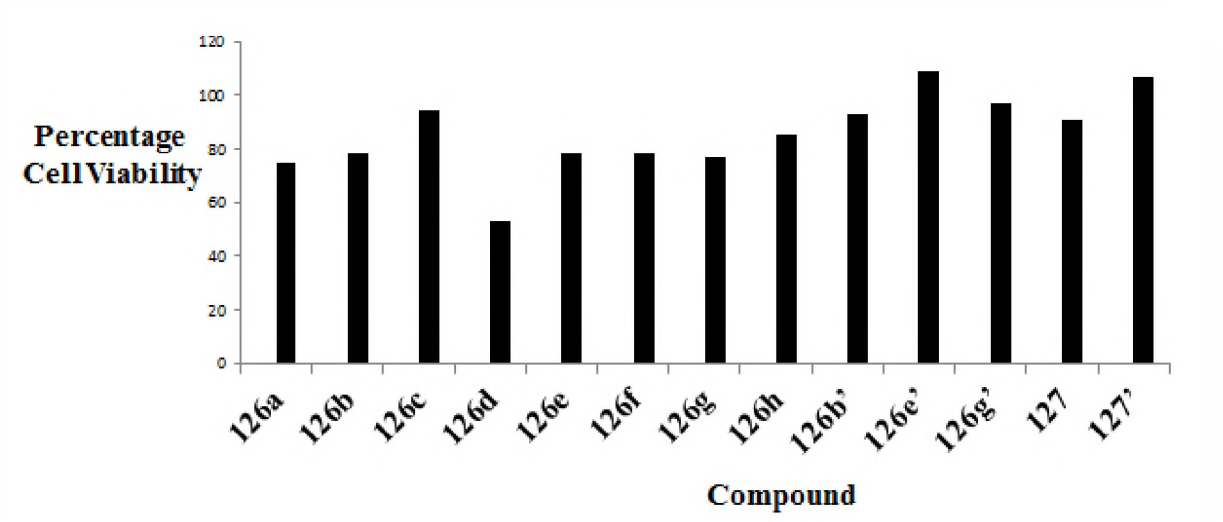

Figure 62. HeLa cell viability obtained in the presence of **126a-h**, **127** and **127'**.

These results against the *Trypanosomas* parasite (*T. brucei*) at 20 μM indicated that **126a**, **126d**, **126e**, **126e'** and **127** were all shown to be active against the parasite (Table 10 and Figure 63).

Table 10. Percentage viability of *T, brucei* in the presence of **126a-h**, **127** and **127'** at 20 μM.

Compound	*T. brucei* Parasite viability (%)	Standard deviation
126a	23.9	0.2
126b	108	1
126c	106	7
126d	20	0.4
126e	23	2
126f	102	5
126g	70	4
126h	114	6
126b'	84	0.2
126e'	18	1
126g'	99	1
127	7	2
127'	105	4

5-bromo-2,3-bis-(2-hydroxybenzylimino)pyridine **127** showed the best activity, limiting the parasite viability to 7%. When the activity of **127** was compared to 5-bromo-2,3-bis(2-hydroxybenzylamino)pyridine **127'** with parasite viability of 105% (Table 10 and Figure 59 and 60), we deduced that the imino units are responsible for the activity. It was also observed that the 2-hydroxyl and the 3,5-dihalo groups are important for activity in the mono-imino

compounds. For example, compound **126e** decreased parasite viability to 23% while **126e'**, which is the hydrogenated derivative of **126e**, gave a parasite viability of 18.33% (Table 10 and Figures 63 and 64).

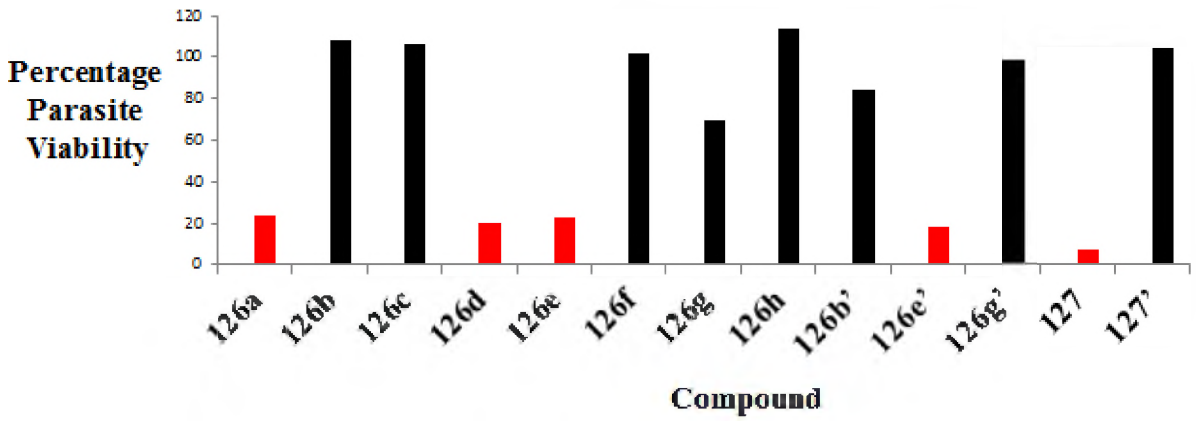

Figure 63. Percentage *T. brucei* parasite viability obtained for **126a-h**, **127** and **127'** at 20 μM.

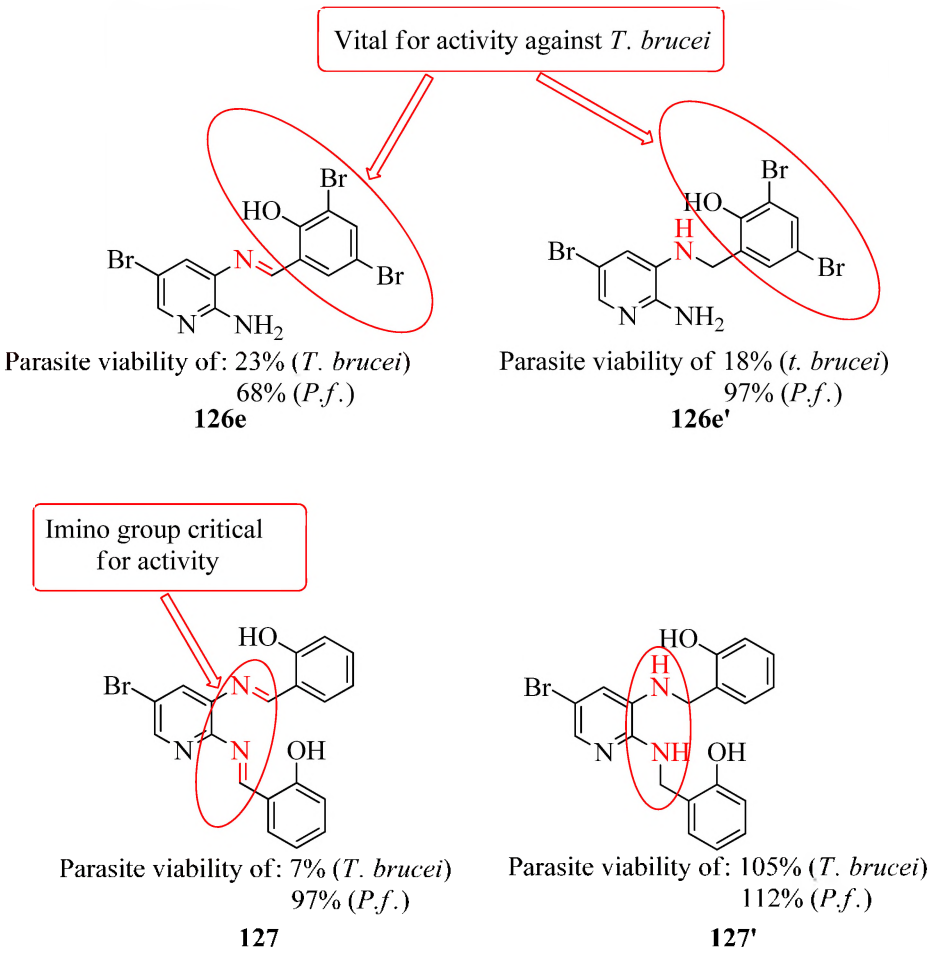

Figure 64. Imino group is critical for activities against parasitic protozoan.

Compound **126a** which has hydroxyl group at positions 3 and 4 of the its benzyl ring and **126d** which has chlorine atom at positions 3 and 5 of its benzyl ring are active against *T. brucei* with parasite viability of 24 and 20%. The half maximal inhibitory concentrations (IC_{50}) of **126a**, **126d**, **126e**, **126e'** and **127** are 1.3, 6.6, 11.2, 6.5 and 42.9 μM, respectively. The pentamidine standard **6** has a corresponding IC_{50} of 0.01 μM – a hundred to a thousand times more potent. Nonetheless, the synthesized imines in this study can be considered to be interesting lead compounds due to their low cytotoxicity at these concentrations.

The pLDH assay (*P. falciparum* strain 3D7) was carried out at 20 μM. The results of the assay showed that **126a** and **126d** also have promising activities against *P. falciparum* with percentage viabilities of 35 and 32%, respectively (Table 11 and Figure 65). The presence of hydroxyl groups at position 3 and 4 (**126a**), chlorine atoms at positions 3 and 5 (**126d**) and bromine atoms at positions 3 and 5 (**126e**) may be consider as necessary for anti-protozoan activities (Figure 65).

Table 11. **126a-h**, **127** and **127'** against *P. falciparum* strain 3D7 at 20 μM.

Compound	*P. falciparum* strain 3D7 (% viability)	Standard deviation
126a	35	18
126b	92	3
126c	96	19
126d	31	10
126e	68	7
126f	70	8
126g	51	2
126h	70	1
126b'	103	4
126e'	97	8
126g'	103	3
127	97	13
127'	112	7

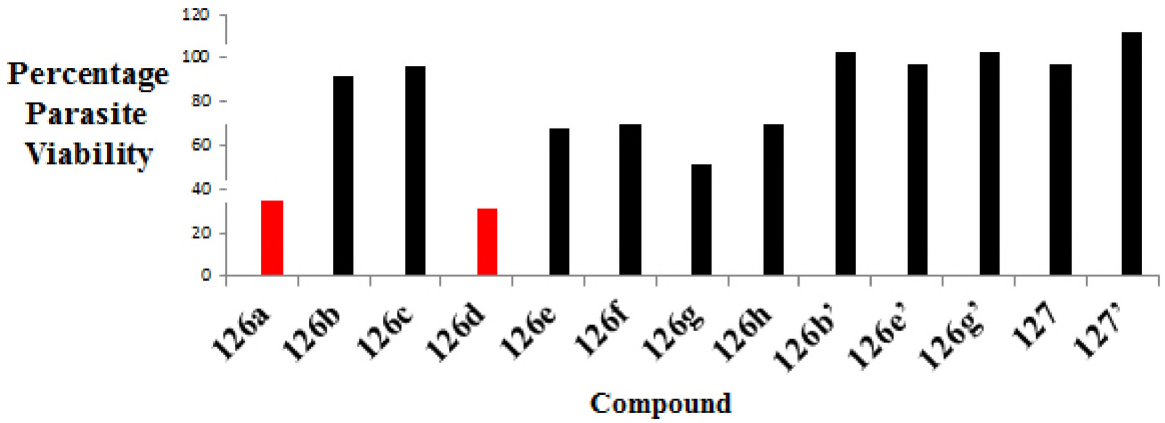

Figure 65. Parasite viability obtained for **126a-h**, **127** and **127'** at 20 μM.

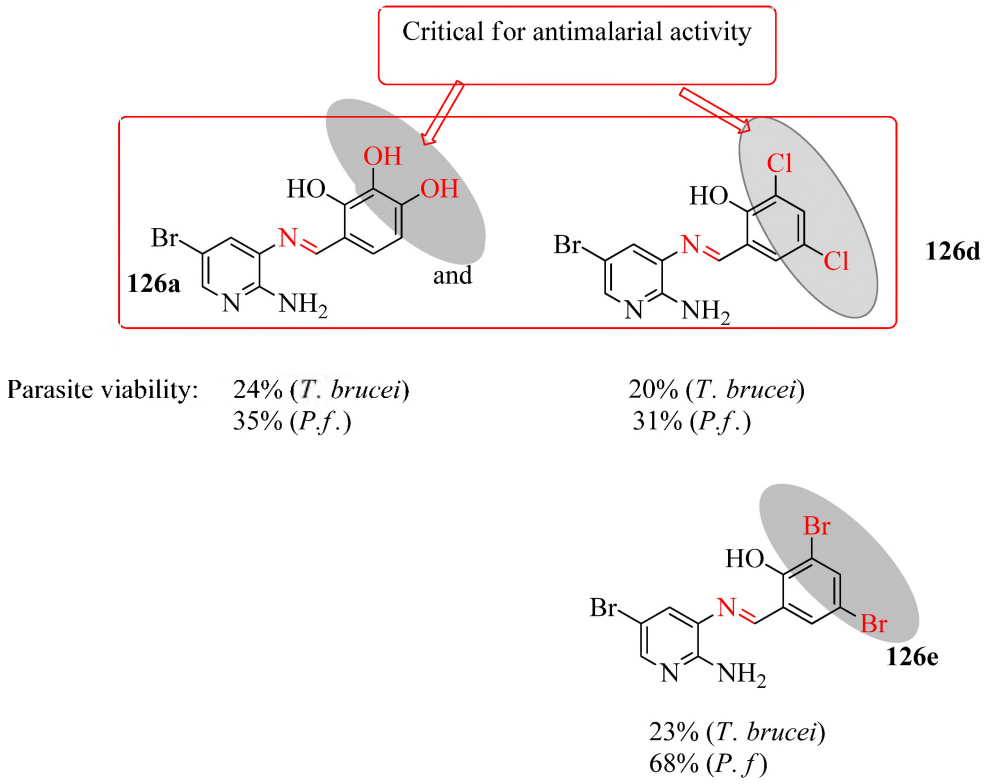

Figure 66. Compounds with activity against both parasites.

2.4. SYNTHESIS OF *N*-2-(PHENYL)-2-HYDROXYBENZYLIMINES 130a-l AND THEIR BENZYLAMINO DERIVATIVES

This reaction used to access *N*-2-(phenyl)-2-hydroxybenzylimines **130a-l** (Scheme 15) was performed according to the method described by Faridoon *et al.*[133] To the appropriate aniline **128** was added to one equivalent of appropriate benzaldehyde **129** in methanol as solvent. Glacial acetic acid was added in a catalytic amount and the resulting mixture was boiled with stirring under reflux. The imino products **130** were generally isolated as precipitates after the completion of the reaction as determined by thin layer chromatography. For derivatives which did not precipitate at the end of the reaction, the solvent (methanol) was evaporated, the residues were neutralized with aqueous sodium carbonate and the desired products were extracted into ethyl acetate; the required products were obtained as coloured solids after evaporation. The yield of the isolated products ranged from 66 to 94% (Table 12).

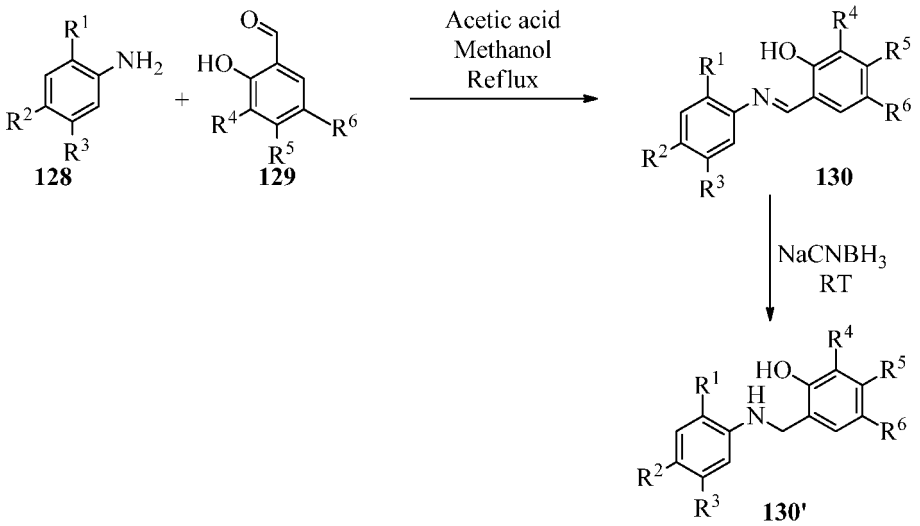

Scheme 15. Synthesis of *N*-(benzyl)-2-hydroxybenzylimines **130a-l**.

NMR and HPLC-MS analyses were used for the structural confirmation of the imines **130a-l**. For example, in *N*-(2-hydroxyl-4-nitrophenyl)-2-hydroxybenzylimine**130k**, the HPLC-MS analysis ($C_{13}H_9BrClN_2O_4$ 370.9434) indicated the presence of $[M+H]^+$ 370.9338 peak. In the ^1H NMR spectrum (Figure 67), the protons of the two hydroxyl groups (O-H) correspond to the signals at 14.83 and 11.68 ppm. These signals do not correlate to any carbon atom(s) in the HSQC spectrum (Figure 68). The imino proton 8-H resonates at 9.18 ppm and the HSQC

spectrum clearly indicates that this signal correlates to the ^{13}C signal at 162.4 ppm on the ^{13}C NMR spectrum (Figures 68 and 69).

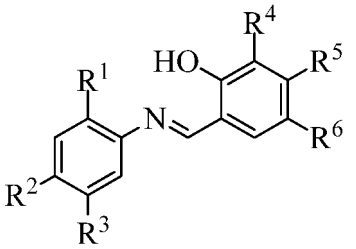

130

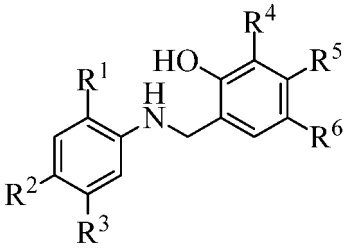

130'

Table 12. *N*-2-(benzyl)-2-hydroxybenzylimines derivatives and yields.

130	R^1	R^2	R3	R^4	R^5	R^6	Yield %
130a	OH	NO_2	H	OH	OH	H	91
130b	OH	NO_2	H	OH	H	H	86
130c	OH	NO_2	H	H	H	Cl	91
130d	H	F	F	OH	OH	H	92
130e	H	F	F	OH	H	H	89
130f	H	F	F	Br	H	Cl	80
130g	H	F	F	Cl	H	Cl	93
130h	H	F	F	Br	H	Br	89
130i	H	F	F	H	H	Cl	92
130j	OH	NO_2	H	Br	H	Cl	93
130k	OH	NO_2	H	Cl	H	Cl	91
130l	OH	NO_2	H	Br	H	Br	93
130b'	OH	NO_2	H	OH	H	H	94
130c'	OH	NO_2	H	H	H	Cl	73
130e'	H	F	F	OH	H	H	70
130g'	H	F	F	Cl	H	Cl	83
130i'	H	F	F	H	H	Cl	70
130j'	OH	NO_2	Br	Br	H	Cl	66
130k'	OH	NO_2	H	Cl	H	Cl	77

The anilino protons 3-H and 4-H are *ortho* to one another and therefore they couple as seen in the COSY spectrum (Figure 70), with a large coupling constant (9.0 Hz); 3-H corresponds to

the doublet at 7.15 ppm. Using HSQC spectrum (Figure 68), this proton (3-H) is shown to correlate to the carbon resonating at 116.6 ppm in the ^{13}C NMR spectrum while 4-H resonates as a doublet of doublets at 8.12 ppm due to its *meta*-arrangement with 6-H and consequently the small coupling between these protons (J = 2.65 Hz). The 4-H signal correlates with the C-4 signal at 124.7 ppm in the HSQC spectrum while the 6-H signal at 8.40 ppm correlates to the ^{13}C signal at 115.3 ppm in the ^{13}C NMR spectrum (Figure 69).

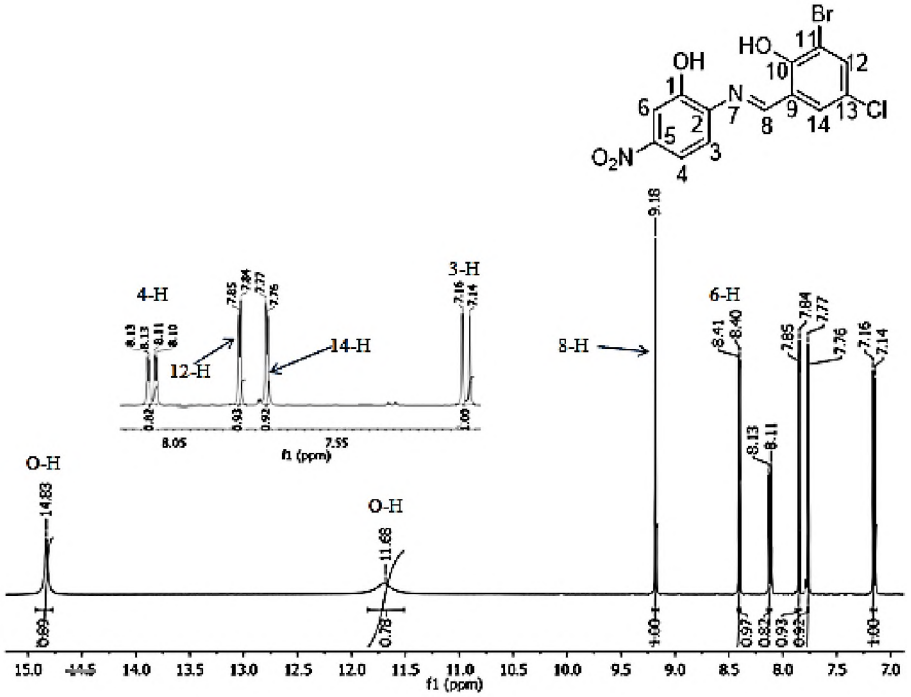

Figure 67. 400 MHz ^{1}H NMR spectrum of **130k** in DMSO-d_6.

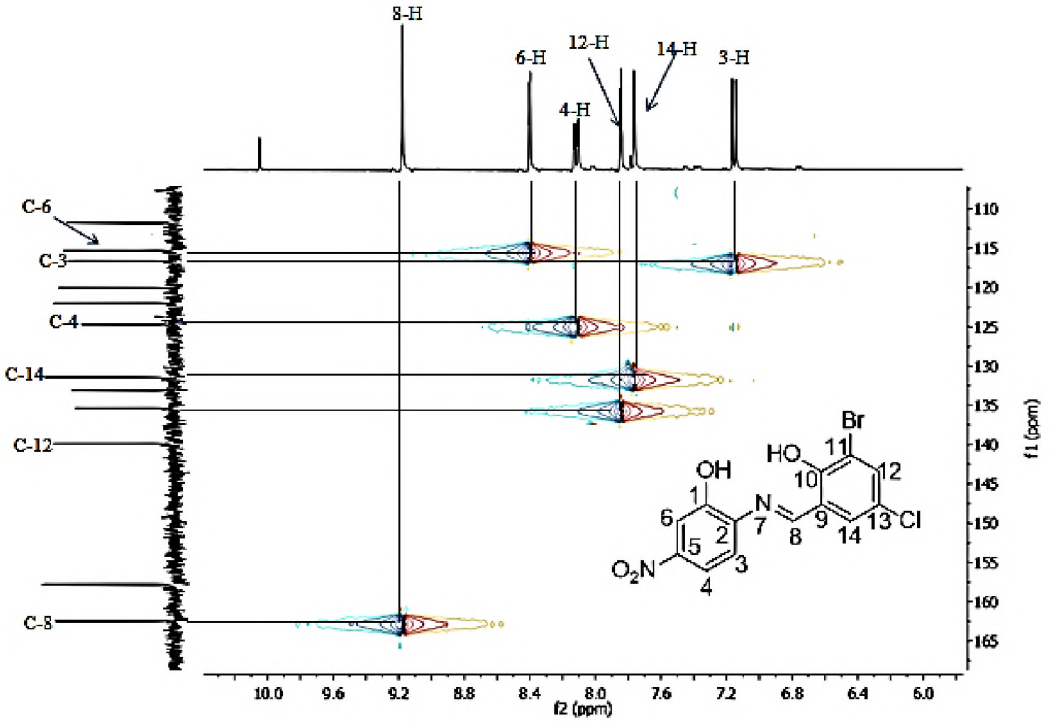

Figure 68. HSQC NMR spectrum of **130k** in DMSO-*d*6.

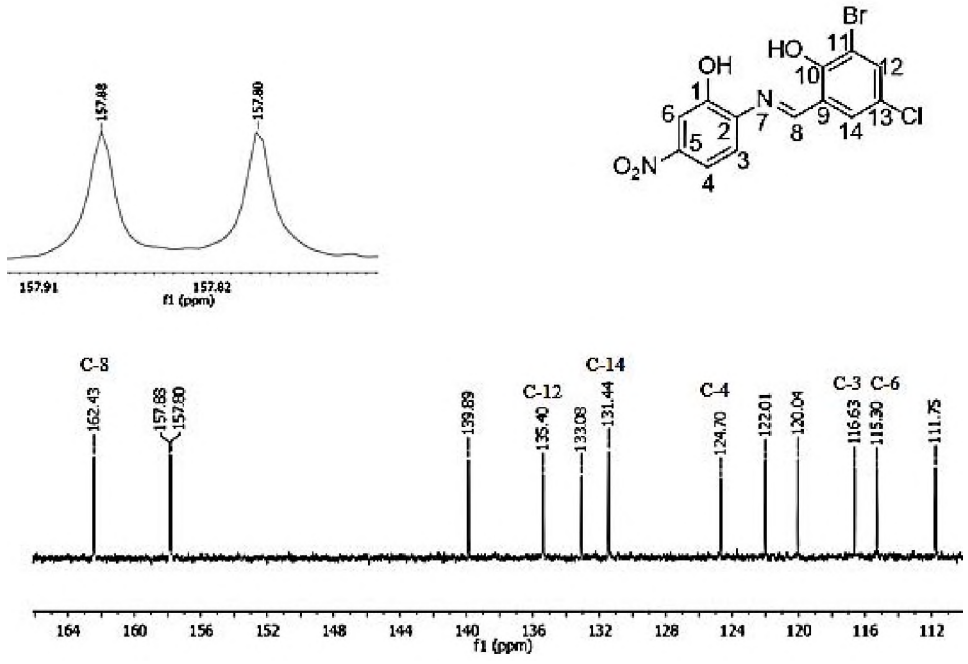

Figure 69. 100 MHz ^{13}C NMR spectrum of **130k** in DMSO-*d*6.

The ^{1}H NMR signal at 7.85 ppm has been assigned to 12-H while the signal at 7.76 ppm corresponds to 14-H. The meta-arrangement between these protons allows for a small coupling between them which was observed with a coupling constant of 2.6 Hz. The HSQC experiment aided in determining the corresponding ^{13}C signals; C-12 corresponds to the signal at 135.4 ppm while C-14 corresponds to the signal at 131.4 ppm. (Figures 67, 68 and 69).

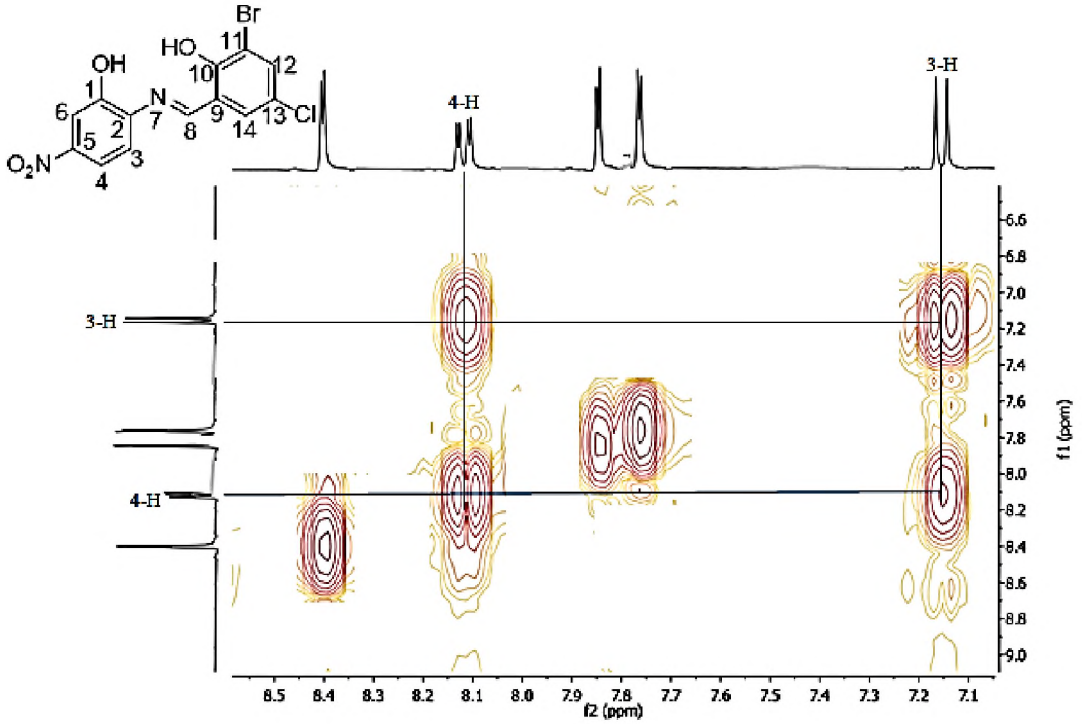

Figure 70. COSY NMR spectrum of **130k** in DMSO-d_6.

Hydrogenation of selected imino products (**130b**, **130c**, **130e**, **130e**, **130g**, **130i**, **130j** and **130k**) with sodium cyanoborohydride at room temperature gave the corresponding secondary amine derivatives**130b'**, **130c'**, **130e'**, **130g'**, **130i'**, **130j'** and **130k'**. A ^{1}H NMR experiment of **130k'** (Figure 71) showed the disappearance of the imino proton and the appearance of a broad signal corresponding to a secondary amino proton (N-H) at 6.04 ppm and the *N*-methylene signal at 4.39 ppm. A DEPT-135 spectrum (Figure 72) of **130k'** also indicates the presence of *N*-methylene carbon (C-8) by a negative signal at 42.1 ppm. The ^{13}C spectrum

(Figure 73) clearly indicates the disappearance of the imino ^{13}C signal while the spectrum shows the *N*-methylene ^{13}C nuclei resonating at 41.6 ppm.

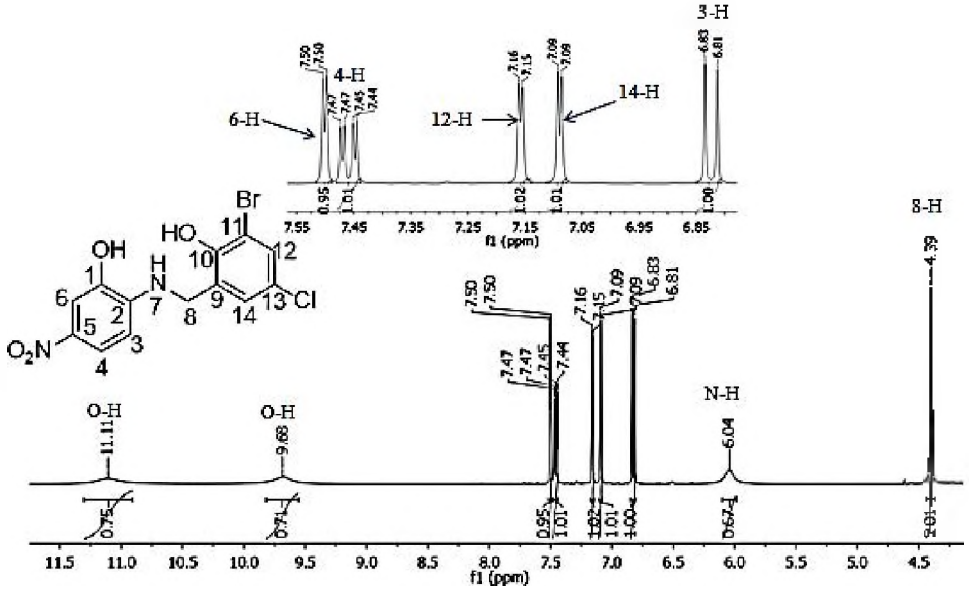

Figure 71. 400 MHz ^{1}H NMR spectrum of **130k'** in DMSO-d_6.

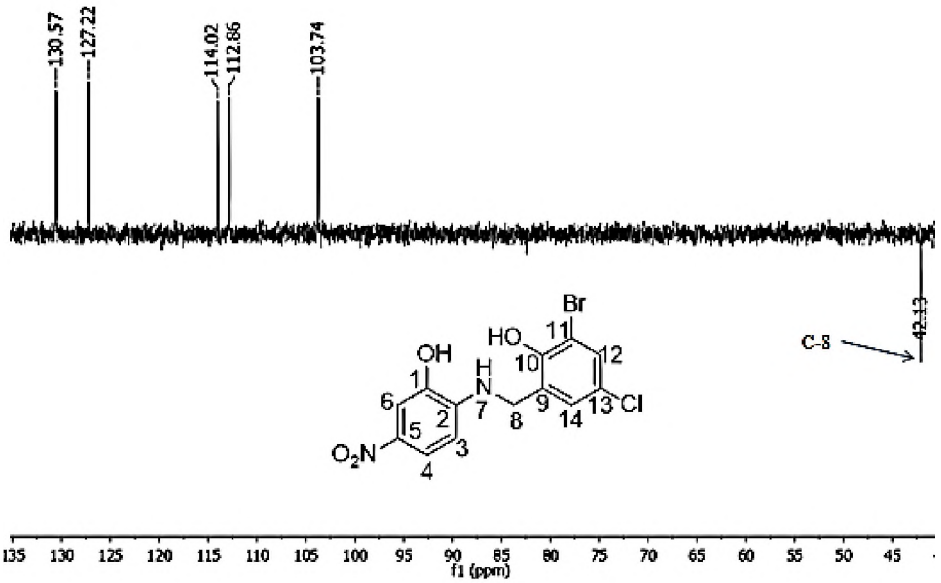

Figure 72. 100 MHz DEPT-135 NMR spectrum of **130k'** in DMSO-d_6.

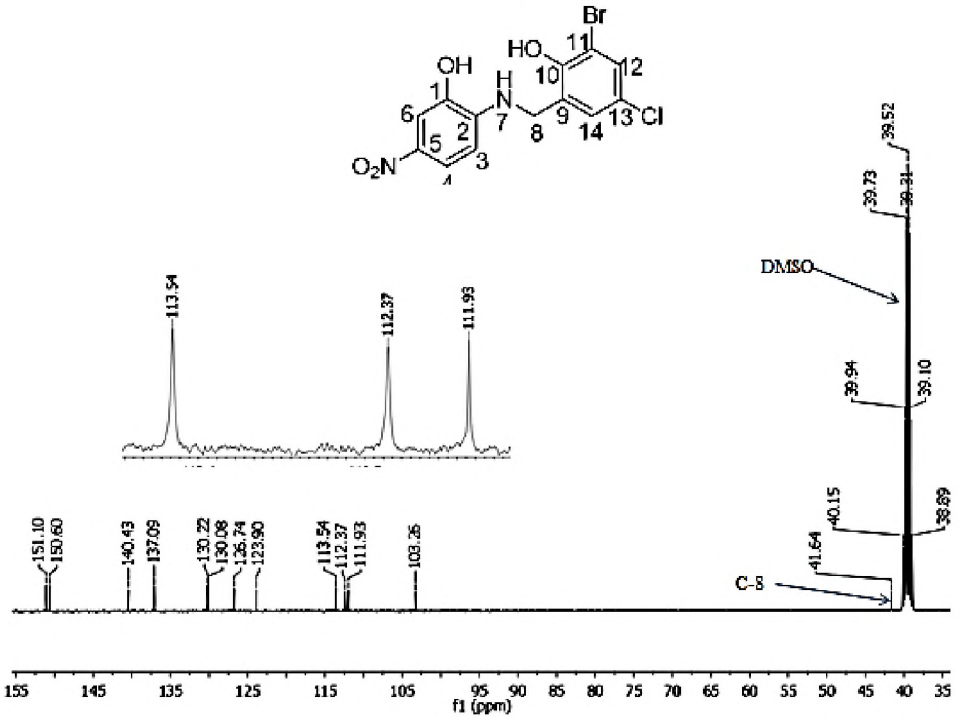

Figure 73. 100 MHz ^{13}C NMR spectrum of **130k'** in DMSO- d_6.

2.4.1. Anti-protozoan activity of *N*-2-(benzyl)-2-hydroxybenzylimines

Cytotoxicity screening of **130 a-l** , **130b'**, **130c'**, **130e'**, **130g'**, **130i'**, **130j'** and **130k'**against HeLa cells 20 μM, revealed that only the benzylamino compounds **130g'** and **130i'** are toxic. When compared to their imino analogues **130g** and **130i**, it was apparent that the presence of the amino group is responsible for their toxicity (Table 13, Figures 74 and 75).

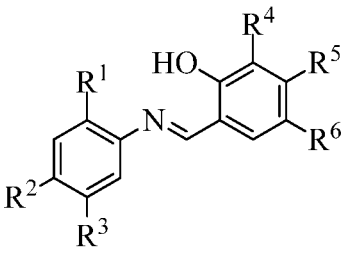

130a-l

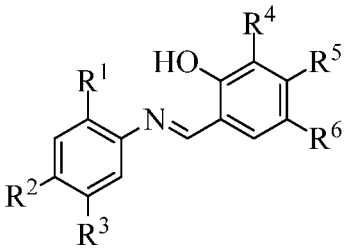

130'

Table 13. Percentage viability of HeLa cells in the presence of **130a-l** at 20 μM.

Compound	HeLa Cell Viability (%)	Standard Deviation
130a	94	5
130b	93	5
130b'	99	2
130c	94	17
130c'	68	4
130d	118	12
130e	74	4
130e'	82	2
130f	98	0.3
130g	86	7
130g'	31	13
130h	111	5
130i	102	4
130i'	14	7
130J	79	12
130j'	74	13
130K	83	4
130k'	87	8
130l	107	0.02

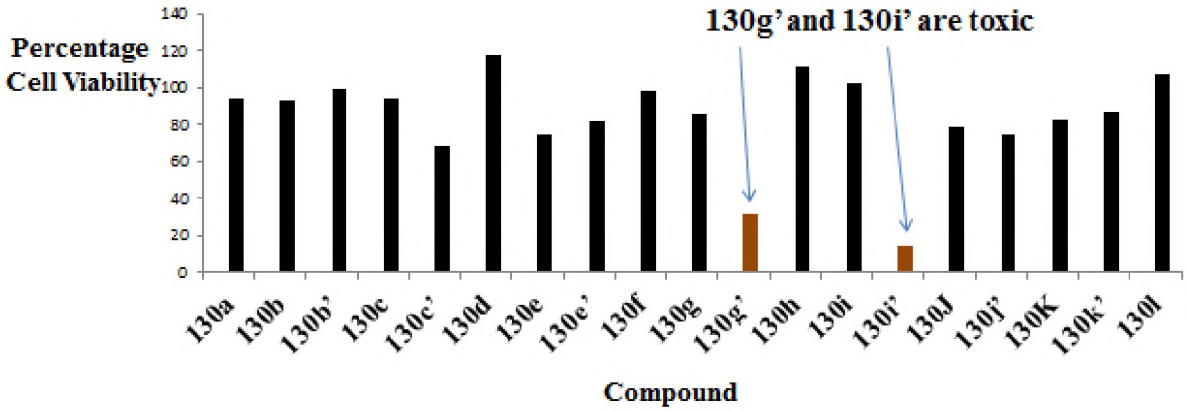

Figure 74 % HeLa cell viability obtained for **130a-l** at 20 μM.

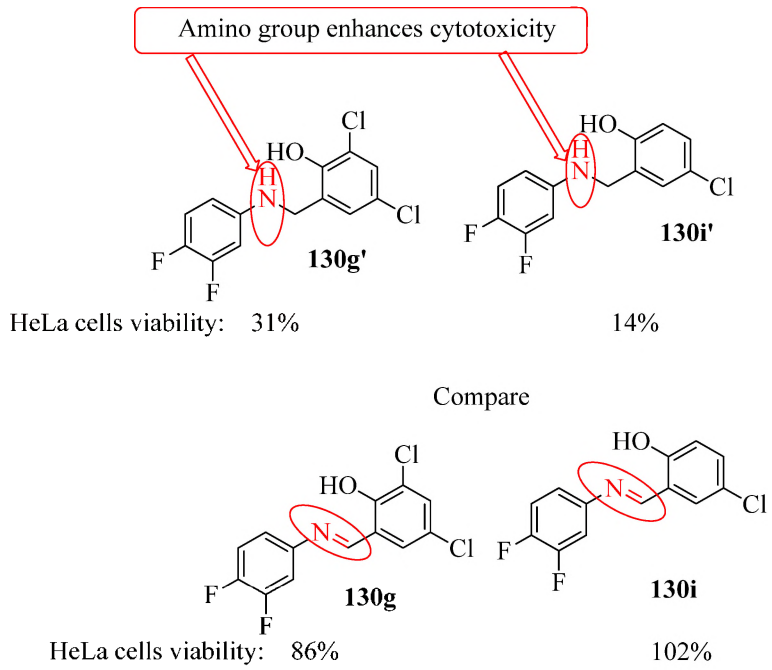

Figure 75. Secondary amino group enhances cytotoxicity.

All of the compounds in this group were able to inhibit *T. brucei* to some extent at 20 μM (Table 14 and Figure 76). Several compounds (highlighted in Table 14) showed significant inhibition of *T. brucei* (reducing the parasite to 25%) [Table 14 and Figure 76]. The structures of these active compounds are given in Figure 77. The active ligands have IC_{50} values ranging from 0.5- 31 μM (Table 15). The pentamidine standard **6** showed an IC_{50} of 0.002 μM in this experiment.

Table 14. Percentage viability of *T. brucei* in the presence of **130a-l** at 20 μM.

Compound	*T. brucei* Parasite viability (%)	Standard Deviation
130a	22	0.1
130b	46	4
130b'	40	2
130c	54	4
130c'	11	3
130d	62	2
130e	44	1
130e'	41	1
130f	12	1
130g	15	0.1
130g'	6	0.1
130h	43	1
130i	17	3
130i'	20	7
130J	18	1
130j'	5	1
130K	7	0.4
130k'	6	2
130l	13	1

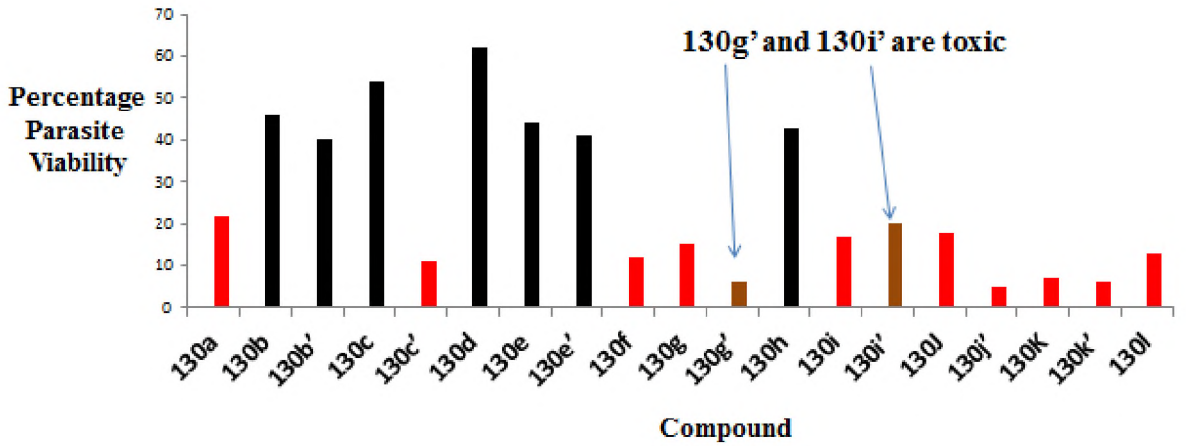

Figure 76. % *T. brucei* parasite viability obtained in the presence of **130a-l** at 20 μM.

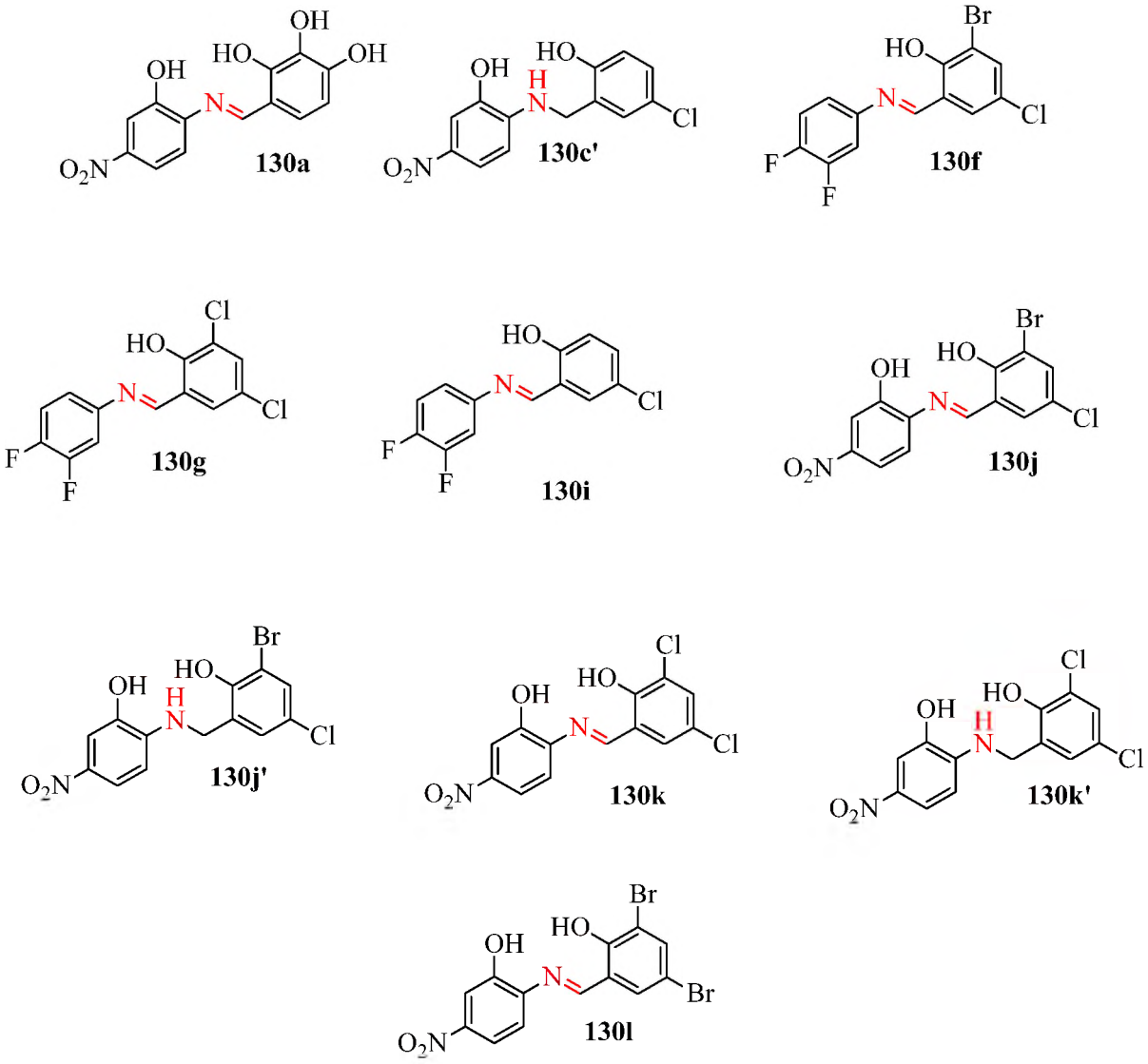

Figure 77. *N*-benzylideneanilines with promising activities against *T. brucei*.

Table 15. IC_{50} of Active *N*-2-(benzyl)-2-hydroxybenzylimines compared with that of pentamidine **6** – a standard anti-trypanosomiasis treatment.

Compound	**130a**	**130c**	**130f**	**130g**	**130i**	**130j**	**130j'**	**130k**	**130k'**	**130l**	**Pentamidine**
IC_{50} (μM)	0.5	25.2	10.9	1.5	31.3	4.3	10.3	3.7	10.6	15.3	0.002

On screening these compounds against *P.falciparum* 20 μM, only four of these compounds showed significant activity against the parasite (Table 16 and Figure 78). To be specific, compounds **130j** and **130k** inhibited the malaria parasite to 27 and 33% viability,

respectively. The parasite inhibition of compounds **130g'** and **130i'** can most likely be attributed to their cytotoxicity. When the anti-plasmodial activity of **130j and 130k** were compared to those of their amino analogues **130j'** and **130k'**, it was observed that the imino group may be responsible for their antimalarial activity (Figure 79). The two compounds **130j** and **130k** have IC_{50} values of 12 and 31 μM, respectively. Chloroquine **16** –a standard has an IC_{50} of 0.01 μM.

Table 16. Percentage viability of *P. falciparum* 3D7 in the presence of **130a-l** at 20 μM.

Compound	*P. falciparum* strain 3D7 Parasite viability (%)	Standard Deviation
130a	63	7
130b	112	3
130b'	79	4
130c	88	1
130c'	53	12
130d	81	8
130e	86	7
130e'	51	1
130f	62	1
130g	50	7
130g'	24	3
130h	91	27
130i	95	7
130i'	20	11
130J	27	10
130j'	104	3
130K	33	5
130k'	121	3
130l	107	4

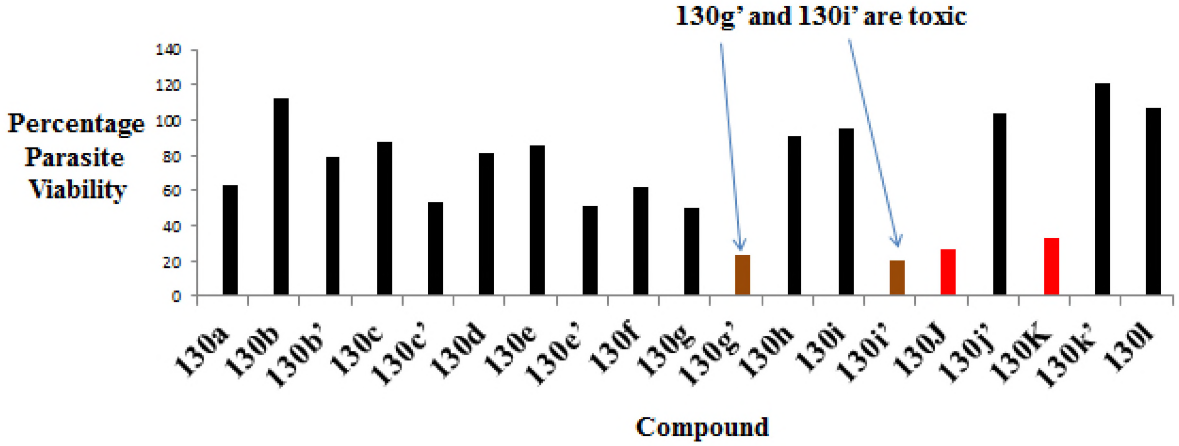

Figure 78. % pLDH parasite viability obtained in the presence of **130a-l** at 20 μM.

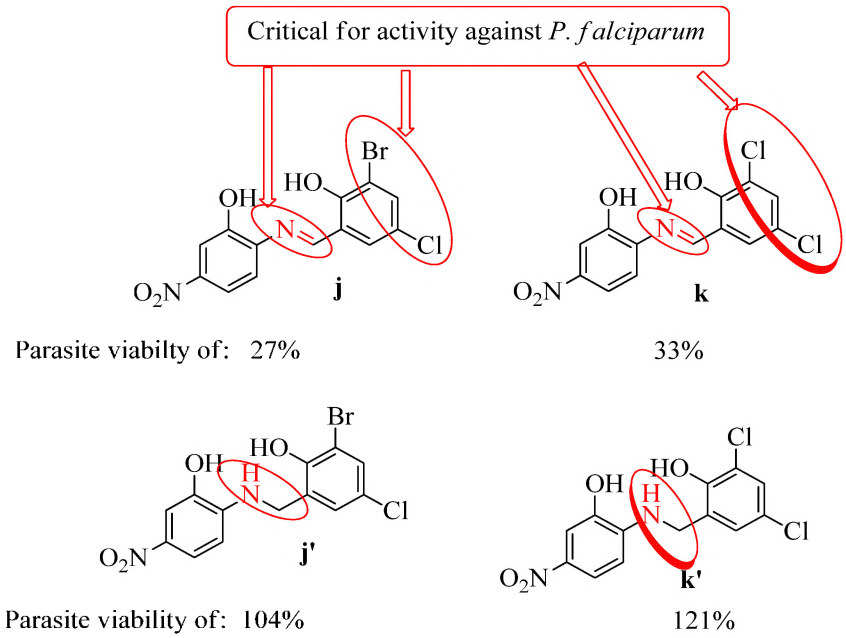

Figure 79. Imino group is critical for activities against *P. falciparum*.

2.5. SYNTHESIS OF *N*-(3,4-DIFLUOROBENZYL)-2-HYDROXY-BENZYLIMINES 133a-e.

In order to improve on the parasite inhibition of the compounds **130a-k**, the synthesis of fluorinated imino compounds **133a-e** were explored. The major structural difference between the compounds and the preceding inhibitors was the introduction of a methylene group

between the imino group and the difluoroaryl group to improve the solubility of the imino compounds. The preparation involved the dissolution of 3,4-difluorobenzylamine **131** in methanol and the addition of one equivalent of an appropriate benzaldehyde **132**. Two drops of glacial acetic acid were added as catalyst and the mixture was stirred at room temperature for twenty minutes – consumption of starting materials was confirmed by thin layer chromatography (Scheme 16). The desired products (**133a-e**) were isolated as yellowish solids with yields in the ranges between 86 and 96%.

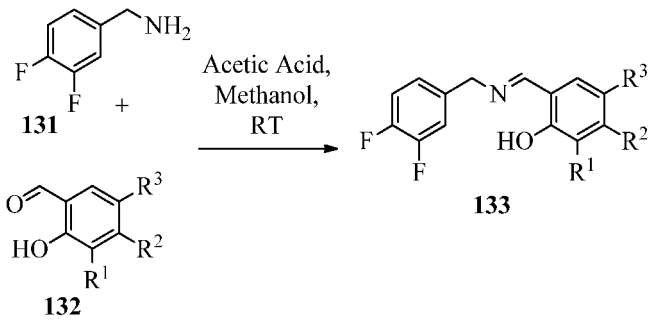

133	R^1	R^2	R^3	Yield %
a	H	H	NO_2	96
b	Br	H	Cl	92
c	OH	OH	H	86
d	OH	H	H	90
e	Cl	H	Cl	94

Scheme 16. Synthesis of *N*-(3,4-difluorobenzyl)-2-hydroxybenzylimines **133a-e**.

^1H, ^{13}C, HSQC, COSY and HMBC experiments were used to elucidate the structures of the isolated products. For the purpose of this discussion, *N*-(3,4-difluorobenzyl)-2-hydroxy-5-nitrobenzylamine **133a** was chosen as a representative to demonstrate that the expected products were formed. The HPLC-MS analysis for compound **133a** ($C_{14}H_{11}F_2N_2O_3$ 293.0659) indicated the presence of $[M+H]^+$ 293.0732 peak. The ^1H NMR spectrum revealed the presence of the imino proton, 7-H (C=N-H) resonating at 8.86 ppm (Figure 80). With the aid of an HSQC experiment, it was apparent that the ^{13}C signal at 167.0ppm corresponds to the imino carbon atom C-7 (Figures 81 and 82). The broad signal at 14.40 ppm in the ^1H NMR spectrum corresponds to the hydroxyl proton (OH) group since the HSQC spectrum did not show any crosspeak corresponding to this signal. The α-methylene protons resonate as a singlet at 4.9 ppm and the HSQC spectrum indicated that the corresponding ^{13}C signal is at 56.2 ppm (C-9). This was further confirmed by the DEPT-135 experiment (Figures 80-83), where this was the only negatively phased signal.

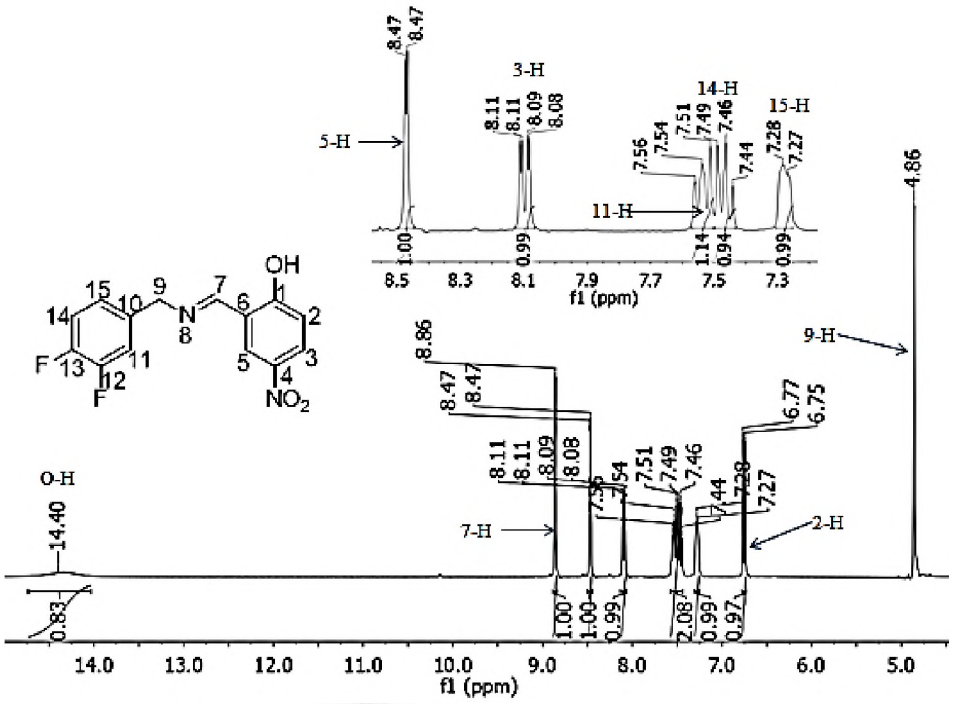

Figure 80. 400 MHz ^{1}H NMR spectrum of **133a** in DMSO-d_6.

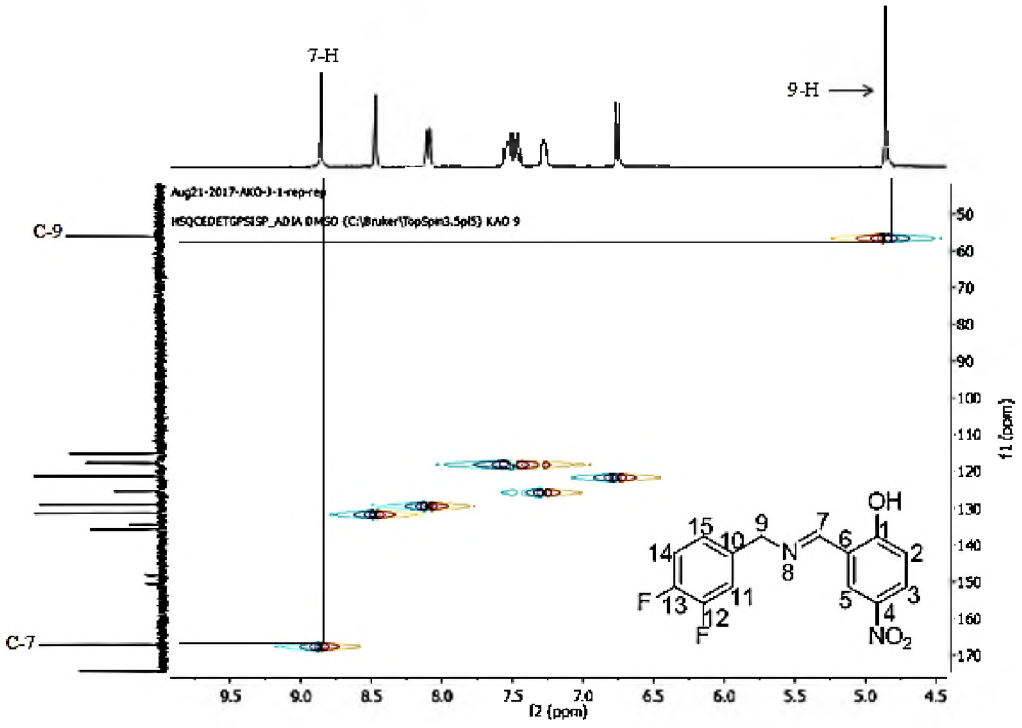

Figure 81. HSQC spectrum of **133a** in DMSO-d_6.

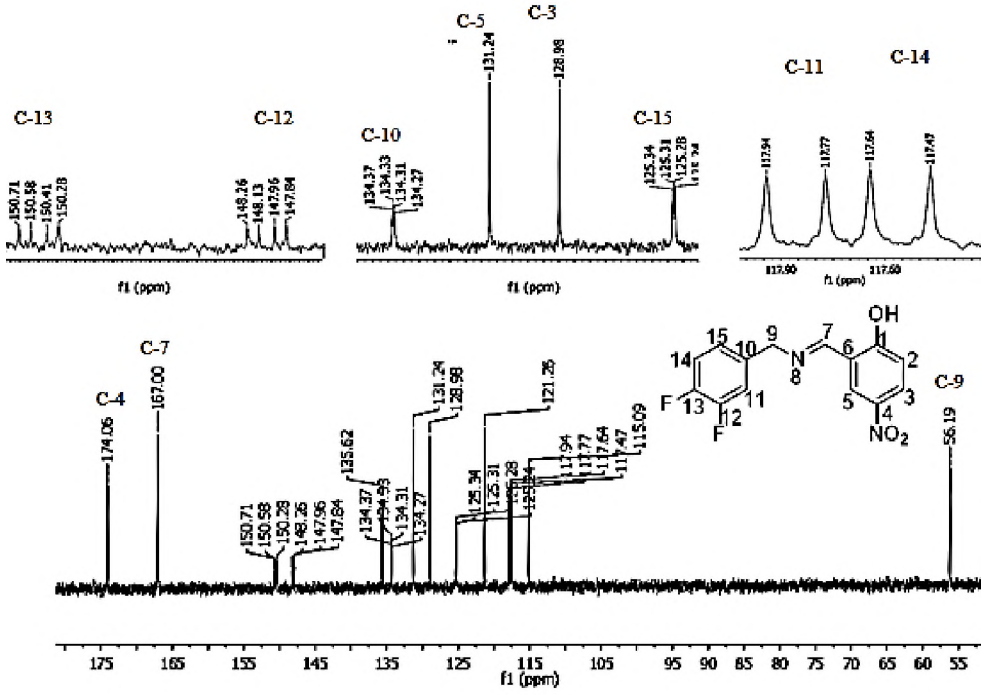

Figure 82. 100 MHz ^{13}C NMR spectrum of **133a** in DMSO-d_6.

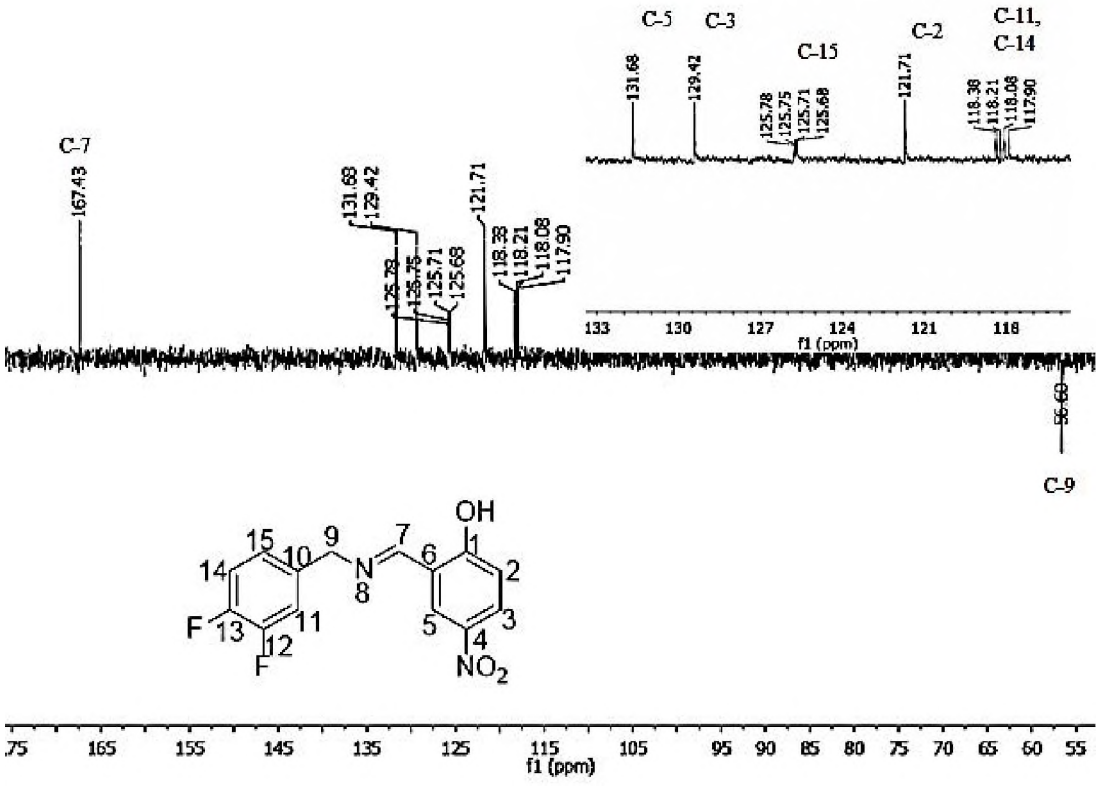

Figure 83. 100 MHz DEPT-135 NMR spectrum of **133a** in DMSO-d_6.

With the aid of a COSY experiment (Figure 84), it was established that the doublet at 6.76 ppm corresponds to 2-H which couples to 3-H with a coupling constant of 9.5 Hz. The signal at 8.10 ppm corresponding to 3-H is a doublet of doublets because of its small additional coupling to 5-H with a coupling constant of 2.9 Hz (Figure 83). The ^{1}H NMR signal at 8.47 ppm corresponds to 5-H (Figures 80).

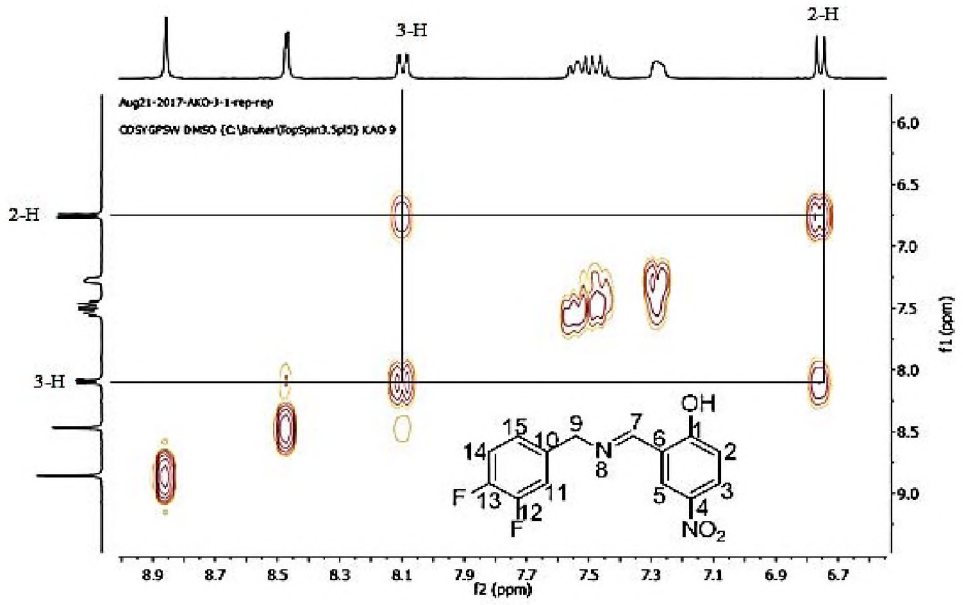

Figure 84. 400 MHz COSY NMR spectrum of **133a** in DMSO-*d*$_6$.

The expanded HSQC spectrum showed the various ^{13}C signals that correlate to the proton signals thus identified. It can be clearly seen that C-2, C-3 and C-5 correspond to the ^{13}C signals resonating at 121.3, 129.0 and 131.6 ppm, respectively on the ^{13}C spectrum (Figures 85 and 86).

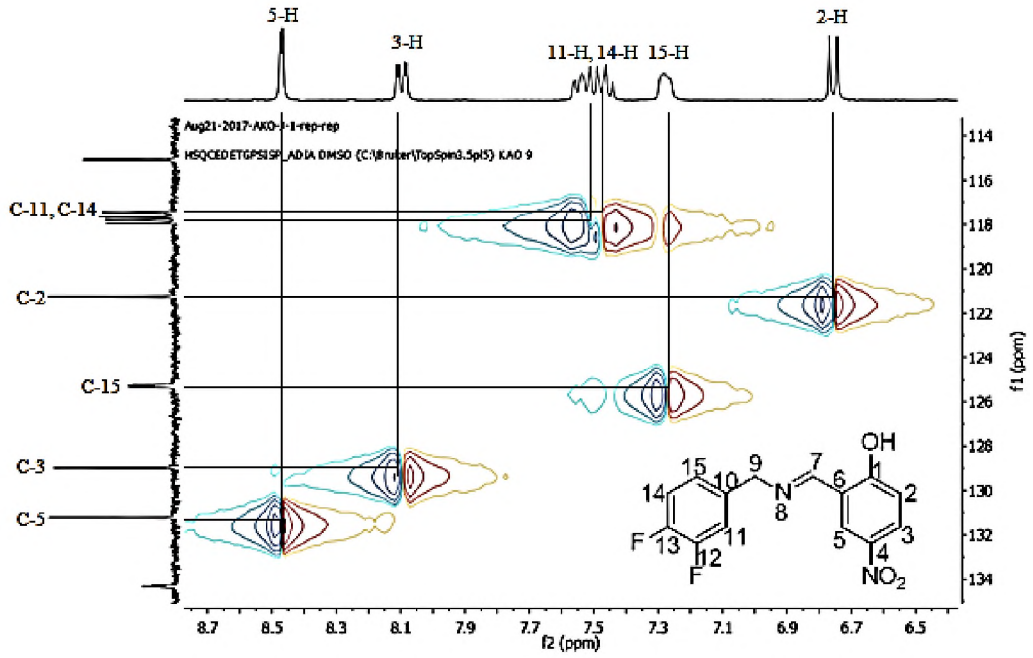

Figure 85. HSQC NMR spectrum of **133a** in DMSO-d_6 (expanded).

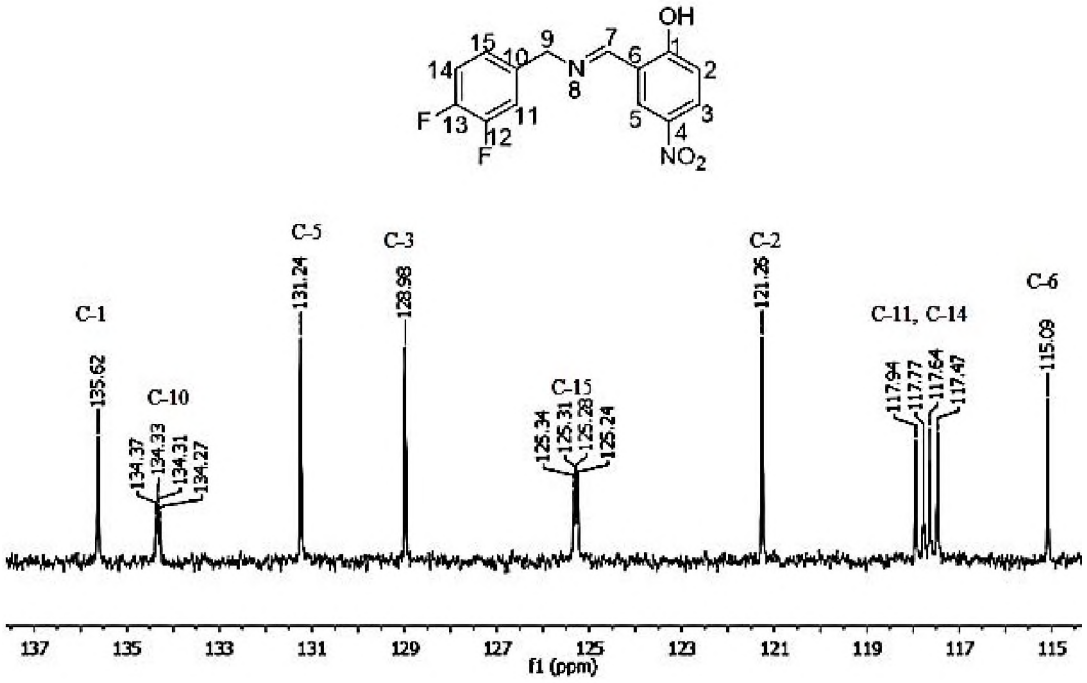

Figure 86. 100 MHz ^{13}C NMR spectrum of **133a** in DMSO-d_6 (expanded).

Nuclei in the 3,4-difluorophenyl ring exhibited complex spin-spin coupling interaction due to the presence of fluorine atoms (13-F and 12-F). ^{19}F couples strongly with nuclei up to three bonds away and this coupling creates extra splitting of the signals that correspond to the

affected ^{1}H and ^{13}C nuclei. As a result, 14-H is split into a multiplet resonating at 7.48 ppm while the signal representing 11-H is split into a multiplet centred at 7.55 ppm. These signals are overlapping. The HSQC experiment showed that proton 14-H correlates to a doublet at 117.6 ppm with a coupling constant of 17.1 Hz ($^{2}J_{C,F}$) and 11-H correlates to the ^{13}C doublet signal at 117.9 ppm with a coupling constant of 17.5 Hz ($^{2}J_{C,F}$). The 15-H and C-15 signals in the ^{1}H and ^{13}C spectra are expected to undergo spin-spin splitting because they are within three bonds of ^{19}F nuclei. The signal at 7.28 ppm appears as a poorly resolved multiplet corresponding to the proton signal for 15-H while the HSQC spectrum indicated that this ^{1}H signal correlates to a ^{13}C signal at 125.2 ppm as a doublet of doublets with coupling constants of 6.7 Hz ($^{2}J_{C,F}$) and 3.5 Hz ($^{3}J_{C,F}$), reflecting its distant relationship to the two fluorine nuclei (Figures 80, 82, 85 and 86).

The ^{13}C signals at 150.5ppm (doublet of doublets; $^{2}J_{C\text{-}F}$ = 30.0, $^{2}J_{C\text{-}F}$ = 12.5 Hz), and 148.1 ppm (doublet of doublets; $^{2}J_{C\text{-}F}$ = 29.7, $^{2}J_{C\text{-}F}$ = 12.5 Hz) show no correlation to any crosspeaks on the HSQC spectrum, therefore they must correspond to C-13 and C-12 (signals appear as doublet of doublets due to successive splitting by the two fluorine nuclei). Probing this relationship with the HMBC experiment, the spectrum shows a 3-bond correlation between 11-H and the methylene carbon C-9, a 3-bond correlation between C-15 and 11-H and a 2-bond correlation between C-12 and 11-H. Therefore the ^{13}C signal at 148.1 ppm corresponds to C-12 while the signal at 150.5 ppm corresponds to C-13 (Figures 86 and 87). There is a 3-bond correlation between 5-H and C-7, a 2-bond correlation between 5-H and C-4, a 3-bond correlation between 5-H and C-1 and a 3-bond correlation between 5-H and C-3, thus, the HMBC spectrum (Figure 88) assisted in assigning C-4 as the signal at 174.1 ppm and C-1 as the signal at 135.6 ppm.

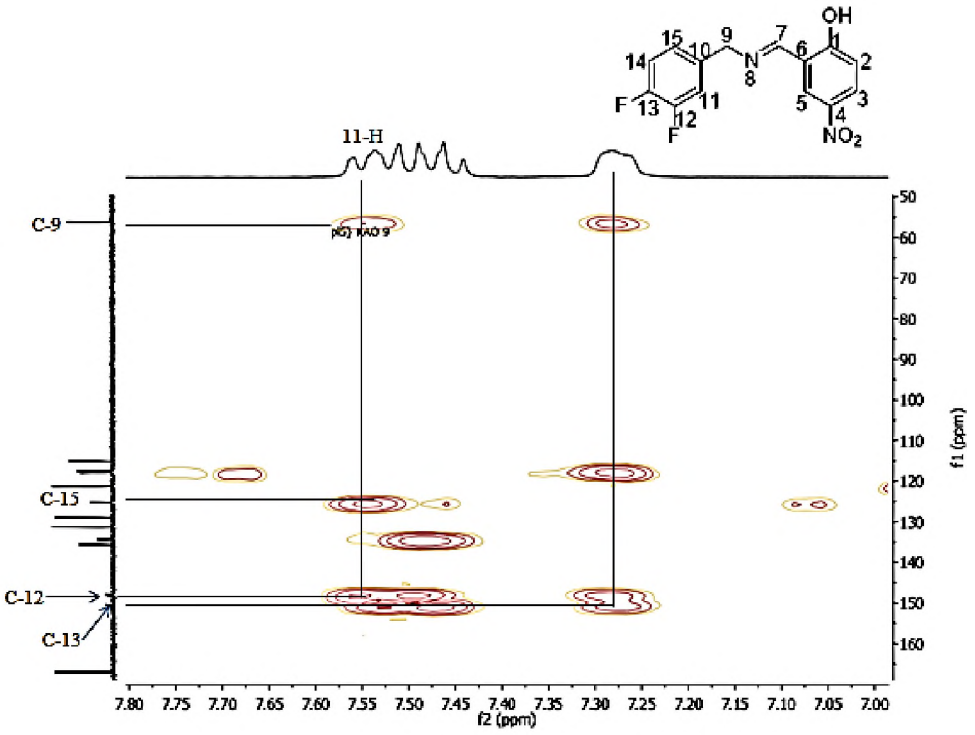

Figure 87. HMBC spectrum of **133a** in DMSO-d_6.

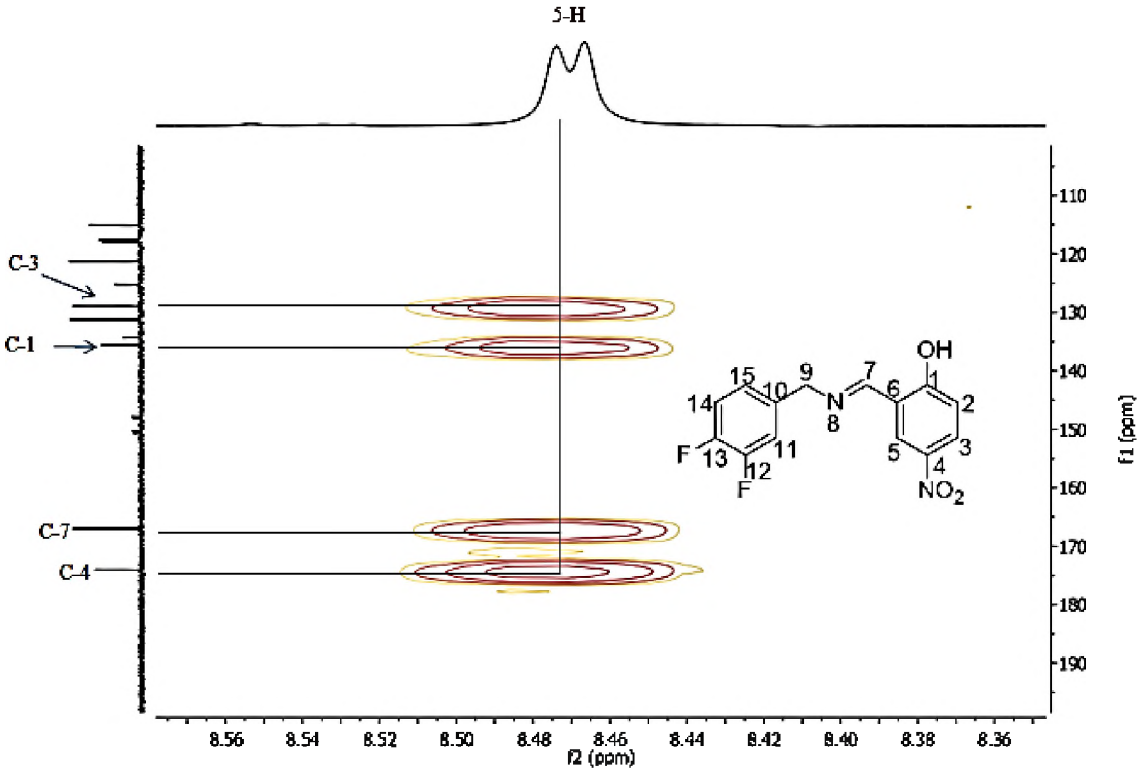

Figure 88. HMBC spectrum of **133a** in DMSO-d_6 (expanded).

2.5.1. Biological activity of *N*-(3,4-difluorobenzyl)imines 133a-e and their Cytotoxicity Activity.

Using ematine as a positive control and a resazurin-based reagent, the overt cytotoxicity of these ligands was determined against HeLa cells at 20 μM. The results indicated that none of the five compounds in this series is significantly cytotoxic because only cell viability of 50% and below was considered cytotoxic (Table 17 and Figure 89). It should be noted that toxicity increases slightly with the introduction of bromine and chlorine atoms at R^1 and R^3 (**133b**; 90%) and more significantly with the introduction of 2 chlorine atoms as R^1 and R^3 (**133e**; 63%).

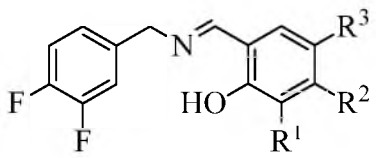

133a-e

Table 17. Viability of HeLa cell and parasite viability in the presence of **133a-e** at 20 μM.

Compound (R^1; R^2; R^3)	HeLa Cell viability (%)	SD	*T.brucei* Parasite viability (%)	SD	*P. f.* strain 3D7 Parasite viability (%)	SD
133a (H; H; NO_2)	112	4	96	5	83	10
133b (Br; H; Cl)	90	4	24	3	88	3
133c (OH; OH; H)	92	1	17	0.3	71	6
133d (OH; H; H)	93	1	102	2	109	1
133e (Cl; H; Cl)	63	7	4	5	38	11

SD – standard deviation

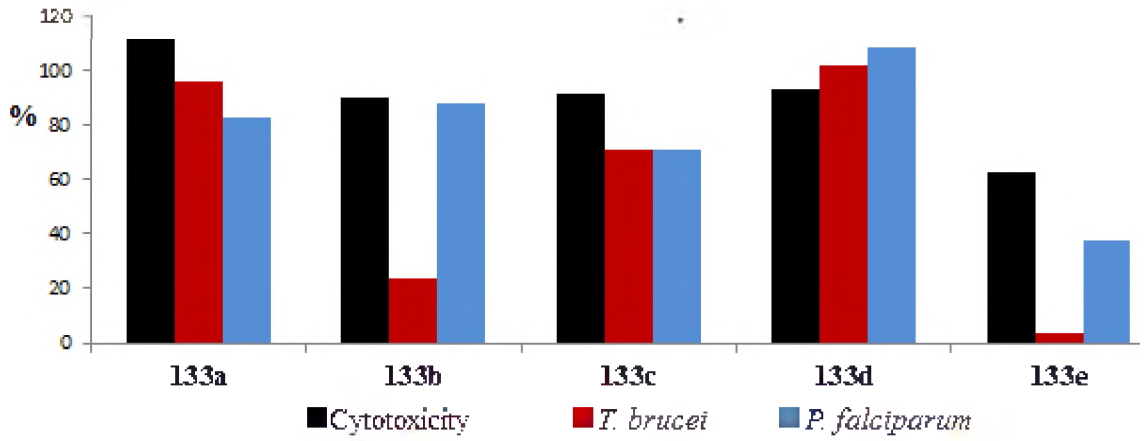

Figure 89. HeLa Cells survival and parasite viability in the presence of **133 a-e** at 20 μM**.**

Compound **133b**, **133c** and **133e** are significantly active against *T. brucei* at 20 μM. It was observed that the presence of hydroxyl groups at R^1 and R^2 (compound **133c**) may be essential for activity against *T. brucei* when compared to compound **133d** where R^1 is a hydroxyl group and R^2 is a hydrogen atom (Table 17 and Figures 89 and 90). When the activity of **133e** against *T. brucei* is compared to that of **133b**, it is clear that the substitution of bromine for chlorine at R^1 (compound **133b**) increases the percentage viability from 4% to 24% (Table 17 and Figures 89 and 90). Therefore the presence of chlorine substituents at R^1 and R^3 can also be considered as important for activity against *T. brucei*. The half maximal inhibitory concentration (IC_{50}) for compounds **133b**, **133c** and **133e** against *T. brucei* was found to be 5.8, 1.5 and 3.7 μM, respectively while the standard (pentamidine **6**) showed an IC_{50} of 0.004 μM. Compound **133e** is also the only compound in this series with promising activity against malaria with a parasite viability of 38% against malaria at 20 μM (Table 17 and Figure 91).

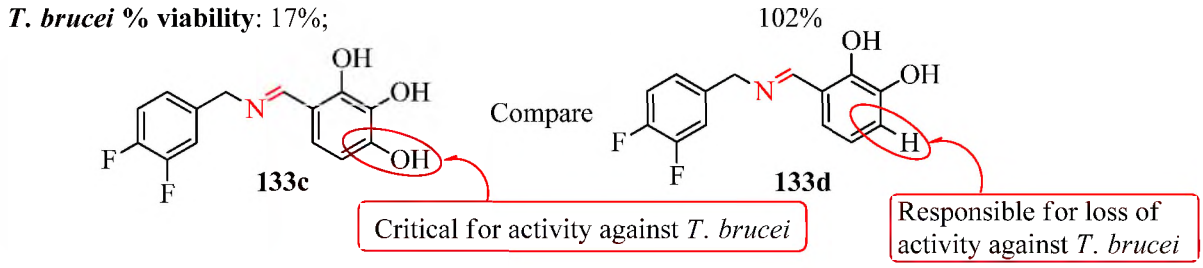

Figure 90. Hydroxyl group at R^2 may be essential for activity against *T. brucei*.

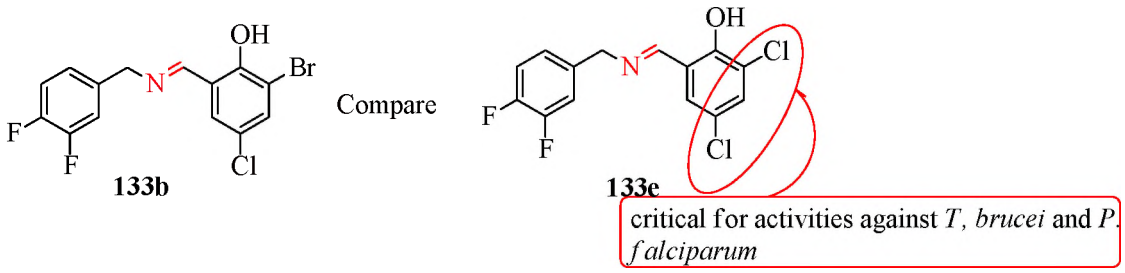

Figure 91. 3,4-dichloro substituents and *p*-hydroxyl substituent enhance activity.

2.6. SYNTHESIS AND ANTIPROTOZOAL ACTIVITY OF (±)-*TRANS-N,N'*-BIS[2-HYDROXYBENZYLIDENYL]CYCLOHEXYL-1,2-DIAMINES 135a-c.

2.6.1. Synthesis of diimines 135a-c

Given the excellent percentage viability of 5-bromo-*N,N*-bis(2-hydroxybenzylimino)pyridine **127** against *T. brucei* (7%) in section 2.1, it was envisaged that replacing the pyridyl unit of 127 with a cyclohexane can improve the solubility of such di-imino compounds. The (±)-*trans*-1,2-bis[2-hydroxybenzylidenyl]cyclohexyl-1,2-diamines **135a-c** were prepared by the condensation (±)-*trans*-1,2-diaminocyclohexane **134** with two equivalents of appropriate benzaldehydes. This condensation reaction was performed using methanol as solvent and a catalytic amount of glacial acetic acid. The reaction was done at room temperature and proceeded to completion within 10 minutes as determined by thin layer chromatography. Precipitates of the crude products were generated by adding hexane dropwise, then filtered and washed with hexane. The three derivatives **135a-c** in this series are solids and yellowish in appearance (Scheme 17).

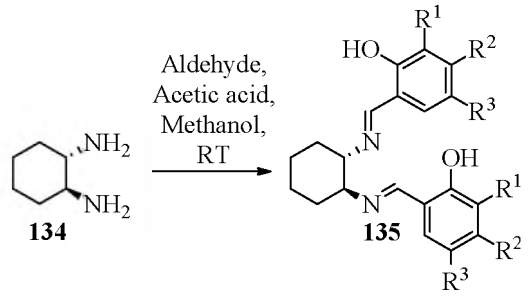

135	R1	R2	R3	Yield %
a	H	H	Cl	89
b	OCH_3	H	H	92
c	Br	H	Cl	91

Scheme 17: Synthesis of (±)-trans-1,2-bis[2-hydroxybenzylimino]cyclohexanes.

The (±)-*trans*-1,2-bis[5-chloro-2-hydroxybenzylimino]cyclohexanes **135a** is used as a representative compound to demonstrate the characterization of these compounds by NMR and HPLC-MS spectroscopies. The HPLC-MS analysis for **135a** ($C_{20}H_{21}Cl_2N_2O_2$ 391.0980) indicated the presence of $[M+H]^+$ 391.0886 peak. The C_2 symmetry of the compounds resulted in a simplification of the NMR spectra. The imino protons (8-H and 8'-H) are seen as a singlet as expected at 8.18 ppm (Figure 92). HSQC experiment (Figure 93) shows that the carbon atoms of the imino groups (C-8, C-8') correspond to the ^{13}C signal at 163.7 ppm (Figure 94) and as a positive signal in the DEPT-135 spectrum (Figure 95). The ^1H signal at 13.18 ppm (Figure 92) corresponds to the hydroxyl protons (OH) – having no correlation in the HSQC spectrum.

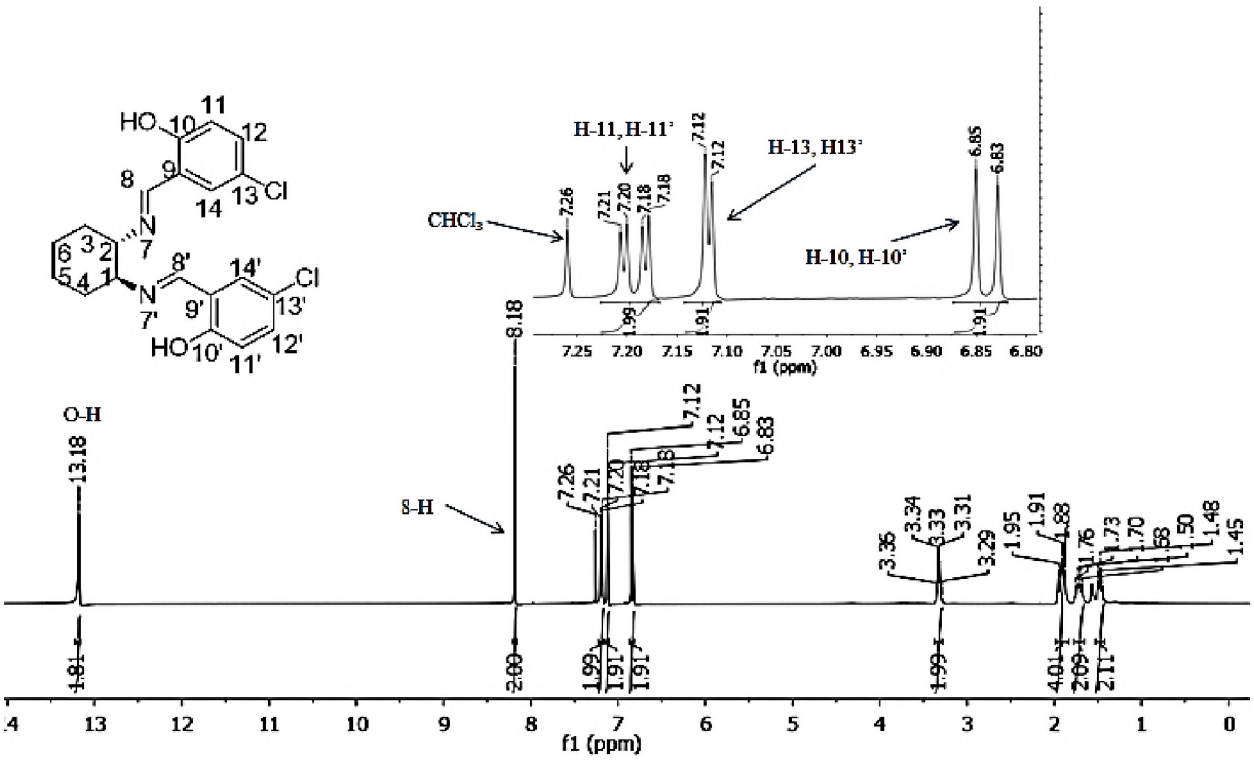

Figure 92. 400 MHz ^1H NMR spectrum of **135a** in $CDCl_3$.

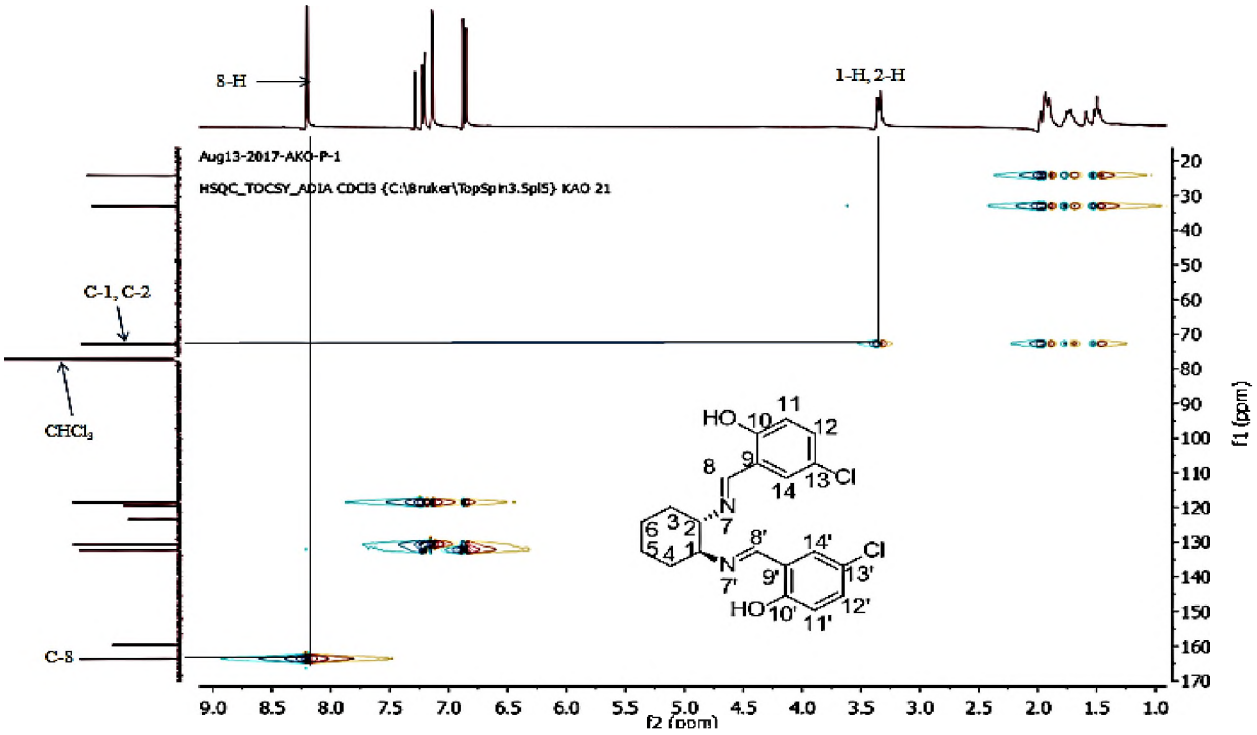

Figure 93. HSQC NMR spectrum of **135a** in $CDCl_3$ (expanded downfield).

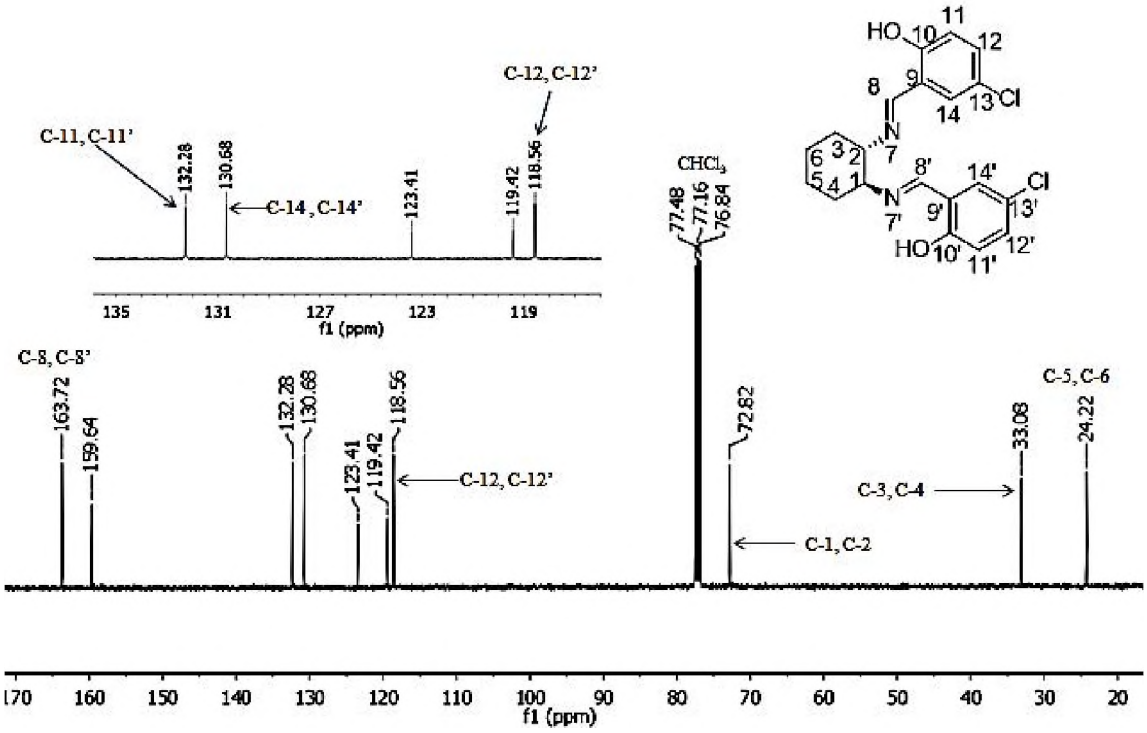

Figure 94. 100 MHz ^{13}C NMR spectrum of **135a** in $CDCl_3$.

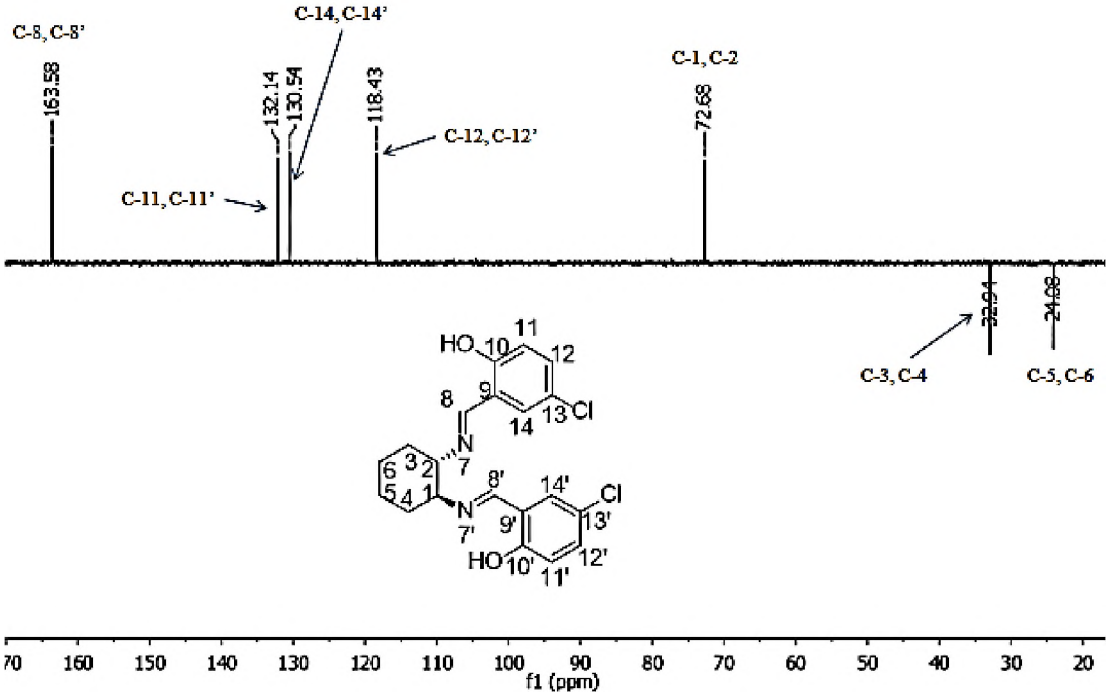

Figure 95. 100 MHz DEPT-135 NMR spectrum of **135a** in $CDCl_3$.

The doublet at 6.84 ppm corresponds to 11-H/ 11'-H while the doublet of doublets signal at 7.17 ppm corresponds to 12-H/ 12' (Figure 92). The doublet at 7.12 ppm corresponds to14-H/ 14'-H. The various coupling constants are in agreement with the crosspeaks observed in the COSY spectrum (Figure 96), confirming the assignment of these protons. With the aid of the HSQC spectrum (Figure 97), the phenyl carbon atoms bearing protons, C-11, C-11' as well as C-12, C-12' were assigned to the ^{13}C signals at 132.3 and 118.6 ppm, respectively while the C-14, C-14' ^{13}C nuclei resonate at 130.7 ppm (Figure 94 and 97).

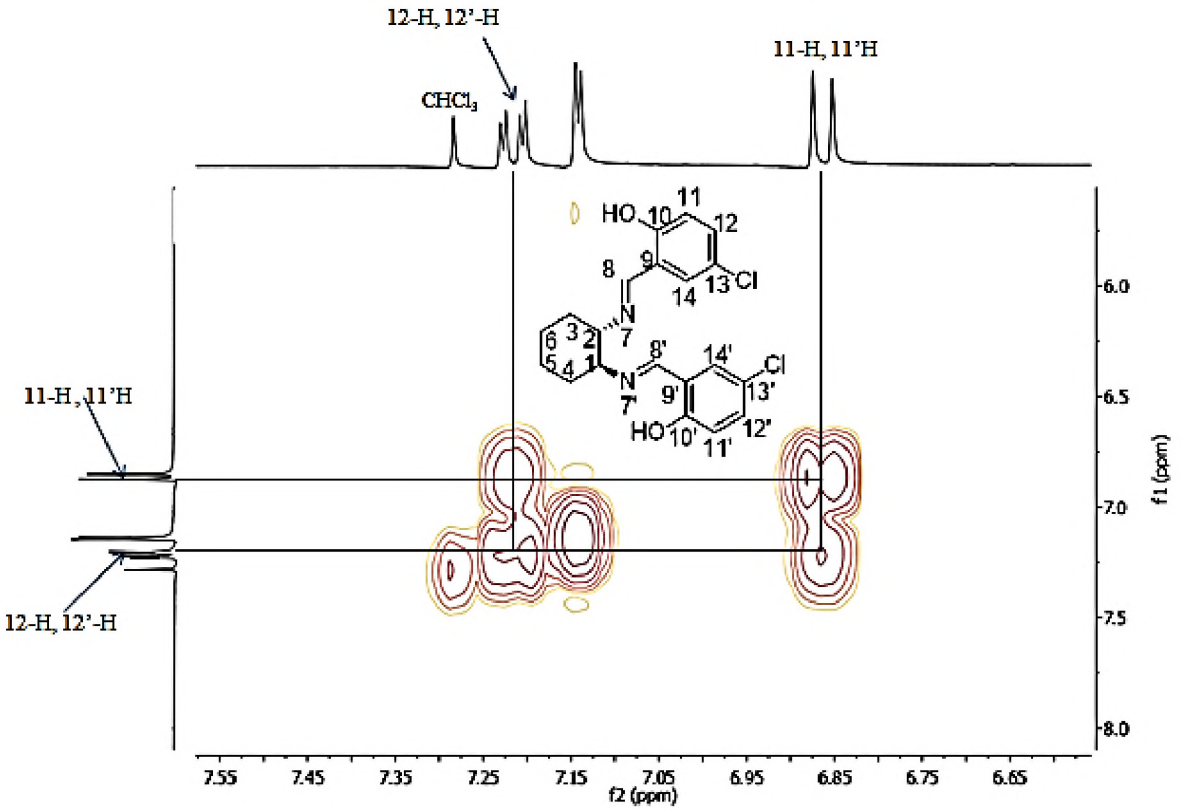

Figure 96. 400 MHz COSY NMR spectrum of **135a** in $CDCl_3$.

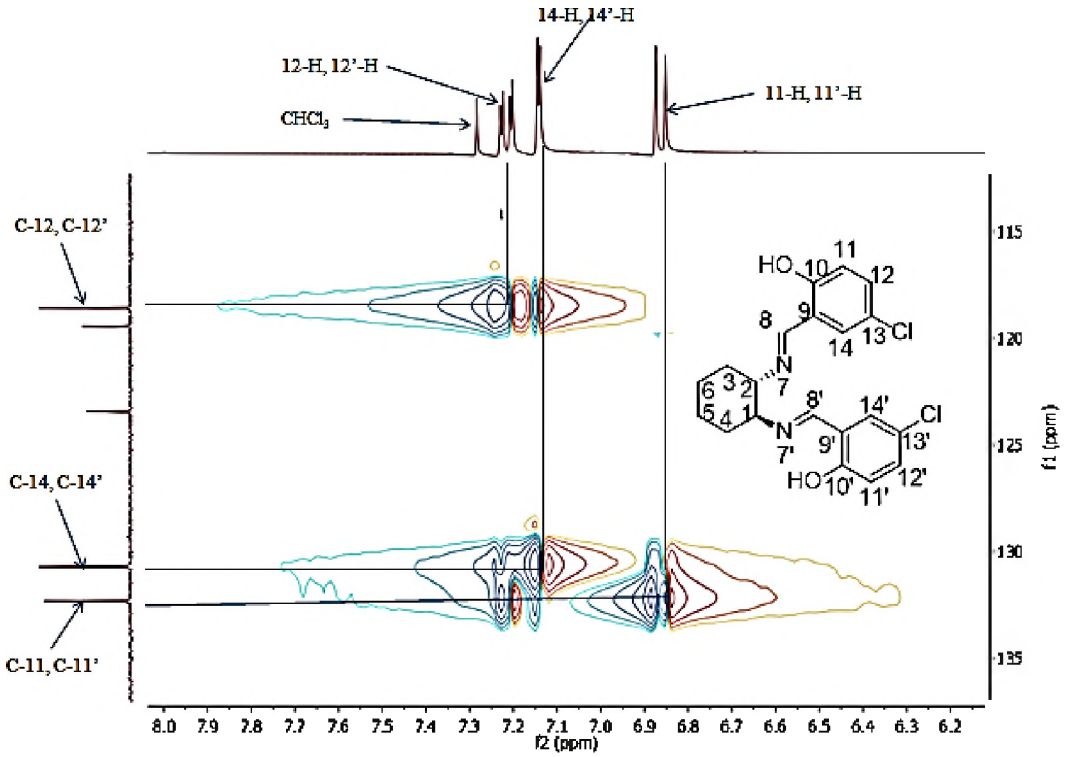

Figure 97. HSQC NMR spectrum of **135a** in $CDCl_3$ (expanded lowfield).

The cyclohexyl methine protons H-1, H-2 (deshielded as expected because of the attached nitrogen atoms) resonate as multiplets between 3.36 – 3.28 ppm (Figure 98) and with the aid of the HSQC spectrum (Figure 93), the signal at 72.8 ppm in the ^{13}C spectrum was assigned to C-1, C-2 (Figure 94). The multiplets between 1.65 – 1.91 ppm in the ^{1}H NMR spectrum represent the signals for 3-H/ 4-H and 5-H/ 6-H while the ^{13}C signals at 33.1 and 24.2 ppm, in the ^{13}C spectrum, represent C-3, C-4 and C-5, C-6 (Figures 94 and 98) respectively. The assignment of the cyclohexyl methine ^{13}C signals was further confirmed by the DEPT-135 spectrum (Figure 95) where two negative signals in the upfield region corresponding to two methylene carbons (C-3, C-4 and C-5, C-6) were unambiguous.

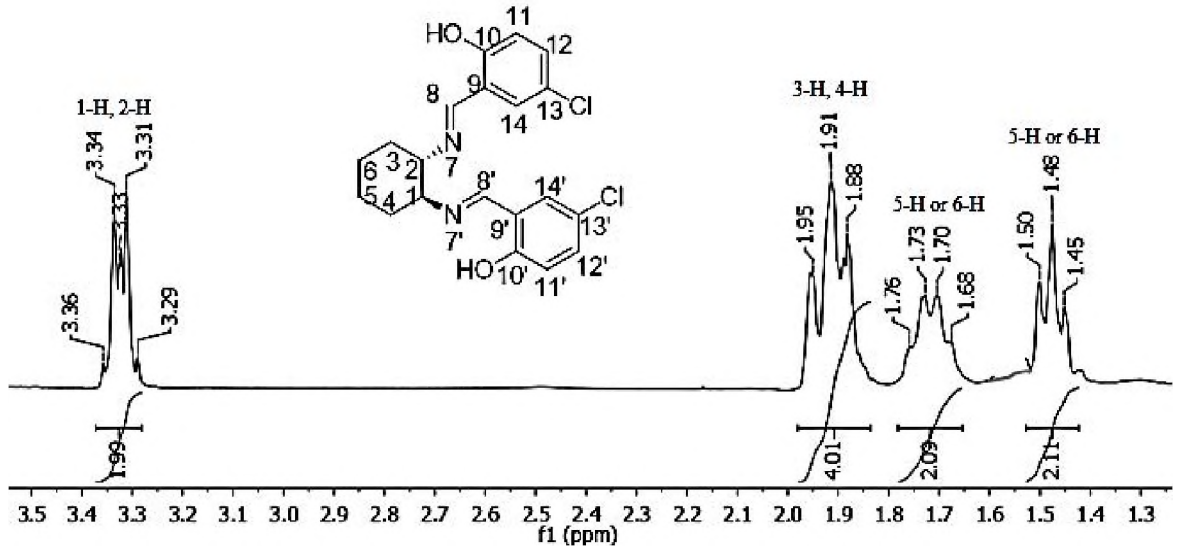

Figure 98. 400 MHz ^{1}H NMR spectrum of **135a** in $CDCl_3$ (expanded).

2.6.1. Anti-Protozoan Activity of cyclohexyl-1,2-diimines 135a-c.

Cytotoxicity studies of the three derivatives indicated that none of the three compounds **135a-c** are significantly cytotoxic to HeLa cells at 20 μM; **135a** and **135b** limited cell viabilities to 82 and 84 %, respectively (Table 18 and Figure 99). Compound **135c** showed a minimal cytotoxicity with cell viability of 58% (cell viability of 50% and below is indicative of significantly cytotoxic compounds).

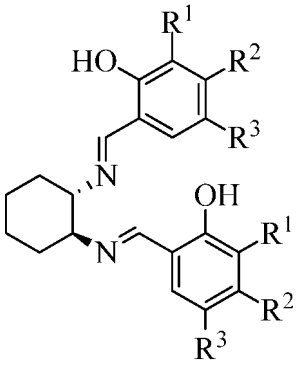

Table 18. Activity of **135a-c** at 20 μM against HeLa cells and parasitic protozoans.

Compound (R^1; R^2; R^3)	HeLa Cell viability (%)	SD	*T.brucei* Parasite viability (%)	SD	*P. f.* strain 3D7 Parasite viability (%)	SD
135a (H; H; Cl)	82	4	88	0.2	79	11
135b (OCH_3; H; H)	84	4	97	3	93	10
135c (Br; H; Cl)	58	2	5	3	13	5

SD – standard deviation

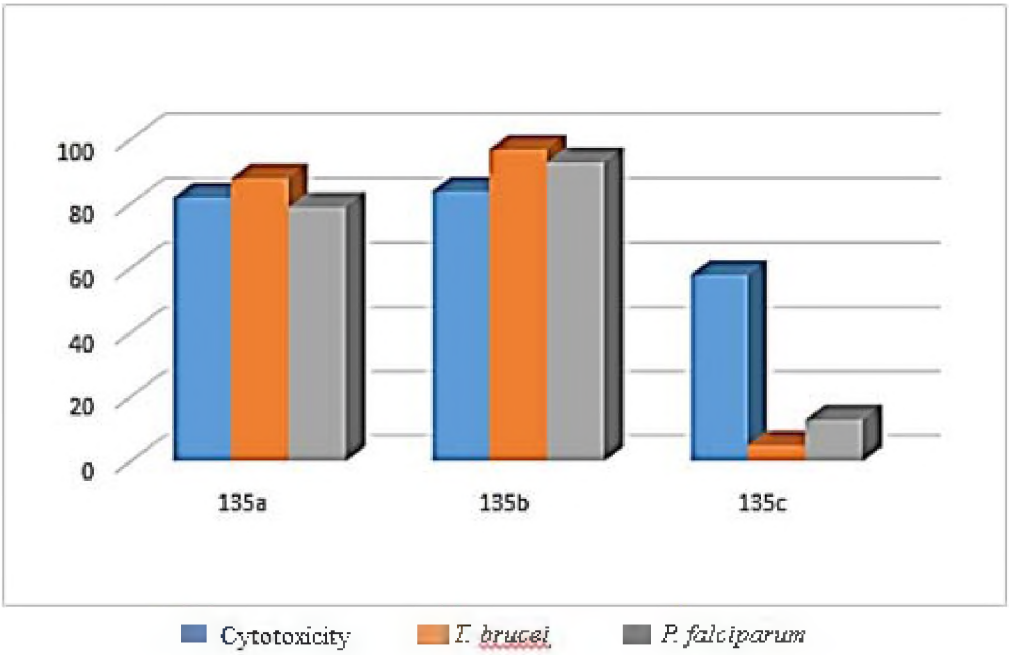

Figure 99. HeLa cells viability and parasite viability in the presence of **135a-c** at 20 μM.

Activity assays against *T. brucei* and *P. falciparum* (3D7 strain) suggests that compound **135c** with electron withdrawing chlorine substituents at R^1 and R^3 was active against both

parasitic protozoans with 5% parasite viability against *T. brucei* and 13% parasite viability against *P. falciparum.* (Table 18, Figure 99). These results suggests that this ligand is a viable scaffold against both parasites and can further be developed into more potent but less toxic molecules that can target both parasites. The presence of bromine and chlorine atoms at R^1 and R^3 respectively, is a key factor for potency in this compound (Figure 100).

The IC_{50} was determined for ligand **135c** and an IC_{50} value of 3.7 μM was obtained against *P. falciparum* (*the* IC_{50} value of the chloroquine **16** – a standard was 0.03 μM). An IC_{50} value of 3.7 μM was also recorded against *T. brucei* for **135c** while 0.004 μM was recorded for pentamidine **6**.

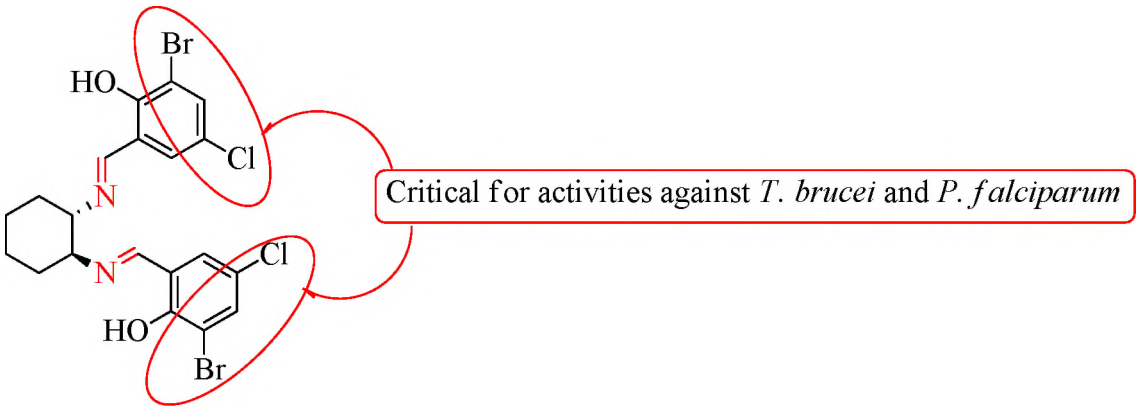

135c

Figure 100. 3-bromo-5-chloro substitution is critical for activity against parasitic protozoans.

2.7. CONCLUSION

This report shows the importance of the imino unit for biological activity in a range of heterocyclic and non-heterocyclic compounds. Compounds synthesized include azabenzimidazoles, benzyliminopyridines and benzylimines and were obtained in good to excellent yields.

For the present study, some of the 2-amino-5-bromo-7-(benzylimino)pyridines and *N*-(phenyl)-2-hydroxybenzylimines were hydrogenated into secondary amines in order to reasonably affirm the selective toxicity of imines to parasitic protozoans.

On screening against HeLa cell lines, it was observed that these compounds are not significantly cytotoxic. The result of bioactivity assay of these compounds showed that the 1-alkylated 7-azabenzimidazole heterocyclic derivatives and 5-bromo-1-[(*N*-substitutedcarbamoyl]methyl}-7-azabenzimid-azoles were not active against these *T. brucei* and *P. falciparum*.

The benzyl, isoxazole and furfuryl derivatives of 5-bromo-1-[(*N*-substitutedcarbamoyl]methyl}-7-azabenzimid-azoles displayed rotational isomerism. 1-{[*N*-(3-chlorobenzyl)carbamoyl}-5-bromo-7-azabenzimidazole **122b** and 1-{[*N*-(2-furfuryl)carbamoyl}-5-bromo-7-azabenzimidazole **122g** were selected as representative compounds for DNMR studies. On subjecting **122b** and **122g** to variable temperature NMR studies, the coalescence temperature T_C and the rate constant k_C were found to be 353 K and 97.7 s^{-1}, respectively for the carbamoyl proton of **122b** while the T_C and k_C for the methylene protons of **122g** were 363 K and 26.6 s^{-1}, respectively. The free energy differences ΔG_o were calculated to be -0.11 kJ mol^{-1} for **122b** and -0.55 kJ $mol^{-1}$for **122g** at 298 K**.** The free energy of activation ΔG^* were calculated (by extrapolation from the graph of temperature against frequency of separation) to be 73.5 kJ mol^{-1} for **122b** and 79.6 kJ mol^{-1} for **122g** . The free energy of activation of 77.3 kJ mol^{-1} for **122b** and 84.6 kJ mol^{-1} for **122g** were also estimated at coalescence by Eyring equation. However, the estimation made from the plot of temperature versus frequency of separation is presumed to be more accurate because it took all experimental temperatures into consideration.

The 2-phenyl-7-azabenzimidazoles and the 2-amino-5-bromo-7-(benzylimino)pyridines were not cytotoxic against HeLa cell lines. These compounds showed good selectivity towards *T. brucei* – **125b** reduced *T. brucei* parasite viability to only 17%, **125d** and **125m** reduced parasite viability to 20% while **125k** to 36%. The 2-amino-5-bromo-7-(benzylimino)pyridines **126a**, **126d** and **126e** were able to reduce *T. brucei* parasite viability to 24, 20 and 23%,m respectively. The 5-bromo-2,3-bis(2-hydroxybenzylimino)pyridine **127** gave the best inhibition against the parasite with a viability of 7%, this is presumed to be due to the fact that there are more carbon-nitrogen double bonds (C=N) in the compound but when this molecule was hydrogenated to 5-bromo-2,3-bis(2-hydroxybenzylamino)pyridine **127'**, the parasite viability rose to 105%. These compounds are worth looking at as a viable novel scaffold that should be optimized in development of new trypanosomiasis drugs.

The anti-protozoan activity of *N*-(phenyl)-2-hydroxybenzylimines, *N*-(benzyl)-2-hydroxybenzylimines and (±)-*trans*-1,2-bis[2-hydroxybenzylimino]cyclohexanes showed that the *T. brucei* parasite viability was reduced to 22% by **130a**, 12% by **130f**, 17% by **130i**, 5% by **130j**, 7% by **130k**, 6% by **130k'** and 13% by **130l**. **130j** and **130k** reduced *P. falciparum* parasite viability to 27 and 33%, respectively but when the imino group in these compounds is hydrogenated to a secondary amino group, the parasite viability against *P. falciparum* were found to be 104 and 121%, respectively, thus making a strong case for the selective toxicity of imines towards parasitic protozoans. **133b**, **133c** and **133e** reduced *T. brucei* parasite viability to 24, 17 and 4%, respectively; however, **133e** also reduced *P. falciparum* parasite viability to 38%. **135c** was able to reduce *T. brucei* parasite viability to 5% and *P. falciparum* parasite viability to 13% and this could be attributed to the fact that two imino units are present in this ligand.

With all these results put together, new scaffolds have been identified for optimization in the development of new anti-parasitic protozoans for the treatment of coinfection that involves both parasites with minimal cytotoxicities. Future work in this area of medicinal chemistry is expected to include the following objectives.

1. Identification of the target enzyme and application of computational method to improve the activity of the 2-phenyl-7-azabenzimidazole and their 2-amino-5-bromo-7-(benzylimino)pyridines analogues in these series with low IC_{50}.
2. Identification of the target enzyme and application of computational method to improve the activity of *N*-(phenyl)-2-hydroxybenzylimines, *N*-(benzyl)-2-hydroxybenzylimines.
3. Optimisation of 5-bromo-2,3-bis(2-hydroxybenzylimino)pyridine and (±)-*trans*-1,2-bis[2-bromo-5-chloro-2-hydroxybenzylimino]cyclohexane to improve activities against *P. falciparum* and *T. brucei* and identification of the relevant target enzymes.

3. EXPERIMENTAL

3.1. GENERAL

All chemicals used were purchased from Sigma-Aldrich Chemical Co. and water used was deionized. Analytical thin layer chromatography (TLC) was performed using precoated silica gel plates and visualized under a UV lamp. Column chromatography was done using silica gel and hexane/ethyl acetate gradient solvent system. Compounds were characterized using Bruker Avance 300 and 400 MHz NMR spectrometers. Chemical shifts for each experiment was reported in parts per million (ppm) relative to residual proton in deuterated solvent used for each experiment (Chloroform, 7.26ppm and DMSO-d_6, 2.5 ppm) and the coupling constants (J) are reported in hertz (Hz), where s = singlet, br s = broad singlet, d =doublets, dd = doublet of doublets, ddd = doublet of doublets of doublets, t = triplet, q =quartet and m = multiplet. The NMR spectra were analysed using mestrenova. IR spectra were recorded on a Perkin Elmer Spectrum 100 FTIR spectrometer with a diamond window. Melting points were determined using hot stage apparatus. Masses of compounds were determined by high-performance liquid chromatography-mass spectrometric (HPLC-MS) experiment was performed using Bruker daltonics compact QTOF MS with electrospray ionization probe, positive mode.

3.2. BIOASSAYS PROCEDURES

3.2.1. Parasite lactate dehydrogenase (pLDH) assay

Malaria parasites (*Plasmodium falciparum* strain 3D7) were maintained in RPMI 1640 medium containing 2 mM L-glutamine and 25 mM Hepes (Lonza). The medium was further supplemented with 5 % Albumax II, 20 mM glucose, 0.65 mM hypoxanthine, 60 µg/mL gentamycin and 2-4 % hematocrit human red blood cells. The parasites were cultured at 37 °C under an atmosphere of 5% CO_2, 5% O_2, 90% N_2 in sealed T25 or T75 culture flasks. Compounds in question were added at 20 μM to parasite cultures in 96-well plates and incubated for 48h in a 37 °C CO_2 incubator. The plates were removed from the incubator after 48h. Aliquots of 20 µL of culture was removed from each well and mixed with 125 µL of a mixture of Malaria solution and NBT/PES solution in a fresh 96-well plate. These solutions measured the activity of the pLDH enzyme in the cultures. A purple product was

formed when pLDH is present, and this product was quantified in a 96-well plate reader by absorbance at 620nm (Abs_{620}). The Abs_{620} reading in each well was thus an indication of the pLDH activity in that well and also the number of parasites in that well.

For each compound concentration, % parasite viability – the pLDH activity in compound-treated wells relative to untreated controls – was calculated. Compounds were tested in duplicate wells, and a standard deviation (SD) was derived. For comparative purposes, chloroquine (an anti-malarial drug) is used as a drug standard and yields IC_{50} values in the range of 0.01-0.05 μM.

3.2.2. Anti-Trypanocidal Activity

To assess anti-trypanocidal activity, compounds were added to *in vitro* cultures of *T.b. brucei* in 96-well plates at a fixed concentration of 20 μM. After an incubation period of 48 hours, the numbers of parasites surviving drug exposure were determined by adding a resazurin based reagent. The reagent contains resazurin which is reduced to resorufin by living cells. Resorufin is a fluorophore (Exc_{560}/Em_{590}) and can thus be quantified in a multi-well fluorescence plate reader.

Results are expressed as % parasite viability – the resorufin fluorescence in compound-treated wells relative to untreated controls. Compounds were tested in duplicate wells, and a standard deviation (SD) was determined. Pentamidine (an existing drug treatment for trypanosomiasis) at 1μM was used as a positive control drug standard.

3.2.3. Cytotoxicity Determination

To assess the overt cytotoxicity of the compounds, they were incubated at a fixed concentration of 20 μM in 96-well plates containing HeLa (human cervix adenocarcinoma) cells for 48 hours. The numbers of cells surviving drug exposure were also determined by using the resazurin based reagent and reading resorufin fluorescence in a multiwell plate reader.

Results were expressed as % cell viability – the resorufin fluorescence in compound-treated wells relative to untreated controls. Compounds were tested in duplicate wells, and a standard deviation (SD) was also included. For the cytotoxicity assay, results were also expressed as % cell viability, based on fluorescence reading in treated wells vs. untreated control well. Emetine (which induces cell apoptosis) was used as a control drug standard.

3.3. SYNTHESIS OF 2,3-DIAMINO-5-BROMOPYRIDINE AND 5-BROMO-7-AZABENZIMIDAZOLE

2-Amino-5-bromopyridine **112**, 2-amino-3,5-dibromopyridine **112b**, 2-amino-5-bromo-3-nitropyridine **114** and 2,3-diamino-5-bromopyridine **115** are known. The procedures for their synthesis have been reported previously.[119]

2-amino-5-bromopyridine 112

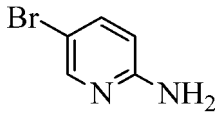

A solution of 2-aminopyridine (28.2 g, 300 mmol) in acetic acid (50 mL) was place in a 200 mL three necked flask equipped with stirrer, dropping funnel and reflux condenser. The solution in the flask was cooled to 15 °C and a solution of bromine (15.4 mL, 301mmol) in acetic acid (30 mL) was added dropwise. The mixture was stirred vigorously for one hour. The reaction temperature was raised to room temperature and after 30 minutes, the temperature was increased to 50 °C. The mixture was stirred for two hours; the mixture was then diluted with deionized water (75 mL) and neutralized with 40% aqueous sodium hydroxide solution to generate a precipitate. The precipitate was filtered and washed with deionized water (3 × 100 mL). The residue was dried and washed with hot petroleum ether to give *2-amino-5-bromopyridine* **112** as a white solid (39.4 g, 76%); m.p. 132-134 °C; δ_H/ppm (300 MHz; $CDCl_3$) 8.08 (1H, dd, J = 2.5, 0.6 Hz, Ar-H), 7.48 (1H, dd, J = 8.7, 2.5 Hz, Ar-H), 6.40 (1H, dd, J = 8.7, 0.7 Hz, ArH) and 4.58 (2H, s, NH_2); δ_C/ppm (75 MHz; $CDCl_3$) 157.2, 148.7, 140.2, 110.2 and 108.3 (Ar-C).

2-Amino-3,5-dibromopyridine 112b

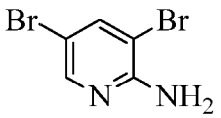

The petroleum ether filtrate from the procedure described for the preparation of 2-amino-5-bromopyridine was concentrated to give a crystalline solid as *2-amino-3,5-dibromopyridine* **112b** (11 g, 10.6%); m.p. 113-118 °C; δ_H/ppm (400 MHz; DMSO-d_6) 8.01 (1H, d, J = 2.0 Hz, Ar-H), 7.93 (1H, d, J = 2.0 Hz, Ar-H) and 6.44 (2H, s, NH_2); δ_C/ppm (100 MHz; DMSO-d_6) 155.4, 147.8, 139.2, 104.4 and 103.5 (Ar-C).

2-amino-5-bromo-3-nitropyridine 114

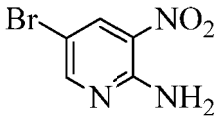

Sulphuric acid (60 mL) was placed a 200 mL three-necked flask equipped with stirrer, dropping funnel, condenser and thermometer and cooled to 0 °C. 2-amino-5-bromopyridine (10.0 g, 57. 8 mmol) was added in 20 portions and stirred to dissolve. Nitric acid (3 mL) was added drop by drop while stirring at 0 °C. The mixture was stirred for one hour at 0 °C, one hour at 25 °C and one hour at 60 °C. The mixture was cooled to room temperature, poured into crushed ice and neutralized with 40% sodium hydroxide (160 mL). The precipitate was filtered and washed with deionized water (3 × 150 mL). The residue was dried at room temperature to give *2-amino-5-bromo-3-nitropyridine* **114** as a yellow solid (10.2 g, 81%); m.p. 203-206 °C; δ_H/ppm (400 MHz; DMSO-d_6) 8.50 (1H, d, J = 2.3 Hz, Ar-H), 8.48 (1H, d, J = 2.3 Hz, Ar-H) and 8.05 (2H, s, NH_2). δ_C/ppm (100 MHz; DMSO-d_6) 156.4, 152.5, 136.2, 127.1 and 103.6 (Ar-C).

2,3-diamino-5-bromopyridine 115

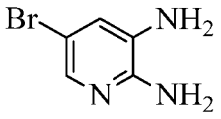

2-amino-5-bromo-3-nitropyridine (10 g, 45.9 mmol), reduced iron (2.7 g) anhydrous ethanol (3.5 mL), deionized water (1 mL) and concentrated hydrochloric acid (0.05 mL) were added into a 25 mL round bottom flask. The mixture was refluxed at 98 °C while the progress of the reaction was monitored by thin layer chromatography. At the completion of the reaction, the iron was filtered and thoroughly washed with hot anhydrous ethanol. The combined filtrate was evaporated to dryness to give *2,3-diamino-5-bromopyridine* **115** residue as a brown solid (6.7 g, 78%); m.p. 162-164 °C; δ_H/ppm (300 MHz; DMSO-d_6) 7.28 (1H, d, J = 2.2 Hz), 6.80 (1H, d, J = 2.2 Hz), 5.62 2H, (2H, s, NH_2) and 5.01 (2H, s, NH_2); δ_H/ppm (75 MHz; DMSO-d_6) 147.5, 134.1, 132, 119.1 and 106.5 (Ar-C).

5-bromo-7-azabenzimidazole 116

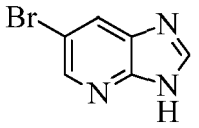

To a stirred solution of 2,3-diamino-5-bromopyridine (10 g, 53.2 mmol) in triethyl orthoformate (53.1 mL, 319.1 mmol), was added acetic anhydride (42.5 mL, 478.6 mmol) The mixture was stirred at 110 °C for 6 hours. Thereafter, the mixture was cooled to room temperature and concentrated under reduced pressure. The crude residue was dissolved in 10% sodium hydroxide solution (30 mL) and the solution was refluxed at 110°C for thirty minutes. After cooling to room temperature, the pH was adjusted to 6 with few drops of glacial acetic acid. The solution was poured into 100 mL ice cubes and stirred. The precipitate was filtered and washed with deionized water (3 × 100 mL) The crude residue was dried and washed with ethyl acetate (2 × 50 mL) and *5-bromo-7-azabenzimidazole* **116** was isolated as a brown solid (10.3 g, 98 %); m.p. dec. > 300 °C [HPLC-MS: m/z calculated for $C_6H_5BrN_3$ $(M+1)^+$ 197.9667. Found 197.9661]; δ_H/ppm (400 MHz; DMSO-d_6) 13.12 (1H, br s, NH), 8.50 (1H, s, Ar-H), 8.43 (1H, d, J = 1.6 Hz, Ar-H) and 8.29 (1H, d, J = 1.5 Hz, Ar-H); δ_C/ppm (100 MHz; DMSO-d_6) 149.9, 145.6, 144.1, 132.0, 126.3 and 112.8 (Ar-C).

3.4. SYNTHESIS OF *N*-ALKYLATED-5-BROMO-7-AZABENZIMIDAZOLES 119a-h.

1-Allyl-5-bromo-7-azabenzimidazole

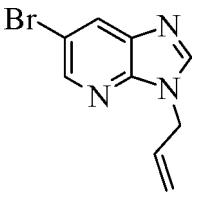

A mixture of 5-bromo-7-azabenzimidazole (200 mg, 1 mmol) and caesium carbonate (651.6 mg, 2 mmol) in 1-methylpyrrolidinone (10 mL) was stirred at room temperature for 15 minutes. To the solution was added allyl bromide (0.1 mL, 1 mmol). The resulting mixture was stirred vigorously at room temperature for 2 hours while the progress of the reaction was monitored by thin layer chromatography. At the completion of the reaction, the organic crude

product was extracted into ethyl acetate (2 × 70 mL). The combined organic phase was thoroughly washed with deionized water (4 × 140 mL), dried with anhydrous sodium sulphate and filtered. The solvent was removed *in vacuo*. The residue was purified using column chromatography on silica gel; elution with ethyl acetate-hexane (2 : 1) to afford *1-allyl-5-bromo-7-azabenzimidazole* **119a** as a brown oil (320.9 mg, 96%) [HPLC-MS: m/z calculated for $C_9H_8BrN_3$ $(M)^+$ 236.9902. Found 237.2171]; δ_H/ppm (400 MHz; $CDCl_3$) 8.42 (1H, d, *J* = 2.0 Hz, Ar-H), 8.19 (1H, d, *J* = 2.0 Hz, Ar-H), 8.04 (1H, s, Ar-H), 6.04 (1H, ddd, *J* = 16.6, 10.5, 5.7 Hz, C-*CH*=C), 5.30 (1H, d, *J* = 10.5 Hz, C-C=*CH*$_{trans}$), 5.20 (1H, d, *J* = 17.6 Hz, C-C=*CH*$_{cis}$) and 4.87 (2H, d, *J* = 5.7 Hz, CH_2); δ_C/ppm (100 MHz; $CDCl_3$) 145.6, 145.3, 145.1, 136.5, 131.8 (Ar-C), 130.5 (C-*C*H=C), 119.2 (Ar-C), 114.1 (C=*C*H_2) and 45.9 (CH_2).

1-Propargyl-5-bromo-7-azabenzimidazol 119b

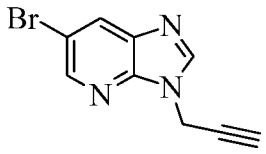

The procedure described for the synthesis of **119a** was used using 5-bromo-7-azabenzimidazole (200 mg, 1.00 mmol), caesium carbonate (652 mg, 2.00 mmol) 1-methylpyrrolidinone (10 mL) and propargyl bromide (1.00 mmol). The crude product was purified (column chromatography; elution with ethyl acetate – hexane 2:1) to yield *5-bromo-1-propargyl-7-azabenzimidazole* **119b** as a white solid (127.5 mg, 54%); m.p. 102-104 °C [HPLC-MS: m/z calculated for $C_9H_7BrN_3$ $(MH+2)^+$ 237.9823. Found 237.9598]; δ_H/ppm (300 MHz; $CDCl_3$) 8.47 (1H, d, *J* = 2.0 Hz, Ar-H), 8.26 (1H, s, Ar-H), 8.22 (1H, d, *J* = 2.0 Hz, Ar-H), 5.05 (2H, d, *J* = 2.6 Hz, CH_2) and 2.53 (1H, t, *J* = 2.6 Hz, C≡*CH*); δ_C/ppm (75 MHz; $CDCl_3$) 145.4, 144.34, 144.33, 136.5, 130.6 and 114.3 (Ar-C), 78.8 (CH_2), 75.2 and 75.1 (*C*≡CH and C≡*C*H).

5-Bromo-1-pentyl-7-azabenzimidazole 119c

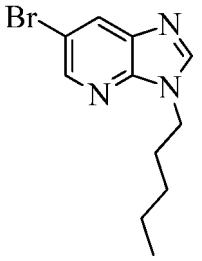

The procedure described for the synthesis of **119a** was used using 5-bromo-7-azabenzimidazole (300mg, 1.5 mmol), caesium carbonate (488.7 mg, 1.5 mmol) 1-methylpyrrolidinone (10 ml) and 1-bromopentane (0.2 ml, 1.7 mmol). The crude product was purified (thin layer chromatography; elution with ethyl acetate – hexane 1:1) to yield *5-bromo-1-pentyl-7-azabenzimidazole* **119c** as a colourless oil (354.0 mg, 88%) [HPLC-MS: m/z calculated for $C_{11}H_{15}BrN_3$ $(M+H)^+$ 268.0449. Found 268.0238]; δ_H/ppm (300 MHz; $CDCl_3$) 8.42 (1H, d, J = 2.0 Hz, Ar-H), 8.18 (1H, d, J = 2.0 Hz, Ar-H), 8.02 (1H, s, Ar-H), 4.24 (2H, t, J = 7.2 Hz, N-CH_2), 1.97 – 1.84 (2H, m, N-C-CH_2), 1.40 – 1.24 (4H, m, N-C-C-CH_2-CH_2) and 0.87 (3H, t, J = 6.9 Hz, CH_3); δ_H/ppm (75 MHz; $CDCl_3$) 145.8, 145.2, 145.1, 136.7, 130.3, 113.9 (Ar-C) 44.1, 29.7, 28.90, 22.2 (CH_2) and 14.0 (CH_3).

5-Bromo-1-(propiophenone)-7-azabenzimidazole 119d

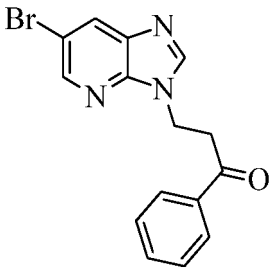

The procedure described for the synthesis of **119a** was used using 5-bromo-7-azabenzimidazole (200 mg, 1 mmol), caesium carbonate (488.7 mg, 1.5 mmol) 1-methylpyrrolidinone (15 mL) and 3-chloropropiophenone (168.6 mg, 1 mmol). The crude product was purified (thin layer chromatography; elution with ethyl acetate – hexane 2:1) to yield *5-bromo-1-(propiophenone)-7-azabenzimidazole* **119d** as a white solid (155.2 mg, 47%); m.p. 104-106 °C [HPLC-MS: m/z calculated for $C_{15}H_{13}BrN_3O$ $(M+H)^+$ 330.0242. Found 330.0089]; δ_H/ppm (400 MHz; $CDCl_3$) 8.40 (1H, d, J = 1.7 Hz, Ar-H), 8.25 (1H, s, Ar-H), 8.14 (1H, d, J = 1.7 Hz, Ar-H), 7.88 (1H, d, J = 7.5 Hz, Ar-H), 7.53 (1H, t, J = 7.4 Hz, Ar-H), 7.41 (2H, t, J = 7.7 Hz, Ar-H), 4.72 (2H, t, J = 6.0 Hz, N-CH_2), 3.62 and (2H, t, J =

6.0 Hz, $COCH_2$). δ_C/ppm (100 MHz; $CDCl_3$) 197.0 (C=O), 146.7, 145.6, 144.9, 136.7, 136.1, 133.8, 130.4, 128.8, 128.1, 114 (Ar-C), 38.8 (N-CH_2), and 37.8 (CO-CH_2).

1-Benzyl-5-bromo-7-azabenzimidazole 119e

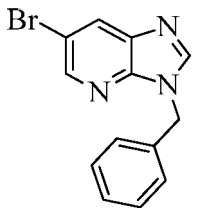

The procedure described for the synthesis of **119a** was used using 5-bromo-7-azabenzimidazole (200 mg, 1 mmol), caesium carbonate (488.7 mg, 1.5 mmol) 1-methylpyrrolidinone (15 mL) and benzyl bromide (0.12mL, 1 mmol). The crude product was purified (thin layer chromatography; elution with ethyl acetate – hexane 2:1) to yield *1-benzyl-5-bromo-7-azabenzimidazole* **119e** as a white solid (224.8 mg, 78%); m.p. 116-118 °C [HPLC-MS: m/z calculated for $C_{13}H_{11}BrN_3$ $(M+H)^+$ 288.0136. Found 287.9823]; δ_H/ppm (400 MHz; $CDCl_3$) 8.46 (1H, d, J = 2.0 Hz, Ar-H), 8.21 (1H, d, J = 2.0 Hz, Ar-H), 8.02 (1H, s, Ar-H), 7.37 – 7.27 (5H, m, Ar-H) and 5.43 (2H, s, CH_2); δ_C/ppm (100 MHz; $CDCl_3$) 145.8, 145.4, 145.15, 136.5, 135.5, 130.5, 129.2, 128.6, 127.9, 114.2 (Ar-C) and 47.4 (CH_2).

5-Bromo-1-(4-nitrobenzyl)- 7-azabenzimidazole 119f

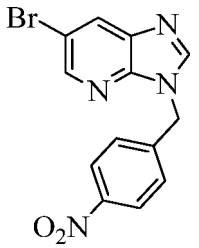

The procedure described for the synthesis of **119a** was used using 5-bromo-7-azabenzimidazole (200 mg, 1 mmol), caesium carbonate (488.7 mg, 1.5 mmol) 1-methylpyrrolidinone (20 mL) and 4-nitrobenzyl bromide (216.0 mg, 1 mmol). The crude product was purified (thin layer chromatography; elution with ethyl acetate – hexane 3:1) to yield *6-bromo-1-(4-nitrobenzyl)- 7-azabenzimidazole***119f** as a brown solid (236.5 mg, 71%); m.p. 150-152 °C [HPLC-MS: m/z calculated for $C_{13}H_{10}BrN_4O_2$ $(M+1)^+$ 332.9987. Found 332.9738]; δ_H/ppm (400 MHz; $CDCl_3$) 8.47 (1H, d, J = 1.9 Hz, Ar-H), 8.26 (1H, s, Ar-H), 8.25 (1H, d, J = 1.8 Hz, Ar-H), 8.19 (2H, d, J = 8.6 Hz, Ar-H), 7.46 (2H, d, J = 8.6 Hz, Ar-H)

and 5.58 (2H, s, CH_2); δ_C/ppm (100 MHz; $CDCl_3$) 148.1, 146.1, 145.4, 144.8, 142.5, 135.8, 130.7, 128.6, 124.4, 114.9 (Ar-C) and 46.8 (CH_2).

5-bromo-1-(3,4-dichlorobenzyl)-7-azabenzimidazole 119g

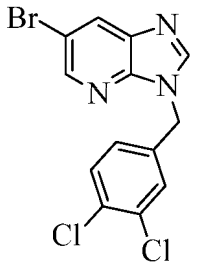

The procedure described for the synthesis of **119a** was used using 5-bromo-7-azabenzimidazole (200 mg, 1 mmol), caesium carbonate (488.7 mg, 1.5 mmol) 1-methylpyrrolidinone (20 mL) and 3,4-dichlorobenzylchloride (0.14 mL, 1 mmol). The crude product was purified (thin layer chromatography; elution with ethyl acetate – hexane 2:1) to yield *5-bromo-1-(3,4-dichlorobenzyl)-7-azabenzimidazole* **119g** as a white solid (274.9 mg, 77%); m.p. 128-130 °C [HPLC-MS: m/z calculated for $C_{13}H_9BrCl_2N_3$ $(M+H)^+$ 355.9357. Found 355.9106]; δ_H/ppm (400 MHz; $CDCl_3$) 8.46 (1H, d, J = 1.2 Hz, Ar-H), 8.23 (1H, d, J = 1.2 Hz, Ar-H), 8.05 (1H, s, Ar-H), 7.40 (2H, d, J = 8.6 Hz, Ar-H), 7.12 (1H, dd, J = 8.2, 1.5 Hz, Ar-H) and 5.39 (2H, s, CH_2); δ_C/ppm (100 MHz; $CDCl_3$) 145.7), 145.6, 144.8, 136.5, 135.7, 133.4, 132., 131.2, 130.8, 129.8, 127.1, 114.5 (Ar-C) and 46.3 (CH_2).

1-benzoyl-5-bromo-7-azabenzimidazole 119h

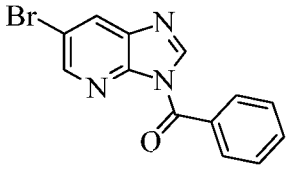

The procedure described for the synthesis of **119a** was used using 5-bromo-7-azabenzimidazole (200 mg, 1 mmol), caesium carbonate (488.7 mg, 1.5 mmol) 1-methylpyrrolidinone (20 mL) and benzoyl chloride (0.12 mL, 1 mmol). The crude product was purified (thin layer chromatography; elution with ethyl acetate – hexane 2:1) to yield *1-benzoyl-5-bromo-7-azabenzimidazole* **119h** as a white solid (244.7 mg, 81%); m.p. 90-94 °C [HPLC-MS: m/z calculated for $C_{13}H_8BrN_3O$ $(M)^+$ 300.9851. Found 301.1463]; δ_H/ppm (400 MHz; $CDCl_3$) 8.73 (1H., d, J = 2.2 Hz, Ar-H), 8.70 (1H, d, J = 2.2 Hz, Ar-H), 8.44 (1H, s, Ar-H), 7.85 – 7.80 (2H, m, Ar-H), 7.76 (1H, t, J = 7.5 Hz, Ar-H) and 7.64 (2H, t, J = 7.7 Hz,

Ar-H); δ_C/ppm (100 MHz; $CDCl_3$) 166.7, 155.2, 148.7, 145.7, 134.2, 131.5, 129.8, 129.5, 126.6, 125.9 and 117.3 (Ar-C).

3.5. SYNTHESIS OF 2-BROMOACETAMIDES 121a-l, 123a-b.

N-Benzyl-2-bromoacetamide 121a

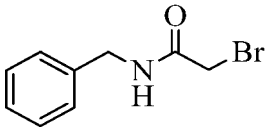

In a 50 mL round bottomed flask evacuated and filled with nitrogen, a solution of benzylamine (0.1mL, 0.92 mmol) was prepared in dry dichloromethane (25 mL) under nitrogen. Potassium carbonate (254.3 mg, 1.84 mmol) was added and the resulting mixture was stirred at 0 °C for 20 minutes under nitrogen. Bromoacetyl bromide (0.08 mL, 0.9 mmol) was added slowly at 0 °C and the mixture was stirred vigorously under nitrogen for 20 minutes at room temperature. The crude product was extracted into dichloromethane (2 ×70 mL), the combined organic phase was washed with deionized water (2 ×70 mL), dried with anhydrous magnesium sulphate, filtered and concentrated *in vacuo* until the volume was reduced to about 10 mL. The residual solution was diluted with hexane (50 mL) and the precipitate formed is filtered under pressure to yield N-*benzyl-2-bromoacetamide* **121a** as a white solid (205.7 mg, 98%); m.p. 144-146 °C [HPLC-MS: m/z calculated for $C_9H_{11}BrNO$ $(M+H)^+$ 228.0024. Found 227.9601]; υ_{max}/cm^{-1}: 2970 (NH), 1658 (C=O); δ_H/ppm (300 MHz; $CDCl_3$) 7.27-7.35 (5H, m, Ar-H), 4.46 (2H, d, *J* 5.8, NHC*H*$_2$), 3.90 (2 H, s, $COCH_2Br$), δ_C/ppm (75 MHz; $CDCl_3$) 164. 0 (C=O), 135.8, 129.0, 127.9 and 127.7 (Ar-C), 44.2 (NH*C*H_2) and 28.9 (CO*C*H_2).

2-Bromo-*N*-(3-chlorobenzyl)acetamides 121b

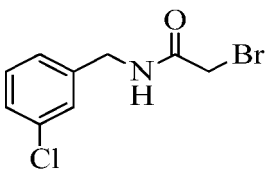

The procedure described for **121a** using 3-chlorobenzylamie (0.1 mL, 0.8 mmol), potassium carbonate (227.7 mg, 1.6 mmol) and bromoacetyl bromide (0.07 mL. 0.8 mmol) to yield *2-*

bromo-N-*(3-chlorobenzyl)acetamides* **121b** as a white solid (203.9 mg, 94.7%); m.p. 72-74 °C [HPLC-MS: m/z calculated for $C_9H_{10}BrClNO$ $(MH+2)^+$ 263.9634. Found 263.9688]; υ_{max}/cm^{-1}: 3265 (NH), 1652 (C=O); δ_H/ppm (300 MHz; $CDCl_3$) 7.29 – 7.26 (3H, overlapping m, Ar-H), 7.20 – 7.14 (1H, m, Ar-H), 6.88 (1H, s, NH), 4.46 (2H, d, *J* = 6.0 Hz, NHC*H*$_2$) and 3.95 (2H, s, COC*H*$_2$Br); δ_C/ppm (75 MHz; $CDCl_3$) 165.8 (C=O), 139.4, 134.8, 130.3, 128.0, 127.8 and 125.9 (Ar-C), 43.7 (NH*C*H$_2$) and 29.2 (CO*C*H$_2$).

2-Bromo-*N*-(3-nitrobenzyl)acetamides 121c

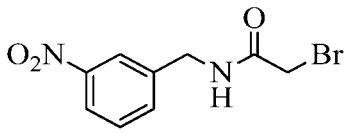

The procedure described for **121a** using 3-nitrobenzylamine hydrochloride (250 mg, 1.3 mmol), potassium carbonate (366.4 mg, 2.7 mmol) and bromoacetyl bromide (0.12m L, 1.3 mmol) to yield *2-bromo*-N-*(3-nitrobenzyl)acetamides* **121c** as a yellow solid (334.1 mg, 92%); m.p. 115-120 °C [HPLC-MS: m/z calculated for $C_9H_{10}BrN_2O_3$ $(M+H)^+$ 272.9875. Found 272.9953]; υ_{max}/cm^{-1}: 3281 (NH), 1643 (C=O); δ_H/ppm (300 MHz; MeOD-*d*$_4$) 8.19 (1H, s, Ar-H), 8.14 (1H, d, *J* = 8.4 Hz, Ar-H), 7.71 (1H, d, *J* = 7.6 Hz, Ar-H), 7.58 (1H, t, *J* = 7.9 Hz, Ar-H), 4.51 (2H, s, NHC*H*$_2$) and 3.91 (2H, s, COC*H*$_2$Br). δ_C/ppm (75 MHz; MeOD-*d*$_4$) 169.8 (C=O), 142.1, 134.8, 130.8 and 123.2 (Ar-C), 43.7 (NH*C*H$_2$) and 28.6 (CO*C*H$_2$).

2-Bromo-*N*-phenethylacetamide 121d

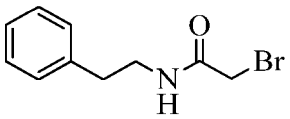

The procedure described for **121a** using phenylethylamine hydrogen chloride (141.9 mg, 0.9 mmol), potassium carbonate (235.0 mg, 1.7 mmol) and bromoacetyl bromide (0.07 mL, 0.9 mmol) to yield *2-bromo*-N-*phenethylacetamide* **121d** as a white solid (188.8 mg, 87%); m.p. 80-82 °C [HPLC-MS: m/z calculated for $C_{10}H_{13}BrNO$ $(M+H)^+$ 242.0180. Found 242.0296]; υ_{max}/cm^{-1}: 3240 (NH), 1651 (C=O); δ_H/ppm (300 MHz; MeOD-*d*$_4$) 7.31 – 7.16 (5H, , Ar-H), 3.79 (2H, s, COC*H*$_2$Br), 3.43 (2H, t, *J* = 7.3 Hz, NHC*H*$_2$), 2.81 (2H, t, *J* = 7.3 Hz, PhC*H*$_2$); δ_C/ppm (75 MHz; MeOD-*d*$_4$) 169.4, 140.2, 129.8, 129.5 and 127.4 (Ar-C), 42.5 (*C*OCH$_2$), 36.2 (NH*C*H$_2$) and 28.7 (*C*H$_2$Ph).

2-Bromo-*N*-(3,4-difluorophenyl)acetamides 121e

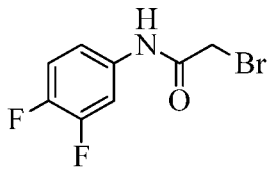

The procedure described for **121a** using 3,4-difluoroaniline (0.1 mL, 2.02 mmol), potassium carbonate (558.4 mg, 4.04 mmol) and bromoacetyl bromide (0.18 mL, 2.02 mmol) to yield *2-bromo*-N-*(3,4-difluorophenyl)acetamide* **121e** as solid (476.3 mg, 94.3%); m.p. 122-124 °C [HPLC-MS: m/z calculated for $C_8H_7BrF_2NO$ $(M+H)^+$ 249.9679. Found 249.9745]; υ_{max}/cm^{-1}: 3281 (NH), 1644 (C=O); δ_H/ppm (300 MHz; MeOD-d_4) 7.73 – 7.64 (1H, m, Ar-H), 7.21 (2H, dd, J = 16.7, 7.7 Hz, Ar-H), 3.95 (2H, s, COCH_2Br); δ_C/ppm (75 MHz; MeOD-d_4) 167.6 (C=O), 149.6, 146.57 (d, $J_{C,F}$ = 12.9 Hz), 118.3 (d, $J_{C,F}$ = 18.2 Hz), 117.39 – 116.87 (m), 111.0, 110.4 (dd, $^1J_{C,F}$ = 22.0, $^2J_{C,F}$ = 2.2 Hz) [Ar-C] and 29.4 (COCH_2).

2-Bromo-*N*-(3-fluorobenzyl)acetamides 121f

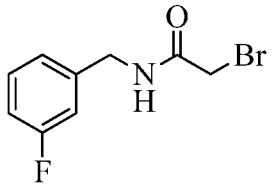

The procedure described for **121a** using 3-fluorobenzylamine (0.1 mL, 0.9 mmol), potassium carbonate (243.2 mg, 1.8 mmol) and bromoacetyl bromide (0.08 mL, 0.9 mmol) to yield *2-bromo*-N-*(3-fluorobenzyl)acetamide* **121f** as a white solid (201.4 mg, 93%); m.p. 58-60 °C [HPLC-MS: m/z calculated for $C_9H_{10}BrFNO$ $(M+H)^+$ 245.9930. Found 246.0006]; υ_{max}/cm^{-1}: 3267 (NH), 1657 (C=O); δ_H/ppm (300 MHz; $CDCl_3$) 7.25 – 6.97 (4H, overlapping m, Ar-H), 6.86 (1H, d, J = 6.0 Hz, NH), 4.43 (2H, d, J = 6.0 Hz, NHCH_2), 3.94 (2H, s, COCH_2Br); δ_C/ppm (75 MHz; $CDCl_3$) 165.8 (C=O), 134.5 (d, $J_{C,F}$ = 1.2 Hz), 124.1 – 123.5 (overlapping m), 117.7 (d, $J_{C,F}$ = 17.5 Hz) and 116.9 (d, $J_{C,F}$ = 18.4 Hz) [Ar-C], 43.3 (NHCH_2) and 29.1 (COCH_2).

2-Bromo-*N*-(furan-2-ylmethyl)acetamides 121g

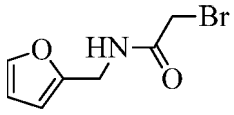

The procedure described for **121a** using furfurylamine (0.2 mL, 1.4 mmol), potassium carbonate (373.2 mg, 2.7 mmol) and bromoacetyl bromide (0.1 mL, 1.4 mmol) to yield *2-bromo*-N-*(furan-2-ylmethyl)acetamide* **121g** as a white solid (483.0 mg, 98%); m.p. 80-82 °C [HPLC-MS: m/z calculated for C_7H_9BrNO $(M+H)^+$ 217.9816. Found 217.9883]; υ_{max}/cm^{-1}: 3276 (NH), 1645 (C=O); δ_H/ppm (400 MHz; DMSO-d_6) 8.75 (1H, t, J = 5.6 Hz, N-H), 7.59 (1H, d, J = 1.0 Hz, Ar-H), 6.40 (1H, dd, J = 3.0, 1.9 Hz, Ar-H), 6.27 (1H, d, J = 2.6 Hz, Ar-H), 4.28 (2H, d, J = 5.6 Hz, NH*CH*$_2$), 3.88 (2H, s, CO*CH*$_2$Br); δ_C/ppm (100 MHz; DMSO-d_6) 165.9 (C=O), 151.6, 142.4, 110.5 and 107.2 (Ar-C), 36.0 (NH*C*H$_2$) and 29.3 (CO*C*H$_2$).

2-Bromo-*N*-(3-fluorophenyl)acetamides 121h

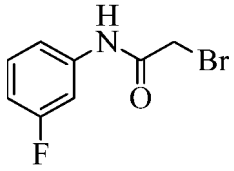

The procedure described for **121a** using 3-fluoroaniline (0.2 mL, 2.1 mmol), potassium carbonate (290.2 mg, 2.1 mmol) and bromoacetyl bromide (0.2 mL, 2.1 mmol) to yield *2-bromo*-N-*(3-fluorophenyl)acetamides* **121h** as a white solid (229.3 mg, 95%); m.p. 100-104 °C [HPLC-MS: m/z calculated for C_8H_8BrFNO $(M+H)^+$ 231.9773. Found 231.9843]; υ_{max}/cm^{-1}: 3279 (NH), 1673 (C=O); δ_H/ppm (400 MHz; DMSO-d_6) 8.41(1H, s, N-H), 7.46, 7.29, 7.28, 6.86, 4.10 (CO*CH*$_2$Br); (100 MHz; DMSO-d_6) 169.30 (C=O), 165.3, 161.0 – 160.9 (m), 131.7 (d, $^1J_{C,F} = {}^2J_{C,F} = 9.2$ Hz), 130.5 (dd, $^1J_{C,F} = 14.6$, $^2J_{C,F} = 9.4$ Hz), 110.2 (dd, $^1J_{C,F} = 37.6$, $^2J_{C,F} = 23.0$ Hz) and 106.0 (dd, $J_{C,F} = 26.4$, 6.0 Hz) [Ar-C] and 30.3 (CO*C*H$_2$).

2-bromo-*N*-(3,4-difluorobenzyl)acetamides 121i

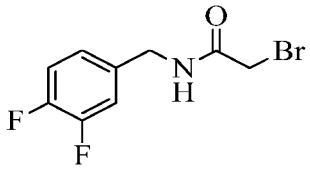

The procedure described for **121a** using 3,4-difluorobenzylamine (0.1 mL, 0.9 mmol), potassium carbonate (235.0 mg, 1.7 mmol) and bromoacetyl bromide (0.07 mL, 0.9 mmol) to yield *2-bromo-N-(3,4-difluorobenzyl)acetamide* **121i** as a white solid (215.5 mg, 96%); m.p. 78-80 °C [HPLC-MS: m/z calculated for $C_9H_9BrF_2NO$ $(MH+1)^+$ 265.9835. Found 263.9890];

υ_{max}/cm^{-1}: 3272 (NH), 1656 (C=O); δ_H/ppm (400 MHz; DMSO-d_6) 8.86 (1H, s, NH), 7.38 (dd, J = 19.2, 8.6 Hz, 1H), 7.34 – 7.26 (m, 1H), 7.11 (s, 1H), 4.28 (2H, d, J = 5.9 Hz, CO*CH*$_2$Br), 3.92 (2H, s, CO*CH*$_2$Br); δ_C/ppm (100 MHz; DMSO-d_6) 166.4 (C=O), 150.1 (dd, $^1J_{C,F}$ = 84.2, $^2J_{C,F}$ = 12.6 Hz), 147.7 (dd, $^1J_{C,F}$ = 83.0, $^2J_{C,F}$ = 12.7 Hz), 136.8 (dd, $^1J_{C,F}$ = 5.4, $^2J_{C,F}$ = 3.7 Hz), 123.9 (dd, $^1J_{C,F}$ = 6.5, $^2J_{C,F}$ = 3.4 Hz), 117.4 (d, $J_{C,F}$ = 17.0 Hz) and 116.2 (d, $J_{C,F}$ = 17.3 Hz) {Ar-C}, 41.5 ($NHCH_2$) and 29.4 ($COCH_2$).

_N_-(2-acetyphenyl)-2-bromoacetamide 121j

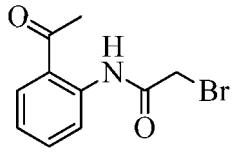

The procedure described for **121a** using 2-aminoacetophenone (0.25 mL, 2.1 mmol), potassium carbonate (565.0 mg, 8.2 mmol) and bromoacetyl bromide (0.18 mL, 2.1 mmol) to yield N-*(2-acetyphenyl)-2-bromoacetamide* **121j** as a white solid (583.3 mg, 90%); m.p 62-64 °C [HPLC-MS: m/z calculated for $C_{10}H_{11}BrNO_2$ $(M+H)^+$ 255.9973. Found 256.0046]; υ_{max}/cm^{-1}: 3156 (NH), 1690, 1646 (C=O); δ_H/ppm (400 MHz; DMSO-d_6) 11.74 (1H, NH), 8.33 (1H, d, J = 8.4 Hz, Ar-H), 8.02 (1H, d, J = 7.9 Hz, Ar-H), 7.62 (1H, t, J = 7.8 Hz, Ar-H), 7.26 (1H, t, J = 7.6 Hz, Ar-H), 4.23 (2H, s, CO*CH*$_2$Br), 2.64 (3H, s, CO*CH*$_3$); δ_C/ppm (100 MHz; DMSO-d_6) 202.5, 165.4 (C=O), 138.3, 134.2, 131.7, 124.5, 123.7 and 120.6 (Ar-C), 30.5 ($COCH_2$) and 28.7 ($COCH_3$).

2-bromo-1-morpholinoethanone 121k

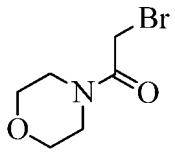

The procedure described for **121a** using morpholine (0.25 mL, 2.9 mmol), potassium carbonate (600.0 mg, 4.3 mmol) and bromoacetyl bromide (0.25 mL, 2.9 mmol) to yield *2-bromo-1-morpholinoethanone* **121k** as yellow oil (608.2 mg, 97%); [HPLC-MS: m/z calculated for $C_6H_{11}BrNO_2$ $(M+H)^+$ 207.9973. Found 208.0032]; υ_{max}/cm^{-1}: 1636 (C=O); δ_H/ppm (400 MHz; $CDCl_3$) 3.82 (2H, s, CO*CH*$_2$Br), 3.72 – 3.68 (2H, m, CH_2), 3.68 – 3.63 (2H, m, CH_2), 3.61 – 3.57 (2H, m, CH_2), 3.51 – 3.47 (2H, m, CH_2); δ_C/ppm (100 MHz; $CDCl_3$) 165.4 (C=O), 66.6 ($COCH_2Br$) 66.4, 47.2, 42.4 and 25.5 (CH_2).

2-bromo-*N*-(isoxazol-3-yl)acetamides 121l

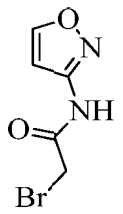

The procedure described for **121a** using 3-aminoisoxazole (0.1 mL, 1.4 mmol), potassium carbonate (373.2 mg, 2.7 mmol) and bromoacetyl bromide (0.11 mL, 1.4 mmol) to yield *2-bromo*-N-*(isoxazol-3-yl)acetamide* **121l** as a white solid (266.0 mg, 96.1%); m.p. 108-110 °C [HPLC-MS: m/z calculated for $C_5H_6BrN_2O_2$ $(M+H)^+$ 204.9612. Found 204.9668]; υ_{max}/cm^{-1}: 3061 (NH), 1607 (C=O); δ_H/ppm (300 MHz; $CDCl_3$) 9.50 (1H, *J* = 1,5 Hz, Ar-H), 8.33 (d, *J* = 1.5 Hz, Ar-H), 7.08 (1H, s, N-H) and 4.03 (2H, s, CO*CH*$_2$Br); δ_C/ppm (75 MHz; $CDCl_3$) 164.2 (C=O), 159.5, 157.2 and 99.3 (Ar-C) and 28.4 (CO*C*H$_2$).

***N,N'*-(ethane-1,2-diyl)bis[2-bromoacetamide] 123a**

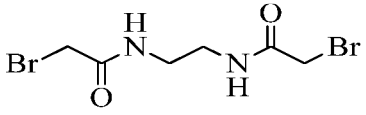

The procedure described for **121a** using ethylenediamine (0.2 mL, 2.9 mmol), potassium carbonate (801.6 mg, 5.8 mmol) and bromoacetyl bromide (0.5 mL, 5.8 mmol) to give N,N'-*(ethane-1,2-diyl)bis(2-bromoacetamide)* **123a** as a white solid (7851 mg, 90%); m.p. 142-144 °C [HPLC-MS: m/z calculated for $C_6H_{11}Br_2N_2O_2$ $(M+H)^+$ 300.9187. Found 301.1459]; υ_{max}/cm^{-1}: 3283, 3091 (NH), 1649 (C=O); $^{\delta}H$/ppm (400 MHz; DMSO-d_6) 8.32 (s, 2H), 3.84 (4H, s, CO*CH*$_2$Br x 2), 3.16 – 3.13 (4H, m, NH*CH*$_2$ x 2); $^{\delta}C$/ppm (100 MHz, DMSO-d_6) 166.2 (C=O), 38.5 (CO*C*H$_2$Br) and 29.5 (NH*C*H$_2$).

***N,N'*-[(1R,2R)-cyclohexane-1,2-diyl]bis{2-bromoacetamide} 123b**

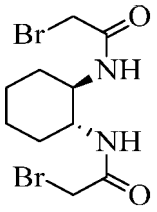

The procedure described for **121a** using (±)trans-1,2-diaminocyclohexane (0.2 mL 1.7mmol), potassium carbonate (470mg, 3.4 mmol) and bromoacetyl bromide (0.3 mL, 3.4 mmol) to yield N,N'-*((1R,2R)-cyclohexane-1,2-diyl)bis(2-bromoacetamide)* **123b** as a white solid (587.5 mg, 97%); m.p. 218-220 °C [HPLC-MS: m/z calculated for $C_{10}H_{17}Br_2N_2O_2$ $(M+H)^+$ 354.9657. Found 354.97868]; υ_{max}/cm^{-1}: 3242, 3076 (NH), 1641 (C=O); δ_H/ppm (400 MHz; DMSO-d_6) 8.12 (2H, d, J = 7.6 Hz, NH), 3.77 (4H, s, CO*CH*$_2$Br), 3.53 (2H, broad s, NH*CH* x 2), 1.77 (2H, d, J = 6.3 Hz,), 1.65 (2H, broad s, 2H) and 1.22 (4H, d, J = 5.8 Hz, 4H); δ_C/ppm (100 MHz, DMSO-d_6) 165.6 (C=O), 52.1 (CO*C*H$_2$Br), 31.5 (NH*C*H), 29.7 and 24.2 (CH_2).

3.6. SYNTHESIS OF 1-{[*N*-(BENZYL) CARBAMOYL]METHYL}-5-BROMO-7-AZABENZIMIDAZOLES 122a-l, *N,N'*-BIS[2-(5-BROMO-7-AZABENZIMIDAZOL-1-yl)ACETAMIDO]-1,2-ETHYLENEDIAMINE 124a and (±)-*TRANS-N,N'*-BIS[2-(5-BROMO-7-AZABENZIMIDAZOL-1-YL)ACETAMIDO]CYCLOHEXANE 124b.

1-{[*N*-(benzyl) carbamoyl]methyl}-5-bromo-7-azabenzimidazole 122a

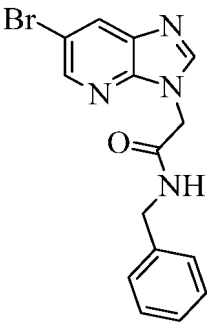

A mixture of 5-bromo-7-azabenzimidazole (100 mg, 0.5 mmol) and caesium carbonate (488.73, 1.5 mmol) in 1-methylpyrrolidinone (20 mL) was stirred at room temperature for 15 minutes. *N-benzyl-2-bromoacetamide* **121a** (114.0 mg, 0.5 mmol) was added to the solution. The resulting mixture was stirred vigorously at room temperature for 30 minutes while the progress of the reaction was monitored by thin layer chromatography. At the completion of the reaction, the organic crude product was extracted into ethyl acetate (2 × 70 mL). The

combined organic phase was thoroughly washed with deionized water (4 × 140 mL), dried with anhydrous sodium sulphate and filtered. The dried crude solution was concentrated to about 10 mL *in-vacuo* and diluted with hexane (40 mL) to precipitate the product. The precipitate was filtered and dried to give *1-{[*N*-(benzyl)carbamoyl]methyl}-5bromo-7-azabenzimidazole* **122a** as a white solid (148.4 mg, 86%); m.p. 172-174 °C [HRMS: m/z calculated for $C_{15}H_{13}BrN_4O$ $[M+H]^+$ 345.0351. Found 345.0345]; υ_{max}/ cm^{-1} 3269 (NH), 1652 (C=O); δ_H/ppm (400 MHz; DMSO-d_6) 8.84 and 8.80 (1H, 2 x t, J = 5.8 Hz, NH), 8.50 (1H, s, Ar-H), 8.45 and 8.43 (1H, 2 x d, J = 2.0 Hz, Ar-H), 8.39 and 8.31 (1H, 2 x d, J = 2.0 Hz, Ar-H), 7.30 (5H, m, Ar-H), 5.08 and 5.06 (2H, 2 x s, COCH_2), and 4.33 and 4.31 (2H, 2 X d, J = 1.5 Hz, NHCH_2); δ_C/ppm (100 MHz; DMSO-d_6) 166.3 and 166.2 (C=O), 154.5, 148.3, 148.0, 145.9, 144.3, 143.9, 138.8, 136.0, 129.6, 128.3, 127.9, 127.4, 127.3, 127.0, 126.9, 121.7, 113.1 and 113.0 (Ar-C), 47.2, 45.3 (COCH$_2$), 42.4 and 42.3 (NHCH$_2$).

1-{[*N*-(3-chlorobenzyl) carbamoyl]methyl}-5-bromo-7-azabenzimidazole 122b

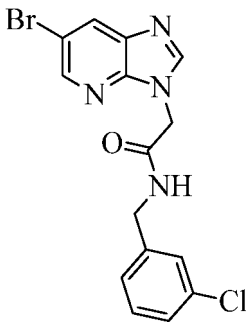

The procedure described for the synthesis of **122a** was followed using 5-bromo-7-azabenzimidazole (100 mg, 0.5 mmol), caesium carbonate (489, 1.5 mmol) 1-methylpyrrolidinone (20 mL) and 2-bromo-*N*-(3-chlorobenzyl)acetamide (131 mg, 0.5 mmol). *1-{[*N*-(3-chlorobenzyl)carbamoyl]methyl}-5bromo-7-azabenzimidazole* **122b** was precipitated as a white solid (167.0 mg, 88%); m.p. 164-163 °C [HPLC-MS: m/z calculated for $C_{15}H_{13}BrClN_4O$ $(M+H)^+$ 378.9961. Found 379.0050]; υ_{max}/cm^{-1} 3265 (NH), 1651 (C=O); δ_H/ppm (400 MHz; DMSO-d_6) 8.89 and 8.82 (1H, 2 x t, J = 5.8, NH), 8.50 (1H, s, Ar-H), 8.49 and 8.46 (1H, 2 x d, J = 2.1Hz and 1.8 Hz, Ar-H), 8.39 and 8.31 (1H, 2 x d, J = 2.1 Hz and 1.8 Hz, Ar-H), 7.38 – 7.29 (3H, m, Ar-H), 7.25 (1H, d, J = 7.2 Hz, Ar-H), 5.11 and 5.07 (COCH_2) and 4.34 and 4.33 (2H, overlapping, NHCH_2); δ_C/ppm (100 MHz; DMSO-d_6) 166.50 and 166.4 (C=O), 154.5, 148.3, 148.0, 145.9, 144.3, 144.0, 141.5, 141.46, 136.0,

133.05, 133.03, 130.16, 130.15, 129.6, 127.9, 127.1, 126.92, 126.89, 126.82, 125.98, 125.9, 113.1 and 113.0 (Ar-C), 47.17, 45.44 and 45.43 (CO*C*H$_2$), 41.8 and 41.7 (NH*C*H$_2$).

1-{[*N*-(3-nitrobenzyl) carbamoyl]methyl}-5-bromo-7-azabenzimidazole 122c

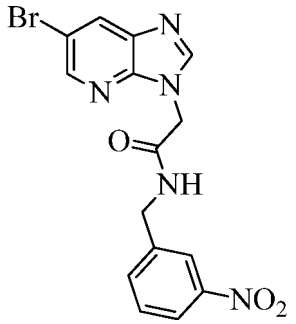

The procedure described for the synthesis of **122a** was followed using 5-bromo-7-azabenzimidazole (100 mg, 0.50 mmol), caesium carbonate (488.7, 1.50 mmol) 1-methylpyrrolidinone (20 mL) and 2-bromo-*N*-(3,4-difluorobenzyl)acetamide (136.5 mg, 0.50 mmol). The desired product was precipitated to give *1-{[*N*-(3-nitrobenzyl)carbamoyl]methyl}-5-bromo-7-azabenzimidazole* **122c** as a white solid (156.1 mg, 80%); m.p. 160-161 °C [HPLC-MS: m/z calculated for $C_{15}H_{13}BrN_5O_3$ $(M+H)^+$ 390.0202. Found 390.0326]; υ_{max}/cm^{-1}:3288 (NH), 1650 (C=O); δ_H/ppm (400 MHz; DMSO-*d*$_6$) 9.00 and 8.94 (1H, 2 x t, *J* = 5.9, 5.8 Hz, NH), 8.50 (1H, s, Ar-H), 8.48 and 8.44 (1H, 2 x d, *J* = 2.1, 2.0 Hz, Ar-H), 8.38, 8.29 (1H. 2 x d, *J* = 2.1, 2.0 Hz, Ar-H), 8.15 (1H, s, Ar-H), 8.11 (1H, d, *J* = 8.0 Hz, Ar-H), 7.75 (1H, d, *J* = 7.5 Hz, Ar-H), 7.63 (1H, td, *J* = 8.0, 2.5 Hz, Ar-H), 5.13 and 5.08 (2H, 2 X s, CO*CH*$_2$) and 4.47 and 4.45 (2H, 2 x d, *J* = 5.9 Hz, NH*CH*$_2$); δ_C/ppm (100 MHz; DMSO-*d*$_6$) 166.7 and 166.6 (C=O), 154.5, 148.3, 148.0, 147.9, 147.8, 145.9, 144.3, 144.0, 141.4, 141.37, 136.0, 134.1, 134.0, 129.8, 129.6, 127.9, 121.95, 121.93, 121.9, 121.7, 121.6, 113.1 and 113.0 (Ar-C), 47.2 and 45.4 (CO*C*H$_2$), 41.8 and 41.7 (NH*C*H$_2$).

1-{[*N*-(phenethyl) carbamoyl]methyl}-5-bromo-7-azabenzimidazole1 122d

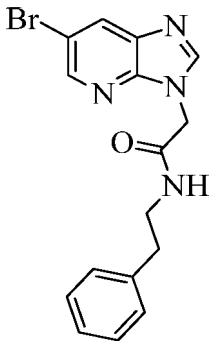

The procedure described for the synthesis of **122a** was used using 5-bromo-7-azabenzimidazole (100 mg, 0.5 mmol), caesium carbonate (488.7, 1.5 mmol) 1-methylpyrrolidinone (20 mL) and 2-bromo-*N*-(3,4-difluorobenzyl)acetamide (121.01 mg, 0.5 mmol). The desired product precipitated to give *1-{[*N*-(phenethyl) carbamoyl]methyl}-5bromo-7-azabenzimidazole1* **122d** as a white solid (158.1 mg, 88%); m.p. 160-162 °C [HPLC-MS: m/z calculated for $C_{16}H_{16}BrN_4O$ $(M+H)^+$ 359.0507. Found 359.0595]; υ_{max}/cm^{-1}: 3272 (NH), 1671 (C=O); δ_H/ppm (400 MHz; DMSO-d_6) 8.50 – 8.42 (2H, m, Ar-H), 8.39 – 8.20 (1H, m, Ar-H), 7.31 – 7.17 5H, (5H, m, Ar-H), 4.96 (2H, d, J = 8.0 Hz, COCH_2), 3.29 (2H, m, NHCH_2), 2.78 – 2.69 (2H, m, CH_2Ph); δ_C/ppm (100 MHz; DMSO-d_6) 166.1, 166.0 (C=O), 154.4, 148.2, 148.0, 145.9, 144.3, 144.0, 139.2, 139.2, 135.9, 129.5, 128.6, 128.32, 128.30, 127.8, 126.2, 126.1, 121.6, 113.1 and 112.9 (Ar-C), 47.15 and 45.20 (COCH_2), 40.47 and 40.38 (NHCH_2), 34.95 and 34.94 (CH_2Ph).

1-{[*N*-(3,4-difluorophenyl) carbamoyl]methyl}-5-bromo-7-azabenzimidazole 122e

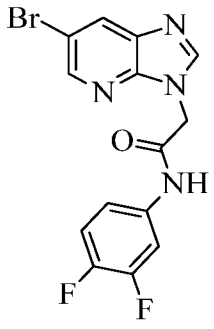

The procedure described for the synthesis of **122a** was followed using 5-bromo-7-azabenzimidazole (100.0 mg, 0.5 mmol), caesium carbonate (488.7, 1.5 mmol) 1-methylpyrrolidinone (20 mL) and 2-bromo-*N*-(3,4-difluorophenyl)acetamide (125.0 mg, 0.5 mmol). The desired product was precipitated to give *1-{[*N*-(3,4-difluorophenyl) carbamoyl]methyl}-5-bromo-7-azabenzimidazole* **122e** as a white solid (150.5 mg, 82%); m.p. 200-202 °C [HPLC-MS: m/z calculated for $C_{14}H_{10}BrF_2N_4O$ $(M+H)^+$ 367.0006. Found

367.0095]; υ_{max}/cm^{-1}: 3214 (NH), 1678 (C=O); δ_H/ppm (400 MHz; DMSO-d_6) 10.71 (1H, d, J = 34.2 Hz, N-H), 8.52 (1H, d, J = 4.6 Hz, Ar-H), 8.51 – 8.40 (2H, m, Ar-H), 7.73 (1H, dtd, J = 9.9, 7.5, 2.4 Hz, Ar-H), 7.41 (1H, dt, J = 18.2, 9.1 Hz, Ar-H), 7.35 – 7.27 (1H, m, Ar-H), 5.23 (2H, d, J = 17.0 Hz, $COCH_2$); δ_C/ppm (100 MHz; DMSO-d_6) 165.46 (s), 165.37 – 165.36 (m) [C=O], 154.4, 150.23 – 150.21 (m), 150.10 – 150.08 (m), 148.4, 148.10 – 147.92 (m), 147.85 – 147.80 (m), 147.7 – 147.6 (m), 146.68 – 146.65 (m), 146.55 – 146.53 (m), 146.0 – 145.8 (m), 144.3, 144.1, 135.96 – 135.90 (m), 135.6 (d, J = 3.2 Hz), 135.6 – 135.5 (m), 135.5 – 135.4 (m), 129.6 (d, J = 14.1 Hz), 128.1, 121.9, 117.7, 117.6, 115.6 – 115.4 (m), 113.2, 113.13 – 112.99 (m), 108.3 and 108.1 [Ar-C], 47.6 and 45.5 ($COCH_2$).

1-{[*N*-(3-fluorobenzyl)carbamoyl]methyl}-5-bromo-7-azabenzimidazole 122f

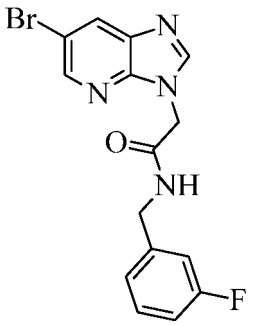

The procedure described for the synthesis of **122a** was used using 5-bromo-7-azabenzimidazole (100 mg, 0.5 mmol), caesium carbonate (488.7, 1.5 mmol) 1-methylpyrrolidinone (20 mL) and 2-bromo-*N*-(3-fluorobenzyl)acetamide (123.0 mg, 0.5 mmol). The desired product was precipitated to give *1-{[*N*-(3-fluorobenzyl) carbamoyl]methyl}-5-bromo-7-azabenzimidazole* **122f** as a white solid (141.3 mg, 78%); m.p. 170-172 °C [HPLC-MS: m/z calculated for $C_{15}H_{13}BrFN_4O$ $(M+H)^+$ 363.0257. Found 363.0324]; υ_{max}/cm^{-1}:3275 (NH), 1656 (C=O); δ_H/ppm (400 MHz; DMSO-d_6) 8.89 and 8.83 (1H, 2 x t, J = 5.8, 5.7 Hz, N-H), 8.51 (1H, s, Ar-H), 8.49 and 8.45 (1H, 2 x d, J = 2.1 Hz, Ar-H), 8.39 and 8.32 (1H, dd, J = 2.1 Hz, Ar-H), 7.37 (1H, dd, J = 14.1, 7.7 Hz, Ar-H), 7.15 – 7.04 (3H, overlapping m, Ar-H), 5.11 and 5.07 (2H, 2 x s, $COCH_2$) and 4.35 and 4.34 (2H, 2 x d, J = 5.8 Hz, $NHCH_2$); δ_C/ppm (100 MHz; DMSO-d_6)166.5, 166.4 (C=O), 163.5, 161.1, 154.5, 148.3, 148.0, 145.9, 144.3, 143.9, 141.9 (dd, $^1J_{C,F}$ = 7.2, $^2J_{C,F}$ = 3.5 Hz), 136.0, 130.3, 130.2, 129.6, 127.9, 123.3 (d, $J_{C,F}$ = 2.6 Hz), 123.2 (d, $J_{C,F}$ = 2.6 Hz), 121.8, 114.0, 114.0, 113.8, 113.7, 113.72, 113.7, 113.6, 113.5, 113.1 and 113.0 [Ar-C], 47.16 and 45.38 ($COCH_2$), 41.9 and 41.8 ($NHCH_2$).

1-{[*N*-(2-furfuryl) carbamoyl]methyl}-5-bromo-7-azabenzimidazole 122g

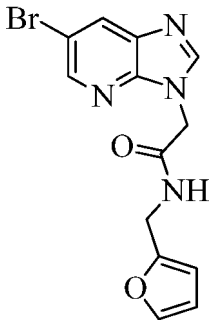

The procedure described for the synthesis of **122a** was used using 5-bromo-7-azabenzimidazole (100 mg, 0.5 mmol), caesium carbonate (488.7, 1.5 mmol) 1-methylpyrrolidinone (20 mL) and **2**-bromo-*N*-(furan-2-ylmethyl)acetamide (109.5 mg, 0.5 mmol). *1-{[*N*-(2-furfuryl)carbamoyl]methyl}-5-bromo-7-azabenzimidazole* **122g** was isolated as a white solid (150.8 mg, 90%); m.p. 170-171°C [HPLC-MS: m/z calculated for $C_{13}H_{12}BrN_4O_2$ $(M+H)^+$ 335.0143. Found 335.0217]; υ_{max}/cm^{-1}: 3280 (NH), 1662 (C=O); δ_H/ppm (400 MHz; DMSO-d_6) 8.86 – 8.78 (1H, m, NH), 8.48 (1H, s, Ar-H), 8.49 and 8.44 (1H, 2 x d, J = 2.1 Hz, Ar-H), 8.38 and 8.28 (1H, 2 x d, J = 2.1 Hz, Ar-H), 7.59 (1H, d, J = 0.6 Hz, Ar-H), 6.42 – 6.40 (1H, m, Ar-H), 6.29 (1H, t, J = 3.3 Hz, Ar-H), 5.04 and 5.01 (2H, 2 X s, COCH_2) and 4.31 (2H, t, J = 5.0 Hz, NHCH_2); δ_C/ppm (100 MHz; DMSO-d_6) 8.86 – 8.78 (1H, m, N-H), 8.50 – 8.43 (2H, overlapping m, Ar-H), 166.2, 166.1 (C=O), 154.4, 151.6, 151.61, 148.2, 148.0, 145.9, 144.3, 143.9, 142.3, 135.9, 129.6, 127.9, 121.7, 113.1, 113.0, 110.5, 107.24 and 107.21 (Ar-C), 47.1 and 45.1 (COCH_2), 35.70 and 35.68 (NHCH_2).

1-{[*N*-(3-fluorophenyl) carbamoyl]methyl}-5-bromo-7-azabenzimidazole 122h

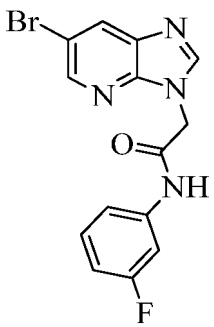

The procedure described for the synthesis of **122a** was used using 5-bromo-7-azabenzimidazole (100 mg, 0.5 mmol), caesium carbonate (488.73, 1.5 mmol) 1-methylpyrrolidinone (20 mL) and 2-bromo-*N*-(3-fluorophenyl)acetamide (116.49 mg, 0.5 mmol). *1-{[*N*-(3-fluorophenyl) carbamoyl]methyl}-5-bromo-7-azabenzimidazole* **122h** was isolated as a white solid (132.7 mg, 76%); m.p. 246-249 °C [HPLC-MS: m/z calculated for $C_{14}H_{11}BrFN_4O$ $(M+1)^+$ 349.0100. Found 349.0116]; υ_{max}/cm^{-1}: 3333 (NH), 1682 (C=O); δ_H/ppm (400 MHz; DMSO-d_6) 10.65 (1H, s, NH), 8.52 (1H, s, Ar-H), 8.50 (1H, d, J = 2.2 Hz, Ar-H), 8.45 (1H, d, J = 2.2 Hz, Ar-H), 7.55 (1H, dt, J = 11.6, 2.1 Hz, Ar-H), 7.42 – 7.29 (2H, overlapping m, Ar-H), 6.91(1H, td, J = 8.5, 2.0 Hz, Ar-H) and 5.26 (2H, s, COCH_2); δ_C/ppm (100 MHz; DMSO-d_6) 165.5 (C=O), 163.3, 160.9, 154.4, 148.4, 144.3, 130.7 – 130.5 (m), 128.1, 121.9, 114.94 – 114.86 (m), 113.25 – 113.18 (m), 110.2 – 109.9 (m) and 106.2 – 105.7 (m) [Ar-C] and 47.6 (CO*C*H$_2$).

1-{[*N*-(3,4-difluorobenzyl) carbamoyl]methyl}-5-bromo-7-azabenzimidazole 122i

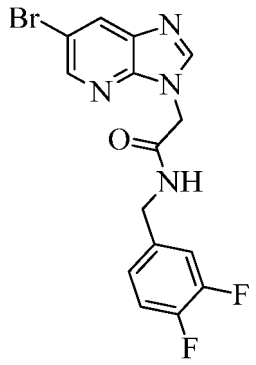

The procedure described for the synthesis of **122a** was used using 5-bromo-7-azabenzimidazole (100 mg, 0.5 mmol), caesium carbonate (488.7, 1.5 mmol) 1-methylpyrrolidinone (20 mL) and **2**-bromo-*N*-(3,4-difluorobenzyl)acetamide (132.0 mg, 0.5 mmol). *1-{[*N*-(3,4-difluorobenzyl)carbamoyl]methyl}-5-bromo-7-azabenzimidazole* **122i** was isolated as a white solid (160.1 mg, 84%); m.p. 160-162 °C [HPLC-MS: m/z calculated for $C_{15}H_{12}BrF_2N_4O$ $(M+H)^+$ 381.0162. Found 381.0301]; υ_{max}/cm^{-1}: 3274 (NH), 1648 (C=O); δ_H/ppm (400 MHz; DMSO-d_6) 8.89 and 8.82 (1H, 2 x t, J = 5.8 Hz, NH), 8.50 (1H, s, Ar-H), 8.49 and 8.45 (1H, 2 x d, J = 2.0 Hz, Ar-H) 2.0 Hz, 1H), 8.39 and 8.30 (1H, 2 x d, J = 2.0 Hz, Ar-H), 7.43 – 7.30 (2H, m, Ar-H), 7.16 – 7.11 (1H, m, Ar-H), 5.08 (2H, 2 x s, COCH_2), 4.31 (2H, 2 X d, J = 5.8 Hz, NHCH_2); δ_C/ppm (100 MHz; DMSO-d_6) 166.6, 166.5 (C=O), 154.4, 150.6 (d, $J_{C,F}$ = 1.3 Hz), 150.4 (d, $J_{C,F}$ = 1.5 Hz), 149.7 (d, $J_{C,F}$ = 4.5 Hz), 149.6 (d, J = 4.4

Hz), 148.3, 148.1 (d, $J_{C,F}$ = 1.5 Hz), 148.0, 147.3 (d, J = 4.6 Hz), 147.1 (d, J = 4.4 Hz), 145.9 (s), 144.3, 143.9, 136.8 (dd, $^{1}J_{C,F}$ = 6.5, $^{2}J_{C,F}$ = 2.5 Hz), 136.0, 129.6, 127.9, 124.0 (dd, $^{1}J_{C,F}$ = 6.5, $^{2}J_{C,F}$ = 3.5 Hz), 123.9 (dd, $^{1}J_{C,F}$ = 6.5, $^{2}J_{C,F}$ = 3.4 Hz), 121.7, 117.4 (d, $J_{C,F}$ = 1.2 Hz), 117.2 (d, $J_{C,F}$ = 1.1 Hz), 116.3, 116.2, 116.16, 116.0, 113.1 and 113.0 [Ar-C], 47.2 and 45.4 (CO*C*H2) 41.4 and 41.3 (NH*C*H$_2$).

1-{[*N*-(2-acetyphenyl)carbamoyl]methyl}-5-bromo-7-azabenzimidazole 122j

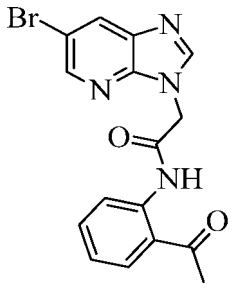

The procedure described for the synthesis of **122a** was used using 5-bromo-7-azabenzimidazole (100 mg, 0.5 mmol), caesium carbonate (488.7, 1.5 mmol) 1-methylpyrrolidinone (20 mL) and 2- *N*-(2-acetylphenyl)-2-bromoacetamide (128.0 mg, 0.5 mmol). *1-{[N-(2-acetylphenyl)carbamoyl]methyl}-5-bromo-7-azabenzimidazole* **122j** was isolated as a white solid (130.62 mg, 70%); m.p. 181-183 °C [HPLC-MS: m/z calculated for $C_{16}H_{14}BrN_4O_2$ $(M+H)^+$ 373.0300. Found 373.0392]; υ_{max}/cm^{-1}: 3055 (NH), 1658, 1608 (C=O); δ_H/ppm (400 MHz; DMSO-d_6) 12.29 (1H, s, NH), 8.62 (1H, s, Ar-H), 8.56 (1H, d, J = 2.1 Hz, Ar-H), 8.19 (1H, d, J = 2.1 Hz, Ar-H), 7.92 (1H, d, J = 8.0 Hz, Ar-H), 7.66 (1H, dd, J = 11.3, 4.1 Hz, Ar-H), 7.45 (1H, d, J = 8.0 Hz, Ar-H), 7.34 (1H, t, J = 7.5 Hz, Ar-H), 2.28 (3H, s, COC*H*$_3$), 2.25 and 2.08 (2H, s, COC*H*$_2$); δ_C/ppm (100 MHz; DMSO-d_6) 158.7, 154.7 (C=O), 148.9, 146.5, 145.3, 138.5, 132.0, 128.3, 126.6, 124.3, 122.9, 122.7, 119.5, 116.2 and 114.5, 17.8 (CO*C*H$_3$) and 14.8 (CO*C*H$_2$).

5-bromo-1-[2-(morpholino)-2-oxoethyl]-7-azabenzimidazole 122k

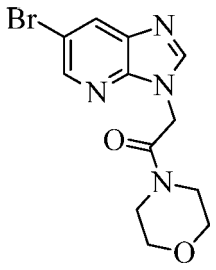

The procedure described for the synthesis of **122a** was used using 5-bromo-7-azabenzimidazole (100 mg, 0.5 mmol), caesium carbonate (488.7, 1.5 mmol) 1-methylpyrrolidinone (20 mL) and 2-bromo-1-morpholinoethanone (287.7 mg, 0.5 mmol). *5-bromo-1-[2-(morpholino)-2-oxoethyl]-7-azabenzimidazole* **122k** was isolated as a white solid (137.2 mg, 84%); m.p. 218-220 °C [HPLC-MS: m/z calculated for $C_{12}H_{14}BrN_4O_2$ $(M+H)^+$ 325.0300. Found 325.0351]; υ_{max}/cm^{-1}: 1656 (C=O); δ_H/ppm (400 MHz; DMSO-d_6) 8.44 (1H, d, J = 2.0 Hz, Ar-H), 8.41 (1H, s, Ar-H), 8.39 (1H, d, J = 2.0 Hz, Ar-H), 5.30 (2H, s, COCH_2), 3.71 – 3.67 (2H, m, CH_2), 3.64 – 3.58 (4H, t, 2 x CH_2), 3.46 – 3.43 (2H, t, CH_2); δ_C/ppm (100 MHz; DMSO-d_6) 165.5 (C=O), 148.6, 146.6, 144.3, 136.4, 130.0 and 113.3 (Ar-C), 66.0, 65.9, 45.1, 44.7 and 42.4 (CO*C*H_2).

1-{[N-(isoxazol-3-yl) carbamoyl]methyl-5-bromo-7-azabenzimidazole 122l

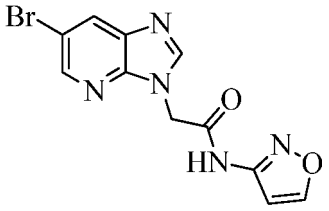

The procedure described for the synthesis of **122a** was used using 5-bromo-7-azabenzimidazole (100 mg, 0.5 mmol), caesium carbonate (488.7, 1.5 mmol) 1-methylpyrrolidinone (20 mL) and 2-bromo-*N*-(isoxazol-3-yl)acetamide (102.5 mg, 0.5 mmol). *1-{[*N*-(isoxazol-3-yl)carbamoyl]methyl-5-bromo-7-azabenzimidazole* **122l** was isolated as a white solid (125.6 mg, 78%); m.p. 242-244 °C [HPLC-MS: m/z calculated for $C_{11}H_9BrN_5O_2$ $(M+H)^+$ 321.9939. Found 322.0021]; υ_{max}/cm^{-1}: 3685 (NH), 1696 (C=O); δ_H/ppm (400 MHz; DMSO-d_6) 11.61 (d, 2 x s, Ar-H), 8.81 (d, J = 9.3 Hz, 2H), 8.51 (1H, s, Ar-H), 8.49 and 8.41 (1H, 2 xd, J = 2.0 Hz, 1H), 8.47 – 8.44 (1H, m, Ar-H), 6.85 (1H, d, J = 9.3 Hz, Ar-H) and 5.28 (2H, d, J = 14.2 Hz, $COCH_2$); δ_C/ppm (100 MHz; DMSO-d_6)165.8,

165.7 (C=O), 160.5, 160.4, 157.2, 157.1, 148.3, 147.9, 144.3, 144.1, 129.7, 121.9, 113.2 and 113.1, 98.99 and 98.95 (Ar-C), 47.5 and 45.6 ($COCH_2$).

_N,N'_-bis[2-(5-bromo-7-azabenzimidazol-1-yl)acetamido]-1,2-ethylenediamine 124a

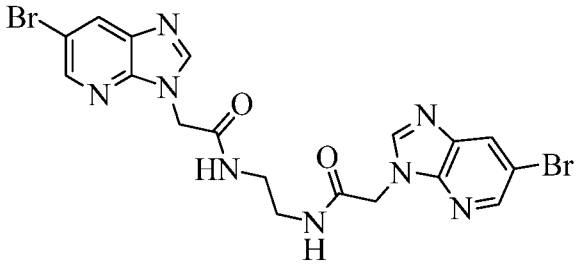

The procedure described for the synthesis of **122a** was used using 5-bromo-7-azabenzimidazole (200.0 mg, 1 mmol), caesium carbonate (488.7, 1.5 mmol) 1-methylpyrrolidinone (20 mL) and N,N′-(ethane-1,2-diyl)bis(2-bromoacetamide) (151.0 mg, 0.5 mmol). N,N'-*bis[2-(5-bromo-7-azabenzimidazol-1-yl)acetyl]-1,2-ethylenediamine* **124a** was isolated as a white solid (386.1 mg, 72%); m.p. 284-286 °C [HPLC-MS: m/z calculated for $C_{18}H_{17}Br_2N_8O_2$ $(M+H)^+$ 534.9841. Found 534.9836]; υ_{max}/cm^{-1}: 3282, 3086 (NH), 1659 (C=O); δ_H/ppm (400 MHz; DMSO-d_6) 8.46 (2H, s, Ar-H), 8.44 (2H, d, J = 1.7 Hz, Ar-H), 8.38 (d, J = 1.5 Hz, 2H), 6.52 (2H, s, Ar-H), 4.96 (4H, s, $NHCH_2$), 3.19 (4H, s, $COCH_2$); δ_C/ppm (100 MHz; DMSO-d_6) 165.1 (C=O), 148.1, 146.1, 143.9, 135.9, 129.6 and 112.9 (Ar-C), 59.8 $NHCH_2$) and 14.1 $COCH_2$).

(±)-*Trans-N,N'*-bis[2-(5-bromo-7-azabenzimidazol-1-yl)acetamido]cyclohexane 124b

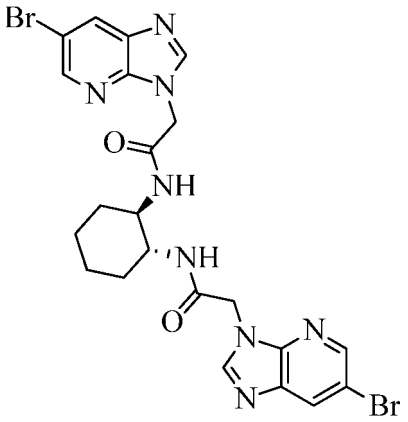

The procedure described for the synthesis of **122a** was followed using 5-bromo-7-azabenzimidazole (200 mg, 1 mmol), caesium carbonate (488.7, 1.5 mmol) 1-methylpyrrolidinone (20 mL) and N,N'-[(1*R*,2*R*)-cyclohexane-1,2-diyl]bis(2-

bromoacetamide) (178.0 mg, 0.5 mmol). *Trans(±)-1,2-bis[2-(5-bromo-7-azabenzimidazol-1-yl)acetamido]cyclohexane* **124b** was isolated as a white solid (507.6 mg, 86%); m.p. 288-300°C [HPLC-MS: m/z calculated for $C_{22}H_{23}Br_2N_8O_2$ $(MH+2)^+$ 591.0310. Found 591.0309]; υ_{max}/cm^{-1}: 3273, 3083(NH), 1653 (C=O); δ_H/ppm (400 MHz; DMSO-d_6) 8.53 – 8.51 (m, 2H), 8.47 – 8.30 (m, 6H), 5.08 – 4.86 (m, 4H), 3.57 (s, 2H), 1.80 (d, J = 9.0 Hz, 2H), 1.64 (s, 2H), 1.35 – 1.15 (m, 4H); δ_C/ppm (100 MHz; DMSO-d_6) 165.97 – 165.70 (m, C=O), 154.4, 148.2, 148.1 (x 2), 146, 144.3, 143.9 (x 2), 135.9 (x 2), 129.6 (x 2), 127.9, 121.8, 113.1, 112.9 [ArC], 52.5 – 51.9 (m, $COCH_2$), 47.3, 45.15 (x 2), 31.85 – 31.29 (m) and 24.24.

3.7. GENERAL SYNTHETIC PROCEDURE FOR 2-PHENYLAZABENZ-IMIDAZOLES 125a-n.

2-(*2*-hydroxy-5-nitrophenyl)-7-azabenzimidazole 125a

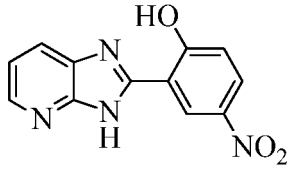

In a 50 ml round bottomed flask, 2,3-diaminopyridine (100.00 mg, 0.9 mmol) and 2-hydroxy-5-nitrosalicylaldehyde (153.8 mg, 0.9 mmol) was dissolved in nitrobenzene (10 mL) and the mixture was refluxed while stirring vigorously at 170 °C. The progress of the reaction was monitored by thin layer chromatography. After the completion of the reaction, the mixture was cooled to room temperature and diluted with 50 mL ethyl acetate, stirred and filtered under vacuum. The filtrate was washed twice with 40 mL ethyl acetate until no nitrobenzene was present to give 2-*(2-hydroxy-5-nitrophenyl)-7-azabenzimidazole* **125a** as brown solid (183.9 mg, 78%); m.p. dec. > 300 °C [HPLC-MS: m/z calculated for $C_{12}H_9N_4O_3$ $(M+H)^+$ 257.0674. Found 257.0474]; δ_H/ppm (400 MHz; DMSO-d_6) 14.08 (1H, s, NH), 9.18 (1H, d, J = 2.8 Hz, Ar-H), 8.46 (1H, dd, J = 4.8, 1.4 Hz, Ar-H), 8.28 (1H, dd, J = 9.2, 2.8 Hz, Ar-H), 8.15 (1H, dd, J = 8.0, 1.2 Hz, Ar-H), 7.37 (1H, dd, J = 8.1, 4.8 Hz, Ar-H) and 7.24 (1H, d, J =

9.2 Hz, Ar-H); δC/ppm (100 MHz; DMSO-d_6) 164.2, 151.7, 145.3, 139.9, 134.6, 128.0, 124.0, 119.6, 118.8 and 113.1 (Ar-C).

2-(2,3,4-trihydroxyphenyl)-7-azabenzimidazole 125b

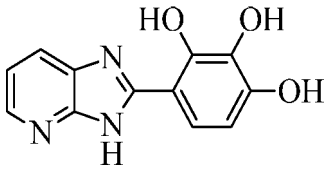

The procedure described for **125a** was followed using 2,3-diaminopyridine (100.0 mg, 0.92 mmol), nitrobenzene (10 mL) and 2,3,4-trihydroxybenzaldehyde (141.8 mg, 0.9 mmol). *2-(2,3,4-trihydroxyphenyl)-7-azabenzimidazole* **125b** was isolated as a brown solid (163.3 mg, 73%); m.p. dec. > 300 °C [HPLC-MS: m/z calculated for $C_{12}H_9N_3O_3$ $(M+2)^+$ 245.0644. Found 245.0581]; δH/ppm (400 MHz; DMSO-d_6): 12.71 (1H, s, NH), 8.67 (1H, s, OH), 7.85 (1H, d, J = 5.7 Hz, Ar-H), 7.35 (1H, d, J = 7.5 Hz, Ar-H), 6.97 (1H, d, J = 8.5 Hz, Ar-H), 6.62 (1H, m, J = 7.5, 4.9 Hz, Ar-H), 6.44 (1H, d, J = 8.4 Hz, Ar-H) and 5.76 (2H, s, O-H); δC/ppm (100 MHz; DMSO-d_6) 163.4, 154., 150.3, 150.2, 145.4, 132.4, 130.2, 124.8, 123.8, 113.0 and 107.8 (Ar-C).

2-(3,5-dichloro-2-hydroxyphenyl)-7-azabenzimidazole 125c

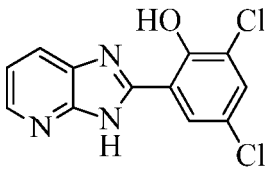

The procedure described for **125a** was followed using 2,3-diaminopyridine (100 mg, 0.9 mmol), nitrobenzene (10 mL) and 3,5-dichlorosalicylaldehyde (175.7 mg, 0.9 mmol). *2-(3,5-dichloro-2-hydroxyphenyl)-7-azabenzimidazole* **125c** was isolated as brown solid (206. 2 mg,

80%); m.p. dec. > 300 °C [HPLC-MS: m/z calculated for $C_{12}H_8Cl_2N_3O$ $(M+H)^+$ 280.0044. Found 279.9831]; δ_H/ppm (400 MHz; DMSO-d_6) 14.03 (1Hs, NH), 8.45 (1H, d, J = 4.6 Hz, Ar-H), 8.20 (1H, d, J = 2.4 Hz, Ar-H), 8.14 (1H, d, J = 7.9 Hz, Ar-H), 7.72 (1H, d, J = 2.4 Hz, Ar-H) and 7.37 (1H, dd, J = 8.1, 4.8 Hz, Ar-H); δ_C/ppm (100 MHz; DMSO-d_6) 153.4, 151.5, 145.2, 131.4, 124.8, 122.8, 122.3, 119.3 and 114.2 (Ar-C).

2-(2,3-dihydroxyphenyl)-7-azabenzimidazole 125d

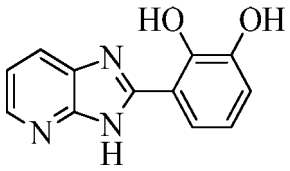

The procedure described for **125a** was followed using 2,3-diaminopyridine (100 mg, 0.9 mmol), nitrobenzene (10 mL) and 2,3-dihydroxybenzaldehyde (127.1 mg, 0.9 mmol). *2-(2,3-dihydroxyphenyl)-7-azabenzimidazole* **125d** was isolated as a brown solid (142.3 mg, 68%); m.p. dec. > 300 °C [HPLC-MS: m/z calculated for $C_{12}H_{10}N_3O_2$ $(M+H)^+$ 228.0773. Found 228.0752]; δ_H/ppm (400 MHz; DMSO-d_6) 13.59 (1H, s, NH), 12.96 (1H, s, OH), 9.27 (1H, s, OH), 8.39 (1H, s, Ar-H), 8.06 (1H, d, J = 51.9 Hz, Ar-H), 7.57 (1H, s, Ar-H), 7.32 (1H, dd, J = 8.0, 4.8 Hz, Ar-H), 6.94 (1H, d, J = 7.6 Hz, Ar-H) and 6.84 (1H, t, J = 7.4 Hz, Ar-H); δ_C/ppm (100 MHz; DMSO-d_6) 153.8, 147.5, 146.4, 144.4, 129.9, 125.9 – 125.3, 123.4, 119.1, 118.7, 118.1, 116.9 – 116.6 and 112.1 (Ar-C).

2-(3-hydroxyphenyl)-7-azabenzimidazole 125e

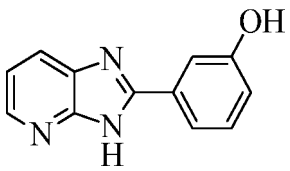

The procedure described for **125a** was followed using 2,3-diaminopyridine (100 mg, 0.9 mmol), nitrobenzene (10 mL) and 3-hydroxybenzaldehyde (112.4 mg, 0.9 mmol). *2-(2-hydroxyphenyl)-7-azabenzimidazole* **125e** was isolated as a brown solid (118.5 mg, 61%);

m.p. dec. > 300 °C [HPLC-MS: m/z calculated for $C_{12}H_{10}N_3O$ $(M+H)^+$ 212.0824. Found 212.0859]; δ_H/ppm (400 MHz; DMSO-d_6) 13.34 (1H, s, NH), 9.97 (1H, s, OH), 8.31 (1H, s, Ar-H), 7.99 (1H, s, Ar-H), 7.62 (2H, d, J = 6.4 Hz, Ar-H), 7.36 (1H, t, J = 8.0 Hz, Ar-H), 7.24 (1H, dd, J = 8.0, 4.8 Hz, Ar-H) and 6.96 – 6.91 (1H, m, Ar-H); δ_C/ppm (100 MHz; DMSO-d_6) 158.1, 144.2, 131.0, 130.6, 118.6, 118.2, 118.0 and 113.9 (Ar-C).

2-(4-chlorophenyl)-7-azabenzimidazole 125f

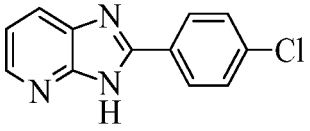

The procedure described for **125a** using 2,3-diaminopyridine (100 mg, 0.9 mmol), nitrobenzene (10 mL) and 4-chlorobenzaldehyde (129.3 mg, 0.9 mmol). *2-(4-chlorophenyl)-7-azabenzimidazole* **125f** was isolated as brown solid (185.9 mg, 88%); m.p. dec. > 300 °C [HPLC-MS: m/z calculated for $C_{12}H_9ClN_3$ $(M+H)^+$ 230.0485. Found 230.0502]; δ_H/ppm (400 MHz; DMSO-d_6) 13.50 (1H, s, NH), 8.35 (1H, d, J = 3.8 Hz, Ar-H), 8.24 (2H, d, J = 8.5 Hz, Ar-H), 8.02 (1H, d, J = 5.1 Hz, Ar-H), 7.65 (2H, d, J = 8.5 Hz, Ar-H) and 7.26 (1H, dd, J = 8.0, 4.8 Hz, Ar-H). δ_C/ppm (100 MHz; DMSO-d_6) 151.6, 149.5, 144.6, 136.0, 135.7, 129.6, 129.0, 128.9, 126.4 and 120.99 – 117.30 (Ar-C).

2-(5-chloro-2-hydroxyphenyl)-7-azabenzimidazole 125g

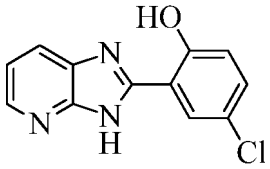

The procedure described for **125a** was followed using 2,3-diaminopyridine (100 mg, 0.9 mmol), nitrobenzene (10 mL) and 5-chlorosalicyaldehyde (144.0 mg, 0.9 mmol). *2-(5-chloro-2-hydroxyphenyl)-7-azabenzimidazole* **125g** was isolated as a brown solid (174.0 mg, 77%); m.p. dec. > 300 °C [HPLC-MS: m/z calculated for $C_{12}H_9ClN_3O$ $(M+H)^+$ 246.0434. Found 246.0471]; δ_H/ppm (400 MHz; DMSO-d_6) 13.11 (1H, s, NH), 8.44 (1H, s, ArH), 8.25 – 8.02 (2H, m, Ar-H), 7.45 (1H, dd, J = 8.8, 2.4 Hz, Ar-H), 7.35 (1H, dd, J = 8.0, 4.8 Hz, Ar-H) and 7.08 (1H, s, Ar-H); δ_C/ppm (100 MHz; DMSO-d_6) 118.8, 113.0, 109.8, 106.1 and 105.8 (Ar-C).

2-(4-methoxy-3-nitrophenyl)-7-azabenzimidazole 125h

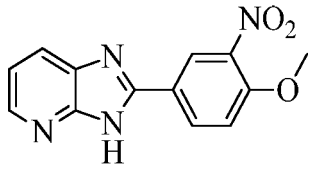

The procedure described for **125a** was followed using 2,3-diaminopyridine (100 mg, 0.9 mmol), nitrobenzene (10 mL) and 4-methoxyl-3-nitrobenzaldehyde (166.7 mg, 0.9 mmol). *2-(4-methoxy-3-nitrophenyl)-7-azabenzimidazole* **125h** was isolated as a brown solid (201.4 mg, 81%); m.p. dec. > 300 °C [HPLC-MS: m/z calculated for $C_{13}H_{11}N_4O_3$ $(M+H)^+$ 271.0831. Found 271.0874]; δ_H/ppm (400 MHz; DMSO-d_6) 13.78 (1H, S, NH), 8.40 (1H, s, Ar-H), 8.06 (1H, s, Ar-H), 7.78 – 7.69 (2H, m, Ar-H), 7.53 (1H, d, J = 8.2 Hz, Ar-H), 7.29 (1H, dd, J = 8.0, 4.7 Hz, Ar-H) and 3.96 (3H, s, O-CH_3); δ_C/ppm (100 MHz; DMSO-d_6) 151.0, 144.8, 138.9, 131.8, 127.3, 127.3, 118.7, 118.6, 118.6, 115.6, 115.6 and 115.5 (Ar-C) and 57.0 (O-CH_3).

2-(2-hydroxy-5-nitrophenyl)5-bromo-7-azabenzimidazole 125i

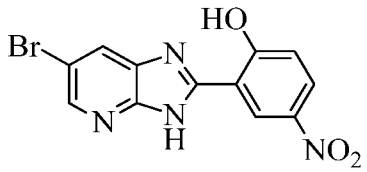

The procedure described for **125a** was followed using 2,3-diamino-5-bromopyridine (100 mg, 0.5 mmol), nitrobenzene (10 mL) and 2-hydroxyl-5-nitrobenzaldehyde (88.6 mg, 0.5 mmol). *2-(2-hydroxy-5-nitrophenyl)-5-bromo-7-azabenzimidazole* **125i** was isolated as a black solid (133.2 mg,75 %); m.p. dec. > 300 °C [HPLC-MS: m/z calculated for $C_{12}H_8N_4O_3$ $(M+H)^+$ 334.9780. Found 334.9832]; δ_H/ppm (400 MHz; DMSO-d_6) 13.86 (1H, s, NH), 9.12 (1H, s, Ar-H), 8.50 (1H, s, Ar-H), 8.36 (1H, s, Ar-H), 8.26 (1H, d, J = 8.4 Hz, Ar-H) and 7.22 (1H, d, J = 9.1 Hz, Ar-H); δ_C/ppm (100 MHz; DMSO-d_6) 163.7, 152.4, 145.3, 139.6, 127.7, 124.0, 118.4 and113.8, 112.8 (Ar-C).

2-(5-chloro-2-hydroxyphenyl)-5-bromo-7-azabenzimidazole 125j

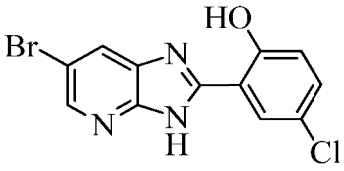

The procedure described for **125a** was followed using 2,3-diamino-5-bromopyridine (100 mg, 0.53 mmol), nitrobenzene (10 mL) and 5-chlorosalicylaldehyde (83.0 mg, 0.5 mmol). *2-(2-hydroxy-5-chlorophenyl)-5-bromo-7-azabenzimidazole* **125j** was isolated as a black solid (153.1 mg, 89%); m.p. dec. > 300 °C [HPLC-MS: m/z calculated for $C_{12}H_8BrClN_3O$ $(M+H)^+$ 323.9539. Found 323.9614]; δ_H/ppm (400 MHz; DMSO-*d*$_6$) 13.13 (2H, s, NH or OH), 8.46 (1H, s, Ar-H), 8.31 (1H, s, Ar-H), 8.18 (1H, s, Ar-H), 7.43 (1H, d, *J* = 8.1 Hz, Ar-H) and 7.06 (1H, d, *J* = 8.7 Hz, Ar-H); δ_C/ppm (100 MHz; DMSO-*d*$_6$) 156.9, 153.0, 145.0, 132.2, 126.4, 123.0, 119.2 and 113.6 (Ar-C).

2-(2-hydroxy-3-methoxyphenyl)-5-bromo-7-azabenzimidazole 125k

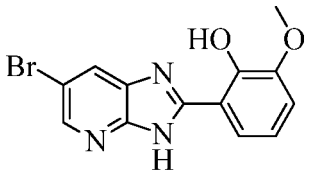

The procedure described for **125a** was followed using 2,3-diamino-5-bromopyridine (100 mg, 0.5 mmol), nitrobenzene (10 mL) and *o*-vanillin (80.6 mg, 0.5 mmol). *2-(2-hydroxy-3-methoxyphenyl)-5-bromo-7-azabenzimidazole* **125k** was isolated as a black solid (106.9 mg, 63%); m.p. dec.> 300 °C [HPLC-MS: m/z calculated for $C_{13}H_{11}BrN_3O_2$ $(M+1)^+$ 320.0034. Found 320.0078]; δ_H/ppm (400 MHz; DMSO-*d*$_6$) 13.75 (1H, d, *J* = 202.5 Hz, NH), 12.68 (1H, d, *J* = 156.7 Hz, OH), 8.47 (1H, s, Ar-H), 8.23 (1H, d, *J* = 7.9 Hz, Ar-H), 7.68 (1H, dd, *J* = 11.9, 7.7 Hz, Ar-H), 7.13 (1H, d, *J* = 7.8 Hz, Ar-H), 6.96 (1H, t, *J* = 8.0 Hz, Ar-H), 3.84 (3H, s, O-CH_3); δ_C/ppm (100 MHz; DMSO-*d*$_6$) 148.6, 144.7, 135.3, 129.8, 123.3, 119.0, 118.2, 114.7 and 113.5 (Ar-C) and 55.8 (O-CH_3).

2-(3,4-dihydroxyphenyl)-5-bromo-7-azabenzimidazole 125l

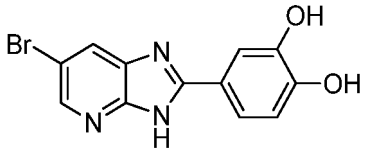

The procedure described for **125a** was followed using 2,3-diamino-5-bromopyridine (100 mg, 0.5 mmol), nitrobenzene (10 mL) and 3,4-dihydroxybenzaldehyde (73.2 mg, 0.5 mmol). *2-(3,4-dihydroxyphenyl)-5-bromo-7-azabenzimidazole* **125l** was isolated as a black solid (108.4 mg, 66.8%); m.p. dec. > 300 °C [HPLC-MS: m/z calculated for $C_{12}H_9BrN_3O_2$ $(M+H)^+$ 305.9878. Found 305.9779]; δ_H/ppm (400 MHz; DMSO-d_6) 13.42 (1H, s, NH), 9.64 (1H, s, OH), 9.32 (1H, s, OH), 8.32 (1H, s, Ar-H), 8.23 (1H, d, J = 8.1 Hz, ArH), 7.65 (1H, s, Ar-H), 7.53 (1H, d, J = 7.8 Hz, Ar-H) and 6.89 (1H, d, J = 8.1 Hz, Ar-H); δ_C/ppm (100 MHz; DMSO-d_6) 148.6, 145.7, 135.3, 129.9, 123.3, 120.4, 119.0 (s), 115.8 and 114.4(Ar-C).

2-(2,3,-dihydroxyphenyl)-5-bromo-7-azabenzimidazole 125m

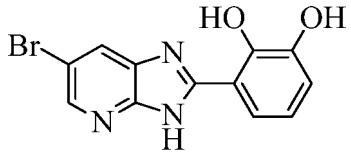

The procedure described for **125a** was followed using 2,3-diamino-5-bromopyridine (100 mg, 0.5 mmol), nitrobenzene (10 mL) and 2,3-dihydroxybenzaldehyde (073.2 mg, 0.5 mmol). *2-(2,3,-dihydroxyphenyl)-5-bromo-7-azabenzimidazole* **125m** was isolated as a black solid (115.2 mg,71 %); m.p. dec. > 300 °C [HPLC-MS: m/z calculated for $C_{12}H_9BrN_3O_2$ $(M+H)^+$ 305.9878. Found 305.9778]; δ_H/ppm (400 MHz; DMSO-d_6) 13.99 (1H, NH), 12.71 (1H, s, OH), 9.34 (1H, s, OH), 8.46 (1H, s, Ar-H), 8.22 (1H, s, Ar-H), 7.61 (1H, d, J = 34.1 Hz, Ar-H), 6.89 (2H, d, J = 47.4 Hz, Ar-H). δ_C/ppm (100 MHz; DMSO-d_6) 154.5, 146.3, 144.3, 119.2, 118.3, 116.9 and 113.4 (Ar-C).

3.8. GENERAL METHOD FOR THE SYNTHESIS OF 2-AMINO-5-BROMO-7-(BENZYLIMINO) PYRIDINES 126a-h, b', e', f', 127 and 127'.

2-Amino-5-bromo-7-(2,3,4-trihydroxybenzylimino)pyridine 126a.

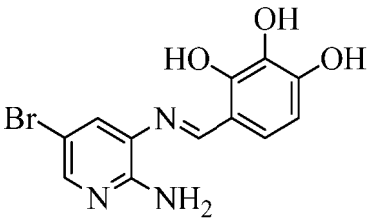

In a 50 ml round bottomed flask equipped with a reflux condenser, 2,3-diamino-5-bromopyridine (100 mg, 0.5 mmol) was dissolved in methanol (20 mL). 1 Equivalent of 2,3,4-trihydroxybenzaldehyde (81.7 mg, 0.5 mmol) and acetic acid (0.2 mL) were added. The resulting mixture was stirred under reflux and progress of the reaction was monitored by thin layer chromatography. At the completion of the reaction, the crude solution was cooled to room temperature, diluted with hexane (50 mL) and the precipitate filtered under vacuum and washed with hexane (3 × 50 mL) to afford *2-amino-5-bromo-7-(2,3,4-trihydroxybenzylimino)pyridine* **126a** as a yellow solid (111.7 mg, 65%); m.p. 150-152 °C [HPLC-MS: m/z calculated for $C_{12}H_{11}BrN_3O_3$ $(M+H)^+$ 323.9984. Found 323.9894]; υ_{max}/cm^{-1}: 3459, 3296 (NH), 3147 (OH), 1645 (C=N); δ_H/ppm (400 MHz; DMSO-d_6) 8.70 (1H, s, N=C-H), 7.90 (1H, d, J = 2.1 Hz, Ar-H), 7.57 (1H, d, J = 2.1 Hz, Ar-H), 7.00 (1H, d, J = 8.5 Hz, Ar-H), 6.45 (1H, d, J = 8.5 Hz, Ar-H) and 6.03 (2H, s, NH_2); 2-amino-5-bromo-7-(2,3,4-trihydroxybenzylimino)pyridine δ_C/ppm (100 MHz; DMSO-d_6) 164.5 (N=C-H), 153.2, 150.7, 150.1, 145.0, 132.4, 131.7, 126.8, 124.1, 113.0, 107.9 and 105.7 (Ar-C).

2-Amino-5-bromo-7-(2-hydroxy-3-methoxybenzylimino)pyridine 126b

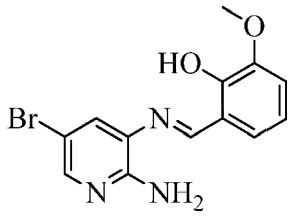

The procedure described for the synthesis of **126a** was followed using 2,3-diamino-5-bromopyridine (100 mg, 0.5 mmol), *o*-vanillin (80.6 mg, 0.5 mmol), methanol (10 mL) and glacial acetic acid (0.2 mL). *2-amino-5-bromo-7-(2-hydroxy-3-methoxybenzylimino)pyridine* **126b** was isolated as a brown solid (138.3 mg, 81%); m.p. 136-140 °C [HPLC-MS: m/z calculated for $C_{13}H_{13}BrN_3O_2$ $(M+H)^+$ 322.0191. Found 322.0079]; υ_{max}/cm^{-1}: 3441, 3349 (NH), 3237 (OH), 1590 (C=N); δ_H/ppm (400 MHz; DMSO-d_6) 11.90 (1H, s, O-H), 9.42 (1H, s, N=C-H), 7.74 (1H, d, J = 2.1 Hz, Ar-H), 7.44 (1H, dd, J = 7.9, 1.1 Hz, Ar-H), 7.33 (1H, d, J = 2.1 Hz, Ar-H), 7.15 (1H, dd, J = 8.0, 1.1 Hz, Ar-H), 6.91 (1H, t, J = 7.9 Hz, ArH) and 5.70 (2H, s, NH_2), 3.84 (3H, s, O-CH_3); δ_C/ppm (100 MHz; DMSO-d_6) 160.6 (N=C-H), 150.0, 148.0, 143.0, 140.8, 135.3, 123.7, 123.3, 120.1, 118.9, 118.8 and 115.7 (Ar-C) and 56.0 (O-CH_3).

2-Amino-5-bromo-7-(5-chloro-2-hydroxybenzylimino)pyridine 126c

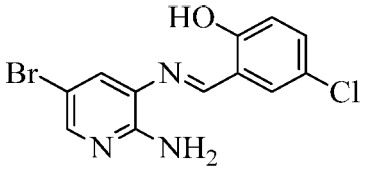

The procedure described for the synthesis of **126a** was followed using 2,3-diamino-5-bromopyridine (100 mg, 0.5 mmol), 5-chlorosalicylaldehyde (83.0 mg, 0.5 mmol), methanol (10 mL) and glacial acetic acid (0.2 mL). *2-amino-5-bromo-7-(5-chloro-2-hydroxybenzylimino)pyridine* **126c** was isolated as a yellow solid (131.6 mg, 76%): m.p. 116-118 °C [HPLC-MS: m/z calculated for $C_{12}H_{10}BrClN_3O$ $(M+H)^+$ 325.9696. Found 325.9566]; υ_{max}/cm^{-1}: 3483, 3295 (NH), 3143 (OH), 1579 (C=N); δ_H/ppm (400 MHz; DMSO-d_6) 11.57 (1H, s, OH), 8.84 (1H, s, N=C-H), 7.94 (1H, d, J = 2.2 Hz, Ar-H), 7.90 (1H, d, J = 2.7 Hz, Ar-H), 7.58 (1H, d, J = 2.2 Hz, Ar-H), 7.44 – 7.39 (1H, dd, Ar-H), 7.00 (1H, d, J = 7.3 Hz, Ar-H), 6.24 (2H, s, NH_2); δ_C/ppm (100 MHz; DMSO-d_6) 160.2 (N=C-H), 157.7, 153.7, 146.1, 132.8, 131.42, 129.7, 126.6, 123.0 , 122.0,118.5 and 105.4 (Ar-C).

2-Amino-5-bromo-7-(3,5-dichloro-2-hydroxybenzylimino)pyridine 126d

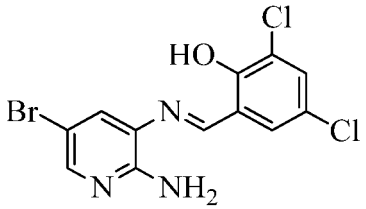

The procedure described for the synthesis of **126a** was followed using 2,3-diamino-5-bromopyridine (100 mg, 0.5 mmol), 3,5-dichlorosalicylaldehyde (101.1 mg, 0.5 mmol), methanol (10 mL) and glacial acetic acid (0.2 mL). *2-amino-5-bromo-7-(3,5-dichloro-2-hydroxybenzylimino)pyridine* **126d** was isolated as an orange solid (145.4 mg, 76%); m.p. 108-110 °C [HPLC-MS: m/z calculated for $C_{12}H_9BrCl_2N_3O$ $(M+H)^+$ 359.9306. Found 359.9229]; υ_{max}/cm^{-1}: 3464, 3376 (NH), 1574 (C=N); δ_H/ppm 400 MHz; DMSO-d_6) 13.18 (1H, s, OH), 9.42 (1H, s, N=C-H), 7.97 (1H, d, J = 2.5 Hz, Ar-H), 7.78 (1H, d, J = 1.9 Hz, Ar-H), 7.74 (1H, d, J = 2.4 Hz, Ar-H), 7.38 (1H, d, J = 2.0 Hz, Ar-H) and 5.85 (2H, s, NH_2). δ_C/ppm (100 MHz; DMSO-d_6) 162.8 (N=C-H), 154.4, 153.4, 146.8, 132.2, 130.4, 130.2, 127.8, 122.7, 121.8, 121.6 and 105.3 (Ar-C).

2-Amino-5-bromo-7-(3,5-dibromo-2-hydroxybenzylimino)pyridine 126e

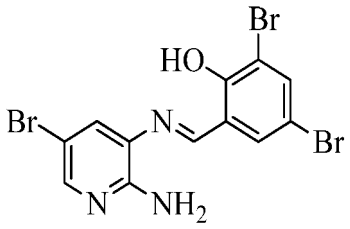

The procedure described for the synthesis of **126a** was followed using 2,3-diamino-5-bromopyridine (100 mg, 0.5 mmol), 3,5-dibromosalicylaldehyde (148.4 mg, 0.5 mmol), methanol (10 mL) and glacial acetic acid (0.2 mL). *2-amino-5-bromo-7-(3,5-dibromo-2-hydroxybenzylimino)pyridine* **126e** was isolated as an orange solid (209.8 mg, 88%); m.p. 118-120 °C [HPLC-MS: m/z calculated for $C_{12}H_9Br_3N_3O$ $(M+H)^+$ 447.8295. Found 447.6101]; υ_{max}/cm^{-1}: 3461, 3373 (NH),3067 (OH), 1615 (C=N); δ_H/ppm (400 MHz; DMSO-d_6) 13.44 (1H, s, OH), 9.38 (1H, s, N=C-H), 8.09 (d, J = 2.3 Hz, 1H, Ar-H), 7.95 (d, J = 2.2 Hz, 1H, Ar-H), 7.79 (d, J = 2.0 Hz, 1H, Ar-H), 7.39 (d, J = 2.0 Hz, 1H, Ar-H) and 5.83 (s, 2H, NH_2); δ_C/ppm (100 MHz; DMSO-d_6) 160.1 (N=C-H), 156.3, 149.3, 141.0, 137.7, 135.7, 134.6, 124.7, 121.9, 119.7, 111.3 and 110.3 (Ar-C).

2-Amino-5-bromo-7-(2-hydroxy-4-methoxybenzylimino)pyridine 126f

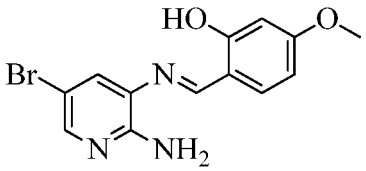

The procedure described for the synthesis of **126a** was followed using 2,3-diamino-5-bromopyridine (100 mg, 0.5 mmol), 4-methoxysalicylaldehyde (80.6 mg, 0.5 mmol), methanol (10 mL) and glacial acetic acid (0.2 mL). *2-amino-5-bromo-7-(2-hydroxyl-4-methoxybenzylimino)pyridine* **126f** was isolated as a yellow solid; m.p. 116-118 °C [HPLC-MS: m/z calculated for $C_{13}H_{13}BrN_3O_2$ $(M+H)^+$ 322.0191. Found 322.0006]; (133.2 mg, 78%); υ_{max}/cm^{-1}: 3483, 3297 (NH_2), 3155 (O-H), 1605 (N=C); δ_H/ppm (400 MHz; DMSO-d_6) 12.30 (1H, s, OH), 8.78 (1H, s, N=C-H), 7.91 (1H, d, J = 2.0 Hz, Ar-H), 7.59 (2H, overlapping multiplets Ar-H), 6.57 (1H, dd, J = 8.6, 2.4 Hz, Ar-H), 6.50 (1H, d, J = 2.4 Hz, Ar-H), 6.10 (2H, s, NH_2) and 3.80 (3H, s, O-CH_3); δ_C/pp (100 MHz; DMSO-d_6) 163.8 (N=C-H), 163.3, 162.0, 153.3, 145.2, 133.8, 131.7, 126.8, 113.7, 106.9, 105.6, 100.8 (Ar-C) and 55.5 (O-CH_3).

2-amino-5-bromo-7-(3,4-dihydroxybenzylimino)pyridine 126g

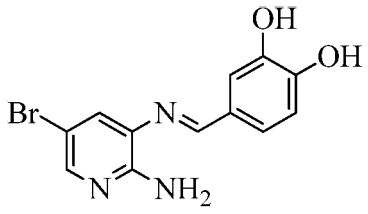

Nohana *et al.*, reported the synthesis of 2-amino-5-bromo-7-(3, 4-dihydroxyphenylimino) pyridine **126g** under microwave irradiation.[124]

The procedure described for the synthesis of **126a** was employed here using 2,3-diamino-5-bromopyridine (100 mg, 0.5 mmol), 3,4-dihydroxybenzaldehyde (73.2, 0.5 mmol), methanol (10 mL) and glacial acetic acid (0.2 mL). *2-amino-5-bromo-7-(3,4-dihydroxybenzylimino)pyridine* **126g** was isolated as a yellow solid (116.0 mg, 71%); m.p. 138-140 °C [HPLC-MS: m/z calculated for $C_{12}H_{11}BrN_3O_2$ $(M+H)^+$ 308.0034. Found 308.0741]; υ_{max}/cm^{-1}: 3421, 3344 (NH_2), 3076 (OH), 1588 (C=N); δ_H/ppm(400 MHz; DMSO-*d*$_6$) 9.46 (2H, s, OH), 8.49 (1H, s, Ar-H), 7.85 (1H, d, *J* = 2.0 Hz, Ar-H), 7.52 (1H, d, *J* = 2.0 Hz, Ar-H), 7.43 (1H, d, *J* = 1.6 Hz, Ar-H), 7.28 (1H, dd, *J* = 8.1, 1.6 Hz, Ar-H), 6.84 (1H, d, *J* = 8.1 Hz, Ar-H), 6.02 (2H, s, NH_2); δ_C/ppm (100 MHz; DMSO-*d*$_6$) 160.8 (N=C-H), 153.8, 149.6, 145.6, 144.7, 132.8, 127.9, 125.1, 122.7, 115.4, 115.1 and 105.5 (Ar-C).

2-amino-5-bromo-7-(3-ethoxy-2-hydroxybenzylimino)pyridine 126h

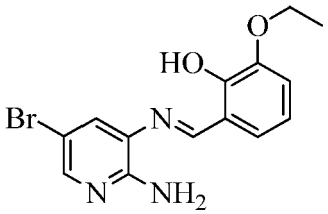

The procedure described for the synthesis of **126a** was followed using 2,3-diamino-5-bromopyridine (100 mg, 0.5 mmol), 3-ethoxysalicylaldehyde (88.07 mg, 0.5 mmol), methanol (10 mL) and glacial acetic acid (0.2 mL). *2-amino-5-bromo-7-(3-ethoxy-2-hydroxybenzylimino)pyridine* **126h** was isolated as an orange solid (153.2 mg, 86%); m.p. 130-132 °C [HPLC-MS: m/z calculated for $C_{14}H_{15}BrN_3O_2$ $(M+H)^+$ 336.0347. Found 336.0277]; υ_{max}/cm^{-1}: 3439, 3352 (NH), 3235 (OH), 1591 (C=N); δ_H/ppm (400 MHz; DMSO-*d*$_6$) 12.07 (1H, s, OH), 9.41 (1H, s, N=C-H), 7.75 (1H, d, *J* = 2.1 Hz, Ar-H), 7.41 (1H, d, *J* = 7.2 Hz, Ar-H), 7.33 (1H, d, *J* = 2.1 Hz, Ar-H), 7.13 (1H, d, *J* = 7.2 Hz, Ar-H), 6.89 (1H, t, *J* =

7.9 Hz, Ar-H), 5.71 (2H, s, NH_2), 4.08 (2H, q, J = 6.9 Hz, O-CH_2), 1.36 (3H, t, J = 6.9 Hz, CH_3); δ_C/ppm (100 MHz; DMSO-d_6) 161.01 (N=C-H), 150.3, 147.1), 142.8, 140.7, 135.3, 123.8, 123.7), 119.9, 118.9, 118.8 and 116.9 (Ar-C), 64.1 (O-CH_2) and 14.7 (CH_3).

5-bromo-2,3-bis(2-hydroxybenzylimino) pyridine 127

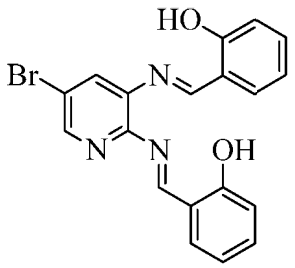

The procedure described for the synthesis of **126a** was followed using 2,3-diamino-5-bromopyridine (100 mg, 0.5 mmol), salicylaldehyde (0.1 mL, 1.6 mmol), methanol (20 mL) and glacial acetic acid (0.4 mL). *5-bromo-2,3-bis(2-hydroxybenzylimino)pyridine* **127** was isolated as a yellow solid (168.0 mg, 80%); m.p. 142-144 °C [HPLC-MS: m/z calculated for $C_{19}H_{15}BrN_3O_2$ $(M+H)^+$ 396.0347. Found 396.0249]; υ_{max}/cm^{-1}: 1605 (C=N); δ_H/ppm (400 MHz; DMSO-d_6) 12.90 (1H, s, OH), 12.42 (1H, s, OH), 9.50 (1H, s, N=C-H), 9.00 (1H, s, N=C-H), 8.52 (1H, s, Ar-H), 8.21 (1H, s, Ar-H), 7.80 (1H, d, J = 7.4 Hz, Ar-H), 7.71 (1H, d, J = 7.3 Hz, Ar-H), 7.46 (2H, d, J = 5.5 Hz, Ar-H) and 7.00 (4-H, dd, J = 12.6, 6.9 Hz, Ar-H); δ_C/ppm (100 MHz; DMSO-d_6) 166.4 (N=C-H), 164.3 (N=C-H), 161.1, 160.4, 150.3 – 149.8 (overlapping m), 146.7, 140.2 – 139.9 (overlapping m), 134.5, 134.2, 133.0, 132.3, 131.1, 119.6, 119.4, 119.3, 119.3, 118.7, 116.8 and 116.8 [Ar-C].

3.9. GENERAL PROCEDURE FOR THE REDUCTION OF IMINES TO AMINES

5-bromo-2,3-bis(2-hydroxybenzylamino) pyridine 127'

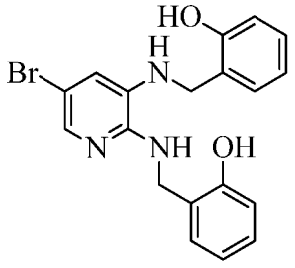

100 mg (0.3 mmol) of **127** was dissolved in methanol (10 mL) and the solution was cooled to below 10°C. Sodium cyanoborohydride (39.3 mg, 0.6 mmol) was added and the mixture stirred vigorously at room temperature. The progress of the reaction was monitored by thin layer chromatography. At the completion of the reaction, the crude mixture was concentrated under pressure, ethyl acetate (50 mL) and deionized water (50 mL) were added and the crude product extracted into ethyl acetate, dried with anhydrous sodium sulphate and concentrated *in vacuo*. The residue was purified using column chromatography on silica gel; elution with ethyl acetate - hexane (1:1) to afford the product *5-bromo-2,3-bis(2-hydroxybenzylamino)pyridine* **127'** as a white solid (92.1 mg, 92%); m.p. 94-98 °C [HPLC-MS: m/z calculated for $C_{19}H_{19}BrN_3O_2$ $(M+H)^+$ 400.0660. Found 400.0730]; υ_{max}/cm^{-1}: 3388 (NH), 3069, 2957 (OH); δ_H/ppm (400 MHz; DMSO-d_6) 10.01 (1H, s, OH), 9.60 (1H, s, OH), 7.35 (1H, d, J = 2.0 Hz, Ar-H), 7.15 (2H, dd, J = 10.0, 3.9 Hz, Ar-H), 7.07 (2H, td, J = 8.5, 1.5 Hz, Ar-H), 6.84 (1H, d, J = 8.0 Hz, Ar-H), 6.76 (3H, dt, J = 15.3, 7.6 Hz, Ar-H), 6.57 (d, J = 2.0 Hz, 1H), 6.55 (1H, t, J = 5.5 Hz, NH), 5.74 (1H, t, J = 5.3 Hz, NH), 4.42 (2H, d, J = 5.5 Hz, CH_2) and 4.19 (2H, d, J = 5.3 Hz, CH_2); δ_C/ppm (100 MHz; DMSO-d_6) 155.3, 155.2, 146.3, 132.6, 132.4, 129.3, 128.7, 128.0, 127.9, 126.1, 124.1, 118.9, 118.8, 115.5, 115.0, 114.5, 106.6 (Ar-C), 41.3 and 21.0 (CH_2).

2-amino-5-bromo-7-(2-hydroxy-4-methoxybenzylamino)pyridine 126b'

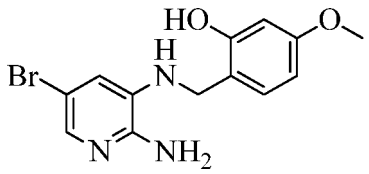

To the procedure described for the preparation of **127'** using **126b** (100 mg, 0.3 mmol), methanol (10 mL) and sodium cyanoborohydride (23.4 mg, 0.4 mmol). *2-amino-5-bromo-7-(2-hydroxy-4-methoxybenzylamino)pyridine* **126b'** was isolated as a white solid (89.4 mg, 89%); m.p. 122-124 °C [HPLC-MS: m/z calculated for $C_{13}H_{15}BrN_3O_2$ $(MH+2)^+$ 326.0347. Found 326.0392]; υ_{max}/cm^{-1}: 3374, 3348, 3273 (NH), 2923, 2852 (OH); δ_H/ppm (400 MHz; DMSO-d_6) 9.63 (1H, s, O-H), 7.26 (1H, d, J = 2.0 Hz, Ar-H), 7.05 (1H, d, J = 8.4 Hz, Ar-H), 6.56 (1H, d, J = 2.0 Hz, Ar-H), 6.41 (1H, d, J = 2.5 Hz, Ar-H), 6.36 (1H, dd, J = 8.4, 2.5 Hz, Ar-H), 5.75 (2H, s, NH_2), 5.45 (1H, t, J = 5.5 Hz, N-H), 4.10 (2H, d, J = 5.5 Hz, CH_2) and 3.67 (3H, s, O-CH_3); δ_C/ppm (100 MHz; DMSO-d_6) 159.3, 156.0, 147.4, 133.2, 132.2, 129.4, 116.7, 114.9, 106.9, 104.3 and 101.1 (Ar-C), 55.0 (CH_2) and 40.8 (O-CH_3).

2-amino-5-bromo-7-(2-hydroxy-3-methoxybenzylamino) pyridine 126e'

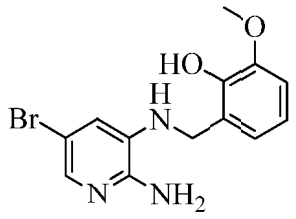

To the procedure described for the preparation of **127'** using **126e** (100 mg, 0.3 mmol), methanol (10 mL) and sodium cyanoborohydride (23.4 mg, 0.4 mmol). *2-amino-5-bromo-7-(2-hydroxy-3-methoxybenzylamino)pyridine* **126e'** was isolated as a white solid (90.4 mg, 90%); m.p 116-118 °C [HPLC-MS: m/z calculated for $C_{13}H_{15}BrN_3O_2$ $(M+H)^+$ 324.0347. Found 324.0383]; υ_{max}/cm^{-1}: 3434, 3369, 3268 (NH), 2933 (OH); δ_H/ppm (400 MHz; DMSO-d_6) 9.50 (1H, s, OH), 7.36 (1H, d, J = 2.1 Hz, Ar-H), 6.83 (1H, d, J = 2.1 Hz, Ar-H), 6.76 (1H, dd, J = 7.6, 1.4 Hz, Ar-H), 6.73 – 6.67 (2H, overlapping m, Ar-H), 6.32 (1H, t, J = 5.7 Hz, NH), 5.16 (2H, s, NH_2), 4.42 (2H, d, J = 5.7 Hz, CH_2), 3.76 (3H, s, O-CH_3); δ_C/ppm (100 MHz; DMSO-d_6) 147.8, 146.3, 144.4, 133.0, 132.5, 126.9, 121.2, 118.6, 118.5, 110.8, 106.1 (Ar-C) and 55.7 (O-CH_3) and 45.2 (CH_2).

2-amino-5-bromo-7-(2-hydroxy-3,5-dibrombenzylamino) pyridine 126f'

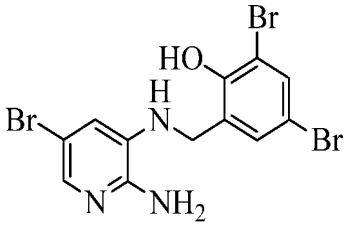

To the procedure described for the preparation of **127'** using **126f** (100 mg, 0.22 mmol), methanol (10 mL) and sodium cyanoborohydride (16.8 mg, 0.3 mmol). *2-amino-5-bromo-7-(2-hydroxy-3,5-dibromobenzylamino)pyridine* **126f'** was isolated as a white solid (93.9 mg, 94.4%); m.p. 122-124 °C [HPLC-MS: m/z calculated for $C_{12}H_{11}Br_3N_3O$ $(MH+2)^+$ 451.8452. Found 451.8467]; υ_{max}/cm^{-1}: 3409, 3830 (NH), 2930 (OH); δ_H/ppm (400 MHz; DMSO-d_6) 11.97 (1H, s, O-H), 7.62 (1H, d, J = 2.4 Hz, Ar-H), 7.41 (1H, d, J = 2.1 Hz, Ar-H), 7.35 (1H, d, J = 2.4 Hz, Ar-H), 6.90 (d, J = 2.1 Hz, 1H, Ar-H), 6.84 (1H, t, J = 6.0 Hz, N-H), 5.24 (2H, s, NH_2) and 4.41 (2H, d, J = 6.0 Hz, CH_2); δ_C/ppm (100 MHz; DMSO-d_6) 152.0, 145.9, 133.3, 133.0, 132.2, 132.0, 130.8, 119.3, 112.3, 110.2 and 106.7 (Ar-C) and 40.9 (CH_2).

3.10. SYNTHESIS OF *N*-(PHENYL)-2-HYDROXYBENZYLIMINES 130a-l AND *N*-(PHENYL)-2-HYDROXYBENZYLAMINES 130b', c', e', g', i', j' and k'.

N-(2-hydroxy-4-nitrophenyl)-2,3,4-trihydroxybenzylimine 130a

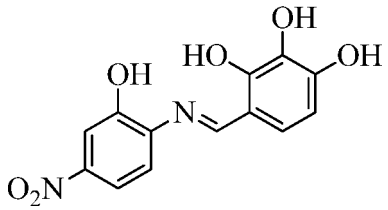

To a methanolic (20 ml) solution of 100 mg (0.7 mmol) of 2-amino-5-nitrophenol and 2,3,4-trihydroxybenzaldehyde (100.2 mg, 0.7 mmol) in 50 ml flask equipped with a reflux condenser was added two drops of glacial acetic acid as catalyst. The solution was stirred under reflux while the progress of the reaction was monitored by thin layer chromatography. At the completion of the reaction, the crude solution was cooled to room temperature, diluted with hexane (30 mL) and the precipitate filtered washed with hexane (3 × 30 mL) to afford N-*(2-hydroxy-4-nitrophenyl)-2,3,4-trihydroxybenzylimine* **130a** as a brown solid (172.4 mg, 91.4 %); m.p. dec. > 300 °C [HPLC-MS: m/z calculated for $C_{13}H_{11}N_2O_6$ $(M+H)^+$ 291.0617. Found 291.0673]; υ_{max}/cm^{-1}: 1591 (C=N), 1504 (N=O); δ_H/ppm (400 MHz; DMSO-d_6) 13.91 (1H, s, OH), 11.35 (1H, s, OH), 9.71 (1H, s, OH), 8.94 (1H, s, N=C-H), 8.46 (1H, s, OH), 8.26 (1H, d, J = 2.7 Hz, Ar-H), 8.02 (1H, dd, J = 9.0, 2.7 Hz, Ar-H), 7.10 (1H, d, J = 9.0 Hz, Ar-H), 6.98 (1H, d, J = 8.6 Hz, Ar-H) and 6.41 (1H, d, J = 8.6 Hz, Ar-H); δ_C/ppm (100 MHz; DMSO-d_6) 162.9 (N=C-H), 157.2, 153.4, 150.5, 140.0, 135.0, 132.6, 124.3, 122.9, 116.1, 114.4, 112.4, and 108.0 (Ar-C).

N-(2-hydroxy-4-nitrophenyl)-2,3-dihydroxybenzylimine 130b

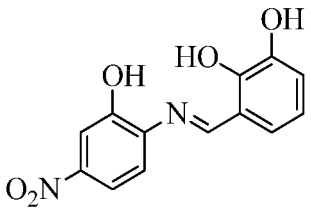

The procedure described for the synthesis of **130a** was followed using 2-amino-5-nitrophenol (100 mg, 0.7 mmol), 2,3-dihydroxybenzaldehyde 0.7 mmol), methanol (20 mL) and glacial acetic acid (two drops). N-*(2-hydroxy-4-nitrophenyl)-2,3-dihydroxybenzylimine* **130b** was isolated as a brown solid (153.3 mg, 86%); m.p. 146-148 °C [HPLC-MS: m/z calculated for

$C_{13}H_{11}N_2O_5$ $(M+H)^+$ 275.0668. Found 274.9680]; υ_{max}/cm^{-1}: 1620 (C=N), 1503 (N=O); δ_H/ppm (400 MHz; DMSO-d_6) 11.43 (1H, s, OH), 9.16 (1H, s, OH), 9.09 (1H, s, N=C-H), 8.31 (1H, d, J = 2.7 Hz, Ar-H), 8.08 (1H, dd, J = 9.0, 2.7 Hz, Ar-H), 7.14 (2H, d, J = 8.8 Hz, Ar-H), 6.96 (1H, dd, J = 7.8, 1.4 Hz, Ar-H) and 6.79 (1H, t, J = 7.8 Hz, Ar-H); δ_C/ppm (100; MHz, DMSO-d_6) 165.0 (N=C-H), 158.1, 150.6, 146.3, 140.4, 135.7, 124.2, 123.4, 119.8, 119.5, 119.0, 116.8 and 115.6 (Ar-C).

N-(2-hydroxy-4-nitrophenyl)-5-chloro-2-hydroxybenzylimine 130c

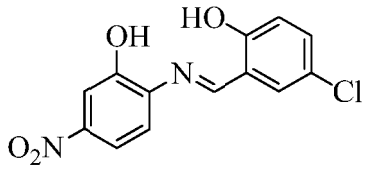

The procedure described for the synthesis of **130a** was followed using 2-amino-5-nitrophenol (100 mg, 0.7 mmol), 5-chloro salicylaldehyde (0.7 mmol), methanol (20 mL) and glacial acetic acid (two drops). *N-(2-hydroxy-4-nitrophenyl)-5-chloro-2-hydroxybenzylimine* **130c** was isolated as an orange solid (91.6 mg, 91%); m.p. 110-116 °C [HPLC-MS: m/z calculated for $C_{13}H_{10}ClN_2O_4$ $(M+H)^+$ 293.0329. Found 293.0411]; υ_{max}/cm^{-1}: 1593 (C=N), 15488 (N=O); δ_H/ppm (400 MHz; DMSO-d_6) 13.07 (1H, s, OH), 11.36 (1H, s, OH), 9.08 (1H, s, N=C-H), 8.26 (1H, d, J = 2.8 Hz, Ar-H), 8.09 (1H, dd, J = 9.0, 2.8 Hz, Ar-H), 7.82 (1H, d, J = 2.7 Hz, Ar-H), 7.45 (1H, dd, J = 8.8, 2.7 Hz, Ar-H), 7.12 (1H, d, J = 9.0 Hz, Ar-H) and 7.00 (1H, d, J = 8.8 Hz, Ar-H); δ_C/ppm; δ_C/ppm (100 MHz; DMSO-d_6) 161.2 (N=C-H), 156.2, 157.8, 140.2, `138.1, 135.3, 128.4, 127.9, 126.6, 117.2, 116.3, 112.3 and 109.1 (Ar-C).

N-(3,4-difluorophenyl)-2,3,4-trihydroxybenzylimine 130d

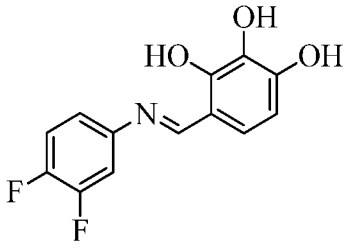

The procedure described for the synthesis of **130a** was followed using 3,4-difluoroaniline (0.1 mL, 1.1 mmol), 2,3,4-trihydroxybenzaldehyde (1.1 mmol), methanol (20 mL) and glacial acetic acid (two drops). N-*(3,4-difluorophenyl)-2,3,4-trihydroxybenzylimine* **130d** was isolated as a brown solid (255.5 mg, 92%); m.p. 138-140 °C [HPLC-MS: m/z calculated for $C_{13}H_{10}F_2NO_3$ $(M+H)^+$ 266.0628. Found 266.0603]; υ_{max}/cm^{-1}: 3316, 3225(OH), 1629 (C=N); δ_H/ppm (400 MHz; DMSO-*d*$_6$) 13.08 (1H, s, OH), 9.79 (1H, s, OH), 8.76 (1H, s, N=C-H), 8.51 (1H, s, O-H), 7.58 – 7.50 (1H, m, Ar-H), 7.49 – 7.43 (1H, m, Ar-H), 7.24 – 7.19 (1H, m, Ar-H), 6.95 (1H, d, *J* = 8.5 Hz, Ar-H) and 6.45 (1H, d, *J* = 8.5 Hz, Ar-H); δ_C/ppm (100 MHz; DMSO-*d*$_6$) 164.45 (N=C-H), 151.0 (d, $J_{C,F}$ = 13.5 Hz), 150.8, 150.75, 148.6 (d, $J_{C,F}$ = 13.7 Hz, $J_{C,F}$), 145.42 (dd, $^1J_{C,F}$ = 7.1, $^2J_{C,F}$ = 3.1 Hz), 132.4, 124.4, 118.4 (dd, $^1J_{C,F}$ = 6.3, $^2J_{C,F}$ = 3.0 Hz), 117.89 (d, $J_{C,F}$ = 17.7 Hz), 112.3, 109.9 (d, $J_{C,F}$ = 18.2 Hz) and 108.0 [Ar-C].

N-(3,4-difluorophenyl)-2,3-dihydroxybenzylimine 130e

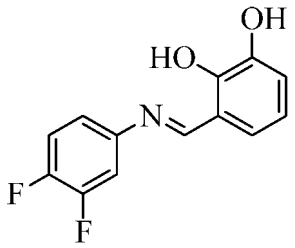

The procedure described for the synthesis of **130a** was followed using 3,4-difluoroaniline (0.1 ml, 1.1 mmol), 2,3,-dihydroxybenzaldehyde (1.1 mmol), methanol (20 mL) and glacial acetic acid (two drops). N-*(3,4-difluorophenyl)-2,3-dihydroxybenzylimine* **130e** was isolated as a red solid (232.2 mg, 89%); m.p. 98-100 °C [HPLC-MS: m/z calculated for $C_{13}H_9F_2NO_2$ $(M)^+$ 249.0601. Found 249.1589]; υ_{max}/cm^{-1}:3259 (OH), 1626 (C=N); δ_H/ppm (400 MHz; DMSO-*d*$_6$) 12.57 (1H, s, OH), 9.24 (1H, s, OH), 8.90 (1H, s, N=C-H), 7.61 (1H, ddd, *J* = 12.0, 7.3, 2.5 Hz, Ar-H), 7.51 (1H, dd, *J* = 19.4, 8.9 Hz, Ar-H), 7.28 (1H, dd, *J* = 5.8, 3.1 Hz, Ar-H), 7.09 (1H, dd, *J* = 7.8, 1.3 Hz, Ar-H), 6.97 (1H, dd, *J* = 7.8, 1.3 Hz, Ar-H) and 6.80 (1H, t, *J* = 7.8 Hz, Ar-H); δ_C/ppm (100 MHz; DMSO-*d*$_6$) 165.0 (N=C-H), 151.0 ($J_{C,F}$ = 13.6 Hz), 149.05, 148.6, 147.0 (d, $J_{C,F}$ = 12.9 Hz), 145.6, 145.3 ($^1J_{C,F}$ = 7.0 Hz, $^2J_{C,F}$ = 3.1 Hz), 122.8, 119.3, 118.9, 118.7 ($^1J_{C,F}$ = 6.5 Hz, $^2J_{C,F}$ = 3.1 Hz), 117.9 (d, $J_{C,F}$ = 17.9 Hz) and 110.3 (d, $J_{C,F}$ = 18.4 Hz) [Ar-C].

***N*-(3,4-difluorophenyl)-3-bromo-5-chloro-2-hydroxybenzylimine 130f**

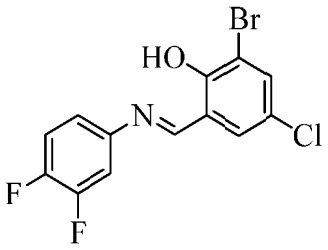

The procedure described for the synthesis of **130a** was followed using 3,4-difluoroaniline (0.1 ml, 1.1 mmol), 3-bromo-5-chlorosalicylaldehyde (1.1 mmol), methanol (20 mL) and glacial acetic acid (two drops). N-*(3,4-difluorophenyl)-3-bromo-5-chloro-2-hydroxybenzylimine* **130f** was isolated as a white solid (290.3 mg, 80%); m.p. 94-96 °C [HPLC-MS: m/z calculated for $C_{13}H_7BrClF_2NO$ $(M+H)^+$ 345.9446. Found 346.3259]; υ_{max}/cm^{-1} : 3053 (OH), 1599 (C=N); δ_H/ppm (400 MHz; DMSO-d_6) 13.95 (1H, s, OH), 8.98 (1H, s, N=C-H), 7.88 (1H, d, J = 2.5 Hz, Ar-H), 7.74 (1H, d, *J* = 2.5 Hz, Ar-H), 7.70 (1H, ddd, *J* = 11.9, 7.4, 2.5 Hz, Ar-H), 7.58 (1H, dd, *J* = 19.3, 8.9 Hz, Ar-H) and 7.41 – 7.37 (1H, m, Ar-H); δ_C/ppm (100 MHz; DMSO-d_6) 163.5 (N=C-H), 156.2, 135.2, 131.4 (s), 122.8, 120.3, 118.9, 118.3 (overlapping m), 118.1, 111.0 (overlapping m) and110.8 [Ar-C].

***N*-(3,4-difluorophenyl)-3,5-dichloro-2-hydroxylbenzylimine 130g**

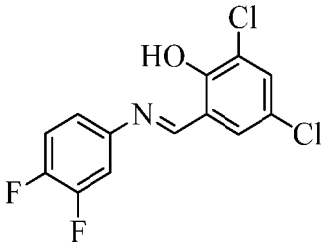

The procedure described for the synthesis of **130a** was followed using 3,4-difluoroaniline (0.1 ml, 1.1 mmol), 3,4-dichlorosalicyaldehyde (1.1 mmol), methanol (20 mL) and glacial acetic acid (two drops). N-*(3,4-difluorophenyl)-3,5-dichloro-2-dihydroxybenzylimine* **130g** was isolated as a yellow solid (294.2 mg, 93%); m.p. 97-98 °C [HPLC-MS: m/z calculated for $C_{13}H_7Cl_2F_2NO$ $(M)^+$ 300.9873. Found 301.1477]; υ_{max}/cm^{-1}: 1606 (C=N); δ_H/ppm (400 MHz; DMSO-d_6) 13.77 (1H, s, OH), 8.98 (1H, s, N=C-H), 7.73 (1H, d, *J* = 2.5 Hz, Ar-H), 7.71 – 7.64 (2H, overlapping m, Ar-H), 7.55 (1H, dd, *J* = 19.3, 8.9 Hz, Ar-H) and 7.36 (1H, dd, *J* = 5.8, 3.1 Hz, Ar-H); δ_C/ppm (100 MHz; DMSO-d_6) 163.4 (N=C-H), 155.2, 150.5 (dd, $J_{C,F}$ = 97.3, 13.2 Hz), 148.0 (dd, $^1J_{C,F}$ = 97.1, $^2J_{C,F}$ = 13.1 Hz), 143.7 (dd, $^1J_{C,F}$ = 7.2, $^2J_{C,F}$ = 3.2

Hz), 132.4, 130.7, 122.4, 121.6, 120.5, 119.0 (dd, $^{1}J_{C,F}$ = 6.6, $^{2}J_{C,F}$ = 3.1 Hz), 118.1 (d, $J_{C,F}$ = 18.2 Hz) and 110.8 (d, $J_{C,F}$ = 18.7 Hz) [Ar-C].

***N*-(3,4-difluorophenyl)-3,5-dibromo-2-hydroxybenzylimine 130h**

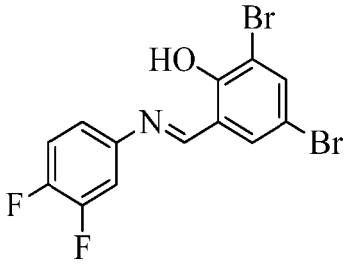

The procedure described for the synthesis of **130a** was followed using 3,4-difluoroaniline (0.1 ml, 1.1 mmol), 3,4-dibromosalicylaldehyde (1.1 mmol), methanol (20 mL) and glacial acetic acid (two drops). N-*(3,4-difluorophenyl)-3,5-dibromo-2-hydroxybenzylimine* **130h** was isolated as a brown solid (364.4 mg, 89%); m.p. 92-94 °C [HPLC-MS: m/z calculated for $C_{13}H_8Br_2F_2NO$ $(MH+2)^+$ 391.8940. Found 391.8984]; υ_{max}/cm^{-1} : 3052 (OH), 1606 (C=N); δ_H/ppm (400 MHz; DMSO-d_6) 13.96 (1H, s, OH), 8.96 (1H, s, N=C-H), 7.94 (1H, d, J = 2.3 Hz, Ar-H), 7.83 (1H, d, J = 2.3 Hz, Ar-H), 7.68 (1H, ddd, J = 11.8, 7.3, 2.5 Hz, Ar-H), 7.56 (1H, dd, J = 19.3, 8.9 Hz, Ar-H) and 7.37 (1H, d, J = 8.8 Hz, Ar-H); δ_C/ppm (100 MHz; DMSO-d_6) 163.3 (N=C-H), 156.6, 151.10 – 150.0 (m), 148.7 – 147.4 (m), 143.6 (dd, $^{1}J_{C,F}$ = 7.2, $^{2}J_{C,F}$ = 3.3 Hz), 137.7, 134.4, 120.9, 119.0 (dd $^{1}J_{C,F}$ = 6.6, $^{2}J_{C,F}$ = 3.2 Hz), 118.2 (d, $J_{C,F}$ = 18.1 Hz), 111.3, 110.8 (d, $J_{C,F}$ = 18.7 Hz) and 109.8 [Ar-C].

***N*-(3,4-difluorophenyl)-5-chloro-2-hydroxybenzylimine 130i**

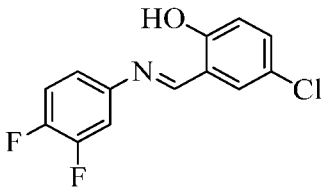

The procedure described for the synthesis of **130a** was followed using 3,4-difluoroaniline (0.1 ml, 1.1 mmol), 5-chlorosalicylaldehyde (1.1 mmol), methanol (20 mL) and glacial acetic acid (two drops). N-*(3,4-difluorophenyl)-5-chloro-2-hydroxybenzylimine* **130i** was isolated as a yellow solid (258.9 mg, 92.4%); m.p. 94-96 °C [HPLC-MS: m/z calculated for $C_{13}H_9ClF_2NO$ $(MH+2)^+$ 270.0340. Found 270.2235]; υ_{max}/cm^{-1}: 1603 (C=N); δ_H/ppm (400

MHz; DMSO-d_6) 12.46 (1H, s, OH), 8.91 (1H, s, N=C-H), 7.73 (1H, d, J = 2.7 Hz, Ar-H), 7.63 – 7.49 (2H, m, Ar-H), 7.46 (1H, dd, J = 8.8, 2.7 Hz, Ar-H), 7.28 (d1H, t, J = 3.9, 3.1 Hz, Ar-H) and 7.01 (1H, d, J = 8.8 Hz, Ar-H); δ_C/ppm (100 MHz; DMSO-d_6) 162.7 (d, J = 1.7 Hz, Ar-C), 158.7 (N=C-H), 145.5 – 145.3 (m), 133.0, 130.7, 122.7, 120.6, 118.7, 118.7, 118.0 (d, $J_{C,F}$ = 18.0 Hz) and 110.6 (d, $J_{C,F}$ = 18.4 Hz) [Ar-C].

S

***N*-(2-hydroxy-4-nitrophenyl)-3-bromo-5-chloro-2-hydroxybenzylimine 130j**

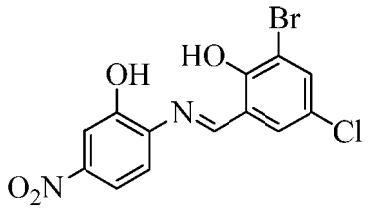

The procedure described for the synthesis of **130a** was followed using 2-amino-5-nitrophenol (100 mg, 0.7 mmol), 2-bromo-5-chloro salicylaldehyde (0.7 mmol), methanol (20 mL) and glacial acetic acid (two drops). N-*(2-hydroxy-4-nitrophenyl)-3-bromo-5-chloro-2-hydroxybenzylimine* **130j** was isolated as a brown solid (224.6 mg, 93%); m.p. above 300 °C [HPLC-MS: m/z calculated for $C_{13}H_9BrClN_2O_4$ $(M+1)^+$ 370.9434. Found 370.9338]; υ_{max}/cm^{-1}: 3087 (OH), 1622 (C=N); $^{\delta}H$/ppm (400 MHz; DMSO-d_6) 14.77 (1H, s, OH), 11.67 (1H, s, OH), 9.16 (1H, s, N=C-H), 8.38 (1H, d, J = 2.7 Hz, Ar-H), 8.10 (1H, dd, J = 9.0, 2.7 Hz, Ar-H), 7.82 (d, J = 2.5, Hz, Ar-H), 7.75 (1H, d, J = 2.5 Hz, Ar-H) and 7.15 (1H, d, J = 9.0 Hz, Ar-H); $^{\delta}C$/ppm (100 MHz; DMSO-d_6) 162.4 (N=C-H), 157.88, 157.80, 139.9, 135.4, 133.1, 131.4, 124.7, 122.0, 120.0, 116.6, 115.3 and 111.8 (Ar-C).

***N*-(2-hydroxy-4-nitrophenyl)-3,5-dichloro-2-hydroxybenzylimine 130k**

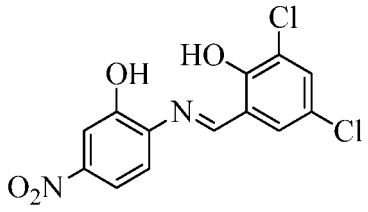

The procedure described for the synthesis of **130a** was followed using 2-amino-5-nitrophenol (100 mg, 0.65 mmol), 3,5-dichlorosalicylaldehyde (0.65 mmol), methanol (20 mL) and glacial acetic acid (two drops). N-*(2-hydroxy-4-nitrophenyl)-3,5-dichloro-2-hydroxybenzylimine* **130k** was isolated as a yellow solid (193.5 mg, 91%); m.p above 300 °C [HPLC-MS: m/z calculated for $C_{13}H_9Cl_2N_2O_4$ $(MH+2)^+$ 328.9939. Found 329.1707]; υ_{max}/cm^{-1} : 3355 (OH), 1623 (C=N); δ_H/ppm (400 MHz; DMSO-d_6) 14.68 (1H, s, OH), 9.20

(1H, s, N=C-H), 8.40 (1H, d, J = 2.7 Hz, Ar-H), 8.12 (1H, dd, J = 9.0, 2.7 Hz, Ar-H), 7.74 (2H, d, J = 1.6 Hz, Ar-H) and 7.16 (1H, d, J = 9.0 Hz, Ar-H); δ_C/ppm (100 MHz; DMSO-d_6) 162.9 (N=C-H), 158.3, 157.4, 140.3, 133.7, 133.1, 131.2, 125.1, 122.6, 122.0, 120.8, 117.1 and 115.8 (Ar-C).

***N*-(2-hydroxy-4-nitrophenyl)-3,5-dibromo-2-hydroxybenzylimine 130l**

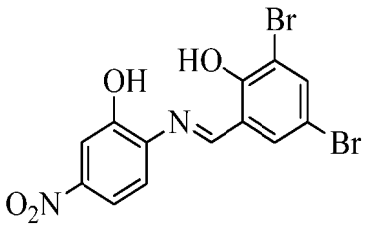

The procedure described for the synthesis of **130a** was followed using 2-amino-5-nitrophenol (100 mg, 0.7 mmol), 3,5-dibromosalicylaldehyde (0.7 mmol), methanol (20 mL) and glacial acetic acid (two drops). N-*(2-hydroxy-4-nitrophenyl)-3,5-dibromo-2-hydroxybenzylimine* **130l** was isolated as a yellow solid (250.4 mg, 92.6%); m.p. 144-146 °C [HPLC-MS: m/z calculated for $C_{13}H_9Br_2N_2O_4$ $(MH+2)^+$ 416.8929. Found 416.9012]; υ_{max}/cm^{-1}: 3087 (OH), 1625 (C=N); δ_H/ppm (400 MHz; DMSO-d_6) 14.84 (1H,s, OH), 9.19 (1H, s, N=C-H), 8.41 (1H, d, J = 2.7 Hz, Ar-H), 8.13 (1H, dd, J = 9.1, 2.7 Hz, Ar-H), 7.95 (1H, d, J = 2.4 Hz, Ar-H), 7.90 (1H, d, J = 2.5 Hz, Ar-H) and 7.16 (1H, d, J = 9.0 Hz, Ar-H); δ_C/ppm (100 MHz; DMSO-d_6) 162.3 (N=C-H), 158.3, 157.8, 139.9, 137.9, 134.4, 124.7, 120.7, 116.6, 115.3, 113.1, 112.2 and 108.9 (Ar-C).

***N*-(2-hydroxy-4-nitrophenyl)-2,3-dihydroxybenzylamine 130b'**

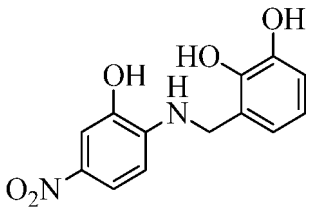

To the procedure described for **127'** using *N*-(2-hydroxy-4-nitrophenyl)-2,3-dihydroxybenzylimine 130b (100 mg, 0.36 mmol), methanol (10 mL) and sodium

cyanoborohydride (34.4 mg, 0.55 mmol). N-*(2-hydroxy-4-nitrophenyl)-2,3-dihydroxybenzylimine* **130b'** was isolated as a colourless oil (93.9 mg, 94%); [HPLC-MS: m/z calculated for $C_{13}H_{13}N_2O_5$ $(M+H)^+$ 277.0824. Found 277.0857]; υ_{max}/cm^{-1} : 3310 (NH); δ_H/ppm (400 MHz; DMSO-d_6) 11.55 (1H, s, OH), 9.77 (1H, s, OH), 7.94 (1H, dd, J = 8.6, 2.5 Hz, Ar-H), 7.70 (1H, d, J = 2.5 Hz, Ar-H), 7.31 (1H, d, J = 8.6 Hz, Ar-H), 7.13 (3H, overlapping m, Ar-H), 6.96 (1H, s, NH) and 4.82 (2H, s, CH_2); δ_C/ppm (100 MHz; DMSO-d_6) 151.0, 145.0, 143.2, 140.5, 137.7, 125.6, 118.7, 118.6, 114.1, 113.1, 112.1 and 103.4 (Ar-C) and 41.6 (CH_2).

N-(2-hydroxy-4-nitrophenyl)-5-chloro-2-hydroxybenzylamine 130c'

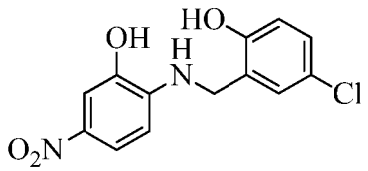

To the procedure described for **127'** using *N*-(2-hydroxy-4-nitrophenyl)-2-hydroxy-5-chlorobenzylimine **130c** (100 mg, 0.3 mmol), methanol (10 mL) and sodium cyanoborohydride (32.2 mg, 0.5 mmol). N-*(2-hydroxy-4-nitrophenyl)-5-chloro-2-hydroxybenzylamine* **130e'** was isolated as a yellow solid (64.8 mg, 73.3%); m.p. 110-116 °C [HPLC-MS: m/z calculated for $C_{13}H_{12}ClN_2O_4$ $(M+H)^+$ 295.0485. Found 295.0493]; υ_{max}/cm^{-1}: 3313 (NH); δ_H/ppm (400 MHz; DMSO-d_6) 10.01 (1H, s, OH), 7.43 (1H, dd, J = 8.6, 2.7 Hz, Ar-H), 7.15 (1H, overlapping m, Ar-H), 7.08 (1H, dd, J = 8.6, 2.7 Hz, Ar-H), 6.85 (1H, d, J = 8.6 Hz, Ar-H), 6.80 (1H, d, J = 8.6 Hz, Ar-H), 5.97 (1H, s, OH) and 4.29 (2H, s, CH_2); δ_C/ppm (100 MHz; DMSO-d_6) 154.0, 151.1, 140.5, 137.4, 127.5, 127.4, 127.4, 122.5, 116.5, 113.3, 112.3, 103.2 (Ar-C) and 40.5 (CH_2).

N-(3,4-difluorophenyl)-2,3-dihydroxybenzylamine 130e'

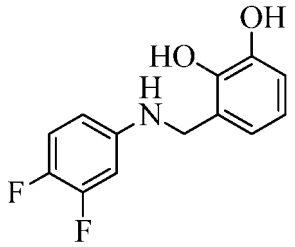

To the procedure described for **127'** using *N*-(3,4-difluorophenyl)-2,3-dihydroxybenzylimine **130e** (100 mg, 0.4 mmol), methanol (10 mL) and sodium cyanoborohydride (37.8 mg, 0.6 mmol). N-*(3,4-difluorophenyl)-2,3-dihydroxybenzylamine* **130e'** was isolated as a colourless oil (70.3 mg, 70%); [HPLC-MS: m/z calculated for $C_{13}H_{12}F_2NO_2$ $(M+H)^+$ 252.0836. Found 251.9935]; υ_{max}/cm^{-1}: 3201 (NH); δ_H/ppm (400 MHz; DMSO-d_6) 7.08 (1H, ddd, J = 19.9, 9.3, 5.0 Hz, Ar-H), 6.66 (1H, t, J = 7.0 Hz, Ar-H), 6.57 (1H, d, J = 7.7 Hz, Ar-H), 6.55 – 6.40 (2H, overlapping m, Ar-H), 6.39 – 6.33 (1H, m, Ar-H) and 4.12 (2H, d, J = 11.9 Hz, CH_2); δ_C/ppm (100 MHz; DMSO-d_6) 172.06 – 171.94 (m), 151.18 – 150.95 (m), 149.66 – 149.36 (m), 144.94 (s), 143.13 (s), 125.71 (s), 118.90 (s), 118.69 (s), 117.9-117.5 (m), 114.00 (s), 108.0 (dd, $^1J_{C,F}$ = 3.3, $^2J_{C,F}$ = 2.1) and 100.4 (d $J_{C,F}$ = 1.5) [Ar-C] and 41.9 (CH_2).

N-(3,4-difluorophenyl)-3,5-dichloro-2-hydroxylbenzylamine 130g'

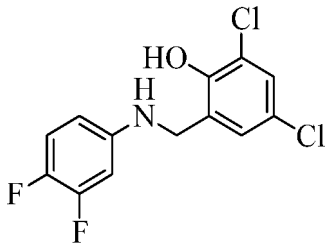

To the procedure described for **127'** using *N*-(3,4-difluorophenyl)-2-hydroxy-3,5-dichlorobenzylimine **130g** (100 mg, 0.3 mmol), methanol (10 mL) and sodium cyanoborohydride (31.2 mg, 0.5 mmol). N-*(3,4-difluorophenyl)-3,5-dichloro-2-hydroxybenzylamine* **130g'** was isolated as a colourless oil (76 mg, 83%); [HPLC-MS: m/z calculated for $C_{13}H_{10}Cl_2F_2NO$ $(M+H)^+$ 304.0107. Found 304.0140]; υ_{max}/cm^{-1} : 3316 (N-H); δ_H/ppm (400 MHz; DMSO-d_6) 7.35 (d, J = 2.6 Hz, 1H), 7.15 (d, J = 2.6 Hz, 1H), 7.08 (dd, J = 19.9, 9.3 Hz, 1H), 6.51 (ddd, J = 13.6, 6.9, 2.8 Hz, 1H), 6.32 (dd, J = 5.1, 3.9 Hz, 1H) and 4.23 (s, 2H); δ_C/ppm (100 MHz; DMSO-d_6) 150.05 (N=C-H), 149.98 (dd, $^1J_{C,F}$ = 241.3, $^2J_{C,F}$ = 13.2 Hz), 145.92 (dd, $^1J_{C,F}$ = 9.1, $^2J_{C,F}$ = 1.3 Hz), 141.23 (dd, $^1J_{C,F}$ = 232.1, $^2J_{C,F}$ = 12.8 Hz), 130.7, 127.1, 126.4, 123.0, 121.9, 117.5 (d, $J_{C,F}$ = 16.3 Hz), 107.7 (dd, $^1J_{C,F}$ = 5.4, $^2J_{C,F}$ = 2.7 Hz) and 100.3 (d, $J_{C,F}$ = 20.5 Hz) [Ar-C] and 41.9 (CH_2).

N-(3,4-difluorophenyl)-5-chloro-2-hydroxybenzylamine 130i'

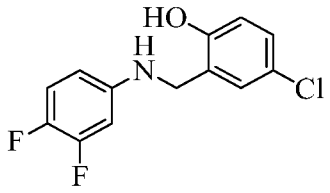

To the procedure described for **127'** using *N*-(3,4-difluorophenyl)-2-hydroxy-5-chlorobenzylimine **130i** (100 mg, 0.4 mmol), methanol (10 mL) and sodium cyanoborohydride (35.3 mg, 0.6 mmol). N-*(3,4-difluorophenyl)-5-chloro-2-hydroxybenzylamine* **130i'** was isolated as a white solid (75.5 mg, 70%); m.p. 68-70 °C [HPLC-MS: m/z calculated for $C_{13}H_{11}ClF_2NO$ $(M+H)^+$ 270.0497. Found 270.0532]; υ_{max}/cm^{-1}: 3249 (NH); δ_H/ppm (400 MHz; DMSO-d_6) 9.89 (s, OH), 7.16 (1H, d, J = 2.6 Hz, Ar-H), 7.12 – 7.04 (2H, overlapping multiplets, Ar-H), 6.83 (1H, d, J = 8.6 Hz, Ar-H), 6.54 – 6.47 (1H, m, Ar-H), 6.31 (2H, overlapping m, Hz, Ar-H and NH) and 4.13 (2H, d, J = 6.1 Hz, CH_2); δ_C/ppm (100 MHz; DMSO-d_6) 154.4 (N=C-H), 146.6 (dd, $J_{C,F}$ = 9.1, 1.3 Hz), 128.1, 128.1, 127.8, 127.8, 122.9, 117.9 (d, $J_{C,F}$ = 17.4 Hz), 117.0, 116.98, 108.1 (dd, $^1J_{C,F}$ = 5.4, $^2J_{C,F}$ = 2.7 Hz) and 100.5 (d, $J_{C,F}$ = 20.4 Hz) [Ar-C] and 61.6 (d, J = 5.3 Hz CH_2).

_N_-(2-hydroxy-4-nitrophenyl)-3-bromo-5-chloro-2-hydroxybenzylamine 130j'

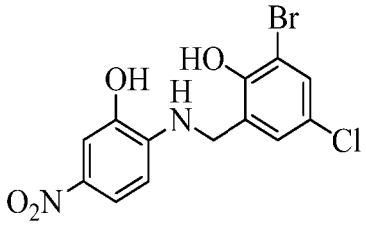

To the procedure described for **127'** using *N*-(2-hydroxy-4-nitrophenyl)-2-hydroxy-3-bromo-5-chlorobenzylimine **130j** (100 mg, 0.3 mmol), methanol (10 mL) and sodium cyanoborohydride (25.4 mg, 0.4 mmol). N-*(2-hydroxy-4-nitrophenyl)-3-bromo-5-chloro-2-hydroxybenzylamine* **130j'** was isolated as a yellow solid (74.7 mg, 66%); m.p. 138-140 °C [HPLC-MS: m/z calculated for $C_{13}H_{11}Br_2ClN_2O_4$ $(MH+2)^+$ 374.9590. Found 374.9633]; υ_{max}/cm^{-1}:3316 (NH); 138-140 °C δ_H/ppm (400 MHz; DMSO-d_6) 11.11 (1H, s, OH), 9.69 (1H, s, OH), 7.50 (1H, d, J = 2.5 Hz, Ar-H), 7.46 (1H, dd, J = 8.6, 2.7 Hz, Ar-H), 7.16 (1H, d, J = 2.5 Hz, Ar-H), 7.09 (1H, d, J = 2.7 Hz, Ar-H), 6.82 (1H, d, J = 8.6 Hz, Ar-H), 6.04 (1H, s, NH) and 4.39 (2H, s, CH_2); δ_C/ppm (100 MHz; DMSO-d_6) 151.1, 150.6, 140.4, 137.1, 130.2, 130.1, 126.7, 123.9, 113.5, 112.4, 111.9, 103.3 (Ar-C) and 41.6 (CH_2).

***N*-(2-hydroxy-4-nitrophenyl)-3,5-dichloro-2-hydroxybenzylamine 130k'**

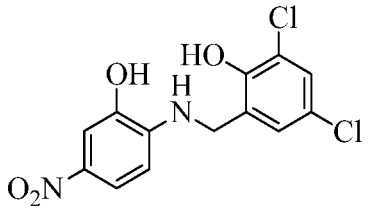

To the procedure described for **127'** using *N*-(2-hydroxy-4-nitrophenyl)-3,5-dichloro-2-hydroxybenzylimine **130k** (100 mg, 0.3 mmol), methanol (10 mL) and sodium cyanoborohydride (28.8 mg, 0.5 mmol). N-*(2-hydroxy-4-nitrophenyl)-3,5-dichloro-2-hydroxybenzylamine* **130k'** was isolated as a yellow solid (75.7 mg, 77%); m.p. 140-142 °C [HPLC-MS: m/z calculated for $C_{13}H_{11}Cl_2N_2O_4$ $(M+H)^+$ 329.0096. Found 329.0127]; υ_{max}/cm^{-1}: 3245 (NH); δ_H/ppm (400 MHz; DMSO-d_6) 11.11 (1H, s, O-H), 9.83 (1H, s, OH), 7.46 (1H, dd, J = 8.6, 2.7 Hz, Ar-H), 7.38 (1H, d, J = 2.6 Hz, Ar-H), 7.13 (1H, d, J = 2.6 Hz, Ar-H), 7.09 (1H, d, J = 2.7 Hz, Ar-H), 6.82 (1H, d, J = 8.6 Hz, Ar-H), 6.03 (1H, s, NH) and 4.38 (2H, s, CH_2); δ_C/ppm (100 MHz; DMSO-d_6) 151.1, 149.6, 140.5, 137.1, 130.3, 127.2, 126.2, 123.3 , 121.7, 113.5, 112.4 and 103.2 (Ar-C) and 41.3 (CH_2).

3.11. SYNTHESIS OF *N*-(3,4-DIFLUOROBENZYL-2-HYDROXYBENZYLIMINES 133a-e.

***N*-(3,4-difluorobenzyl)-2-hydroxy-5-nitrobenzylimine 133a**

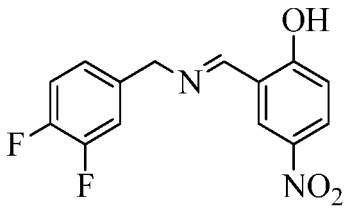

In a round bottom flask equipped with a stirrer, a methanolic solution (20 ml) of 3,4-difluorobenzylamine (0.2 ml, 1.7 mmol) and 2-hydroxy-5-nitrobenzaldehyde was added glacial acetic acid (2 drops) and the resulting solution was stirred at room temperature while the reaction progress was monitored by thing layer chromatography. At the completion of the reaction, the crude mixture was diluted with hexane (50 mL), the precipitate was filtered and washed with hexane (3 × 40 mL). N-*(3,4-difluorobenzyl)-2-hydroxy-5-nitrobenzylimine* **133a**

was isolated as yellow a solid (476.9 mg, 96%); m.p. 130-132 °C [HPLC-MS: m/z calculated for $C_{14}H_{11}F_2N_2O_3$ $[M+H]^+$ 293.0659. Found 293.0732]; υ_{max}/cm^{-1} : 3071 (OH), 1646 (C=N); δ_H/ppm (400 MHz; DMSO-*d*6) 8.67 (1H, s, N=C-H), 7.76 (1H, d, *J* = 2.6 Hz, Ar-H), 7.56 (1H, d, *J* = 2.6 Hz, Ar-H), 7.54 – 7.35 (3H, m, Ar-H), 7.28 – 7.21 (1H, m, Ar-H) and 4.84 (2H, s, CH_2); δ_C/ppm (100 MHz; DMSO-*d*6) 166.0 (N=C-H), 160.8, 135.3, 135.1 (dd, $^2J_{C,F}$ = 5.9, $^2J_{C,F}$ = 3.9 Hz), 131.0, 125.0 (dd, $^2J_{C,Fu}$ = 6.6, $^3J_{C,F}$ = 3.4 Hz), 119.7, 118.1, 117.9, 117.7, 117.4, 117.3 and 113.3 [Ar-C] and 57.8 (CH_2).

_N_-(3,4-difluorobenzyl)-3-bromo-5-chloro-2-hydroxybenzylimine 133b

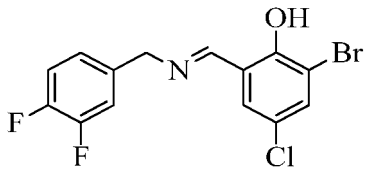

The procedure described for the synthesis of **133a** was followed using 3,4-difluorobenzylamine (0.2 ml, 1.7 mmol), 3-bromo-5-chlorosalicyaldehyde (1.7 mmol), methanol (20 mL) and glacial acetic acid (two drops). N-*(3,4-difluorobenzyl)-3-bromo-5-chloro-2-hydroxybenzylimine* **133b** was isolated as a yellow solid (564.0 mg, 92%); m.p. 110-112 °C [HPLC-MS: m/z calculated for $C_{14}H_{10}BrClF_2NO$ $(MH+2)^+$ 361.9602. Found 361.8230]; υ_{max}/cm^{-1}: 3100 (OH), 1629 (C=N); δ_H/ppm (400 MHz; DMSO-*d*6) 14.34 (1H, s, OH), 8.86 (1H, s, N=C-*H*), 8.47 (1H, d, *J* = 2.8 Hz, Ar-H), 8.09 (1H, dd, *J* = 9.5, 2.8 Hz, Ar-H), 7.50 (1H, dt, *J* = 19.2, 8.8 Hz, Ar-H), 7.28 (1H. s, Ar-H), 6.75 (1H, d, *J* = 9.5 Hz, Ar-H) and 4.86 (s, 2H, C*H*2). δ_C/ppm (100 MHz; DMSO-*d*6) 174.1 (N=*C*-H), 167.0, 135.6, 134.3 (dd, $^2J_{C,F}$ = 5.7, $^2J_{C,F}$ = 3.8 Hz), 131.3, 129.0, 125.3 (dd, ^1J = 6.7, $^2J_{C,F}$ = 3.5 Hz), 121.3, 118.0, 117.9, 117.7, 117.5 and 115.1 [Ar-C] and 56.2 (CH_2).

_N_-(3,4-difluorobenzyl)-2,3,4-trihydroxybenzylimine 133c

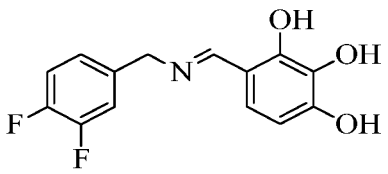

The procedure described for the synthesis of **133a** was followed using 3,4-difluorobenzylamine (0.2 ml, 1.7 mmol), 2,3,4-trihydroxybenzaldehyde (1.7 mmol), methanol (20 mL) and glacial acetic acid (two drops). N-*(3,4-difluorobenzyl)-2,3,4-trihydroxybenzylimine* **133c** was isolated as a yellow solid (408.3 mg, 86%); m.p. 190-192 °C

[HPLC-MS: m/z calculated for $C_{14}H_{12}BrF_2NO_3$ $(M+H)^+$ 280.0785. Found 280.0865]; υ_{max}/cm^{-1}: 3054 (OH), 1626 (C=N); δ_H/ppm (400 MHz; DMSO-d_6) 8.46 (1H, s, N=C-*H*), 7.50 – 7.37 (2H, m, Ar-H), 7.20 (1H, dddd, J = 8.5, 4.3, 2.0, 1.4 Hz, Ar-H), 6.74 (1H, d, J = 8.6 Hz, Ar-H), 6.29 (1H, d, J = 8.5 Hz, Ar-H) and 4.72 (2H, s, CH_2); δ_C/ppm (100 MHz; DMSO-d_6) 166.4 (N=*C*-H), 154.0, 150.3 (dd, $^2J_{C,F}$ = 75.2, $^2J_{C,F}$ = 12.7 Hz), 149.2, 147.8 (dd, J = 74.2, 12.5 Hz), 136.7 (dd, $^1J_{C,F}$ = 5.6, $^2J_{C,F}$ = 3.7 Hz), 132.6, 124.5 (dd, $J_{C,F}$ = 6.5, 3.4 Hz), 123.0, 117.6 (d, $J_{C,F}$ = 17.0 Hz), 116.8 (d, $J_{C,F}$ = 17.2 Hz), 111.2 and 107.1 [Ar-C] and 58.8 (CH_2).

_N_-(3,4-difluorobenzyl)-2,3-dihydroxybenzylimine 133d

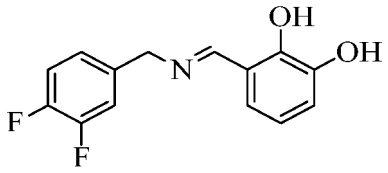

The procedure described for the synthesis of **133a** was followed using 3,4-difluorobenzylamine (0.2 ml, 1.7 mmol), 3,4-dihydroxybenzaldehyde (1.7 mmol), methanol (20 mL) and glacial acetic acid (two drops). N-*(3,4-difluorobenzyl)-2,3-dihydroxybenzylimine* **133d** was isolated as a yellow solid (402.8 mg, 90%); m.p. 88-90 °C [HPLC-MS: m/z calculated for $C_{14}H_{12}F_2NO_2$ $(M+H)^+$ 264.0836. Found 264.0754]; υ_{max}/cm^{-1}: 3268 (OH), 1632 (C=N); δ_H/ppm (400 MHz; DMSO-d_6) 8.64 (1H, s, N=C-*H*), 7.49 – 7.36 (2H, m, Ar-H), 7.23 – 7.17 (1H, m, Ar-H), 6.95 – 6.85 (2H, m, Ar-H), 6.69 (1H, t, J = 7.7 Hz, Ar-H) and 4.79 (2H, s, CH_2) ; δ_C/ppm (100 MHz; DMSO-d_6) 172.4 (N=*C*-H), 167.3, 150.4, 147.5 (dd, $^1J_{C,F}$ = 54.8, $^2J_{C,F}$ = 12.6), 146.0, 124.6 (dd, $^1J_{C,F}$ = 6.4, $^2J_{C,F}$ = 3.2 Hz), 122.0, 118.6, 118.13, 118.10, 117.7, 117.5 and 116.9 (d, $^1J_{C,F}$ = 17.4) [Ar-C] and 60.2 (CH_2).

_N_-(3,4-difluorobenzyl)-3,5-dichloro-2-hydroxybenzylimine 133e

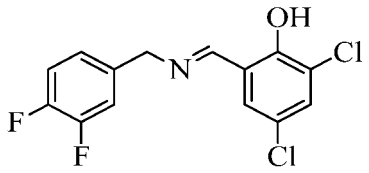

The procedure described for the synthesis of **133a** was followed using 3,4-difluorobenzylamine (0.2 ml, 1.7 mmol), 3,5-dichlorosalicyaldehyde (1.7 mmol), methanol (20 mL) and glacial acetic acid (two drops). N-*(3,4-difluorobenzyl)-3,5-dichloro-2-hydroxybenzylimine* **133e** was isolated as a yellow solid (503.03 mg, 93.6%); m.p. 120-122 °C [HPLC-MS: m/z calculated for $C_{14}H_{10}Cl_2F_2NO$ $(M+H)^+$ 316.0107. Found 316.0174]; υ_{max}/cm^{-1}: 3090 (OH), 1630 (C=N); δ_H/ppm (400 MHz; DMSO-d_6) 14.60 (1H, s, OH), 8.69

(1H, s, N=C-H), 7.62 (1H, d, J = 2.6 Hz, Ar-H), 7.52 (1H, d, J = 2.6 Hz, Ar-H), 7.47 (2H, ddd, J = 17.1, 8.0, 5.4 Hz, Ar-H), 7.23 (1H, s, Ar-H) and 4.84 (2H, s, CH_2); δ_C/ppm (100 MHz; DMSO-d_6) 166.5 (N=*C*-H), 160.6 – 160.0 (m), 135.5 (dd, $^1J_{C,F}$ = 5.2, $^2J_{C,F}$ = 2.1 Hz), 133.0 (d, $J_{C,F}$ = 5.9 Hz), 130.7 (d, $J_{C,F}$ = 5.4 Hz), 125.4 (dd, $^1J_{C,F}$ = 6.7, $^2J_{C,F}$ = 4.0 Hz), 123.7 – 123.3 (m), 120.0 (d, $J_{C,F}$ = 5.5 Hz), 118.8 (d, $J_{C,F}$ = 4.4 Hz), 118.3 (d, $J_{C,F}$ = 5.9 Hz), 118.1 (d, $J_{C,F}$ = 5.6 Hz), 117.8 (d, $J_{C,F}$ = 5.8 Hz) and 117.6 (d, $J_{C,F}$ = 6.0 Hz) [Ar-C] and 58.32 (CH_2).

3.12. PROCEDURE FOR THE SYNTHESIS OF (±)-*TRANS-N,N'*-BIS[2-HYDROXYPHENYLIMINO)CYCLOHEXANES 135a-c.

(±)-*Trans-N,N'*-bis(3-chloro-2-hydroxyphenylimino)cyclohexane 135a

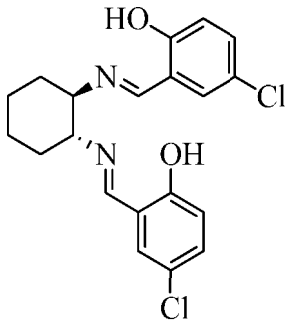

The procedure described for the synthesis of **133a** was followed using (±)-*trans*-1,2-diaminocyclohexane (0.1 ml, 0.83 mmol), 5-chlorosalicylaldehyde (1.66 mmol), methanol (20 mL) and glacial acetic acid (two drops). *(±)-trans-1,2-bis(3-chloro-2-hydroxyphenylimino)-cyclohexane* **135a** was isolated as a yellow solid (289.1 mg, 89%); m.p. 150-152 °C [HPLC-MS: m/z calculated for $C_{20}H_{21}Cl_2N_2O_2$ $(M+H)^+$ 391.0980. Found 391.0886]; υ_{max}/cm^{-1}: 2907 (OH), 1631 (C=N); δ_H/ppm (400 MHz; $CDCl_3$) 13.18 (2H, s, OH), 8.18 (2H, s, N=C-*H*), 7.19 (2H, dd, J = 8.8, 2.6 Hz, Ar-H), 7.12 (2H, d, J = 2.6 Hz, Ar-H), 6.84 (2H, d, J = 8.8 Hz, Ar-H), 3.37 – 3.29 (2H, m, N*CH* x 2), 1.92 (4H, t, J = 14.8 Hz, CH_2 x 2), 1.72 (2H, dd, J = 22.1, 11.2 Hz, CH_2) and 1.48 (2H, t, J = 9.8 Hz, CH_2); δ_C/ppm (100 MHz; $CDCl_3$) 163.7 (N=C-H), 159.6, 132.3, 130.7, 123.4, 119.4 and 118.6 (Ar-C), 72.8 (N*C*H), 33.1 and 24.2 (*C*H_2).

(±)-*Trans*-1,2-bis(2-hydroxy-3-methoxyphenylimino)cyclohexane 135b

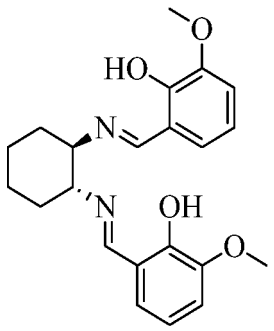

The procedure described for the synthesis of **133a** was followed using (±)-*trans*-1,2-diaminocyclohexane (0.1 ml, 0.8 mmol), 2-methoxylsalicylaldehyde (1.7 mmol), methanol (20 mL) and glacial acetic acid (two drops). *(±)-Trans-1,2-bis(2-hydroxy-3-methoxyphenylimino)cyclohexane* **135b** was isolated as a yellow solid(292.0 mg, 92%); m.p 140-142 °C [HPLC-MS: m/z calculated for $C_{22}H_{27}N_2O_4$ $(M+H)^+$ 383.1971. Found 383.2004]; υ_{max}/cm^{-1}: 2938 (OH), 1624 (C=N); δ_H/ppm (300 MHz; $CDCl_3$) 13.82 (2H, s, OH x 2), 8.25 (2H, s, N=C-*H* x 2), 6.85 (2H, dd, *J* = 7.7, 1.8 Hz, Ar-H), 6.78 (2H, dd, *J* = 7.8, 1.8 Hz, Ar-H), 6.71 (2H, t, *J* = 7.7 Hz, Ar-H), 3.86 (6H, s, O-CH_3 x 2), 3.31 (2H, dd, *J* = 5.6, 3.8 Hz, NCH x 2), 1.90 (4H, ddd, *J* = 15.9, 13.4, 6.1 Hz, CH_2 x 2), 1.78 – 1.64 (2H, m, CH_2), 1.55 – 1.43 (2H, m, CH_2); δ_C/ppm (75 MHz; $CDCl_3$) 164.9 (N=C-H), 151.7, 148.4, 123.3, 118.5, 118.0 and 114.0 (Ar-C), 72.5 (OCH_3), 56. 1 (NCH), 33.1 (CH_2) and 24.2 (CH_2).

(±)-*Trans*-1,2-bis(3-bromo-5-chloro-2-hydroxyphenylimino)cyclohexane 135c

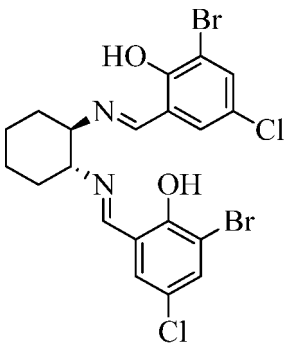

The procedure described for the synthesis of **133a** was followed using (±)-*trans*-1,2-diaminocyclohexane (0.1 ml, 0.8 mmol), 3-bromo-5-chlorosalicylaldehyde (1.7 mmol),

methanol (20 mL) and glacial acetic acid (two drops). *(±)-Trans-1,2-bis(3-bromo-5-chloro-2-hydroxyphenylimino)cyclohexane* **135c** was isolated as a yellow solid (413.4 mg, 90.7%); m.p. 198-200 °C [HPLC-MS: m/z calculated for $C_{20}H_{19}Br_2Cl_2N_2O_2$ $(M+H)^+$ 546.9190. Found 546.9150]; υ_{max}/cm^{-1}: 2944 (OH), 1626 (C=N); δ_H/ppm (400 MHz; $CDCl_3$) δ 14.31 (2H, s, OH), 8.15 (2H, s, N=C-*H*), 7.51 (2H, d, *J* = 2.5 Hz, Ar-H), 7.12 (2H, d, *J* = 2.5 Hz, Ar-H), 3.40 – 3.31 (2H, m, NC*H* x 2), 1.92 (4H, t, *J* = 14.3 Hz, C*H*$_2$ x 2), 1.69 (2H, dd, *J* = 21.6, 11.5 Hz, C*H*$_2$), 1.46 (2H, t, *J* = 10.1 Hz, CH_2); δ_C/ppm (100 MHz; $CDCl_3$) 163.4, 157.4, 135.3, 130.1, 123.4, 119.1 and 111.8 (Ar-C), 72.2 (N*C*H), 33.0 (*C*H_2) and 24.0 (*C*H_2).

4. REFERENCE

1. Stuart, H. The Protista. *Essential Microbiology*; John Wiley & Sons, Ltd: West Sussex, England, 2005. pp 224-226.
2. Centre for Disease Control and Prevention. About Parasites: Protozoa. https://www.cdc.gov/parasites/about.html. (Accessed July 4, 2017).
3. Encyclopaedia Britannica. Protozoan Microorganism. https://www.britannica.com/science/protozoan. (Accessed July 4, 2017).
4. World Health Organization Report, 2017. Trypanosomiasis, human African (sleeping sickness). http://www.who.int/mediacentre/factsheets/fs259/en/. (Accessed March 15, 2017).
5. Steverding, D. The history of African Trypanosomiasis. *Parasit. Vectors.* ***2008****, 1, 1-8.*
6. World Health Organization. Human African trypanosomiasis. The history of sleeping sickness. http://www.who.int/trypanosomiasis_african/country/history/en/index6.html. (Accessed March 15, 2017).
7. Centre for Disease Control and Prevention. Parasites- African Trypanosomiasis (also known as sleeping sickness): Causal Agents. https://www.cdc.gov/parasites/sleepingsickness/biology.html. (Accessed March, 22, 2017).
8. Matthews, K. R. *J.Cell Sci.* **2005**, 15, 283-290.
9. Jatin M. Vyas. New York Times, 2010, http://www.nytimes.com/health/guides/disease/sleeping-sickness/overview.html. (Accessed August, 1, 2017).
10. U. S. National Library of Medicine. Sleeping Sickness. https://medlineplus.gov/ency/article/001362.htm. (Accessed August 1, 2017).
11. World Health Organization. Trypanosomiasis, human African (sleeping sickness): Fact sheets. http://www.who.int/mediacentre/factsheets/fs259/en/. (Accessed August 1, 2017).
12. Simarro, P. P.; Diarra A.; Postigo, J. A. R.; Franco, J. R.; Jannin, J. G. *PLoS Negl. Trop. Dis.* **2011**, 5, 1-7.
13. Headrick, D. R. *PLoS Negl. Trop. Dis.* **2014**, 8, 1-8.

14. Brein, A.; Todd, J. L. *BMJ*. **1907**, 132-134.
15. Wilkinson, S. R.; Kelly, J. M. Trypanocidal drugs: mechanisms, resistance and new targets. *Expert Rev. Mol. Med.*, **2009**, 11: e31, doi: 10.1017/S1462399409001252.
16. Boibessot, C. M. R.; Turner, D. G.; Watson, E.; Goldie, G.; Connel, A.; McIntosh, M. H.; Grant, G. G.; Skellern. *ActaTropica*. **2002**, 84, 219-228.
17. Ndoutamia, G.; Moloo, S. K.; Murphy, N. B.; Peregrine, A. S. *Antimicrob. Agents Chemother*. **1993**, 37, 1163-1166.
18. Ranjithkumar, M.; Saravanan, B. C.; Yadav, S. C.; Kumar, R.; Singh, R.; Dey, S. *Trop. Anim. Health Prod.* **2014**, 46, 371-377.
19. Vincent, I. M.; Creek, D.; David, G.; Watson, D. G.; Kamleh, M. A.; Debra, J.; Woods, D. J.; Wong, P. E.; Burchmore, R. J. S.; Michael, P.; Barrett, M. P. *PLoS Pathog*. **2010**, 6, 1-9.
20. Fairlamb, A. H. *Trends in Parasitol*. **2003**, 19, 488-494.
21. Mungube, E. O.; Vitouley, H. S.; Allegye-Cudjoe, E.; Diall, O.; Boucoum, Z.; Diarra, B.; Sanogo, Y.; Randolph, T.; Bauer, B.; Karl-Hans, Z.; Peter-Henning, C. *Parasit. Vectors*. **2015**, 5, 1-9.
22. Plouffe, D. M.; Wree, M.; Du, A. Y.; Meister, S.; Li, F.; Patra, K.; Lubar, A.; Okitsu, S. L.; Flannery, E. L.; Kato, K.; Tanaseichuk, O.; Comer, E.; Zhou, B.; Kuhen, K;, Zhou, Y.; Leroy, D.; Schreiber, S. L.; Scherer, C. A.; Vinetz, J.; Winzeler, E. A. *Cell Host Microbe. **2016**, 19, 114-126.*
23. Stuart, H. The Protista. *Essential Microbiology*; John Wiley & Sons, Ltd: West Sussex, England, 2005. Pp 229-230.
24. David Sullivan. Malariology Overview-History, Life cycle, Epidemiology, Pathology and Control. Johns Hopkins Bloomberge School of Public Health. http://ocw.jhsph.edu/courses/Malariology/PDFs/lecture1.pdf. (Accessed September 29, 2017).
25. Centre for Disease Control and Prevention. The History of Malaria, an Ancient Disease. https://www.cdc.gov/malaria/about/history/. (Accessed March 15, 2017)
26. Centres for Disease Control and Prevention. Biology. https://www.cdc.gov/malaria/about/biology/ (Accessed March 15, 2017).
27. Medicines for Malaria Venture. Parasite lifecycle. http://www.mmv.org/malaria-medicines/parasite-lifecycle. (Accessed March 15, 2017).
28. Haemers, T. *Synthesis and evaluation of fosmidomycin analogues as antimalarial agents*. A Ph.D. Dissertation; Gent University, Netherlands, 2007.

29. Garcia-Basteiro, A. L.; Basat, Q.; Alonso, P. L. *Mediterr J Hematol Infect Dis.* **2012**, 4, 1-13.
30. Hill, A. V. S. *Philos. Trans. R. Soc. Lond. B Biol. Sci.*, **2011**, 366, 2806-2814.
31. Hovlid, M. L.; Winzeler, E. A. *Trends Parasitol.*, **2016**, 32, 697-707.
32. John Hopkins Bloomberg School of Public Health. Malaria epidemiology. http://ocw.jhsph.edu/courses/Malariology/PDFs/lecture3.pdf. (Assessed April 6, 2017)
33. Newby, G.; Bennett, A.; Larson, E.; Cotter, C.; Shretta, R.; Phillips, A. A.; Feachem, R. G. A. *Lancet*. **2016**. 387, 1775-1784.
34. Max Roser. Our World in Data: Malaria. https://ourworldindata.org/malaria/. (Accessed August 5, 2017).
35. (a)The World Bank. World Development Report, 2009. http://siteresources.worldbank.org/INTWDRS/Resources/47736513275253473 07/8392086-1327528510568/WDR09_bookweb_1.pdf. (Accessed August 5, 2017). (b) Hay, S. I.; Snow, R. W. *PLoS Med.* **2006**, 3(12), 1-5. (c) Guerra, C. A.; Gikandi, P.W.; Tatem, A. J.; Noor, A. M.; Smith, D. L.; Hay, S. I.; Snow, R. W. *PLoS Med.* **2008**, 5(2), 300-311. (d) Hay, S. I.; Guerra, C. A.; Gething, P. W.; Patil, A. P.; Tatem, A, J.; Abdisalan, M.; Noor, A. M.; Kabaria, C. W.; Manh, B. H.; Elyazar, I. R . F.; Brooke, S.; Smith, D. L.; Moyeed, R. A.; Snow, R. W. *PLoS Med.* **2009**, 6(3), 286-302.
36. Bartoloni, A.; Zammarchi, L. *Mediterr. J. Hematol. Infect Dis.* 2012, 4, 1-10.
37. Centre for Disease Control and Prevention. Disease. https://www.cdc.gov/malaria/about/disease.html. (Accessed *August 5, 2017*).
38. *Annemarie Ryu. We eradicated smallpox, so why not malaria? Harvard college of global health review. 2010. https://hcghr.wordpress.com/2010/01/13/we-eradicated-smallpox-so-why-not-malaria/. (Accessed August 4, 2017).*
39. *Dichlorodiphenyltrichloroethane.* http://chem11ddt.weebly.com/benefits-and-disadvantages-to-ddt.html. *(Accessed August 4, 2017).*
40. Preserved articles. DDT has several drawbacks and environmental impact.as follows. http://www.preservearticles.com/2012030625225/ddt-has-several-drawbacks-and-environmental-impactas-follows.html. (Accessed August 4, 2017).
41. United for Sight. Eradication Efforts: Malaria vs Smallpox. http://www.uniteforsight.org/global-health-history/module4. (Accessed August 4, 2017).

42. Africa Fighting Malaria. The benefits and risks in the use of DDT. http://www.fightingmalaria.org/news/638.html. (Accessed August 4, 2017).
43. World Health Organization. WHO called to return to the Declaration of Alma-Ata. http://www.who.int/social_determinants/tools/multimedia/alma_ata/en/. (Accessed August 4, 2017).
44. Bill & Melinda Gates Foundation. Gates Foundation Commits More than $500 Million to Tackle Burden of Infectious Diseases in Developing Countries. 2014. https://www.gatesfoundation.org/Media-Center/Press-Releases/2014/11/ASTMH-Address. (Accessed August 4, 2017).
45. Alonso, P. L.; Brown, G.; Arevalo-Herrera, M.; Binka, F.; Chitnis, C.; Collins, F.; Doumbo, O. K.; Greenwood, B.; Hall, B. F.; Levine, M. M.; Mendis, K.; Newman, R. D.; Plowe, C. V.; Rodrı´guez, M. H.; Sinden, R.; Slutsker, L.; Tanner, M. *PLoS Med.* **2011**, 8(1), 1-99.
46. Marcel, T.; Brian, G.; Whitty, C. J. M.; Ansah, E. K.; Price, R. N.; Dondorp, A. M.; Seidlein, L.V.; Baird, J. K.; Beeson J. G.; Freya, J.I.; Hemingway, F. J.; Kevin, M.; Faith, O. *BioMed Center*. **2015**, 13(167), 2-22.
47. Bruce-Chwatt, L. J. *Bull. World Health Organ.* **1962**, 27(2), 287-290.
48. John McMurry. Organic Chemistry. **2015**. Ninth edition. Cengage learning, Boston, United States. pp 468.
49. Antimalaria quinolones. https://www.drugs.com/drug-class/antimalarial-quinolines.html. (Accessed May 4, 2017).
50. Foley, M.; Tille, L. *Pharmacol. Ther.* **1998**, 79(1), 55-87.
51. O'PJeill, P. M.; Bray, P. G.; Hawley, S. R.; Ward, S. A.; Park, B. K. *Pharmacol. Ther.* **1998**, 77(1), 29-58.
52. Achan, J.; Talisuna, A. O.; Erhart, A.; Yeka, A.; Tibenderana, J. K.; Baliraine, F. N.; Rosenthal, P. J.; D'Alessandro, U. *Malar. J.* **2011**. 10:144. 1-12.
53. Yadav, N.; Sharma, C.; Awashi, S. K. *RSC. Adv.* **2014**, 4, 5469.
54. Deshpande, S.; Kuppast, B. *Med. Chem.* **2016**, 6(1), 1-11.
55. Bray, P. G.; Ward, S. A; O'Neill, P.M. *Current Topics in Microbio. Immunol.* **2005**, 295, 338.
56. Homewood, C. A.; Warhurst, D. C.; Peters, W.; Baggaley, V. C. *Nature*, **1972,** 235, 50-52.
57. Diribe, C. O.; Warhurst, D. C. *Biochem. Pharmacol.* **1985**, 34, 3019-3027.

58. Shaun, R.; Hawley, Bray P. G.; Mungthin, M.; Atkinson J. D.; O'Neill P. M.; Ward S. A. *Antimicrob. Agents Chemother.* **1998**, 42, 682-686.
59. Verdier, F.; Bras, J. L.; Clavier, F.; Hatin, I.; Marie-Claude, B. C. *Antimicrob. Agents Chemother.* **1985**, 27, 561-564.
60. Roberts, L.; Egan, T. J.; Joiner, K. A.; Hoppe, H. C. *Antimicrob.l Agents Chemother.* **2008,** 52, 1840-1842.
61. Goldberg, D. E.; Slater, A. F. G. *Parasitology*. **1992**, 8, 280-283.
62. Sullivan, D. J. *Int. J. Parasitol.* **2002**, 32, 1645–1653.
63. Fitch, C. D. *Science*, 1**970**, 169, 289-290.
64. Pandeya, S. N.; Alka, T. *Int. j. pharm. pharm. Sci.* **2011**, 3, 53-61.
65. Reynolds K. A. Design and Synthesis of Quinoline, Cinchona Alkaloids and Other Potential Inhibitors of Leishmaniasis. PhD Thesis; Eskitis Institute for Cell and Molecular Therapies Science, Environment, Engineering and Technology, Griffith University, **2011**.
66. Zhang, L.; Zheng, L.; Guo, B.; Hua, R. *J. Org. Chem.* **2014**, 79, 11541-11548.
67. White, N. J.; Hien, T. T.; Nosten, F. H. *Trends Parasitol.* **201**5, 31, 607-609.
68. Das, A. K. *Ann. Med. Health Sci. Res.* **2015**, 5(2), 93-102.
69. Klayman, D. L.; Lin, A. J.; Action, N.; Scovill, J. P.; Hoch, J. M.; Milhous, W. K.; Theoharides, A. D. *J. Nat. Prod.* **1984**, 47, 715-717.
70. Meshnick, S. R. *Int. J. Parasitol.* **2002**, 32, 1655-1660.
71. Presser, A.; Feichtinger, *A. MONATSH CHEM.* **2017**, 148, 63-68.
72. Olliaro, P. L.; Haynes, R. K.; Meunier, B.; Yuthavong, Y. *Trends Parasitol.* **2001**, 17(3), 122-126.
73. O'Neill, P.M.; Posner, G.H. *J. Med. Chem.* **2004**, 47(12), 2945-2064.
74. Persico, M.; Quintavalla, A.; Rondinelli, F.; Trombini, C.; Lombardo, M.; Fattorusso, C.; Azzarito, V.; Taramelli, D.; Parapini, S.; Corbett, Y.; Chianese, G.; Fattorusso, E.; Taglialatela-Scafati, O. *J. Med. Chem.*. **2011,** 54, 8526-8540.
75. Hye-Sook, K.; Khurshida, B.; Naoki, O.; Yusuke, W.; Takahiro, T.; Araki, M.; Masatomo, N.; Kevin, J. M. *J. Med. Chem.* **2002**, 45, 4732-4736.
76. Constantino, M. G.; Beltrame Jr, M.; Jose da Silva, G. V. Synth. Commun. 1996, 26, 321-329.
77. Ellis, G. L.; Amewu, R.; Hall, C.; Rimmer, K.; Ward, S. A.; O'Neill, P. M. *Bioorganic Med. Chem. Lett.* **2008**, 18, 1720-1724.
78. Yuthavong, Y. *Microb. Infec.* **2002**, 4, 175-182.

79. Nzila, A.; Ward, S. A.; Marsh, K.; Sims, P. F. G.; Hyde, J. E. *Trends Parasitol.* **2005**, vol. 21, 292-298.
80. Nzila, A.; Ward, S. A.; Marsh, K.; Sims, P. F. G.; Hyde, J. E. *Trends Parasitol.* **2005**, vol. 21, 334-339.
81. Purcell, W.T.; Ettinger D. S. *Curr. Oncol. rep.* **2003**, 5, 114-125.
82. Gaillard, T.; Madamet, M.; Tsombeng, F.F.; Dormoi, J.; Pradines, B. *Malar. J.* **2016**, 15: 556, 1-10.
83. Collin, F.; Karkare, S.; Maxwell, A. *Appl. Microbiol. Biotechnol.* **2011**, 92, 479-497.
84. Charest, M. G.; Lerner, C.D.; Brubaker, J.D.; Siegel, D. R.; Myers, A. G. *Science.* **2005**, 308, 395-398.
85. Charest, M.G.; Dionicio, R.; Siegel, D. R.; Myers, A. G. *J. Am. Chem. Soc.* **2005**, 127, 8292-8293.
86. Krakauer, T.; Buckley, M. *Antimicrob. Agents Chemother.* **2003**, 47(11), 3630–3633.
87. Chopra, I; Roberts M. *Microbiol. Mol. Biol. Rev.* 2001, 65(2), 232-260.
88. Cai, G.; Deng, L.; Xue, J.; Moreno, S. N. J.; Striepen, B.; Song, Y. *Bioorganic Med. Chem. Lett.* **2013**, 23(7), 2158-2161.
89. Deng, L.; Endo, K.; Kato, M., Cheng, G.; Yajima, S.; Song, Y. *ACS Med. Chem. Lett.* **2011**, 2, 165-170.
90. Odoma, A. R.; Voorhis, W. C. V. *Mol. Biochem. parasitol.* **2010**. 170(2), 108-111.
91. Zhang, B.; Watts, K. M.; Hodge, D.; Kemp, L. M.; Hunstad, D A.; Hicks, L. M.; Odoma, A. R. *Biochem.* **2011**. 50, 3570-3577.
92. Nair, S. C.; Carrie, F.; Brooks, C. F.; Goodman, C. D.; Strurm, A.; McFadden, G. I.; Sundriyal, S.; Anglin, J.L.; Song, Y.; Moreno, S. N. J.; Striepen, B. *J. Exp. Med.* **2011**. 208, 1547-1559.
93. Masini, T.; Kroezan, B. S.; and Hirsch, A. K.; H. *Drug Discov. Today.* **2013**, 18, 1256-1262.
94. Bodill, T.; Conibear, A. C.; Blatch, G. L.; Lobb, K. A.; Kaye, P. T. *Bioorganic Med. Chem.* **2011**, 19, 1321-1327.
95. Na-Bangchang, K.; Ruengweerayut, R.; Karbwang, J.; Chauemung, A.; Hutchinson, D. *Malar. J.* **2007**,6, 1-10.
96. Lell, B.; Ruangweerayut, R.; Wiesner, J.; Missinou, M. A.; Schindler, A.; Baranek, T.; Hintz, M.; Hutchinson, D.; Jomaa, H.; Kremsner, P. G. *Antimicrob. Agent Chemother.* **2003**, 47, 735-738.

97. Jansson, A. M.; Więckowska, A.; Björkelid, C.; Yahiaoui S.; Sooriyaarachchi, S.; Lindh, M.; Bergfors, T.; Dharavath, S.; Desroses, M.; Suresh, S.; Andaloussi, M.; Nikhil, R.; Sreevalli, S.; Srinivasa, B. R.; Larhed, M.; Jones, T. A.; Karlen, A.; Mowbray, S. L. *J. Med. Chem.* **2013,** 56, 6190-6199.

98. Adeyemi, C. M.; Faridoon; Isaacs, M.; Mnkandhla, D.; Hoppe, H.; Krause, R. W. M.; Kaye, P. T. *Bioorganic Med. Chem.* **2016,** 24, 6231-6138

99. Rajeshwaran, G. G.; Nandakumar, M.; Sureshbabu, R.; Mohanakrishnan, A. K. *Org. Lett.* **2011**, 13, 1270-1273.

100. Zhao, Y.; Kappes, B.; Franklin, R. M. *The J. Biol. Chem.* **1993**, 268, 4347-4354.

101. Chapman, T. M.; Osborne, S. A.; Bouloc, N.; Large, J. M.; Wallace, C.; Birchall, K.; Ansell, K. H.; Jones, H. M.; Taylor, D.; Clough, B.; Green, J. L.; Holder, A. A. *Bioorganic Med. Chem. Lett.* **2013**, 23, 3064-3069.

102. Gaji, R. Y.; Checkley, L.; Reese, M. L.; Ferdig, M. T.; Arrizabalaga, G. *Antimicrob. Agents Chemother.* **2014,** 58, 2598-2607.

103. Ansell, K. H.; Jones, H. M.; Whalley, D.; Hearn, A.; Taylor, D. L.; Patin, E. C.; Chapman, T. M.; Osborne, S. A.; Wallace, C.; Birchall, K.; Large, J.; Bouloc, N.; Smiljanic-Hurley, E.; Clough, B.; Moon, R. W.; Green, J. L.; Holder, A. A. *Antimicrob. Agents Chemother.* **2014**, 58, 6032-6043.

104. Chapman, T. M.; Osborne, S. A.; Wallace, C.; Birchall, K.; Bouloc, N.; Jones, H. M.; Ansell, K. H.; Taylor, D. L.; Clough, B.; Green, J. L.; Holder, A. A. *J. Med. Chem.* **2014**, 57, 3570-3587.

105. Holder, A. A. H.; Veigel C. *Trends in Parasitology.* **2008**, 25, 1-3.

106. Bansal, A.; Singh, S.; More, K. R.; Hans, D.; Nangalia, K.; Yogavel, M.; Sharma, A.; Chitnis, C. E. *J. Bio. Chem.* **2013**, 288, 1590-1602.

107. Barsanti, P. A.; Pan, Y.; Lu, Y.; Jain, R.; Cox, M.; Aversa, R. J.; Dillon, M. P.; Elling, R.; Hu, C.; Jin, X.; Knapp, M.; Lan, J.; Ramurthy, S.; Rudewicz, P.; Setti, L.; Subramanian, S.; Mathur, M.; Taricani, L.; Thomas, G.; Xiao, L.; Yue, Q. *ACS Med. Chem. Lett.* **2014**, 6, 42-46.

108. Singh, M. P.; Joseph, T.; Kumar, S.; Bathini, Y.; Lown, J. W. *Chem. Res.Toxicol* **1992**, 5, 597-607.

109. Kidwai, M.; Jahan, A.; Bhatnagar, D. *J. Chem. Sci.* **2010**, 122(4), 607-612.

110. Karimi-Jaberi Z.; Amiri, M. *E-J CHEM.*, **2012**, 9(1), 167-170.

111. John B. Wright. The Chemistry of the Benzimidazoles. **1951**. http://pubs.acs.org/doi/pdf/10.1021/cr60151a002. (Accessed August 6, 2017).

112. XU, Y.; Brenning, B. G.; Kultgen, S. G.; Foulks, J. M.; Clifford, A.; Shuping, L.; Chan, A.; Merx, S.; McCullar, M.V.; Kanner, S. B.; Koc-Kan; H. *ACS Med. Chem. Lett.* **2015**, 6, 63-67.

113. Ndakala, A. J.; Gessner, R. K.; Gitari, P. W.; October, N.; White, K. L.; Hudson, A.; Fakorede, F.; Shackleford, D. M.; Kaiser, M.; Yeates, C.; Charman, S. A.; Chibale, K. *J. Med. Chem.* **2011**, 54, 4581-4589.

114. Shahul, H. P.; Chinnapattu, M.; Shanbag, G.; Manjrekar, P'; Koushik, K.; Raichurkar, A.; Patil, V.; Jatheendranath, S.; Rudrapatna, S. S.; Barde, S. P.; Rautela, N.; Awasthy, D.; Morayya, S.; Narayan, C.; Kavanagh, S.; Saralaya, R.; Bharath, S.; Viswanath, P.; Mukherjee, K.; Bandodkar, B.; Srivastava, A.; Panduga, V.; Reddy, J.; Prabhakar, K. R.; Sinha, A.; Jiménez-Díaz, M. B.; Martínez, M. S.; Angulo-Barturen, I.; Ferrer, S.; Sanz, L. M.; Gamo, F, J.; Duffy, S.; Avery, V. M'; Magistrado, P. A.; Lukens, A. K.; Wirth, D. F.; Waterson, D.; Balasubramanian, V.; Iyer, P. S.; Narayanan, S.; Hosagrahara, V.; Sambandamurthy, V. K.; Ramachandran, S. *J.Med. Chem.*, **2014**, 57, 5702-5713.

115. Johannes, J. W.; Chuaqui, C.; Cowen, S.; Devereaux, E.; Gingipalli, L.; Molina, A.; Wang, T.; Whitston, D.; Wu, X.; Hai-Jun, X.; Zinda, M. *Bioorganic Med. Chem.* **2014**, 24, 1138-1143.

116. Rathelot, P.; Vanelle, P.; Gasquet, M.; Crozet, M. P.; Timon-David, P.; Maldonado, J. *Chem. Eur. J.* **1995**, 30, 503-508.

117. Bringmann, G.; Dreyer, M.; Faber, J. H.; Dalsgaard, P. W.; Staerk, D.; Jaroszewski, J. W.; Ndangalasi, H.; Mbago, F.; Brun, R.; Christensen B. S. *J. Nat. Prod.* **2004**, 67(5), 743-748.

118. Ressurreica, A. S.; Goncalves, D.; Sitoe, A. R.; Albuquerque, I. S.; Gut, J.; Gois, A.; Goncalves, L. M.; Bronze, M. R.; Hanscheid, T.; Biagini, G. A.; Rosenthal, P. J.; Prudencio, M.; O'Neill P.; Mota, M. M.; Lopes, F.; Moreira, R. *J. Med. Chem.* **2013**, 56, 7679-7690.

119. Fox, B. A.; Threlfall, T. L. *Organic Syntheses, Coll.* **1973**, 5, 346; 1964, 44, 34.

120. Wyatt P. and Warren S. Organic Synthesis: Strategy and Control. **2007**. John Wiley and son Ltd. West Sussex, England. PP 750

121. McMurry J. Organic Chemistry. **2012** (ninth edition). Cengage Learning, Boston, USA. PP 819-820.

122. Viron S. J. The nitration of 2-aminopyridines and 2-aminothiozoles. PhD thesis; Mc Gill University, Montreal 2, Canada, **1952.**

123. Kasman S. Investigation of nitroaminopyridines and nitroaminothiazoles. PhD thesis; Mc Gill University, Montreal 2, Canada, **1955**.

124. Bellobono, I. R.; Favini G. *J. Chem. Soc.* (**B**), **1971**, 2034-2037.

125. Bryson, A. *J. Am. Chem. Soc.* **1960**, 82, 4862-4871.

126. Gasparro, F. P.; Kolodny N. H. *J. Chem. Educ.* **1977**, 54, 258-261.

127. Williams, D. H.; Ian, F. Spectroscopic Method in Organic Chemistry, 4th ed.; McGraw-Hill: London, 1987. pp 103.

128. Zimmer, K. Z.; Shoemaker, R.; Ruminski, R. R. *Inorganic Chimica Acta.* **2006**, 359, 1478-1484.

129. Sulima, A.; Cheng, K.; Jacobson, A. E.; Rice, K. C.; Gawrisch, K.; Young-Sok, L. *Magn. Reson. Chem.* **2013**, 51, 82-88.

130. Manna I. K.; Weier, R. M; Swenton L; Lankin D. C. *J. Org. Chem.* **1995**, 60, 960-965.

131. Ramos, N. C.; Echevarria, A.; Valbon, A.; Bortoluzzi ,A. J.; Guedes, G. P.; Rodrigues-Santos, C. E. *Cogent Chemistry.* **2016**, 2, 1-11.

132. Clayden, J. P.; Greeves, N.; Warren, S.; Wothers, P. D. Organic Chemistry. **2005**. Oxford University press, New York, United States. pp 354.

133. Faridoon; Edkins, A. L.; Isaacs, M.; Dumisani, M. D.; Hoppe, H. C.; Kaye, P. T. *Bioorganic Med. Chem. Lett.* **2016**, 26, 3810-3812.